

Plants thrive in diverse environments by developing wood, which is crucial for their structure and growth. This thesis examines the role of xylan in the secondary cell wall integrity (SCWI) of *Arabidopsis* and *Populus*, identifying differences between herbaceous and tree species. By exploring mechanosensing pathways and genetic manipulation of xylan, the thesis reveals how xylan structure impacts SCWI, plant physiology, and drought responses. These insights are pivotal for enhancing biomass production for biofuel and improving plant resilience through priming strategies.

Félix Barbut received his graduate education at the Department of Forest Genetic and Plant Physiology, SLU, Umeå in Sweden. He completed his Master in Science and Technologies for Agriculture, Food, and the Environment at Université Paris-Est Créteil, in France.

Acta Universitatis Agriculturae Sueciae presents doctoral theses from the Swedish University of Agricultural Sciences (SLU).

SLU generates knowledge for the sustainable use of biological natural resources. Research, education, extension as well as environmental monitoring and assessment are used to achieve this goal.

Online publication of thesis summary: <http://epsilon.slu.se/eindex.html>

ISSN 1652-6880

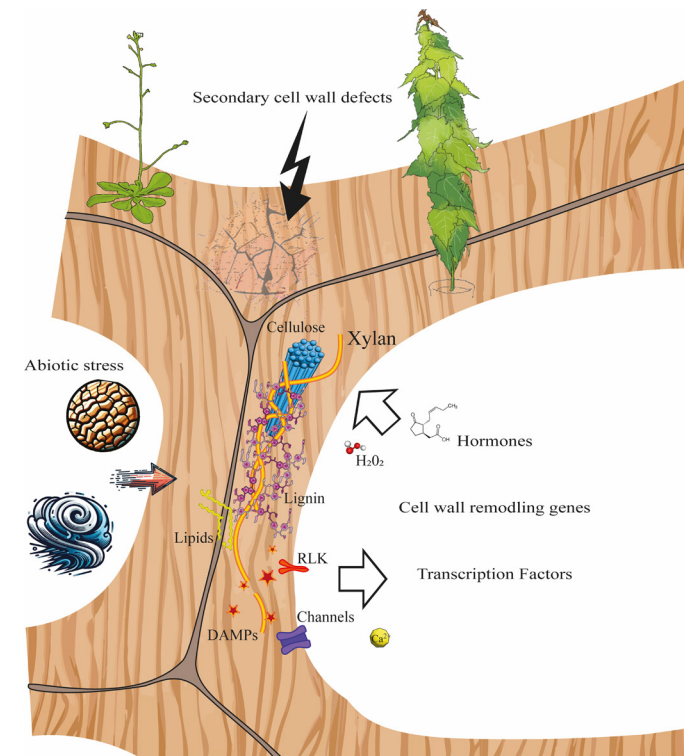
ISBN (print version) 978-91-8046-042-2

ISBN (electronic version) 978-91-8046-043-9



Unraveling the Role of Xylan in the Integrity of Secondary Cell Walls: Insights from *Arabidopsis* and Aspen

FÉLIX BARBUT



Unraveling the Role of Xylan in the Integrity
of Secondary Cell Walls: Insights from
Arabidopsis and Aspen

Félix Barbut

Faculty of Forest Sciences

Department of Forest Genetics and Plant Physiology

Umeå



SWEDISH UNIVERSITY
OF AGRICULTURAL
SCIENCES

DOCTORAL THESIS

Umeå 2024

Acta Universitatis Agriculturae Sueciae

2024:51

Cover: **The role of xylan in secondary cell wall integrity sensing and maintenance in dicots plants.**

(Detailed illustrations of *Arabidopsis thaliana* and *Populus tremula x tremuloides* are expertly drawn by Q. Moindzé based on my original photographs.

Illustration generated in Adobe Illustrator and using IA-generated icons to show stresses)

ISSN 1652-6880

ISBN (print version) 978-91-8046-042-2

ISBN (electronic version) 978-91-8046-043-9

<https://doi.org/10.54612/a.1a1lti3om5>

© 2024 Félix Barbut, <https://orcid.org/0000-0001-5395-6776>

Swedish University of Agricultural Sciences, Department of Forest Genetics and Plant Physiology, Umeå, Sweden

The summary chapter of this thesis is licensed under CC BY NC ND 4.0. To view a copy of this license, visit <https://creativecommons.org/licenses/by-nc-nd/4.0/>. Other licences or copyright may apply to illustrations and attached articles.

Print: Original Tryckeri Umeå 2024

Unraveling the Role of Xylan in the Integrity of Secondary Cell Walls: Insights from *Arabidopsis* and Aspen

Abstract

Plants have conquered lands by developing wood, with cells having secondary cell walls (SCW), which allowed them to thrive in various environments and reach heights up to a hundred meters. Wood is also the main reservoir of the assimilated carbon. Given current societal challenges, there is a pressing need for better utilization of this renewable resource, underscoring the importance of understanding the dynamic process of SCW deposition. In this thesis, I explored the role of xylan in the SCW integrity of *Arabidopsis* and *Populus*, which allowed me to uncover some differences between herbaceous and tree species.

As the SCW integrity sensing pathways are not understood, I first searched for the members of the CrRLK1L family expressed during SCW formation in *Populus* because these proteins function as primary cell wall integrity sensing. I discovered that *Populus* possesses an extended array of lectin domain receptors expressed in tissues forming SCWs, reflecting the trees' adaptation to withstand higher negative vascular pressures and support perennial growth. Moreover, I studied changes following mechanical stimuli in *Populus* stems because mechanosensing pathway overlaps with cell wall integrity sensing. I found that tree growth was increased after repetitive stem bending and that jasmonic acid and polyamine signaling were activated.

To determine the role of xylan in SCW integrity, I studied transgenic plants with altered xylan structure. Removal of the xylan MeGlcA side chain affected the binding of suberin-like compounds to cell walls without inducing any SCW integrity stress responses. Conversely, xylan backbone-impaired plants exhibited altered abscisic acid, ethylene, and cytokinin levels and changes in the expression of signaling and stress-related genes, which could participate in SCW integrity sensing and signaling. Finally, I studied the effect of xylan backbone impairment on drought responses in *Arabidopsis* and *Populus*. Xylan backbone-impaired plants exhibited different susceptibilities to drought, underscoring xylan pivotal role in cell wall architecture and overall plant physiology.

Through this thesis, I have advanced our understanding of plant SCW integrity maintenance and identified potential targets for priming and genetic engineering. These findings hold significant implications for enhancing biomass production for biorefinery and plant resilience.

Keywords: glucuronoxytan, secondary cell wall, *Arabidopsis*, *Populus*, cell wall integrity maintenance, abiotic stress, mechanoperception, genetic engineering, priming effect.

Autor's address: Félix Barbut, Swedish University of Agricultural Sciences, Department of Forest Genetics and Plant Physiology, SE-901-83, Umeå, Sweden; Email: felix.barbut@slu.se

Avslöjande av Xylans roll för sekundära cellväggers integritet: Insikter från *Arabidopsis* och *Asp*

Abstrakt

Växter har erövrat land genom att utveckla ved, med celler som har sekundära cellväggar (SCV), vilket har möjliggjort för dem att trivas i olika miljöer och växa upp till hundra meter höga. Ved är också den huvudsakliga reservoaren för assimilerat kol. Med tanke på dagens samhällsutmaningar finns det ett brådskande behov av att bättre utnyttja denna förnybara resurs, vilket understryker vikten av att förstå den dynamiska processen när SCV bildas. I denna avhandling utforskade jag xylans roll i SCV-integritet hos *Arabidopsis* och *Populus*, vilket gjorde det möjligt för mig att upptäcka vissa skillnader mellan örtartade och trädbaserade arter.

Eftersom signalvägarna som känner av den strukturella integriteten hos SCV inte är förstådda, började jag med att söka efter medlemmar av CrRLK1L-familjen som uttrycks i SCV-bildning i *Populus*, eftersom dessa proteiner fungerar som sensorer för integritet i primära cellväggar. Jag upptäckte att *Populus* har en utvidgad uppsättning av lectin-domänreceptorer uttryckta i vävnader som bildar SCV, vilket speglar trädens anpassning för att motstå högre negativa vaskulära tryck och främja perenn tillväxt. Dessutom studerade jag förändringar efter mekaniska stimuli i *Populus*-stammar eftersom mekanosensorningsvägen överlappar med känslan av cellväggsintegritet. Jag fann att träd tillväxten ökade efter upprepad böjning av stammen och att signalering av jasmonsyra och polyaminer aktiverades.

För att bestämma xylans roll i SCV-integritet studerade jag transgena växter med förändrad xylanstruktur. Borttagning av xylan MeGlcA-sidokedjan påverkade bindningen av suberin-liknande föreningar till cellväggar utan att framkalla några SCV-integritetsstressreaktioner. Tvärtom hade växter med xylan innehållande en kolkedja med nedsatt funktion förändrade nivåer av abscisinsyra, etylen och cytokinin samt förändringar i uttrycket av signal- och stressrelaterade gener, vilket kan spela en roll i SCV att känna integritet och signalering. Slutligen studerade jag hur *Arabidopsis* och *Populus* innehållande xylan med den defekta kolkedjan klarar torka, vilket understryker xylans centrala roll i cellväggsarkitektur och övergripande växtfysiologi.

Genom denna avhandling har jag främjat vår förståelse för underhåll av växt-SCV-integritet och identifierat potentiella mål för priming och genetisk modifiering. Dessa fynd har betydande implikationer för förbättrad biomassa produktion för biorefining och växtresiliens.

Nyckelord: Glukuronoxylan, Sekundär Cellvägg, *Arabidopsis*, *Populus*, Underhåll av Cellväggsintegritet, Abiotisk Stress, Mekanoperception, Genetisk Teknik, Primingeffekt, Receptor-Liknande Kinas.

Déceler le rôle du xylane dans l'intégrité de la paroi cellulaire secondaire : Aperçu sur *Arabidopsis* et le peuplier

Résumé

Les plantes ont conquis les terres en développant du bois, renforcé par des cellules dotées de parois cellulaires secondaires (PCS), ce qui leur a permis de prospérer dans divers environnements et d'atteindre des hauteurs allant jusqu'à cent mètres. Le bois constitue également le principal réservoir de carbone assimilé. Face aux enjeux sociétaux actuels, il devient urgent de mieux utiliser cette ressource renouvelable, ce qui souligne l'importance de comprendre le processus dynamique de dépôt des PCS. Dans cette thèse, j'ai exploré le rôle du xylane dans le maintien de l'intégrité des PCS chez *Arabidopsis* et le peuplier, révélant des différences notables entre les espèces herbacées et arborescentes.

Comme les mécanismes de détection de l'intégrité des PCS restent mal compris, j'ai initialement identifié les membres de la famille *CtRLK1L* exprimés durant la formation des PCS du peuplier. Ces protéines jouent un rôle crucial dans la perception de l'intégrité de la paroi cellulaire primaire. J'ai constaté que le peuplier dispose d'un large spectre de récepteurs à domaine malectine exprimés dans les tissus où se forment les PCS, reflétant l'adaptation des arbres à supporter des pressions vasculaires négatives plus élevées et à soutenir une croissance pérenne. De plus, j'ai examiné les réactions aux stimuli mécaniques dans les troncs de peuplier, observant que la voie des mécanoperceptions interagit avec celle de la détection de l'intégrité de la paroi cellulaire. J'ai découvert que la croissance des arbres était augmentée après des flexions répétées du tronc, et que les voies de signalisation de l'acide jasmonique et des polyamines étaient activées.

Pour déterminer le rôle du xylane dans l'intégrité des PCS, j'ai étudié des plantes transgéniques présentant une structure de xylane modifiée. La suppression de la chaîne latérale MeGlcA du xylane a altéré la liaison des composés de type subérine aux parois cellulaires sans induire de réponses de stress liées à l'intégrité des PCS. Inversement, les plantes présentant une modification de la chaîne carbonée du xylane ont montré des différences dans les niveaux d'acide abscissique, d'éthylène, et de cytokinine, ainsi que des changements dans l'expression des gènes de signalisation et liés au stress, qui pourraient contribuer à la détection et à la signalisation de l'intégrité des PCS. Enfin, j'ai analysé l'impact de l'altération de la chaîne carbonée du xylane sur les réponses à la sécheresse chez *Arabidopsis* et le peuplier. Ces plantes ont montré des susceptibilités différentes à la sécheresse, soulignant le rôle crucial du xylane dans l'architecture de la paroi cellulaire et la physiologie générale de la plante.

À travers cette thèse, j'ai approfondi notre compréhension du maintien de l'intégrité des PCS des plantes et identifié des cibles potentielles pour l'amélioration génétique et les pratiques agricoles. Ces découvertes ont des implications importantes pour l'amélioration de la production de biomasse pour la bioraffinerie et la résilience des plantes.

Mots-clés : Glucuronoxylane, Paroi Cellulaire Secondaire, *Arabidopsis*, Peuplier, Maintien de l'Intégrité de la Paroi Cellulaire, Stress Abiotique, Mécanoperception, Génie Génétique, Effet de Priming, Récepteur Kinase.

Dedication

I dedicate this thesis to my parents Christine and Henry, who have always believed in me and granted me the freedom to find my own path.

I also dedicate this work to all my former teachers and supervisors who knew how to motivate me, enhance my potential, and offer me the opportunity to embrace their knowledge.

“All knowledge is connected to all other knowledge. The fun is in making the connections.” – Arthur C. Aufderheide

“Nature’s economy shall be the base for our own, for it is immutable, but ours is secondary. An economist without knowledge of nature is therefore like a physicist without knowledge of mathematics.” – Carl Linnaeus

Contents

List of publications.....	11
List of figures	15
Abbreviations	17
1. Introduction	21
1.1 The plant cell wall.....	21
1.1.1 Wood cell wall structure and components in dicots	22
Pectins	24
Cellulose.....	25
Hemicelluloses	25
Lignin	26
Structural proteins	27
1.1.2 Xylan of hardwoods	28
Detailed structure of xylan in dicot wood.....	28
Biosynthesis of wood xylan.....	30
1.2 Multi-level hierarchy of players in cell wall integrity maintenance.....	33
1.2.1 Stress molecules to be sensed.....	33
Damage-Associated Molecular Patterns.....	33
Small peptides	34
1.2.2 The perception of cell wall damage with membrane-bound proteins	34
Receptor-like kinases.....	34
Ion channels.....	36
1.2.3 Cell wall damage signal integration and downstream signalization.....	37

1.3	CWI integrity sensing during SCW formation.....	38
1.4	Importance of CWI for engineering plant cell walls.....	41
2.	Hypotheses and Objectives.....	43
3.	Results and Discussion	45
3.1	Identifying potential molecular players involved in secondary wall integrity sensing/signal transduction.....	45
3.1.1	Genome-wide analysis of malectin domain proteins in <i>Populus</i> and <i>Arabidopsis</i> reveals candidates for SCWI maintenance (Paper I).....	45
3.1.2	Secondary wall sensing and signaling during flexure wood formation in aspen highlights possible elements participating in SCWI maintenance related to mechanoperception (Paper II).....	48
3.2	Xylan glucuronic acid side chains provide anchoring for suberin-like aliphatics in secondary cell walls (Paper III)	51
3.3	Exploring the direct and indirect effects of xylan impairment in <i>Arabidopsis</i> and aspen: glucuronoxyylan backbone in pieces (Papers IV and V)	54
3.3.1	Impact of two xylanases, GH10 and GH11, on the secondary cell wall, signaling pathways, growth, and saccharification in aspen (Paper IV)	56
3.3.2	Drought responses of <i>Arabidopsis</i> and aspen with modified xylan backbone (Paper V)	61
4.	Discussion and Conclusions	67
	References	73
	Popular science summary	101
	Populärvetenskaplig sammanfattning.....	103
	Acknowledgements	105

List of publications

This thesis is based on the work contained in the following papers, referred to by Roman numerals in the text:

- I. Vikash Kumar, Evgeniy N. Donev, **Félix R. Barbut**, Sunita Kushwah, Chanaka Mannapperuma, János Urbancsok, and Ewa J. Mellerowicz. (2020). Genome-Wide Identification of Populus Malectin/Malectin-Like Domain-Containing Proteins and Expression Analyses Reveal Novel Candidates for Signaling and Regulation of Wood Development. *Frontiers in Plant Science* 11:588846. <https://doi.org/10.3389/fpls.2020.588846>.
- II. János Urbancsok, Evgeniy N. Donev, Pramod Sivan, Elena van Zalen, **Félix R. Barbut**, Marta Derba-Maceluch, Jan Šimura, Zakiya Yassin, Madhavi L. Gandla, Michal Karady, Karin Ljung, Sandra Winstrand, Leif J. Jönsson, Gerhard Scheepers, Nicolas Delhomme, Nathaniel R. Street, Ewa J. Mellerowicz (2023). Flexure Wood Formation via Growth Reprogramming in Hybrid Aspen Involves Jasmonates and Polyamines and Transcriptional Changes Resembling Tension Wood Development. *New Phytologist* 240 (6): 2312–34. <https://doi.org/10.1111/nph.19307>.
- III. Marta Derba-Maceluch, Madhusree Mitra, Mattias Hedenström, Xiaokun Liu, Madhavi L. Gandla, **Félix R. Barbut**, Ilka N. Abreu, Evgeniy N. János Urbancsok, Thomas Moritz, Leif J. Jönsson, Adrian Tsang, Justin Powlowski, Emma R. Master, Ewa J. Mellerowicz (2023). Xylan Glucuronic Acid Side Chains Fix Suberin-like Aliphatic Compounds to Wood Cell Walls. *New Phytologist* 238 (1): 297–312. <https://doi.org/10.1111/nph.18712>.
- IV. Pramod Sivan, János Urbancsok, Evgeniy N Donev, Marta Derba-Maceluch, **Félix R Barbut**, Zakiya Yassin, Madhavi L Gandla, Madhusree Mitra, Saara E Heinonen, Jan Šimura, Kateřina Cermanová, Michal Karady, Gerhard Scheepers, Leif J Jönsson, Emma R Master,

Francisco Vilaplana, Ewa J Mellerowicz. Modification of Xylan in Secondary Walls Alters Cell Wall Biosynthesis and Wood Formation Programs (Manuscript), BioRxiv doi: <https://doi.org/10.1101/2024.05.02.592170>

- V. **Félix R. Barbut**, Emilie Cavel, Evgeniy Donev, Ioana Gaboreanu, Janos Urbancsok, Garima Pandey, Hervé Demailly, Dianyi Jiao, Zakiya Yassin, Marta Derba-Maceluch, Emma R. Masters, Gerhard Scheepers, Laurent Gutierrez, Ewa J. Mellerowicz. Integrity of Xylan Backbone Affects Plant Responses to Drought (Manuscript)

Papers I-V are reproduced with the permission of the publishers.

The contribution of Félix Barbut to the papers included in this thesis was as follows:

- I. I analyzed co-expression networks, edited, and designed 5 out of 8 figures with Illustrator and PowerPoint from raw files generated from bio-informatic tools, wrote the Introduction, and participated in the writing of the entire paper.
- II. I participated in the design of experiments, preformation, data analysis, and writing. This included setting up the experiment, daily surveying, and harvesting the trees at the end of the experiment. I was responsible for recording the bending movement and measuring the magnitude of the stress.
- III. I designed and performed the majority of experiments with *Arabidopsis*, analyzed the obtained data, and wrote the respective parts of the paper. In particular, I characterized the transgenic *Arabidopsis* lines expressing AnAgu67A and *gux1gux2* mutants. This included isolating the homozygotic lines, selecting the best-expressing lines, evaluating the transgene expression by qPCR, and performing the α -glucuronidase enzymatic activity tests.
- IV. I participated in designing experiments, preparing them, analyzing the data, and writing. This included setting up the experiment, daily surveying, harvesting, and taking pictures of the trees at the end of the experiment.
- V. I took a leading role in designing experiments, preparing them, analyzing the data, and writing the manuscript, starting with the isolation of homozygotic xylanase-expressing *Arabidopsis* lines and selecting the best-expressing ones based on qPCR, selecting transgenic aspen lines, coordinating, and performing the majority of experiments with *Arabidopsis* and aspen, interpreting the data, and writing the manuscript.

List of figures

Figure 1 Wood cell wall structure at different developmental stages: Different components are deposited in the apoplast in sequence. First, the primary cell wall (PCW) is deposited with different pectins, xyloglucan, and cellulose microfibrils. After cell expansion is finished, the three secondary wall (SCW) layers (S1, S2, S3) having different matrix polysaccharide compositions are deposited, and the PCW is transformed into a compound middle lamella (CML). Cellulose microfibrils are deposited at different angles in each SCW layer. Lignin deposition starts in the CML from the corner of the cell. Glucuronoxytan, the main hemicellulose in the SCW, binds cellulose through its major domain and lignin through its minor domain. In mature walls, the plasma membrane is degraded, and the cell dies.	21
Figure 2. GX structure, biosynthetic genes, and sites of fungal enzymatic cleavages targeted in this work.....	30
Figure 3 Overview of sensing and signaling molecules involved in cell wall integrity (from Hamann 2015).....	38

Abbreviations

ABA	Abscisic Acid
ACC	1-Amino Cyclopropane Carboxylic acid
<i>AnAgu67A</i>	α -glucuronidase GH67 of <i>Aspergillus niger</i>
<i>CrRLK1Ls</i>	<i>Catharanthus roseus</i> family of Receptor-Like Kinase 1 Like proteins
Col-0	Columbia-0 ecotype
CWI	Cell Wall Integrity
DAMPs	Damage-Associated Molecular Patterns
DP	Degree of Polymerization
EXTs	Extensins
FER	Feronia
FLAs	Fasciclin-Like Arabinogalactan Proteins
F_v/F_m	Maximum quantum efficiency of photosystem II
G, H, S	Guaiacyl, p-Hydroxyphenyl, and Syringyl
GH	Glycoside Hydrolase
G-layer	Gelatinous Layer
GUX	GlucUronic acid substitution of Xylan
GX	GlucuronoXylan
GXM	Glucuronoxylan Methyl transferase
HG	HomoGalacturonan
IRX	Irregular xylem
JA	Jasmonic Acid

LCCs	Lignin-Carbohydrate Complexes
LRR	Leucine-Rich Repeat
MD, MLD	Malectin Domain, Malectin Like Domain
MeGlcA	4- <i>O</i> -MethylGlucuronic Acid
ML	Middle Lamella
OG	OligoGalacturonide
OSCA	Reduced Hyperosmolality-Induced [Ca ²⁺] Increase
PA	Polyamide
PCW	Primary Cell Wall
PM	Plasma Membrane
PTI	Pathogen-Triggered Immunity
RALFs	Rapid Alkalinization Factors
RG	RhamnoGalacturonan
RLKs	Receptor-Like Kinases
ROS	Reactive Oxygen Species
RWA	Reduced Wall Acetylation
SA	Salicylic Acid
SL	StrigoLactone
SCW	Secondary Cell Wall
SCWI	Secondary Cell Wall Integrity
S1, S2, S3	Layers of the Secondary Cell Wall
TBL	Trichome Birefringence-Like
WAKs	Wall-Associated Kinases
XSC	Xylan Synthase Complex
XyG	XyloGlucan

1. Introduction

1.1 The plant cell wall

Algae, the progenitors of plants, evolved more than a billion years ago from ancestral eukaryotes by the secondary endosymbiosis event with cyanobacteria, which allowed them to photosynthesize (Archibald, 2009). At that time, the prokaryotic cell wall was probably transferred to plants through lateral gene transfers, which shows that cell walls have always been a feature of plants closely related to their autotrophic nature (Niklas, 2004). Approximately half a billion years ago, plants started to conquer lands, and the need for better encapsulation of their cells to resist desiccation led to further cell wall adaptations. The emergence of lignin in tracheophytes is one of these adaptations that permit plants to withstand significant negative water pressure in their conductive systems and gain rigidity to be able to stand upright (Weng and Chapple, 2010). Almost 400 years ago, in 1665, Robert Hooke published *Micrographia*, where he discovered cells by observing honeycomb-like cork cells with suberized cell walls. Today, the vast diversity of cell walls across the plant kingdom offers an avenue of opportunity to understand their physiology better and, with this knowledge, drive the progress toward plant biomass utilization and crop engineering.

The plant cell wall is a crucial and dynamic structure that encapsulates the cell with the unique ability to expand without weakening or breaking. This quality is required for plant growth while providing mechanical strength (Carpita and Gibeaut, 1993; Cosgrove, 2023). Delimited between the plasma membrane and the middle lamellae of the neighboring cell, the cell wall can be viewed as the scaffolding for plant cells, serving as a skeleton. However, it is also an active structure mediating cell-to-cell communication and holding various functions because of its dynamic composite nature and its capacity to generate signaling molecules sensed by transmembrane proteins (Delmer et al., 2024). It also mediates the plant's interaction with its environment, which is crucial to elaborate a precise stress response or to thrive in harsh conditions (Le Gall et al., 2015; Vaahtera et al., 2019).

Moreover, it is the most abundant biomass produced by plants, and numerous examples of bio-economic applications have already been explored. Nevertheless, more knowledge is needed to magnify their potential. The main constituents of cell walls are cellulose, hemicelluloses, pectins, lignin, and proteins. The cell wall composition varies greatly between species, tissues, and developmental stages, and it can be adjusted to mitigate environmental cues thanks to its plasticity (Cosgrove, 2005; Popper et al., 2011; Fangel et al., 2012). The structure and the pivotal role of the cell wall in plants will be discussed here with a focus on the xylan in the secondary cell wall of dicot plants (**Figure 1**).

1.1.1 Wood cell wall structure and components in dicots

The wood cell wall composition of dicots such as aspen or *Arabidopsis* is variable across different stages of wood cell development. It notably differs between growing cells with only primary cell walls (PCW) and maturing ones depositing secondary cell wall (SCW) layers. When PCW is characterized by its extensibility, SCW is formed onto this first layer after cell expansion, reinforcing the wall and providing mechanical support to withstand intense negative pressure for water transport. During this maturation process, the PCW, as well as the thickening SCW, become enriched in the phenolic-based amorphous polymer called lignin. In maturing wood, the main difference in composition between the PCW and SCW is the varied proportion and nature of components such as cellulose and hemicellulose, the absence of pectin in SCW, and the timing of lignin impregnation, which starts in the middle lamella followed by the PCW (Cosgrove, 2023; Delmer et al., 2024). During maturation, the secondary wall is formed in three layers (S1, S2, S3 -from the outer to the inner layer), with the S1 layer being at the transition between PCW and SCW that could act as a scaffold for the other layers. The thickest layer is the S2 (75–85% of the SCW thickness) (Barnett and Bonham, 2004). Additionally, the formation of the innermost tertiary layer can be initiated, for example, the gelatinous layer (G-layer) in the fibers (Mellerowicz and Gorshkova, 2012; Guedes et al., 2017) or the amorphous layer in the parenchyma cells (Wisniewski and Davis, 1989). During the dynamic process of wood formation, the synthesis and incorporation of the different cell wall components are tightly controlled. The following chapters describe the main components found in dicot woody cells of primary, secondary, and tertiary walls.

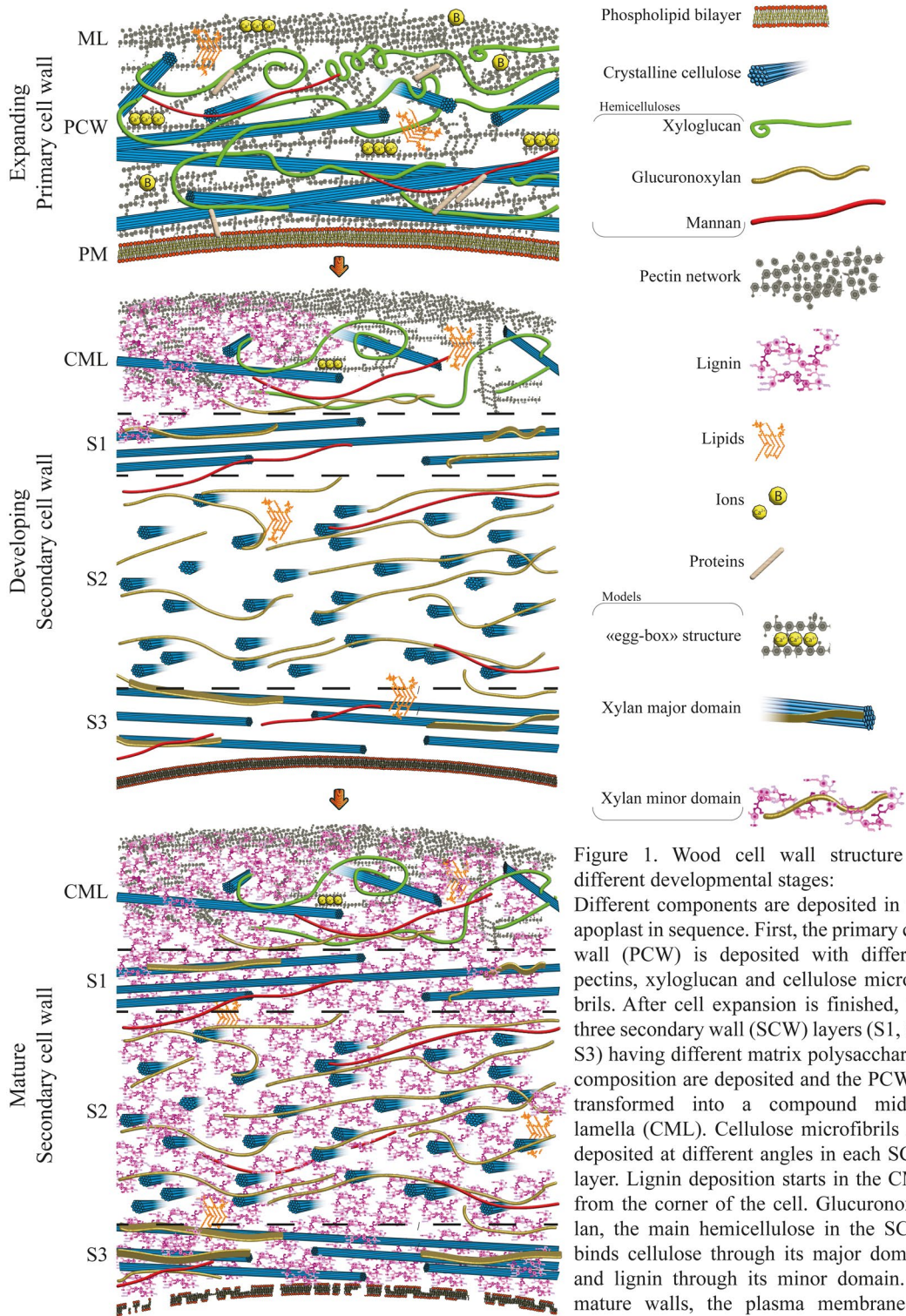


Figure 1. Wood cell wall structure at different developmental stages: Different components are deposited in the apoplast in sequence. First, the primary cell wall (PCW) is deposited with different pectins, xyloglucan and cellulose microfibrils. After cell expansion is finished, the three secondary wall (SCW) layers (S1, S2, S3) having different matrix polysaccharide composition are deposited and the PCW is transformed into a compound middle lamella (CML). Cellulose microfibrils are deposited at different angles in each SCW layer. Lignin deposition starts in the CML from the corner of the cell. Glucuronoxylan, the main hemicellulose in the SCW, binds cellulose through its major domain and lignin through its minor domain. In mature walls, the plasma membrane is degraded, and the cell dies.

Pectins

Pectins are only found in the primary cell wall and middle lamella (about ~50% of the dry weight) and some types of tertiary walls (Mellerowicz et al., 2001; Sivan et al., 2023). They form one of the most complex matrix polysaccharide networks and are composed of galacturonic acid-based polysaccharides named homogalacturonan (HG), rhamnogalacturonan-I (RG-I), and rhamnogalacturonan-II (RG-II). Pectins contain many other sugars such as rhamnose, arabinose, and galactose and some minor sugars like glucuronic acid, fucose, xylose, apiose, Kdo (3-deoxy-D-manno-2-octulosonic acid), and Dha (3-deoxy-D-lyxo-2-heptulosaric acid) some of which can be methylated or acetylated. Given the diverse degree of polymerization (DP) of their backbones and side chains, pectin exhibits an important versatility of physical and chemical properties (O'Neill et al., 1990; Caffall and Mohnen, 2009; Atmodjo et al., 2013; Chen et al., 2015). The middle lamella acts as a cellular glue and is primarily formed by pectins, which place these polymers as a central nod in cell-to-cell adhesion (Daher and Braybrook, 2015). In the primary cell wall, the pectins provide a structural gelatinous network that allows for substantial rearrangement, and their importance for plant growth, development, and defense also lies in their involvement in signaling in response to biotic and abiotic stresses. Apart from interacting with themselves, pectins interact with other macromolecules like cellulose, hemicelluloses, and lignin, as well as ions such as calcium and borate, which ensure the cohesion of the primary wall polysaccharide matrix. Pectins participate extensively in hydrating the PCW, which is necessary for the movement and separation of cellulose microfibrils during growth. Surprisingly, RG-I is also found in the G-layer, highlighting pectin roles even beyond the primary cell wall (Mellerowicz and Gorshkova, 2012). The capacity of HG to form gels and bind calcium is essential for the pH and the ionic status in the apoplast. Finally, the pectins fragments released after biotic cell wall damage are sensed by transmembrane receptors as damage-associated molecular patterns (DAMPs) (Du et al., 2022). Thus, pectins provide structural support and facilitate growth but also play a role in the plant's adaptation.

Cellulose

Cellulose, the load-bearing component of cell walls, is the most important polysaccharide in the SCW (40-60% in dry weight) and represents ~20% of dry weight in primary-walled developing xylem and phloem tissues (Simson and Timell, 1978). It consists of unbranched β -1,4-linked D-glucose polymers of many thousands of residues that coalesce to form crystalline microfibrils made of probably 18 glucan chains connected by hydrogen and van der Waals bonds (Kubicki et al., 2018). The glucan chains surrounding the crystallized core are semi-crystalline and can interact with hemicelluloses such as xyloglucan in PCW, and thus be integrated within the polysaccharide matrix. Surrounded by hemicelluloses and pectins in the PCW, cellulose provides tensile strength comparable to steel while allowing cell extensibility. Cellulose microfibrils spontaneously aggregate together to form bundles potentially affected by the presence of xyloglucan in PCW and xylan in SCW (Cosgrove and Jarvis, 2012). The orientation of the microfibrils is linked to the microtubule's guidance of the membrane-anchored cellulose synthases complexes, which drives the direction of cell expansion in PCW and varies across the SCW layers. The thick SCW S2 layer has a longitudinal microfibril orientation, while the S1 and S3 layers have more horizontal microfibrils that limit radial expansion (Barnett and Bonham, 2004). In the SCW, the degree of cellulose crystallization is higher than in the PCW, which is probably caused by microfibril aggregation. The increased content of cellulose in SCW, as well as the more packed and aligned microfibrils and their bundle structures, provide SCW rigidity and mechanical support (Cosgrove and Jarvis, 2012). The crystallization and DP are even more important in the G-layer, with four times more glucan chains and a higher content (~75%) than in SCWs (Mellerowicz and Gorshkova, 2012).

Hemicelluloses

The hemicelluloses are a heterogeneous group of polysaccharides mainly associated with cellulose (but also lignin and pectins) that confer flexibility and contribute to cell wall diversity. These polysaccharides have a backbone of either one or two types of monosaccharides connected by β (1-4) bonds, mainly xylose, mannose, and glucose, and side chains made of different sugars. In dicotyledonous plants, the main hemicellulose of PCW is

xyloglucan (20-25% d.w.), and the main hemicellulose of SCW is glucuronoxylan (20-30% d.w.) (Scheller and Ulvskov, 2010).

The xyloglucan (XyG) is composed of a glucose backbone substituted with xylose units that can be further linked to galactose and fucose. Notably, xyloglucan can both be linked to pectin via the galactan side chain of RG-I (Keegstra et al., 1973) and to cellulose either spontaneously with hydrogen bonds or by being embedded inside cellulose fibrils during crystallization (Park and Cosgrove, 2015). The central role of XyG in PCW is supported by the myriad of XyG endotransglycosylases existing in cell walls for modification of this hemicellulose (Hayashi, 1989; Hayashi and Kaida, 2011). Mainly found in PCW and ML, XyG is also an important component of the G-layer (~15%) (Nishikubo et al., 2007; Mellerowicz and Gorshkova, 2012).

Dicots PCW is also composed of arabinoglucuronoxylan (5%) and mannans (3-5%) (Zablackis et al., 1995). Arabinoglucuronoxylan, consisting of a xylose backbone with arabinose and glucuronic acid substitution, can also bind to cellulose with a weaker bond than XyG (Mikkelsen et al., 2015). It is cross-linked to pectin by cell wall arabinogalactan protein APAPI (Tan et al., 2013). Mannans, such as glucomannans and galactoglucomannans, are composed of a backbone with two sugars, mannose and glucose, and mannose can be further substituted by acetyl groups and galactose. Closely related to XyG, they share some functions in PCW but are also present in SCW (2-5%) (Yu et al., 2022).

The main SCW hemicellulose of dicots is glucuronoxylan (GX), making about $\frac{1}{3}$ of its dry mass. GX backbone is made of xylose units some of which can be decorated with acetyl groups and glucuronosyl substitutions that can be methylated. The patterning of acetylations and glucuronidations define xylan main domains and varies among species, tissues, and developmental stages affecting GX interaction with other SCW components, such as cellulose (Hao and Mohnen, 2014; Grantham et al., 2017). More details about GX structure, cross-linking, and biosynthesis are depicted in Figure 2 and Section 1.1.2.

Lignin

Formed mainly after the beginning of the SCW program, lignin is a complex phenolic polymer with a high molecular weight and amorphous structure. Its

functions are diverse, ranging from mechanical support and waterproofing to abiotic resistance and defense against pathogens. Lignin complexity lies “simply” in the random arrangement of three monolignol units, *p*-hydroxyphenyl (H), guaiacyl (G), and syringyl (S), interconnected and linked to other cell wall components. Like other components, lignin exhibits considerable variability across species, tissues, developmental stages, and environments (Weng and Chapple, 2010). Dicot lignin is composed of S and G units with a small amount of H units. The xylem cell wall continues to be lignified after programmed cell death (Pesquet et al., 2013), reaching between 17 and 30% of cell wall dry weight in the wood (Panshin and De Zeeuw, 1980; McDougall et al., 1993; Christiernin, 2006). As shown in Figure 1, this lignification process starts from the outer corner of the cell in the ML, progressing to the PCW and creeping through the SCW layers, and the lignin unit profile varies among these locations (Donaldson, 2001). The lignin is incorporated in the frames of cellulose and hemicellulose, filling the gaps and interacting with carbohydrates (Ros Barceló, 1997; Vanholme et al., 2010, 2019). The lignin-carbohydrate complexes (LCCs) resulting from these interactions via either benzyl ether, phenyl glycoside, or γ -esters bonds involve mainly hemicelluloses. For example, the γ -esters bonds connect lignin units to the xylan glucuronic acid (Takahashi and Koshijima, 1988; Watanabe et al., 1989; Balakshin et al., 2014).

Structural proteins

Cell wall proteins, essential for the structure and adaptability of the cell wall, are categorized based on their amino acid composition, solubility, level of glycosylation, and function (Keller, 1993). They include extensins (EXTs), arabinogalactan proteins (AGPs), and proline-rich proteins (PRPs), all being part of the hydroxyproline-rich glycoproteins superfamily (HRGPs), and glycine-rich proteins (GRPs). HRGP common features include specific glycosylation patterns, Hyp-based *O*-glycosylation sites, functional domains, and possible GPI plasma membrane anchoring (Leszczuk et al., 2023). Distinctly, the GRPs contain up to 70% glycine but no glycosylation (Ringli et al., 2001).

EXTs are moderately glycosylated with arabinogalactan II, generating both homopolymeric crosslinking with tyrosine linkages to form extended rods and heteropolymeric crosslinks with pectin, lignin and AGPs (Qi et al., 1995; Held et al., 2004; Nunez et al., 2009; Cong et al., 2013; Tan et al., 2018;

Mishler-Elmore et al., 2021). EXTs help distribute stress more evenly, facilitating the turgor-driven expansion of the cell wall.

AGPs hyperglycosylated with arabinogalactan II and differing in amino acid sequence from EXTs play a role in xylem development during SCW thickening and programmed cell death (Schindler et al., 1995; Showalter, 2001; Iakimova and Woltering, 2017; Leszczuk et al., 2023). FLA11 and FLA12, AGP subclasses with fasciclin domain (FLAs), regulate SCW composition in response to mechanical stress (Ma et al., 2022, 2023). The correlation between the abundance of acidic arabinogalactan II in the G-layer and FLA12-like proteins highlights their significance in the cell wall structure and adaptability (Mellerowicz and Gorshkova, 2012).

PRPs, lightly glycosylated and containing essentially one repetitive motif of (ProHyp-Val-Tyr-Lys)_n, are preponderant in protoxylem and primary xylem (Cassab, 1998). For example, they are linked to SCW formation in poplar, aiding lignin deposition as nucleation sites (Josè-Estanyol and Puigdomènech, 2000; Li et al., 2019).

Cell wall localized GRPs potentially function like collagen with unknown cross-linking mechanisms, possibly via ether bonds involving tyrosine. Other GRPs are known to interact with cell wall-associated kinases, participating in signal transduction and vascular tissue formation, wound healing, and response to environmental stresses (Ringli et al., 2001; Czolpinska and Rurek, 2018; Ma et al., 2021).

1.1.2 Xylan of hardwoods

Detailed structure of xylan in dicot wood

The backbone of GX is made of D-xylopyranosyl units polymerized with β -(1 \rightarrow 4)- glycosidic linkages in equatorial configuration. Every xylose unit alternates in orientation, and two xylose units form a disaccharide: the xylobiose. The type and patterning of the GX substitutions govern its cross-linking capacity and add an additional lever to the plant adaptability arsenal. Research to understand the role of xylan structure in the cross-linking of the cell wall matrix and its interaction with cellulose is driven by the need to facilitate the extraction of CW components for biorefinery applications (Smith et al., 2017). GX substitution residues are acetyl, glucuronic acid (GlcA), and 4-*O*-methyl glucuronic acid (MeGlcA).

GX decorations vary between species, tissue, and development but could also vary throughout single GX molecules. In the major xylan domain, every second xylose in the backbone is typically *O*-acetylated at position O-2 and/or O-3 (Mortimer et al., 2010; Lee et al., 2012; Rennie et al., 2012; Bromley et al., 2013; Busse-Wicher et al., 2014; Chong et al., 2014; Pawar et al., 2016). Acetylation impacts the solubility of GX in water and makes it more resilient to hydrolysis (Pawar et al., 2013; Qaseem and Wu, 2020). It also affects GX binding to cellulose and lignin (Giummarella and Lawoko, 2016; Martínez-Abad et al., 2018). Major domain acetylation every second unit implies that only one side of the GX ribbon is acetylated, facilitating cellulose interactions. In contrast, the minor xylan domain can have consecutively acetylated xyloses (Busse-Wicher et al., 2014; Chong et al., 2014), which would limit the xylan-cellulose interaction (Busse-Wicher et al., 2014).

While (Me)GlcA might have a role similar to acetylation in GX (Xiong et al., 2015), it also could have a distinct impact on cell walls due to its charge that makes the polymer more acidic and hydrophilic. The hardwood GX major domain is substituted with an even pattern, usually every 8th xylose at *O*-2 with α -D-glucuronic acid, which is often 4-*O*-methylated (Mortimer et al., 2015; Busse-Wicher et al., 2016). GX minor domain has an uneven (Me)GlcA substitution pattern. The patterning of substitutions in the GX extensively participates in defining its interaction with cellulose and lignin. When GX is in solution, it forms a 3-fold helical screw, but in the cell wall, the major domain can form a flattened 2-fold helical screw interacting with cellulose, whereas the minor domain having the 3-fold helical screw configuration can interact with lignin (Grantham et al., 2017; Martínez-Abad et al., 2017, 2018). Indeed, the GX docking to (semi)crystalline cellulose microfibrils via hydrogen bonds from the major domain would form a “xylanocellulose” fibril with all the decoration facing outside the microfibril (Grantham et al., 2017). GX MeGlcA side chain can covalently bind to lignin via γ -ester (and maybe α -ester) (Imamura et al., 1994; Balakshin et al., 2014; Giummarella and Lawoko, 2016; Giummarella et al., 2019; Nishimura, 2022). Lignin can also connect non-covalently with electrostatic dipole-dipole interactions between its methyl ethers and the hydroxyl group of GX sugars (Houtman and Atalla, 1995; Kang et al., 2019). Preferably, lignin binds to the 3-fold helical screw configuration of GX, although it can

associate with the 2-fold flat structure of xylan that can adhere to cellulose (Kang et al., 2019; Kirui et al., 2022).

In dicot wood GX, most (if not all) GlcA substitutions are 4-*O* methylated (Ebringerová and Heinze, 2000), increasing the diversity and complexity of the cell wall polymers possibly linked with the evolution and development of secondary xylem (Kulkarni et al., 2012). These methyl groups are probably implicated in the cross-linking of cell wall components as it has been shown that their absence impacts the lignin composition, degree of lignification, and biomass recalcitrance (Urbanowicz et al., 2012).

Besides its backbone substitutions, GX of dicots features a unique tetrasaccharide sequence at the reducing end comprising Xylp-1,4-β-D-Xylp-1,3-α-L-Rhap-1,2-α-D-GalpA-1,4-D-Xyl. This sequence, known as "Sequence 1," is needed for xylan biosynthesis and might function either as a primer or a terminator (Peña et al., 2007). If acting as a primer, "Sequence 1" could initiate the polymerization process, and as a terminator, it might signal the end of the polymerization process, limiting the length of the glucuronoxylan chains (Peña et al., 2007; York and O'Neill, 2008; Urbanowicz et al., 2014).

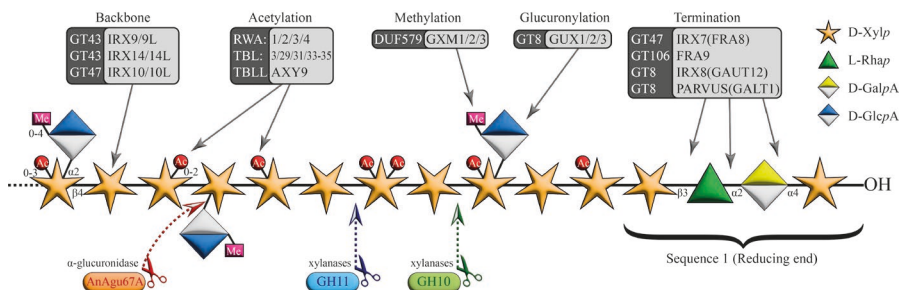


Figure 2. GX structure, biosynthetic genes, and sites of fungal enzymatic cleavages targeted in this work.

Biosynthesis of wood xylan

To generate a proper glucuronoxylan molecule, a plethora of enzymes need to act in concert (**Figure 2**). Originally described after their collapsed (irregular) xylem (*irx*) phenotype, xylan biosynthesis mutants also often show stunted growth and infertility, leading to the discovery of enzymes crucial for xylan backbone elongation, side-chain addition, reducing-end synthesis, and modifications like acetylation. Xylan biosynthetic enzymes

are directly or indirectly associated with the membrane of the Golgi apparatus, where GX is assembled before being transported to the cell wall. These enzymes, belonging to various Carbohydrate-Active enZyme (CAZy) families, form complexes within the Golgi, orchestrating the creation of this complex structure (Rennie and Scheller, 2014; Popa, 2017).

Backbone elongation requires at least three proteins, IRX9, IRX14 (GT43 family), and IRX10 (GT47 family), which form a xylan synthase complex (XSC) to elongate the backbone (Zeng et al., 2010). Only IRX10/10-L (also called XYLAN SYNTHASE 1) has been proven to exhibit β -1,4-xylosyl transferase activity to transfer xylosyl residues from UDP-xylose to the xylo-oligosaccharide when using 2-aminobenzamide β -1,4-xylohexaose (Xyl₆-2AB) as donor (Urbanowicz et al., 2014). Indeed, the role of IRX9 and IRX14 may not be catalytic but rather structural in facilitating IRX10/10L attachment to the membrane. The structure of XSC is still elusive, and more proteins could be involved. Growth impairments in *irx9* and *irx14* mutants were pronounced, suggesting that all proteins involved in the complex have importance regardless of their enzymatic activity (Brown et al., 2005, 2007; Peña et al., 2007; Chong et al., 2014; Zeng et al., 2016; Anders et al., 2023).

The acetylation of GX requires acetyl-CoA transporters from the family of reduced wall acetylation (RWA) (Lee et al., 2011, 2014; Manabe et al., 2011; Pawar et al., 2017), specific members of trichome birefringence-like (TBL) family (Gille et al., 2011) and a TBL-like protein ALTERED XYLOGLUCAN9 (AXY9) (Schultink et al., 2015). Among the 46 TBL members (in *Arabidopsis*), the extensively studied TBL29/ESK1 is capable of transferring the *O*-acetyl group to both the 2-*O* and 3-*O* positions of GX xylopyranose units and when mutated it confers freezing, drought and salt tolerance (Xin and Browse, 1998; Xin et al., 2007; Bischoff et al., 2010; Yuan et al., 2013; Ramírez et al., 2018; Ramírez and Pauly, 2019). However, the *esk1* mutation only partially reduced GX acetylation, with other TBL proteins having distinct roles in the acetylation of GX, such as TBL3 and TBL31 (Yuan et al., 2016). Acetyl-esterases have also been described within the family of GDSL esterases that probably remove some acetyl groups from GX in the Golgi (Zhang et al., 2017; Rastogi et al., 2022).

Glucuronidation of the GX involves three genes from the GT8 family: *GLUCURONIC ACID SUBSTITUTION OF XYLAN 1* (*GUX1*), *GUX2*, and *GUX3*. They all have distinct roles and give rise to the major or minor

domains of GX. GUX1 protein acts during SCW biosynthesis, decorating the xylan backbone (major domain) strictly evenly along with GUX2, creating odd patterns (minor domain) (Bromley et al., 2013). The GUX3 operates during PCW biosynthesis and generates an even pattern with slightly denser GlcA substitution than found in SCW (Mortimer et al., 2015).

The methylation of the glucuronic acid at position *O*-4 involves glucuronoxylan methyl transferase (GXM) proteins, which possess a DUF576 domain. The three described members, GXM1/2/3, are responsible for all methyl substitution in GX (Urbanowicz et al., 2012; Yuan et al., 2014b). The degree of methylation is altered in GX biosynthetic mutants, suggesting a possible fine-tuning of the methyl substitution (Urbanowicz et al., 2012).

Sequence 1 at the reducing end needs several enzymes of different families of glycosyltransferases for its synthesis (Figure 2): IRX7/FRA8 (Zhong et al., 2005), FRA9 (Zhong et al., 2023), IRX8/GAUT12 (Peña et al., 2007), and PARVUS/GATL1 (Lee et al., 2007). While still speculative (Rennie and Scheller, 2014), IRX8/GAUT12 emerges as a candidate for the galacturonic acid transferase due to its homology with GAUT1, while PARVUS/GATL1, located in the ER, might transfer the xylose to an unknown primer, possibly to a lipid (Sterling et al., 2006; Lee et al., 2007; Persson et al., 2007). IRX7/FRA8, an inverting enzyme, could function as a xylosyltransferase specific for the rhamnosyl end (Lee et al., 2009). The newly identified FRA9 protein from the family GT106 could participate in adding the rhamnose to GalA (Zhong et al., 2023).

After GX deposition to the cell wall, beta-xylosidases (GH5) and endo-xylanases/transglycosylases (GH10) have been reported to trim the GX backbone (Suzuki et al., 2002; Goujon et al., 2003) or transglycosylase GX chains (Derba-Maceluch et al., 2015).

The coordination among the different biosynthetic processes is necessary to make functional xylan. It is thought that cell can monitor these processes, among others *via* cell wall integrity (CWI) sensing, to ensure the required coordination.

1.2 Multi-level hierarchy of players in cell wall integrity maintenance

1.2.1 Stress molecules to be sensed

During plant development, but especially under stress, cell wall fragments can be generated as a result of cell wall damage. The cell perceives these molecules as a signal to initiate CWI maintenance program (Hamann, 2012; Wolf et al., 2012). Below, I will primarily explore "self" recognition patterns. For detailed insights into CWI's role in defense and priming following the detection of pathogen-associated molecular patterns (PAMPs), please refer to the comprehensive reviews by Swaminathan et al. (2022) and Hamann (2012).

Damage-Associated Molecular Patterns

Plants have evolved to recognize cell wall damage caused by pathogens, mechanical stress, or cell remodeling by identifying cell wall fragments as signaling molecules known as damage-associated molecular patterns (DAMPs) (Lotze et al., 2007; Zipfel, 2009). So far, signaling activities have been identified for the degradation products of pectins, cellulose, hemicelluloses, and β -1,3-glucan. Cellulose-derived DAMPs, such as cellobiose and cello-oligosaccharides, have been shown to establish pathogen-triggered immunity (PTI) in *Arabidopsis* (de Azevedo Souza et al., 2017). Pectins are targeted for enzymatic degradation by many pathogens, which produce oligogalacturonides (OGs) inducing PTI (Benedetti et al., 2015). Xyloglucan-derived oligosaccharides have been shown to regulate growth and immunity responses in *Arabidopsis* and *Vitis vinifera* (Claverie et al., 2018). Xylobiose (XB) induced ROS, PTI responses, changes in cell wall composition, and hormone signaling in *Arabidopsis* (Dewangan et al., 2023). Callose-derived oligosaccharides were shown to act as DAMPs, activating different immunity responses in both monocots and dicots (Wanke et al., 2020). In addition, DAMPs can also be released as a result of wounding activating immune defenses (Savatim et al., 2014; Melnyk et al., 2018; Pontiggia et al., 2020). In many cases, the structure of DAMPs, specified by the degree of polymerization, backbone identity, and side chain substitution pattern, has been identified as a signature for different stresses or development processes. The constant monitoring of these DAMPs by a complex multilevel perception system allows plants to coordinate important

physiological processes such as defense, growth, and development, all of which require a functional cell wall.

Small peptides

Secreted by the cell, rapid alkalization factors (RALFs) are key signaling molecules in the CW (Zhang et al., 2023). RALFs are 5-kDa cysteine-rich peptides inducing apoplastic alkalization and participating in CWI maintenance (Pearce et al., 2001). They interact with receptor-like kinases (RLKs) and initiate signal transduction pathways to modulate the activity of plasma membrane H^+ -ATPase, affecting pH, cell expansion, ion fluxes, cell wall mechanics, and plant defense (Blackburn et al., 2020). For instance, RALF23 was shown to interact with FERONIA (FER), a member of the *Catharanthus roseus* RLK1-like family (*CrRLK1Ls*) to regulate pollen tube development together with RALF4/19 that interacts with BUDDHA'S PAPER SEAL/ANXUR (BUPS/ANX) *CrRLK1Ls* receptor complex (Morato do Canto et al., 2014; Ge et al., 2017). Additionally, FER-RALF23 interaction enhances immune responses against pathogens, and FER-RALF1 participates in fine-tuning responses to stress and development (Stegmann et al., 2017; Wang et al., 2020). Another type of small peptide is plant elicitor peptides (AtPeps), which were shown to mediate the CWI and PTI responses (Bartels and Boller, 2015; Engelsdorf et al., 2018).

1.2.2 The perception of cell wall damage with membrane-bound proteins

Receptor-like kinases

RLKs, including lectin-RLKs, wall-associated kinases (WAKs), extensin-like kinases, proline-rich extensin-like receptor kinases (PERKs), and *CrRLK1L*, play a key role in ensuring CWI maintenance by sensing cell wall damage-associated molecules (Jose et al., 2020).

The first RLK essential for CWI response was THESEUS1 (THE1) from the *CrRLK1L* family, which functions as a CWI sensor upon cellulose synthesis perturbation (Hématy et al., 2007). All 17 *CrRLK1L* proteins of *Arabidopsis* are characterized by two malectin ectodomains and a Ser/Thr intracellular kinase domain (Franck et al., 2018). Several of them were reported to be involved in both developmental processes and defense responses against biotic and abiotic stress. Their ability to bind carbohydrates with their

malectin domain differs from that in animals; instead, they have a new potential ligand-binding site (Jeong et al., 2012). They can form complexes with co-receptors from LORELEI-like GPI-anchored protein (LLG) protein family when binding to RALFs, which can be associated with LEUCINE-RICH REPEAT EXTENSIN (LRXs) (Li et al., 2015; Zhao et al., 2021). RALF22 was shown to bind to the FER-LLG complex, which promoted LRX, HG, and RALF22 secretion, leading to the formation of a pectin complex involving acidic HG, LRX, and RALF22 that strengthened the growing root hair wall (Schoenaers et al., 2024). Additionally, FER was reported to bind pectin for mechano-perception and salt stress resistance in *Arabidopsis* (Shih et al., 2014; Feng et al., 2018; Dünser et al., 2019; Malivert et al., 2021). FER appears to function as a hub for signaling pathways active in both PTI and development, with its role modulated by interaction with RALF1/6/7/16/19/22/23/33/36/37 (Xie et al., 2022; Cheung, 2024; Schoenaers et al., 2024). THE1 was linked to cellulose biosynthesis defects (Hématy et al., 2007). It could coordinate changes in turgor pressure and cell wall stiffness via abscisic acid (ABA) (Bacete et al., 2022) as well as fine-tune lateral root initiation upon RALF34 binding by regulating cell division through Ca^{2+} and/or hormone signaling (Murphy et al., 2016; Gonneau et al., 2018). FER and ANX1/2, alongside BUPS1/2, are pivotal in sexual reproduction and pollen tube growth by mediating ROS and Ca^{2+} signaling (Boisson-Dernier et al., 2009; Ge et al., 2017). *CrRLK1L* HERKULES1 was shown to participate in pollen tube elongation interacting with brassinosteroid signaling pathway and in salt response together with THE1, attenuating its effect (Guo et al., 2009; Gigli-Bisceglia et al., 2022). Additionally, *CrRLK1L* proteins are engaged in immune responses. For example, FER was shown to enhance PTI and ANX1 to modulate it (Keinath et al., 2010; Mang et al., 2017; Stegmann et al., 2017).

WAKs (26 members in *Arabidopsis*) are known to bind HG (Park et al., 2001; Kanneganti and Gupta, 2008). They have two types of epidermal growth factor (EGF) ectodomains with different abilities to bind calcium, which could be involved in protein-protein interactions with glycine-rich proteins. However, their pectin and OG binding function is not dependent on these domains, even if they help the binding (Decreux et al., 2006; Kohorn et al., 2009; Brutus et al., 2010). WAKs are known to phosphorylate proteins (such as brassinosteroid receptor) and to play a role in immunity, abiotic

stress, and during development (Anderson et al., 2001; Verica and He, 2002; Yue et al., 2022).

Some types of extensins (see “*structural proteins*”) possess a kinase domain and participate in CWD sensing in association with RALFs and CrRLK1Ls. The LRX1 kinase uniquely merges features from LRR and extensins (Baumberger et al., 2001). Similarly, PERKs interact with pectins, aiding in repair and maintaining integrity after cell wall damage (Borassi et al., 2016).

Ion channels

Ion channels and mechanosensitive proteins participate in CWI maintenance either at the signal sensing or integration level (Bacete and Hamann, 2020b). Among these, calcium channels such as MID1-COMPLEMENTING ACTIVITY (MCA) detect plasma membrane stress and impact calcium influx, an essential ion for the plant's response to cell wall damage (Nakagawa et al., 2007; Kamano et al., 2015). Considered mechano-sensing, MCA1 operates downstream of THE1 and increases calcium flow under cell swelling in hypo-osmotic conditions (Engelsdorf et al., 2018). The mechanosensitive channels of small conductance-like (MSLs), for example, MSL10, have been inferred to transduce turgor pressure signal through cytoplasmic Ca²⁺ transient, leading to accumulation of ROS, mechano-inducible gene expression, and programmed cell death (Basu and Haswell, 2020). DEFECTIVE KERNEL 1 (DEK1) is a mechanosensitive channel belonging to the calpain superfamily, which is also involved in calcium-mediated signaling (Amanda et al., 2016) and could also be involved in CWI stress. Additionally, REDUCED HYPEROSMOLALITY-INDUCED [Ca²⁺] INCREASE proteins (OSCs) (Yuan et al., 2014a) and CYCLIC NUCLEOTIDE GATED CHANNELS (CNGCs) could be regulated by ANX1 CrRLK1L signaling module (Boisson-Dernier et al., 2013; Tunc-Ozdemir et al., 2013; Shih et al., 2015). Moreover, GLUTAMATE RECEPTORS (GLRs) (Toyota et al., 2018) are responsive to hyperosmotic stress and wounding and, therefore, could also be contributing to CWI perception (Vaahtera et al., 2019). These different ion channels can help integrate mechanical signals with chemical cues and thus participate in CWI maintenance.

1.2.3 Cell wall damage signal integration and downstream signalization

Recognition of DAMPs by RLKs activates their kinase domain, which initiates specific complex downstream signaling cascade, including Rho-GTPase activation, proton pump regulation, Ca^{2+} signaling via MLO proteins, and transcriptional regulation (Swaminathan et al., 2022). Overlapping signaling cascades between various biological processes, such as abiotic and biotic stresses and CWI maintenance, makes the characterization of CWI downstream players difficult. Downstream signaling for all these processes involves calcium-dependent protein kinases (CDPKs), guanosine nucleotide exchange factors (GEFs), and mitogen-activated protein kinases (MAPKs), which eventually activate transcription factors, and downstream defense genes, including those involved in the production of anti-microbial secondary metabolites. This activation is part of an interconnected defense strategy that includes maintaining CWI and initiating pattern-triggered immunity that can act in concert or independently. NADPH oxidases increase ROS production, both as signaling molecules to propagate defense signals and directly contribute to cell wall structure through protein cross-linking and lignin polymerization. DAMPs-RLK interactions may directly or indirectly modulate cytosolic calcium levels (Knogge et al., 2009; Seybold et al., 2014). Calcium ions act as secondary messengers in signal transduction. Their extracellular concentration influences pectin cross-linking and enzyme activity and regulates the activity of different ion channels, which is critical for activating defense mechanisms under CWI stress.

Furthermore, CWI signal transduction by either RLKs or ion channels, for instance, stimulates stress-phytohormone synthesis, such as salicylic acid (SA) and jasmonic acid (JA), and stress-related processes of callose deposition and lignin synthesis, strengthening the cell wall and sealing off damaged areas, restoring integrity (Heil and Land, 2014; Gigli-Bisceglia and Testerink, 2021). These responses involve specific transcription factors, inducing downstream genes involved in stress response, cell wall modification, and hormone-regulated processes. For example, FER can regulate immunity upon RALF23 binding through MYC2 transcription factor and JA (Guo et al., 2018). Furthermore, FER regulates ABA signaling

through RALF23 binding, activating ABSCISIC ACID-INSENSITIVE 2 (ABI2) phosphatase, which in turn activates many genes, including transcription factors (Fujii et al., 2009; Yu et al., 2012). This signal integration and downstream signaling network highlights the plant's capability to perceive and respond effectively to cell wall damage, coordinating diverse responses to maintain cell wall integrity through development and to cope with adverse conditions (**Figure 3**).

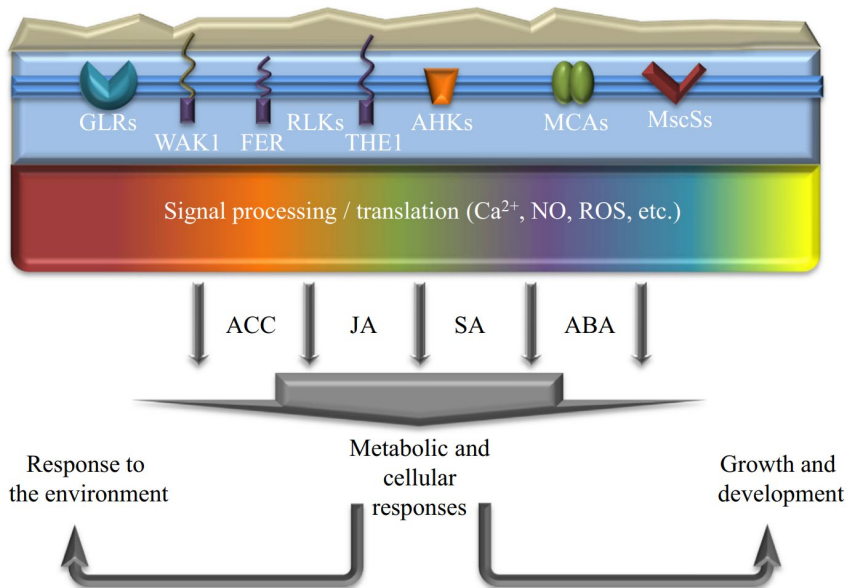


Figure 3 Overview of sensing and signaling molecules involved in cell wall integrity (from Hamann 2015)

1.3 CWI integrity sensing during SCW formation.

Given the complexity inherent in the numerous biological processes involved, studying CWI in the expanding primary cell wall presents considerable challenges. Venturing into exploring secondary cell wall integrity (SCWI) maintenance can thus be regarded as a pioneering effort. Despite technological advances (such as the sequencing of tree genomes, single-cell transcriptomics of developing wood, or advanced microscopy

methods) potentially helping to understand the SCWI, the existence of a dedicated SCWI maintenance system remains elusive. This is because several challenges hinder it:

- 1) Distinguishing SCWI from primary CWI maintenance mechanisms might be difficult, especially in *Arabidopsis*;
- 2) Given that many cells undergo programmed cell death following SCW development, CW rearrangements as a result of SCWI signaling are believed to be less likely;
- 3) Wood formation and SCWI have been studied in *Arabidopsis*, but these processes are not biologically as important for *Arabidopsis* as they are for tree species;
- 4) The narrow timeframe for observing plant responses to SCW defects, from sensing cues to wall maintenance, limits the opportunity to study signaling pathways effectively.

Nevertheless, several studies have provided important insights into the field. The study of Hernández-Blanco et al. (2007) revealed that mutations in SCW-specific cellulose biosynthetic genes (CESA4/IRX5, CESA7/IRX3, and CESA8/IRX1) required for *Arabidopsis* SCW integrity enhanced resistance to fungal and bacterial pathogens. Crossing *irx1*, *irx3*, and *irx5* mutants with mutants in different hormones sensing and biosynthesis-responsible genes, they found that the induced resistance was independent of traditional defense signaling pathways (SA, ET, JA) but instead involved ABA signaling. This ABA signaling suppressed ET/JA-mediated responses and activated biotic defenses. The authors suggested a novel signaling pathway whereby alterations in SCWI activate defenses to pathogens.

Liu et al. (2023) investigated the role of FER and WAKs in sensing and responding to hypolignification in the *ccr1* mutant. They investigated if FER could detect hypolignification via OG sensing since the mutation induced *ARABIDOPSIS* DEHISCENCE ZONE POLYGALACTURONASE 1 (ADGP1) (Gallego-Giraldo et al., 2020). They found that FER was needed to induce ADGP1 and other pectin-modifying enzymes, which were degrading pectin and releasing elicitors (such as GalA₃) that were then sensed by WAKs, transducing the signal and triggering defense response such as PR1 expression (Liu et al., 2023). This research shows that plants have signaling systems triggered by modifications in the SCW.

Ramírez et al. (2018 and 2019) identified *MORE AXILLARY BRANCHES 3* and 4 (*MAX3/4*) as essential genes for the development of *irregular xylem* phenotype and freezing resistance in *tbl29/esk1* mutant with highly reduced GX acetylation. *MAX3/4* are carotenoid cleavage dioxygenases generating carlactone from β -carotene, a precursor to active strigolactones (SL). As other genes acting downstream *MAX3/4* in the biosynthesis of SL or their perception failed to complement *tbl29/esk1* phenotypes, this indicated that the reduced GX acetylation in SCW induces *irregular xylem* phenotype and freezing resistance using not a classical SL signaling but the carlactone activation of unknown downstream signaling responses. Moreover, *max4* partially complemented defects of other SCW mutants but not those of PCW mutants, suggesting that regulation by carlactone could be specific to SCW development.

Potential DAMP signaling from SCW was discovered by Zhao et al. (2013), who studied plasma membrane-bound endo-beta-mannanase *PtrMAN6* in *Populus*. This enzyme suppressed secondary cell wall formation and lignification *via* releasing galactoglucomannan oligosaccharides (GGMOs). Activity of GGMOs was also demonstrated in *Zinnia* xylogenic cultures where their addition induced tracheary element differentiation into metaxylem rather than into protoxylem as well as increased cell population density (Beňová-Kákošová et al., 2006).

While reduced growth is generally observed when altering SCW formation in *Arabidopsis* and transcriptome analyses in these mutants did not reveal changes in CWI-related genes such as members of the *CrRLK1L* family (Faria-Blanc et al., 2018), similar analyses in aspen trees suggested the existence of novel non-cell-autonomous signaling originating from the altered SCW which could stimulate cambial growth while reducing the SCW biosynthesis (Ratke et al., 2018). Transcriptomic analysis in aspen trees having SCW-specific downregulation of GT43 genes involved in xylan backbone biosynthesis revealed that genes associated with cambial cell division were upregulated, while those involved in SCW biosynthesis and programmed cell death were downregulated. Moreover, many signaling genes were also differentially expressed. Increased cambial growth and overall tree growth have been also observed when suppressing SCW trans-xylanase *PtxtXyn10A* in aspen (Derba-Maceluch et al., 2015). These papers collectively suggest the uniqueness of SCWI maintenance mechanisms.

1.4 Importance of CWI for engineering plant cell walls

Plant cell walls (as wood) have served to create tools and energy since the dawn of humankind. Our history is intricately linked to this natural product, and scientific progress has permitted us to broaden the myriad of uses of wood. On the one hand, elaborating new biomaterials elicits the need to better understand the cell wall by challenging its structure and isolating its components. This is depicted by the usage of lignin, hemicellulose, or cellulose for industry (Kai et al., 2016; Rinaldi et al., 2016; Trache et al., 2020; Xu et al., 2023) and by using lignocellulosic biomass both for saccharification to produce 2nd generation of biofuels (Nieminen et al., 2012; Marriott et al., 2016; Smith et al., 2017; Donev et al., 2018; Oliveira et al., 2019). On the other hand, the knowledge of the cell wall as a signaling hub integrating various stresses and developmental adjustments opens new routes to develop crops and forests more resilient to the increasing climatic challenges (Novaković et al., 2018; Wolf, 2022). With the SCW representing a considerable carbon sink after being deposited, a better understanding of the complexity of its regulation and, in particular, of the dynamic adjustment of this regulation to different cues could open major levers to increase the deployment of this widely available and sustainable resource (Xia et al., 2017). Lacking this essential insight, attempts to modify the cell wall could encounter unforeseen difficulties, as the plant compensatory mechanisms would mitigate the modification via the maintenance of its CW integrity (Yoshida et al., 2021) or could compromise plant defense mechanisms. The acquired knowledge could also permit the elaboration of new agricultural applications, such as priming, which is especially needed in preparation for increasing adversary climate conditions and water scarcity (Swaminathan et al., 2022).

2. Hypotheses and Objectives

The general objective of this research was to shed light on and describe the diversity of plant responses to secondary cell wall impairment, focusing on the effect of altered xylan integrity. Xylan impairment can induce both direct effects on cell wall architecture and indirect effects resulting from cell wall integrity sensing. Here, “direct effects” refer to immediate changes in the secondary cell wall’s physical and chemical properties, such as alterations in xylan content and structure. In contrast, “indirect effects” encompass broader physiological and biochemical responses, including adjustments in growth patterns, signaling pathways, gene transcription, and overall cell wall composition triggered by the xylan impairment. We aimed to elucidate these responses in cases of xylan backbone shortening and glucuronic acid side chain removal. Moreover, since the cell wall integrity signaling pathways overlap with general stress response pathways, we investigated if xylan-impaired plants have modified drought responses. These hypotheses were addressed in five papers using *Arabidopsis* and hybrid aspen models. Each paper of this Ph.D. thesis addressed specific questions detailed below:

- ✓ What malectin domain-containing proteins in *Populus* are expressed during secondary wall biosynthesis and thus could potentially be involved in secondary wall integrity sensing? (**Paper I**)
- ✓ What are the molecular and hormonal players that participate in the response to mechanical signals in cells depositing secondary cell walls in the developing wood of aspen? (**Paper II**)
- ✓ What is the response of aspen and *Arabidopsis* to the removal of glucuronic acid (GlcA) xylan decorations from xylan? (**Paper III**)
- ✓ What are the responses of aspen and *Arabidopsis* to the xylan backbone impaired induced by expressing fungal xylanases in secondary walls? (**Papers IV and V**)
- ✓ Do modifications in the xylan backbone in *Arabidopsis* and aspen impact their drought responses, as evidenced by their physiological parameters and growth? (**Paper V**)

3. Results and Discussion

3.1 Identifying potential molecular players involved in secondary wall integrity sensing/signal transduction.

3.1.1 Genome-wide analysis of malectin domain proteins in *Populus* and *Arabidopsis* reveals candidates for SCWI maintenance (**Paper I**).

MD/MLD proteins of *P. trichocarpa* and *Arabidopsis*

Malectin domain (MD) is an extracellular lectin-like motif composed of four antiparallel β -strands, capable of recognizing carbohydrates (CBM57 in CAZy), widespread in prokaryotes and eukaryotes, but especially prevalent in plants (Schallus et al., 2008; Yang et al., 2021). MD serves crucial sensing roles for RLK during cell wall integrity maintenance, defense, and development (Doblas et al., 2018; Franck et al., 2018). Malectin-like domain (MLD) possesses two MDs that form an 85° angle with a connecting β hairpin linker, creating a 30 Å cleft (Moussu et al., 2018). Despite structural similarities to animal MDs shown to bind maltose (Schallus et al., 2008), plant MLDs lack key carbohydrate-binding residues, indicating a divergence in their carbohydrate-binding properties. The investigation of proteins possessing such domains in *Populus* sets the stage for further groundwork to establish the concept of primary and secondary cell wall integrity maintenance in tree species.

First, genome-wide analysis of genes with predicted MD and MLD in *P. trichocarpa* and *Arabidopsis* and their phylogenetic analysis resulted in the identification of 14 clades (**Paper I, Fig. 1, 2**). Certain clades appeared to be unique to *P. trichocarpa* or significantly expanded, suggesting specialized roles potentially related to tree-type lifestyle (wood formation, perennial habit, or extensive defense mechanisms). Altogether, 146 malectin/malectin-like domain-containing proteins were identified in *P. trichocarpa* and 87 in *Arabidopsis*, expanding upon previous studies in strawberry or rice (Zhang et al., 2016; Jing et al., 2020).

Different domain structures and diversification of MD/MLD proteins in *P. trichocarpa* and *Arabidopsis*

Most of the identified proteins had a classical domain structure for RLKs with a MD or MLD extracellular domain that can be accompanied by LRR domains, followed by a transmembrane domain and an intracellular kinase domain (**Paper I, Fig. 1**). This “classical” model allows these proteins to sense cues by binding cell wall polysaccharides or their fragments (DAMPs) or associate with other components such as RALFs (Haruta et al., 2014) or LLG (Li et al., 2015) among others in the apoplastic space and transduce the signal by phosphorylation through their kinase domain. However, few of these proteins did not possess a transmembrane domain (13%), and this feature was typically observed in clade XIV. This clade presents unique domains such as coiled-coil and kinesin domains instead of the classical kinase domain, which was not previously included in *Arabidopsis* or the rice MD family. All three proteins of this clade are predicted to be cytoplasmic (**Paper I, Table. S1**), which, together with their unusual domain structure, points to potential novel functions of this clade. Clade XIII represents proteins without an intracellular domain, some of which did not even possess a transmembrane domain either (*Pt*MDs 136-140) and are predicted to be extracellular (**Paper I, Table. S1**). It is noteworthy to mention that in clades IX to XI, which have MLDs, LRR domains are located after the MLD and before the transmembrane domain. In contrast, within clades I-VII having MDs, LRR domains are located before the malectin domain, followed by the transmembrane domain. This might impact how these proteins can interact with other proteins with their LRR and/or malectin domains. Finally, clade XII, with 42 members in *P. trichocarpa* but only 17 in *Arabidopsis*, indicating great expansion of this clade in *Populus*, grouped proteins known as *Cr*RLK1L (Schulze-Muth et al., 1996). They exhibited an MLD, a transmembrane, and a kinase domain but no LRR domain.

Chromosomal mapping of the *MD/MLD* genes in *P. trichocarpa* revealed many clusters indicative of the family expansion by local gene duplication (**Paper I, Fig. 4**). Exon-intron structure analysis indicates a clear difference between *Cr*RLK1L and other clades supporting the diverse evolutionary history of these genes and their classification (**Paper I, Fig. 3**). Assuming *Cr*RLK1L function in CWI maintenance, it appears that *P. trichocarpa* has developed a robust arsenal for monitoring its CWI (**Paper I, Fig. 2**).

Expression analyses of MD/MLD proteins in aspen identified potential candidates for SCWI maintenance

The expression analysis of *PtMD/MLD* genes in different organs and tissues of aspen and hybrid aspen revealed an important expression in leaves, especially in mature ones and subjected to different abiotic stresses, with several genes also highly expressed in cambial or developing xylem tissues (**Paper I, Fig. 5, 6**). This suggests the roles of *PtMD/MLD* genes in many aspects of tree physiology, including foliar defenses and development and wood biosynthesis. To further investigate the suggested role of *PtMD/MLD* during wood formation, the AspWood database with high spatial resolution of wood developmental zones was used. We found that 89 *PtMD/MLD* genes (61%) were active in secondary vascular tissues, with expression patterns clustering into ten groups indicative of their specific functions at various stages of wood development (**Paper I, Fig. 7**). Many of these genes were peaking in the phloem, and many clades were overrepresented at specific developmental stages. Notably, the genes most expressed during the transition from primary to secondary wall, SCW deposition, and maturation were predominantly from the clade XII (*CrRLKIL* genes). Their distinct expression patterns suggested specialized functions in secondary cell wall development and wood maturation. Among other clades active during wood formation, clade I genes were expressed during secondary cell wall development, clades V and VII genes - during wood maturation, and clades II, VI, VIII, and XIII genes were active at various stages, including the transition between PCW and SCW. Intriguingly, among the 12 *Populus* genes of clade IX, which was expanded in *Arabidopsis*, none was expressed at any stage of vascular development. In contrast, the clades that included predominantly or exclusively *Populus* genes (I, VI, and VII) exhibited significant expression in wood developmental zones where secondary cell wall integrity may be sensed.

Co-expression networks were analyzed to identify putative partners of *PtMD/MLD* proteins active during xylogenesis, focusing on genes expressed during secondary wall formation. The co-expression networks of these genes included genes with known functions in CWI (*RALFL31*), defense against the pathogen (*PUB13*), calcium signaling (*CSCI*), ROS regulation (*PBL19*), and hormonal signaling pathways (*BIMI*, *TPD1*, *LAX3*, *GASA4*) (**Paper I, Fig. 8**).

In conclusion, this study provided a foundation for the characterization of the SCWI by analyzing the MD/MLD protein family in *Populus* and their expression during plant development, stress responses, and wood formation.

3.1.2 Secondary wall sensing and signaling during flexure wood formation in aspen highlights possible elements participating in SCWI maintenance related to mechanoperception (**Paper II**)

Stem flexing in a woody species altered the SCW formation program

To perceive and respond to environmental cues such as wind or mechanical disturbances, plants have developed adaptative strategies to detect these cues and react. One of the well-described reactions to stem bending is the formation of flexure wood, generally followed by physiological changes such as altered growth (Roignant et al., 2018). As the mechanism of mechanoperception and the subsequent molecular events that occur due to stem bending in trees are still elusive, we investigated hormonal and transcriptomic alterations induced by stem flexing in aspen.

The regular stem flexing was beneficial for aspen tree growth. Upon flexure, the stem heights and diameters were 10% larger, and the trees produced significantly more biomass and bigger leaves (**Paper II, Fig. 1**). In parallel, improved saccharification efficiency of untreated wood biomass was recorded (**Paper II, Fig. 4**). This highlights the potential of using mechanical cues to optimize bioenergy crops. However, it is crucial to understand how mechanical stimuli lead to these responses and to test several parameters of mechanostimulation as the nature, force, and frequency of the stress are known to affect its potential beneficial effects on plants (Puijalon et al., 2011; Kouhen et al., 2023).

The faster growth and improved saccharification yield were associated with the development of flexure wood. The observed increase in stem diameter resulted primarily from the increased meristematic activity, which was accompanied by the downregulation of the negative regulator of cell cycle *SKP2B* and upregulation of cyclin *CYCP3;2* (**Paper II, Fig. 2 and Table 3**). Moreover, the wood cells of trees subjected to flexing developed G-layers, leading to increased wood density and reduced fibers SCW thickness both in normal and tension wood. The fiber diameter was unaltered, and the microfibril angle was decreased due to flexing. The alteration of the chemical composition of the wood in flexed trees was observed (**Paper II, Fig. 3**):

they had higher G- and H-lignin levels and lower S/G ratio without a change in total carbohydrates to lignin ratio. Sugar analysis revealed a shift in matrix polysaccharide composition, with decreases in Ara, Xyl, and GlcA but increases in Gal, Glc, and Man. Additionally, a 16% rise in crystalline cellulose and 24% greater cell wall nanoporosity indicated significant structural changes.

Flexure-induced increases in aspen growth and saccharification efficiency underscore the value of mechanical cues in bioenergy optimization, emphasizing the need for deeper molecular understanding for application across species.

Hormonal and transcriptomic changes highlight key candidates potentially involved in secondary cell wall integrity maintenance

Mechanoperception and CWI maintenance mechanisms are interconnected (Bacete and Hamann, 2020b). Yet little is known about how the secondary cell wall maintains its integrity; thus, studying the impact of mechanical cues in trees offers a valuable approach to investigating potential molecular players participating in the response to mechanical stress in the secondary cell wall. Indeed, the development of flexure wood in response to stem flexing was accompanied by hormonal and transcriptomic changes in the cambium and the secondary wall-forming xylem cells. Major changes in different precursors of hormones, their active and deactivated forms were observed in both tissues (**Paper II, Fig. 5**). The most striking response was an increase in JA content in both tissues and an increase in JA-Ile, an active form, in the cambium. In contrast, the content of JA precursor (*cis*OPDA) was reduced in both tissues, suggesting its conversion upon stem flexing to JA and active forms. Early precursors of polyamines (PAs) were found to be downregulated, and their active forms were upregulated in the xylem. While JA is known to be induced after touching *Arabidopsis* leaves (Chehab et al., 2009, 2012; Wang et al., 2024) and could contribute to increased primary xylem production in the roots (Jang et al., 2017, 2019; Jang and Choi, 2018), PAs have so far only been reported to increase after sound treatment in cabbage (Qin et al., 2003). Among other hormones and precursors measured, only some forms of cytokinins were upregulated in the xylem, while ABA, salicylic acid, ethylene, and auxin were downregulated in both tissues, highlighting a complex hormonal interplay at work during flexure wood formation.

Transcriptomic analyses provided further insight into stem flexing response, identifying 167 and 219 DEGs in the cambium and developing xylem, respectively, due to flexure, with 27 genes affected in both tissues (**Paper II, Fig. 6**). These included the genes directly involved in thigmomorphogenesis, genes associated with structural modifications of the wood, and new potential regulators of flexure wood formation. Jasmonate conversion to JA-Ile could have been reduced in the xylem because *JAR1* was downregulated. Surprisingly, no other JA-related genes were detected. Their transcriptomics response could have been dampened after many repetitive mechanical stimulations because plants adapt their sensitivity to avoid overreacting to frequent, non-threatening environmental changes. This desensitization, known as accommodation, helps conserve energy for growth and reduces unnecessary activation of stress responses, ensuring more efficient resource allocation and longer-term survival (Leblanc-Fournier et al., 2014). Upregulation of PAs biosynthetic genes supports their function in flexure wood formation. Other transcriptomic changes emphasized the important roles of ABA, ethylene, cytokinins, and auxin for flexure response. Also, gibberellins and brassinosteroids could be implicated in flexure wood formation as the related transcripts were upregulated in the xylem. The hormonal orchestration in flexed trees hints at a complex regulatory system operating during secondary cell wall development.

We also found that transcriptomic responses of flexure wood and tension wood were similar and distinct from those of opposite wood. About 40% of genes affected by flexure aligned with those differentially regulated between tension and opposite wood induced by gravitational stress (Zinkgraf et al., 2018), with 97% reacting the same way as in tension wood. Notably, 60% of genes, including key regulators *KNAT3* and *MYB52*, were affected only by flexure and not gravity, indicating their potential role in adapting to mechanical stress and affecting secondary cell wall properties. Genes affected in common between tension wood and flexure wood were related to cell wall organization and biosynthesis, such as primary wall cellulose synthases (*CesA*), fasciclin-like arabinogalactan proteins (*FLA11/FLA12*) important for G-layer biosynthesis (Andersson-Gunnerås et al., 2006; Bygdell et al., 2017; Ma et al., 2022) and xylan O-acetyltransferases. Among the upregulated genes, members of the xyloglucan transglycosidases/hydrolases (*XTH*) family, which is known to participate in touch response in *Arabidopsis* (Lee et al., 2005) and to link the plasma

membrane to the cell wall (Zhu et al., 2014) could be important candidates for the sensing of mechanostimuli. Their enzymatic activity is to cleave, and re-join xyloglucan and two members of this family were shown to affect secondary cell wall formation and expression of *THE1* and *WAK2* (Thompson and Fry, 2001; Kushwah et al., 2020). Many other cell wall-related genes, such as genes encoding pectin acetyl- and methylesterases, laccases, and class III peroxidases, were also differentially expressed in either the xylem or cambium of flexed trees. This indicates that flexure modified the cell wall biosynthetic program by activating lignification, altering pectin and xylan composition, and promoting cellulose biosynthesis.

Finally, the flexure-induced co-expression network defined gene clusters, influencing wood development under mechanical stress pinpointing specific genes and pathways altered in response to flexure (**Paper II, Fig. 6**). Particularly, Xylem cluster 1 included upregulated genes with important roles in secondary wall formation including zinc finger transcription factor proteins. Furthermore, the identification of genes related to lignin polymerization and cell wall modification provided insights into the genetic mechanisms that underpin the development of flexure wood.

In conclusion, this research identified potential key players maintaining secondary cell wall integrity in response to mechanical stress in hybrid aspen. Moreover, these insights not only improved our understanding of plant adaptability but also hold promising implications for optimizing bioenergy crops and enhancing wood quality by manipulating signaling pathways related to stress response and growth regulation.

3.2 Xylan glucuronic acid side chains provide anchoring for suberin-like aliphatics in secondary cell walls (**Paper III**)

Xylan MeGlcA reduction does not significantly impact plant growth, wood composition, or saccharification

Wood properties are significantly shaped by interactions among lignin, cellulose, and hemicellulose (Terashima et al., 2009; Lyczakowski et al., 2019; Addison et al., 2020). In the SCW of dicots, glucuronoxylan interacts with lignin and cellulose, which is affected by its decorations, such as methyl glucuronic acid side chains (Busse-Wicher et al., 2014, 2016; Grantham et al., 2017). Studies with *Arabidopsis* mutants of *GlcA Substitution of Xylan*

(*gux1-gux5*) belonging to CAZy Glycosyltransferase family 8 (GT8), responsible for adding GlcA side chains to xylan backbone, show that alterations in xylan glucuronosylation might impact plant growth under specific conditions. When *GUX1* and/or *GUX2* are mutated, xylan extractability and saccharification yields are increased, and interactions between cellulose and xylan are altered, as revealed by NMR (Mortimer et al. 2010; 2015; Lee et al. 2012; 2014; Rennie et al. 2012; Bromley et al. 2013; Lyczakowski et al. 2017; Grantham et al. 2017). However, cell wall and lignocellulose characteristics in *gux1gux2* mutants are likely altered by more than just changes in MeGlcA substitution, as exemplified by increased acetylation and xylan content in the cell wall (Chong et al., 2014; Lee et al., 2014). Post-synthetic MeGlcA removal from the xylan deposited to cell walls can provide a more direct tool to dissect the role of MeGlcA decorations.

To selectively reduce xylan glucuronosylation after xylan deposition into the apoplast in *Arabidopsis* and hybrid aspen, we employed *AnAgu67A*, an *Aspergillus niger* α -glucuronidase from family GH67, hydrolyzing MeGlcA decoration at the terminal nonreducing end of the xylan. The fungal enzyme was targeted to the apoplast by a plant signal peptide, and the apoplastic targeting of the recombinant protein was experimentally verified.

Expressing *AnAgu67A* in hybrid aspen did not notably affect aspen growth, wood composition, or saccharification (**Paper III, Fig. 1, S2**). Although α -glucuronidase activity was confirmed in transgenic lines, reducing MeGlcA content by 20-30% did not significantly change wood polysaccharides or lignin compared to WT. The only observed effect was a slight decrease in stem height, with no major alterations in growth or wood anatomy (**Paper III, Fig. S3**). Moreover, the α -glucuronidase did not affect the γ -ester linkage between xylan and lignin (**Paper III, Fig. S4**). This suggests that the formation of γ -ester linkages between xylan and lignin occurs intracellularly prior to their integration into the cell wall. This point is of key importance for our understanding of secondary cell wall biosynthesis and LCC assembly.

Enhanced extractability of aliphatic compounds in sapwood by *AnAgu67a* α -glucuronidase: Lipids in the wood are connected to xylan

Expression of *AnAgu67A* α -glucuronidase in transgenic aspen significantly reduced the content of bound (extraction-resistant) aliphatic compounds, such as fatty acids, triacylglycerols and diacylglycerols in dioxane-lignin, as

revealed by 2D HSQC NMR analysis making them more extractable (**Paper III, Fig. 2, S4, S5**). In contrast, the content of all (soluble and insoluble) lipids in the wood was unaltered. In agreement there was no change in expression of genes responsible for lipid biosynthesis, whereas the lipidomic analysis of extracted lipids revealed increased presence of mono- and oligomeric suberin components in transgenic lines (**Paper III, Fig. S2, S3**). This suggests that MeGlcA xylan substituent affects the extractability of suberin-like aliphatic compounds without altering their total presence in the wood.

In parallel, the reduced presence of solvent-resistant aliphatic compounds in sapwood cell walls of transgenic lines expressing α -glucuronidase was shown by diminished Fluorol Yellow 088 staining after removal of soluble extractives (**Paper III, Fig. 3**). This effect was verified for both hybrid aspen and *Arabidopsis* where similar reductions of solvent-resistant lipids were observed. Moreover, a similar effect was observed in the *gux1gux2 Arabidopsis* mutant. These observations indicate a role for xylan MeGlcA substitutions in anchoring suberin-like lipids to the cell wall, though the exact mechanism remains unclear. Further research is needed to determine whether these substitutions directly interact with lipids or if they participate in more complex interactions within the cell wall matrix that influence lipid localization and extractability.

Aliphatic, solvent-resistant compounds were detected using FY088 staining in the wood cell walls of different woody species, including softwoods like Norway spruce and Scots pine and hardwoods such as downy birch, goat willow, and European aspen (**Paper III, Fig 5**). The persistence of staining in solvent-extracted samples suggests that they are linked to cell wall polymers. This finding challenges the traditional view where lipids have been thought to be only found in decayed wood but not healthy wood. Semi-quantitative staining intensity analysis showed that hardwoods generally exhibited stronger signals than softwoods, which might reflect variations in the composition or abundance of aliphatic compounds, suggesting species-specific differences in how these lipids are integrated or masked by other extractives. The difference in the presence of solvent-resistant lipids in cell walls between these groups could also be related to a lower xylan content in softwood compared to hardwood. In addition, the distribution of these lipids across different wood cell wall layers, uniformly present in spruce and pine but primarily found in lignified cell walls and absent from nonlignified

gelatinous layers in hardwoods, suggests their association with lignin and/or xylan. This distribution pattern indicates that the incorporation of lipids into cell walls is not random but is governed by specific biochemical processes that link these lipids directly to the structural polymers of the cell wall.

In conclusion, as Dr. Oliveira titled his commentary on this paper “Glucuronic acid: not just another brick in the cell wall,” we found a novel role of xylan MeGlcA in the wood in fastening suberin-like compounds to the cell wall. We also demonstrated the presence of aliphatic compounds in healthy wood and provided indirect evidence for intracellular γ -ester linkage formation between xylan and lignin. Reduction in wall-bound lipids in plants with reduced GlcA substitution of xylan is likely a direct consequence of reduced MeGlcA content without necessarily involving a secondary cell wall integrity signaling system.

3.3 Exploring the direct and indirect effects of xylan impairment in *Arabidopsis* and aspen: glucuronoxylan backbone in pieces (**Papers IV and V**)

The following two studies (**Paper IV and V**) explore plant responses to xylan backbone modification. While the first study focused on hybrid aspen, the second examined *Arabidopsis* and aspen models under drought conditions. These investigations aimed to understand plant responses to modifications in the xylan backbone caused by GH10 and GH11 xylanases targeted to secondary walls and to knocking out/down xylan backbone biosynthetic genes. Additionally, we broadened our understanding of the impacts of these xylan modifications by examining how they have contributed to drought tolerance that could reveal cell wall integrity sensing mechanisms during secondary cell wall development. These studies are multifaceted and afford four main comparisons:

- ***Arabidopsis* and aspen (Paper IV and V):** Both angiosperm eudicot models have much in common, but for aspen, as a perennial tree species, the tight control of SCW development and the maintenance of its integrity might be more prominent. It is also conceivable that conserved genetic programs that could monitor the SCW integrity exist in *Arabidopsis* and aspen, while drought stress coping mechanisms could be drastically different.

- **Targeting the SCW before or after its deposition (Paper V):** Employing fungal xylanase directed to the secondary cell wall during its development thanks to the hybrid aspen signal peptide from gene *PtxtCel9B3* and the promotor from *PtxtGT43B* gene (Ratke et al., 2015), let us disrupt xylan backbone without additional adjustments form the biosynthetic machinery whereas altering biosynthetic genes like *irx9*, *irx10*, and *irx14* could induce some compensatory changes due to metabolic imbalances. Furthermore, comparing the effects of xylanases expressed ubiquitously with those expressed under a wood-specific promoter could help identify changes specific to secondary cell wall damage.
- **Types of xylanases and xylan biosynthetic genes employed (Paper IV and V):** GH10 and GH11 xylanases share the enzymatic activity of cleaving glycosidic bonds in the xylan backbone. A small difference in their activity exists: GH11 is unable to act on the backbone if (Me)GlcA substitutions are present on the +1 subsite and is more affected by the presence of acetylation (Biely et al., 1997; Pell et al., 2004; Kolenová et al., 2006; Vardakou et al., 2008; Kojima et al., 2022). Thus, some differences in the profile of xylo-oligosaccharides between these two enzymes are predicted. Moreover, comparing the impact of different *irx* mutants on plant development could help to deepen the knowledge about their specific roles and offer insights into their different potentials for enhancing plant resilience by stress priming.
- **Different types and intensities of drought treatments (Paper V).** Comparing how the xylan-impaired plants perform under challenging environments sheds light on their viability when grown in field conditions, which is crucial for studying potential applications for biorefinery. Moreover, varied conditions could help to differentiate plants with distinct xylan alterations that could be similar in well-watered conditions. Stressful conditions challenging the plant cell wall integrity sensing can offer new leads to investigate how xylan integrity can be sensed and how its alteration could induce a priming effect.

3.3.1 Impact of two xylanases, GH10 and GH11, on the secondary cell wall, signaling pathways, growth, and saccharification in aspen (**Paper IV**)

Direct effects of xylanases expressed either constitutively or during secondary cell wall development

Expressing GH10 and GH11 xylanases in aspen, either constitutively or during the development of the secondary cell wall, led to several alterations in secondary walls. There was a notable reduction in cell wall matrix xylose content detected by methanolysis-TMS, which was expectedly a direct consequence of the xylanase activity on the backbone, effectively decreasing the overall xylan content in the cell wall (**Paper IV, Fig. 3B**). Xylan reduction was further evidenced by the reduced signal from LM10 antibody used for xylan immunolocalization (**Paper IV, Fig. 4B**). The increase in xylan acetylation was also the result of a direct effect (**Paper IV, Fig. 5B**). This can be attributed to preferred hydrolysis of low acetylated xylan by the xylanases (Biely et al., 1997; Kojima et al., 2022).

The direct impact of these enzymes is further evidenced by a decrease in molecular weight and, consequently, the DP of the xylan chain, as measured by size exclusion chromatography (**Paper IV, Fig. 5C**). Additionally, analyses of oligomeric mass profiling revealed changes in the profiles of xylan oligomers after GH30 digestion, suggesting that the enzymatic action of GH10 and GH11 not only reduces xylan content but also alters its structure (**Paper IV, Fig. 5DE**). These biochemical changes might directly contribute to improved saccharification, as the enzymatic breakdown of the cell wall xylan could enhance the accessibility of cellulose for subsequent enzymatic hydrolysis, leading to increased yields of fermentable sugars, which was experimentally confirmed (**Paper IV, Fig. 6**).

Importantly, alongside these direct effects, there were significant effects, which could be indirect, such as a reduction in lignin content, and which could have also contributed to improved saccharification outcomes. Understanding such indirect effects is very important to generate plants with better biorefinery conversion efficiency.

Understanding the indirect effects of altering the aspen xylan backbone requires exploring a potential secondary cell wall integrity maintenance system

Aspen trees expressing xylanases were shorter, lighter, and displayed important developmental changes with a reduction in secondary cell wall thickness and xylem-to-phloem ratio and overall altered wood composition (**Paper IV, Fig. 1-3**). As these alterations require many molecular players acting in concert, transcription factors and hormones have likely been involved downstream of direct xylanase effects. Revealing the identity of these players will help to engineer plants for different purposes, especially since the improved saccharification in xylanase-expressing lines could have partially resulted from the indirect effects of xylan impairment. The notable decrease in G-lignin and total lignin in transgenic lines could be an example of an indirect yet significant consequence of xylan modification. This conclusion was based on the decreased expression of homologs to *AtMYB85*, *AtMYB52*, and *AtSND2* (Zhong et al., 2008; Geng et al., 2020) and genes encoding several monolignol biosynthetic and polymerizing enzymes revealed by transcriptomics analysis (**Paper IV, Table S8**). Decreased cell wall lignification may be the reaction to maintain the structural integrity of secondary walls weakened by the xylanases. Other examples of cell wall modification in response to xylan integrity impairment include alterations in the cell wall matrix sugar composition (**Paper IV, Fig. 3**). Considering the layered regulation of wood formation by both hormones and transcription factors, it is necessary to delve into a multi-omics approach to understand in detail the secondary cell wall fine-tuning following xylanase impact.

The striking reduction of ABA observed in transgenic lines (**Paper IV, Fig. 7**) indicates that this hormone plays a role in the signaling cascade induced after xylan integrity impairment. This observation is corroborated by the transcriptomic changes, downregulation of biosynthetic genes such as *NCDE1* (Qin and Zeevaart, 1999), and upregulation of negative regulators of ABA like *FCLY* (Huizinga et al., 2010) (**Paper IV, Table 1**). ABA has previously been shown to mediate SCWI impairment-induced biotic stress resistance (Hernández-Blanco et al., 2007). Conversely, ABA signaling in osmotic stress was negatively affected by *THE1* (Bacete et al., 2022). ABA is also known as a regulator of secondary cell wall formation (Chen et al., 2016; Yan et al., 2018; Liu et al., 2021). Even if the reduced cell wall thickness and reduced lignin content observed in xylanase-expressing lines

were similar to phenotypes of *aba2-1* mutant, suggesting that reduced ABA signaling could drive these changes, the SCW biosynthetic genes downregulated in *aba2-1* such as *AtSND1*, *AtNST1*, *AtMYB46*, *AtMYB83*, *AtIRX8*, *AtIRX9*, *AtIRX14*, *AtPAL1*, *AtC4H*, *AtCCR1*, *AtCESA4*, *AtCESA7* and *AtCESA8* (Liu et al., 2021) were not reduced in xylanase-expressing aspen lines suggesting that additional signaling must be involved in these lines. Moreover, among the cell wall-related downregulated genes in xylanase-expressing lines (**Paper IV, Table 2**), there were several genes implicated in xylan decorations, such as homologs of *AtTBL29/ESK1*, *AtTBL31*, *AtRWA3*, or *AtGUX1*, and a homolog of *AtPARVUS* which participates in the synthesis of xylan reducing end (Brown et al., 2007; Kong et al., 2009; Mortimer et al., 2010; Lee et al., 2011; Yuan et al., 2013, 2016; Zhong et al., 2017). Additionally, among downregulated cell wall-related genes in xylanase-expressing lines, there were several GH9 members, including a homolog of *AtCEL1* encoding an endo-1,4- β -glucanase, downregulation of which reduced SCW thickening and lignin biosynthesis in *Arabidopsis* (Tsabary et al., 2003; Shani et al., 2006).

Two other hormones, ethylene, and cytokinins, were also identified as candidates for signaling secondary cell wall impairment in xylanase-expressing lines. An increase in 1-amino cyclopropane carboxylic acid (ACC) content, the direct precursor of ethylene, was observed in these transgenic lines (**Paper IV, Fig. 7**). Transcriptomic analysis identified the negative regulator of ethylene signaling *AtETR2* upregulated (**Paper IV, Table 1**). Its mutation increased ABA sensitivity and affected microtubule dynamic in *Arabidopsis* (Plett et al., 2009; Wilson et al., 2014), suggesting that its function in xylanase-expressing lines could involve hormonal crosstalk with ABA and maintaining microtubule stability. Moreover, for short-term response, ACC itself has been shown to participate in CWI maintenance without involving ethylene perception (Tsang et al., 2011). While auxin and ROS signaling are required downstream ACC signaling, jasmonate, ABA, and ROS signaling are integrated with ethylene signaling probably by the ERFs transcription factors acting as an integrative regulatory hub (Müller and Munné-Bosch, 2015). Several ERF-encoding genes were differentially regulated in xylanase-expressing lines (**Paper IV, Table 1**). This indicates that ERFs transcription factors may participate in mediating the complex hormonal interactions during secondary cell wall integrity maintenance in xylanase-expressing lines. It is noteworthy that the

suppression of primary wall cellulose synthase induced both jasmonate and ethylene overproduction (Ellis and Turner, 2001; Ellis et al., 2002) and that an interplay between ethylene and FERONIA-brassinosteroid signaling has been proposed to control the dark hypocotyl elongation (Deslauriers and Larsen, 2010)

The upregulation of cytokinins, especially *trans*-zeatin (**Paper IV, Fig. 7**) and two homologs of *AtIPT5*, a gene encoding isopentenyl transferase responsible for *trans*-zeatin biosynthesis (**Paper IV, Table 1**), suggests that alterations in xylan structure might trigger cytokinin biosynthesis and signaling. Indeed, we observed an important upregulation of *AtKMD2* homolog (**Paper IV, Table 1**), the encoded protein of which targets for degradation type-B *Arabidopsis* response regulators (ARRs), transcription factors positively regulating cytokinin signaling (Argyros et al., 2008; Kim et al., 2013). These types B ARR negatively impact drought tolerance (Nguyen et al., 2016), suggesting that *AtKMD2* upregulation could increase drought tolerance in xylan defective lines by lowering cytokinin sensitivity through ARR degradation. Additionally, the upregulation of a homolog of *Arabidopsis* CYTOKININ RESPONSE FACTOR 4 (*AtCRF4*) (**Paper IV, Table 1**) with a role in freezing tolerance (Zwack et al., 2016) also suggests that xylanase-expressing lines could have increased freezing resilience. Homolog of *AtARR6*, encoding a type-A ARR, was downregulated in xylanase-expressing lines (**Paper IV, Table 1**). *arr6* mutant displayed altered cell-wall composition and biotic resistance and increased content of pectin- and xylan-related DAMPs, which could prime plants for defense (Bacete et al., 2020; Mérida et al., 2020).

Other important signalling genes differentially regulated in xylanase-expressing lines were homologs of *Arabidopsis* MILDEW RESISTANCE LOCUS O (*AtMLO*) 1 and 4 (**Paper IV, Table 1**) encoding calcium channels (Gao et al., 2022). *AtMLO1* was reported to be activated by a CrRLK1L-LLG-RLCK complex in response to RALF peptides, which was essential to maintain cell wall integrity of growing pollen tubes (Gao et al., 2023). It is also probable that *AtMLO4* and its aspen homolog could participate in CWI functions as *AtMLO4* has been reported in root thigmomorphogenesis and gravity sensing (Chen et al., 2009; Zhu et al., 2021), which are both part of a proprioception mechanism requiring CWI maintenance system (Monshausen and Haswell, 2013; Hamant and Moullia, 2016; Bacete and Hamann, 2020a). In contrast, homologs of *Arabidopsis* OSCA1 encoding

calcium channels in the plasma membrane that permit calcium influx in response to osmotic stress and mechanoperception (Yuan et al., 2014a; Pei et al., 2022) were upregulated in xylanase-expressing lines (**Paper IV, Table 1**). This suggests that OSCA1 channels could play a role in CWI sensing activated by xylanases.

Only one gene distantly related to the *CrRLK1L* family but without a kinase domain, *PtMD138* homologous to *AtLLR3* exhibited differential expression in xylanase-expressing lines where it was downregulated. It encoded an extracellular protein with a malectin-like domain and LRR domains. In *Arabidopsis*, *LLR3* was expressed in the vasculature with a proposed role in lignified tissues (Sultana et al., 2020). In aspen wood-forming tissues, *PtMD138* transcripts peaked in the maturation zone, which could be interpreted as acting in the ray cells (**Paper I, Fig. 7**). The absence of *CrRLK1L* proteins in transcriptomic data of xylanase-expressing lines does not preclude their involvement in SCW integrity sensing. Our analysis would not detect them if these genes were transiently mobilized during the early stages of cell wall integrity impairment or if their activity was regulated at the post-transcriptional rather than transcriptional level following cell wall damage. Finally, peptide signaling could play a role in mitigating the effects of xylanases in transgenic lines, as indicated by the upregulation of *AtCLE45* homolog (**Paper IV, Table 1**). This peptide is known to reduce protophloem formation in *Arabidopsis* root (Depuydt et al., 2013) and thus could be induced to counteract the excess phloem formation in xylanase-expressing lines.

To conclude, unraveling the direct and indirect effects of SCW impairment in xylanase-expressing lines sheds light on adaptative strategies to compensate for the direct impact of the expressed xylanases. It is challenging to pinpoint which biological processes or genes are responsible for the observed phenotypes, such as reduced growth or thinner cell walls, and whether these genes adjust plant physiology to CWI stress and mitigate the negative impact of the direct effect of xylanases. This complexity highlights the need for further research to understand plant SCW integrity maintenance better.

3.3.2 Drought responses of *Arabidopsis* and aspen with modified xylan backbone (**Paper V**)

Both direct and indirect effects from impaired xylan backbone in well-watered conditions play a role in drought responses

Studies with xylan backbone biosynthetic mutants have shown that xylan backbone reduction can lead to a decrease in secondary cell wall thickness and stem rigidity, which in turn can affect the plant's ability to maintain structural integrity and lead to severe dwarfism (Peña et al., 2007; Brown et al., 2009; Wu et al., 2009; Keppler and Showalter, 2010). In **Paper V**, we showed that expression of xylanases from families GH10 and GH11 during secondary cell wall development in *Arabidopsis* led to significant reductions in secondary xylem xylose content and to the *irx* phenotype, similar to phenotypes seen in *irx9*, *irx14*, and *irx10* mutants (**Paper V, Table 1, Fig. 2C**). Traditionally it was thought that xylan impairment leads directly to the *irx* phenotype modifying plants' physiological performance (Turner and Somerville, 1997; Lefebvre et al., 2011; Bensussan et al., 2015). However, recent work has challenged this view, suggesting that the *irx* phenotype, along with associated dwarfism and freezing tolerance, might indirectly arise from regulation by strigolactone-like compounds, as seen in the *esk/tbl29* mutant (Ramírez et al., 2018; Ramírez and Pauly, 2019). Nevertheless, we cannot rule out that the *irx* and other observed phenotypes in *irx9*, *irx14*, and *irx10* mutants and xylanase-expressing lines (**Paper V, Fig. 2C**) could result, at least partially, from the direct effects of xylan structural deficiency. This could explain only partial complementation of freezing tolerance and dwarfism in *irx1*, *irx3*, and *parvus* by *MAX4* mutation (Ramírez and Pauly, 2019).

Our initial hypothesis was that xylan impairment in secondary walls would lead to increased drought tolerance due to the priming effect. However, given the diverse phenotypes we observed across different genotypes and species with varied levels and types of xylan impairment (**Paper V, Fig. 6**), it is essential to emphasize the potential direct impact of these changes on drought responses. For example, vessel deformations could directly affect the observed changes in hydraulic conductivity (**Paper V, Fig 8E**) and represent an important component alongside hypothesized indirect effects. The reduction in vessel size and roundness, a result of *irregular xylem*, may decrease the likelihood of embolism during drought stress (Lovisolo and

Schubert, 1998; Jacobsen et al., 2019; Lens et al., 2022, 2023; Isasa et al., 2023). In tall species like trees where the water column in the vasculature needs to be raised to the heights of tens of meters and thus maintain substantial negative pressures increasing the risks of cavitation, benefits of *irx* could be more important than in smaller plants such as *Arabidopsis* (Cochard and Delzon, 2013). Moreover, with narrower conductive elements, the importance of capillary forces in maintaining negative water potential is greater, which could be advantageous, allowing the plant to draw tightly bound water molecules more effectively from the soil (Sherwin et al., 1998; Fichot et al., 2010). The *irx* phenotype could also allow the plant to retain water longer between intake and evapotranspiration due to slower transport (Stiller, 2009). Conversely, the water-pulling force driven by evapotranspiration would require a higher negative pressure to maintain the same water transport rate, which could limit overall development, as a reduced amount of water would be available for photosynthesis and growth (Martorell et al., 2014). We indeed observed reduced growth in some genotypes (**Paper V, Fig. 3**).

While all types of xylan backbone defects induced in **Paper V** led to reduced xylose content and an *irx* phenotype, each line displayed unique characteristics under well-watered and drought conditions. Noteworthy effects of xylan modification under well-watered conditions include reduced rosette growth in *Arabidopsis irx9* and *irx14* mutants (**Paper V, Fig. 3B**), decreased stem height in aspen GH10 and GH11 lines (**Paper V, Fig. 9B**), and lower F_v/F_m ratios in *irx10*, *irx14*, and GH11 *Arabidopsis* lines (**Paper V, Fig. 5A**) indicative of impaired photosynthetic efficiency. These physiological changes, particularly the lower F_v/F_m ratios, likely reflect disruptions in chloroplast function and light energy conversion, which could affect the plants' ability to optimize water usage effectively (**Paper V, Fig. 7B**).

Strikingly and echoing with changes observed in aspen (**Paper IV, Fig. 3C**), the reduction in lignin was observed in all studied *Arabidopsis* lines except for the *irx14* mutant, which had significantly more lignified secondary xylem (**Paper V, Table. 2**). Although not yet proven, the decreased lignification in xylan-impaired *Arabidopsis* lines was most likely driven by transcriptional regulation as it was shown in xylanase-expressing aspen (**Paper IV, Table S8**) and in *irx8* mutant in *Arabidopsis* (Hao et al., 2014). The origin of increased lignin content in the *irx14* mutant is unknown. Variability in lignin

content would expectantly contribute to variations in drought responses (Yan et al., 2018; Bang et al., 2019; Choi et al., 2023), and the best performance of *irx14* under severe drought is possibly related to its increased lignin content. Additionally, high lignin content in *irx14* could have prevented problems with water conductivity that were evident in other xylan-impaired genotypes, as *irx14* uniquely maintained intact vascular conductivity to the side shoots (**Paper V, Fig. 8**).

Increased stomatal density and pore size reduction were observed in most xylan-impaired *Arabidopsis* lines (**Paper V, Fig. 8B, C**). These traits are influenced by a complex network of hormonal and transcriptional regulations, integrating various signaling pathways and cascades, with ABA playing a crucial role (Shahzad et al., 2021). The observed increase in stomatal density across all *Arabidopsis* lines studied (**Paper V, Fig. 8B**) could result from xylan impairment that indirectly decreases ABA biosynthesis. However, the observed smaller stomatal pore area (**Paper V, Fig. 8C**) cannot be explained by reduced ABA signaling, which generally leads to larger stomatal pores. Indeed, ABA-insensitive mutants typically show both increased stomatal density and larger apertures, enhancing their conductivity through two different pathways where OST1 kinase activates ROS production, increasing pore aperture (Mustilli et al., 2002; Tanaka et al., 2013; Jalakas et al., 2018). Other factors, such as the cell wall composition of guard cells, their mechanical properties, overall water status, and ROS balance, could contribute to pore size reduction in xylan-impaired lines (Singh et al., 2017; Rui et al., 2018; Yi et al., 2022; Keynia et al., 2023). The reduction in stomata pore size in most studied lines and impaired water conductivity in *irx9* and GH11-expressing line GH11.1 could explain their better water retention (**Paper V, Fig. 8**).

ABA signaling is crucial for regulating stomatal behavior during drought responses (Loveys and Kriedemann, 1974; Liu et al., 2022). Aspen xylanase-expressing lines had decreased ABA content (**Paper IV**), whereas some *Arabidopsis* xylan-impaired lines exhibited decreased stomatal closure in response to ABA (**Paper V, Fig. 8C**). For instance, ABA treatment in *irx10* and *irx14* (with smaller pores) further reduced stomate pores but with a lower intensity than in wild type; in *irx9*, stomata closed only after 60 minutes of treatment, while GH10-expressing line (GH10.1) showed greatly attenuated response to ABA treatment.

Drought stress responses of xylan-impaired lines indicate that secondary cell wall integrity could induce priming for this stress

Priming plants for drought resistance involves biological mechanisms that help them adapt to water scarcity more efficiently by activating stress response pathways ahead of actual stress events (Goh et al., 2003; Ding et al., 2012; Virilouvet and Fromm, 2015). Priming can be induced by the perception of cell wall integrity defects (Swaminathan et al., 2022). One way these defects could be perceived is by DAMPs. Xylan impairments induced by expressing xylanases would lead to the release of xylobiose, which has recently been shown to exhibit DAMP activity (Dewangan et al., 2023). We cannot exclude that drought conditions themselves may also trigger the release of additional DAMPs. These molecules activate the plant's stress response systems, increasing their readiness to manage further stress. Mutants with secondary cell wall or xylan alterations have already been shown to resist better to different types of abiotic and biotic stress (Hernández-Blanco et al., 2007; Keppler and Showalter, 2010; Ramírez and Pauly, 2019). Another way that cell wall integrity defect could be perceived in the context of drought is related to structural wall alterations using signaling in common with mechanical stress or osmotic stress (Marshall et al., 2012; Monshausen and Haswell, 2013; Haswell and Verslues, 2015; Zhu, 2016; Bacete and Hamann, 2020b; Rui and Dinneny, 2020). All three sensing pathways to wall impairment can activate downstream signaling cascades involving kinases, calcium signaling, G-protein signaling, and reactive oxygen species (ROS), which finally impact hormone signaling pathways and transcription factors. Maintaining cell wall integrity is crucial, as it is a physical barrier and strengthens the plant's overall resilience. Thus, this coordinated response helps plants manage water stress and sustain growth under challenging conditions.

To further elucidate secondary cell wall integrity signaling, we investigated the impacts of moderate and severe drought conditions on xylan-modified lines and wild type. This analysis revealed distinct phenotypic responses, which not only could open new avenues for exploring how cell wall modifications could contribute to developing drought-resistant crops but also clearly highlighted the differences among these lines. We observed that the *irx10* mutant thrived under moderate drought conditions and that *irx14* was less affected by severe drought than the wild types (**Paper V, Fig. 4**). Other lines generally resisted moderate drought better than the wild type but were

more sensitive to severe drought. After uncontrolled water depletion and re-watering, all *Arabidopsis* lines with xylan reduction in secondary walls survived better than wild type (**Paper V, Fig. 7D**). However, all transgenic lines, except for GH11, exhibited lower water use efficiency (**Paper V, Fig. 7B**).

We also observed differences in drought response between *Arabidopsis* and hybrid aspen lines expressing xylanases, which suggests species-specific adaptations to xylan backbone modifications. Aspens were much more affected in growth by xylan modification than *Arabidopsis* (**Paper V, Figs. 4 and 9**). This suggests that xylan integrity is more important for tree species than it is for herbs. Intriguingly, the drought did not affect GH11-expressing aspen as it did GH10-expressing aspen or wild type (**Paper V, Figs 9 and 10**), contrasting with the result from *Arabidopsis* (**Paper V, Fig. 4B**).

Analyzing drought responses in some xylan deficient lines (exemplified below), it would appear that these plants are in a state akin to drought stress, even without actual water scarcity. In this context, xylan deficiency may act as a priming factor, but the impact of this deficiency could also be detrimental. Similar challenges arise with this priming method as with others, including determining the optimal timing, frequency, and intensity of the priming factors that affect the plant. Indeed, the line between priming and stress response is often blurred; excessive priming could, in fact, prove deleterious to the plant (Kerchev et al., 2020; Ghosh et al., 2021; Raza et al., 2023). Our results highlight the need for careful calibration when applying priming techniques, ensuring they enhance resilience without crossing into harmful stress levels. Indeed, we observed that the leaf temperature of GH10.b hybrid aspen under well-watered conditions equals that of drought-stressed plants (**Paper V, Fig. 9F**), suggesting that alterations in CWI may activate signaling pathways typically associated with drought stress (Cruz De Carvalho, 2008; Pinheiro and Chaves, 2011; Tee et al., 2023). This hypothetically could be due to impaired ROS scavenging from CWI disruptions, resulting in reduced transpiration "cooling," which drastically would reduce growth even under well-watered conditions (Cruz De Carvalho, 2008; Lee and Park, 2012; Xu et al., 2018; Vijayaraghavareddy et al., 2022). This phenomenon is further illustrated by the reduced stomatal pore area of most xylan-defective *Arabidopsis* under well-watered conditions, which matches the Col-0 pore area after ABA treatment (mimicking drought conditions) (**Paper V, Fig. 8C**). This suggests that some

specific drought signaling is already activated in xylan-defective lines, likely through overlapping CWI maintenance systems. More integrative phenotypes such as the WLI/NDVI for *irx9*, *irx14*, and GH11.1 (**Paper V, Fig. 5B**) or general growth reductions also display similar tendencies in these lines, where xylan-deficient plants appear to be in a state akin to drought stress, even without actual water scarcity. Xylan deficiency could potentially act as a priming factor; however, when growth is already reduced in well-watered conditions, the priming effect may become overly intense and harmful. This is illustrated by the *irx14* mutant, which shows better drought resilience than other lines but suffers from growth impairment. Therefore, xylanase lines without growth defects could provide a more advantageous approach. Further studies are needed to understand better the balance between enhanced drought resilience and growth penalties and to optimize xylanase use for improved plant performance under various environmental conditions.

In conclusion, the study of xylan backbone deficiencies in cells developing secondary walls not only enhances our understanding of secondary cell wall integrity sensing and its interaction with drought stress signaling pathways but also underlines the potential of harnessing these pathways for developing drought-resistant crops. Through the detailed examination of how xylan modifications affect various physiological traits under different watering conditions, this research underscores the crucial role of the cell wall in managing plant responses to drought while also highlighting the nuanced differences between plant species and similar transgenic lines (**Paper V, Fig. 6**).

4. Discussion and Conclusions

Exploring the SCWI maintenance system is central to this doctoral thesis work. Increasing environmental and societal pressure on crop production and the necessity for generating more sustainable energy stress the need to understand better how wood is produced and how adversary environmental conditions could impact this dynamic process. The heart of this effort is condensed into understanding more holistically how the signaling machinery operates in the wood to integrate environmental and developmental cues. Aligning with these broad goals, this thesis provided new insight into the secondary cell wall integrity maintenance concept.

While Faria-Blanc et al. (2018) stated that transcriptomic analyses of xylan mutants did not confirm the existence of mechanisms maintaining SCWI in *Arabidopsis*, studying SCWI in *Arabidopsis* glucuronoxylan mutants is challenging due to developmental differences from wild-type plants, especially in *irx9* and *irx14* mutants. While these mutants demonstrate evident secondary wall defects, their morphological and developmental changes are not easy to account for. Secondly, it is still unclear which genes could be good markers for SCWI signaling. Transcriptional responses of genes involved in CWI sensing could be transient and thus overlooked when analyzing mutants or transgenic plants. Also, they could be regulated not at the transcription level but rather through post-translational modifications such as phosphorylation. Thus, studying the downstream response genes, including peptides like RALFs, calcium, ROS, and hormonal signaling, for example, could offer a deeper insight into how plants cope with SCW defects. In that sense, the published data (Faria-Blanc et al., 2018) offers precious insight for further investigations: one illustrative example is the evidence for high induction of *AtGA2ox8* in the stems of *irx10* and *irx14* (ranked first and second most highly induced gene, respectively). Recent studies have shown that this gene is involved in the hormonal interplay between ethylene, JA, and gibberellins during thigmomorphogenesis (Wang et al., 2024).

Many others studied in *Arabidopsis* support the existence of SCWI sensing mechanisms. Notably, research by Hernández-Blanco et al. (2007) and Liu et al. (2023) underscores how alterations in SCW can activate distinct signaling mechanisms, independent of the classical defense pathways, implicating ABA signaling, and FER coupled with OG-sensing pathways, respectively. Other studies revealed that SCW disturbances can induce carlactone or a related compound signaling (Ramírez et al., 2018; 2019), causing collapsed vessels, impairing overall development, and increasing freezing tolerance. These studies suggest that SCWI sensing pathway(s) in *Arabidopsis*, while not as biologically important as in woody species, involves various types of signaling that can integrate environmental and developmental signals into physiological responses. These insights pave the way for reevaluating the existence and functionality of SCWI mechanisms. Thus, while *Arabidopsis* may not prioritize SCW maintenance, the genetic and molecular evidence points towards an operational SCWI sensing system.

This thesis underscores the need for research on SCWI sensing involving woody species, where secondary cell wall functions are more pronounced. Indeed, the annual lifecycle of *Arabidopsis* may not necessitate robust SCW integrity sensing mechanisms focused on long-term structural integrity, unlike perennial trees that require such systems for survival and stress recovery. This, coupled with the technical challenges in sampling secondary xylem tissue in *Arabidopsis*, which requires precise techniques like single-cell extraction or microdissection, limits its use for studying secondary cell walls. In contrast, sampling developing wood tissue in tree species is much easier, providing data with higher resolution compared to mixed-tissue analyses performed so far in *Arabidopsis*, where average gene expression signals from various tissues could mask the differential expression in cells developing secondary walls. Studying intricate SCWI sensing mechanisms in *Arabidopsis* and hybrid aspen afforded comparison between herbaceous plants and woody species, providing comprehensive insights into how plants respond to secondary cell wall xylan impairment. We delved into the molecular and hormonal responses to xylan modifications and mechanical stress, exploring how these stresses affected plant physiology and resilience to drought. Our studies highlighted the conserved structure of malectin domain-containing proteins between *Arabidopsis* and *Populus*, implicating some of these proteins in recognizing and responding to SCW integrity cues. We examined the direct effects of xylan modification on cell wall

architecture and indirect effects involving different signaling pathways through multiple experiments. Each article from **Paper I** to **V** compiled in this thesis contributes separately to better our understanding of SCWI sensing, but their harmonious combination forms this solid conglomerate. Here are the main conclusions of each paper:

Paper I. We identified and characterized malectin and malectin-like domain proteins in *Populus trichocarpa* and *Arabidopsis thaliana*, demonstrating their potential roles in SCWI sensing. 146 MD/MLD proteins were identified in *P. trichocarpa* and 87 in *Arabidopsis*, with significant domain structure diversification suggesting specialized functions related to tree physiology and wood formation. Notably, clade XII (*CrRLK1L* family), which is expanded in *P. trichocarpa*, points to a robust arsenal for monitoring SCWI during wood development in this species.

Paper II. Flexure wood formation in hybrid aspen in response to mechanical stress (stem flexing) led to several physiological changes, including faster growth, and altered wood composition. Hormonal and transcriptomic analyses indicated a complex interplay of hormonal responses, particularly jasmonates, polyamines, ABA, and ethylene. The study underscores the role of mechanoperception in wood formation and the potential of mechanical cues to optimize bioenergy crops. Additionally, specific genes involved in cell wall organization and biosynthesis were identified as key players in the maintenance of SCWI during mechanical stress.

Paper III. We explored the role of MeGlcA substitutions in xylan and their interaction with lignin in secondary cell walls. We demonstrated that altering MeGlcA content, specifically through the expression of *AnAgu67A* α -glucuronidase, did not significantly impact overall plant growth or wood composition but enhanced the extractability of aliphatic suberin-like compounds. This suggests a novel role for xylan MeGlcA in anchoring suberin-like compounds to the wood cell wall, with potential implications for biomass processing. We also showed the presence of lipids in living wood and in a wide range of species for the first time.

Paper IV. Expression of GH10 and GH11 xylanases in hybrid aspen was shown to affect the SCW by reducing xylan content and altering its structure, leading to changes in cell wall composition and saccharification efficiency. We revealed both direct effects of xylanase activity on xylan and indirect effects, such as alterations in lignin content, developmental programs, hormonal status, and transcriptional activation of different signaling pathways. We suggest these changes participate in a complex regulatory mechanism that alters plant growth in response to SCWI sensing, highlighting the intricate relationship between xylan structure and plant stress responses.

Paper V. We investigated the impact of xylan backbone modifications in *Arabidopsis* and hybrid aspen on growth under drought conditions. We showed that modifications in the xylan backbone can induce various physiological responses, including altered growth patterns and drought stress responses. We suggest that xylan deficiencies may prime plants for drought resistance but also could have adverse effects, underlining the need for balanced approaches in crop engineering for drought resistance.

These targeted investigations not only enhance our understanding of SCWI sensing but also suggest new avenues for improving plant robustness against environmental stresses and for generating better-suited trees for biorefinery. Integrating molecular details with physiological outcomes provides a clear picture of the complexities involved in SCW integrity sensing, which are essential for future crop improvement strategies and forestry management.

From our gained experience after this work, to further understand the inherent complexity of these signaling mechanisms, we suggest a variety of new experiments and angles to tackle new knowledge needed in this field:

- **Spatial differentiation and time-dependent experimentation.** To study SCWI effectively, it is crucial to employ advanced sampling techniques such as single-cell extraction or laser microdissection, especially in non-tree species, to avoid collecting mixed tissues. Responses to stress in wood encompass a range of changes that vary over time. For instance, immediate gene expression or protein phosphorylation changes must be captured shortly after stress

induction, while slower changes may reflect long-term adaptations. Designing experiments to sample developing secondary xylem cells in *Arabidopsis* and hybrid aspen precisely after specific stress events, such as a single strong stem flexion or using inducible constructs in a time-dependent manner for further omics approaches, could provide valuable insights into SCWI sensing dynamics.

- **Investigating levels of SCW impairment.** Understanding SCWI maintenance involves discerning the fine line between priming and stressing a plant. Investigating various levels of expression or intensity of stress could clarify key players in this process. This can be achieved by creating multiple transgenic lines, applying different types and intensities of mechanical forces, varying drought stress levels, or using various pathogens to impact the plants.
- **Cross-species comparison.** Extending SCWI sensing and maintenance mechanism studies to other species synthesizing SCW, such as lower vascular plants, gymnosperms, and grasses (among others), can enrich our understanding of these processes through an evolutionary lens. Based on our progress, further studies could also focus on the functional characterization of specific MD/MLD proteins identified in *P. trichocarpa* and *Arabidopsis*, especially those unique or expanded clades associated with tree-specific functions. Investigating their roles in various stress responses and developmental processes could elucidate their precise mechanisms in CWI maintenance.
- **Characterization of SCWI sensors.** Numerous potential sensors have been identified in our research, but their roles in SCWI sensing still need to be proven. This can be accomplished by creating crosses between sensor mutants and SCW-deficient lines. Additionally, examining how these mutants respond to inhibitors of specific signaling pathways would provide further insights. Finally, studying SCW-deficient lines in media containing various hormones could improve our understanding of how different hormones and signaling pathways participate in SCWI.
- **Multidisciplinary approaches.** The complexity of SCWI requires a multidisciplinary approach. Indeed, to grasp the whole picture, collaboration with experts specializing in secondary cell wall

formation, stress responses, and photosynthesis (etc.) is essential. Additionally, contributions from physicists, mathematicians, and bioinformaticians are crucial to interpreting results and developing robust models.

- **Holistic understanding.** With proteins like FERONIA and THESEUS involved in both biotic and abiotic stress signaling and general development, this study area is crucial for unraveling complex hormonal and signaling interactions. Examining a broad spectrum of factors, from transcriptional changes to physiological responses, is essential. We have incorporated a wide range of data in our work, partly thanks to novel approaches. However, further insights could be gained, particularly in analyzing hyperspectral and fluorescence data from *Arabidopsis* using high-throughput phenotyping facilities. This field is set for significant advancements in the future, particularly by computational methods to interpret large datasets. Nonetheless, it remains essential to corroborate these data with physiological measurements to ensure robust and meaningful scientific outcomes.

References

- Addison, B., Stengel, D., Bharadwaj, V. S., Happs, R. M., Doeppke, C., Wang, T., et al. (2020). Selective One-Dimensional ^{13}C - ^{13}C Spin-Diffusion Solid-State Nuclear Magnetic Resonance Methods to Probe Spatial Arrangements in Biopolymers including Plant Cell Walls, Peptides, and Spider Silk. *J. Phys. Chem. B* 124, 9870–9883. doi: 10.1021/acs.jpcc.0c07759.
- Amanda, D., Doblin, M. S., Galletti, R., Bacic, A., Ingram, G. C., and Johnson, K. L. (2016). DEFECTIVE KERNEL1 (DEK1) regulates cell walls in the leaf epidermis. *Plant Physiol.* 172, 2204–2218. doi: 10.1104/pp.16.01401.
- Anders, N., Wilson, L. F. L., Sorieul, M., and Nikolovski, N. (2023). β -1,4-Xylan backbone synthesis in higher plants: How complex can it be? *Front. Plant Sci.* 13, 1–9. doi: 10.3389/fpls.2022.1076298.
- Anderson, C. M., Wagner, T. A., Perret, M., He, Z. H., He, D., and Kohorn, B. D. (2001). WAKs: Cell wall-associated kinases linking the cytoplasm to the extracellular matrix. *Plant Mol. Biol.* 47, 197–206. doi: 10.1023/A:1010691701578.
- Andersson-Gunnerås, S., Mellerowicz, E. J., Love, J., Segerman, B., Ohmiya, Y., Coutinho, P. M., et al. (2006). Biosynthesis of cellulose-enriched tension wood in *Populus*: Global analysis of transcripts and metabolites identifies biochemical and developmental regulators in secondary wall biosynthesis. *Plant J.* 45, 144–165. doi: 10.1111/j.1365-313X.2005.02584.x.
- Archibald, J. M. (2009). Secondary Endosymbiosis. *Encycl. Microbiol. Third Ed.*, 438–446. doi: 10.1016/B978-012373944-5.00360-6.
- Argyros, R. D., Mathews, D. E., Chiang, Y. H., Palmer, C. M., Thibault, D. M., Etheridge, N., et al. (2008). Type B response regulators of *Arabidopsis* play key roles in cytokinin signaling and plant development. *Plant Cell* 20, 2102–2116. doi: 10.1105/tpc.108.059584.
- Atmodjo, M. A., Hao, Z., and Mohnen, D. (2013). Evolving views of pectin biosynthesis. *Annu. Rev. Plant Biol.* 64, 747–779. doi: 10.1146/annurev-arplant-042811-105534.
- Bacete, L., and Hamann, T. (2020a). Plant Biology: Plants Turn Down the Volume to Respond to Cell Swelling. *Curr. Biol.* 30, R804–R806. doi: 10.1016/j.cub.2020.06.001.
- Bacete, L., and Hamann, T. (2020b). The role of mechanoperception in plant cell wall integrity maintenance. *Plants* 9. doi: 10.3390/plants9050574.
- Bacete, L., Mélida, H., López, G., Dabos, P., Tremousaygue, D., Denancé, N., et al. (2020). *Arabidopsis* response reGULATOR 6 (ARR6) modulates plant cell-wall composition and disease resistance. *Mol. Plant-Microbe Interact.* 33, 767–780. doi: 10.1094/MPMI-12-19-0341-R.

- Bacete, L., Schulz, J., Engelsdorf, T., Bartosova, Z., Vaahtera, L., Yan, G., et al. (2022). THESEUS1 modulates cell wall stiffness and abscisic acid production in *Arabidopsis thaliana*. *Proc. Natl. Acad. Sci. U. S. A.* 119. doi: 10.1073/pnas.2119258119.
- Balakshin, M., Capanema, E., and Berlin, A. (2014). “Chapter 4 - Isolation and Analysis of Lignin–Carbohydrate Complexes Preparations with Traditional and Advanced Methods: A Review,” in *Studies in Natural Products Chemistry.*, ed. Atta-ur-Rahman (Elsevier), 83–115. doi: <https://doi.org/10.1016/B978-0-444-63281-4.00004-5>.
- Bang, S. W., Lee, D. K., Jung, H., Chung, P. J., Kim, Y. S., Choi, Y. Do, et al. (2019). Overexpression of OsTF1L, a rice HD-Zip transcription factor, promotes lignin biosynthesis and stomatal closure that improves drought tolerance. *Plant Biotechnol. J.* 17, 118–131. doi: 10.1111/pbi.12951.
- Barnett, J. R., and Bonham, V. A. (2004). Cellulose microfibril angle in the cell wall of wood fibres. *Biol. Rev. Camb. Philos. Soc.* 79, 461–472. doi: 10.1017/S1464793103006377.
- Bartels, S., and Boller, T. (2015). Quo vadis, Pep? Plant elicitor peptides at the crossroads of immunity, stress, and development. *J. Exp. Bot.* 66, 5183–5193. doi: 10.1093/jxb/erv180.
- Basu, D., and Haswell, E. S. (2020). The Mechanosensitive Ion Channel MSL10 Potentiates Responses to Cell Swelling in *Arabidopsis* Seedlings. *Curr. Biol.* 30, 2716–2728.e6. doi: 10.1016/j.cub.2020.05.015.
- Baumberger, N., Ringli, C., and Keller, B. (2001). The chimeric leucine-rich repeat/extensin cell wall protein LRX1 is required for root hair morphogenesis in *Arabidopsis thaliana*. *Genes Dev.* 15, 1128–1139. doi: 10.1101/gad.200201.
- Benedetti, M., Pontiggia, D., Raggi, S., Cheng, Z., Scaloni, F., Ferrari, S., et al. (2015). Plant immunity triggered by engineered in vivo release of oligogalacturonides, damage-associated molecular patterns. *Proc. Natl. Acad. Sci. U. S. A.* 112, 5533–5538. doi: 10.1073/pnas.1504154112.
- Beňová-Kákošová, A., Digonnet, C., Goubet, F., Ranocha, P., Jauneau, A., Pesquet, E., et al. (2006). Galactoglucomannans increase cell population density and alter the protoxylem/metaxylem tracheary element ratio in xylogenetic cultures of zinnia. *Plant Physiol.* 142, 696–709. doi: 10.1104/pp.106.085712.
- Bensussan, M., Lefebvre, V., Ducamp, A., Trouverie, J., Gineau, E., Fortabat, M. N., et al. (2015). Suppression of dwarf and Irregular Xylem phenotypes generates low-acetylated biomass lines in *arabidopsis*. *Plant Physiol.* 168, 452–463. doi: 10.1104/pp.15.00122.
- Biely, P., Vršanská, M., Tenkanen, M., and Kluepfel, D. (1997). Endo- β -1,4-xylanase families: Differences in catalytic properties. *J. Biotechnol.* 57, 151–166. doi: 10.1016/S0168-1656(97)00096-5.
- Bischoff, V., Nita, S., Neumetzler, L., Schindelasch, D., Urbain, A., Eshed, R., et al. (2010). TRICHOME BIREFRINGENCE and its homolog AT5G01360 encode plant-specific DUF231 proteins required for cellulose biosynthesis in *arabidopsis*. *Plant Physiol.* 153, 590–602. doi: 10.1104/pp.110.153320.

- Blackburn, M. R., Haruta, M., and Moura, D. S. (2020). Twenty years of progress in physiological and biochemical investigation of RALF peptides. *Plant Physiol.* 182, 1657–1666. doi: 10.1104/PP.19.01310.
- Boisson-Dernier, A., Lituiev, D. S., Nestorova, A., Franck, C. M., Thirugnanarajah, S., and Grossniklaus, U. (2013). ANXUR Receptor-Like Kinases Coordinate Cell Wall Integrity with Growth at the Pollen Tube Tip Via NADPH Oxidases. *PLoS Biol.* 11. doi: 10.1371/journal.pbio.1001719.
- Boisson-Dernier, A., Roy, S., Kritsas, K., Grobei, M. A., Jaciubek, M., Schroeder, J. I., et al. (2009). Disruption of the pollen-expressed FERONIA homologs ANXUR1 and ANXUR2 triggers pollen tube discharge. *Development* 136, 3279–3288. doi: 10.1242/dev.040071.
- Borassi, C., Sede, A. R., Mecchia, M. A., Salgado Salter, J. D., Marzol, E., Muschietti, J. P., et al. (2016). An update on cell surface proteins containing extensin-motifs. *J. Exp. Bot.* 67, 477–487. doi: 10.1093/jxb/erv455.
- Bromley, J. R., Busse-Wicher, M., Tryfona, T., Mortimer, J. C., Zhang, Z., Brown, D. M., et al. (2013). GUX1 and GUX2 glucuronyltransferases decorate distinct domains of glucuronoxylan with different substitution patterns. *Plant J.* 74, 423–434. doi: 10.1111/tpj.12135.
- Brown, D. M., Goubet, F., Wong, V. W., Goodacre, R., Stephens, E., Dupree, P., et al. (2007). Comparison of five xylan synthesis mutants reveals new insight into the mechanisms of xylan synthesis. *Plant J.* 52, 1154–1168. doi: 10.1111/j.1365-313X.2007.03307.x.
- Brown, D. M., Zeef, L. A. H., Ellis, J., Goodacre, R., and Turner, S. R. (2005). Identification of novel genes in Arabidopsis involved in secondary cell wall formation using expression profiling and reverse genetics. *Plant Cell* 17, 2281–2295. doi: 10.1105/tpc.105.031542.
- Brown, D. M., Zhang, Z., Stephens, E., Dupree, P., and Turner, S. R. (2009). Characterization of IRX10 and IRX10-like reveals an essential role in glucuronoxylan biosynthesis in Arabidopsis. *Plant J.* 57, 732–746. doi: 10.1111/j.1365-313X.2008.03729.x.
- Brutus, A., Sicilia, F., Macone, A., Cervone, F., and De Lorenzo, G. (2010). A domain swap approach reveals a role of the plant wall-associated kinase 1 (WAK1) as a receptor of oligogalacturonides. *Proc. Natl. Acad. Sci. U. S. A.* 107, 9452–9457. doi: 10.1073/pnas.1000675107.
- Busse-Wicher, M., Gomes, T. C. F., Tryfona, T., Nikolovski, N., Stott, K., Grantham, N. J., et al. (2014). The pattern of xylan acetylation suggests xylan may interact with cellulose microfibrils as a twofold helical screw in the secondary plant cell wall of Arabidopsis thaliana. *Plant J.* 79, 492–506. doi: 10.1111/tpj.12575.
- Busse-Wicher, M., Grantham, N. J., Lyczakowski, J. J., Nikolovski, N., and Dupree, P. (2016). Xylan decoration patterns and the plant secondary cell wall molecular architecture. *Biochem. Soc. Trans.* 44, 74–78. doi: 10.1042/BST20150183.
- Bygdell, J., Srivastava, V., Obudulu, O., Srivastava, M. K., Nilsson, R., Sundberg,

- B., et al. (2017). Protein expression in tension wood formation monitored at high tissue resolution in *Populus*. *J. Exp. Bot.* 68, 3405–3417. doi: 10.1093/jxb/erx186.
- Caffall, K. H., and Mohnen, D. (2009). The structure, function, and biosynthesis of plant cell wall pectic polysaccharides. *Carbohydr. Res.* 344, 1879–1900. doi: 10.1016/j.carres.2009.05.021.
- Carpita, N. C., and Gibeaut, D. M. (1993). Structural models of primary cell walls in flowering plants: Consistency of molecular structure with the physical properties of the walls during growth. *Plant J.* 3, 1–30. doi: 10.1111/j.1365-313X.1993.tb00007.x.
- Cassab, G. I. (1998). Plant cell wall proteins. *Annu. Rev. Plant Biol.* 49, 281–309. doi: 10.1146/annurev.arplant.49.1.281.
- Chehab, E. W., Eich, E., and Braam, J. (2009). Thigmomorphogenesis: A complex plant response to mechano-stimulation. *J. Exp. Bot.* 60, 43–56. doi: 10.1093/jxb/ern315.
- Chehab, E. W., Yao, C., Henderson, Z., Kim, S., and Braam, J. (2012). Arabidopsis touch-induced morphogenesis is jasmonate mediated and protects against pests. *Curr. Biol.* 22, 701–706. doi: 10.1016/j.cub.2012.02.061.
- Chen, J., Liu, W., Liu, C. M., Li, T., Liang, R. H., and Luo, S. J. (2015). Pectin Modifications: A Review. *Crit. Rev. Food Sci. Nutr.* 55, 1684–1698. doi: 10.1080/10408398.2012.718722.
- Chen, J., Yu, F., Liu, Y., Du, C., Li, X., Zhu, S., et al. (2016). FERONIA interacts with ABI2-type phosphatases to facilitate signaling cross-talk between abscisic acid and RALF peptide in Arabidopsis. *Proc. Natl. Acad. Sci. U. S. A.* 113, E5519–E5527. doi: 10.1073/pnas.1608449113.
- Chen, Z., Noir, S., Kwaaitaal, M., Hartmann, H. A., Wu, M. J., Mudgil, Y., et al. (2009). Two seven-transmembrane domain MILDEW RESISTANCE LOCUS O proteins cofunction in arabidopsis root thigmomorphogenesis. *Plant Cell* 21, 1972–1991. doi: 10.1105/tpc.108.062653.
- Cheung, A. Y. (2024). FERONIA: A Receptor Kinase at the Core of a Global Signaling Network.
- Choi, S. J., Lee, Z., Kim, S., Jeong, E., and Shim, J. S. (2023). Modulation of lignin biosynthesis for drought tolerance in plants. *Front. Plant Sci.* 14, 1–14. doi: 10.3389/fpls.2023.1116426.
- Chong, S. L., Virkki, L., Maaheimo, H., Juvonen, M., Derba-Maceluch, M., Koutaniemi, S., et al. (2014). O-Acetylation of glucuronoxylan in arabidopsis thaliana wild type and its change in xylan biosynthesis mutants. *Glycobiology* 24, 494–506. doi: 10.1093/glycob/cwu017.
- Christiernin, M. (2006). Composition of lignin in outer cell-wall layers. in Available at: <https://api.semanticscholar.org/CorpusID:135935616>.
- Claverie, J., Balacey, S., Lemaître-Guillier, C., Brulé, D., Chiltz, A., Granet, L., et al. (2018). The cell wall-derived xyloglucan is a new DAMP triggering plant immunity in *vitis vinifera* and *arabidopsis thaliana*. *Front. Plant Sci.* 871, 1–14. doi: 10.3389/fpls.2018.01725.

- Cochard, H., and Delzon, S. (2013). Hydraulic failure and repair are not routine in trees. *Ann. For. Sci.* 70, 659–661. doi: 10.1007/s13595-013-0317-5.
- Cong, F., Diehl, B. G., Hill, J. L., Brown, N. R., and Tien, M. (2013). Covalent bond formation between amino acids and lignin: Cross-coupling between proteins and lignin. *Phytochemistry* 96, 449–456. doi: 10.1016/j.phytochem.2013.09.012.
- Cosgrove, D. J. (2005). Growth of the plant cell wall. *Nat. Rev. Mol. Cell Biol.* 6, 850–861. doi: 10.1038/nrm1746.
- Cosgrove, D. J. (2023). Structure and growth of plant cell walls. *Nat. Rev. Mol. Cell Biol.* doi: 10.1038/s41580-023-00691-y.
- Cosgrove, D. J., and Jarvis, M. C. (2012). Comparative structure and biomechanics of plant primary and secondary cell walls. *Front. Plant Sci.* 3, 1–6. doi: 10.3389/fpls.2012.00204.
- Cruz De Carvalho, M. H. (2008). Drought stress and reactive oxygen species: Production, scavenging and signaling. *Plant Signal. Behav.* 3, 156–165. doi: 10.4161/psb.3.3.5536.
- Czolginska, M., and Rurek, M. (2018). Plant glycine-rich proteins in stress response: An emerging, still prospective story. *Front. Plant Sci.* 9, 1–13. doi: 10.3389/fpls.2018.00302.
- Daher, F. B., and Braybrook, S. A. (2015). How to let go: Pectin and plant cell adhesion. *Front. Plant Sci.* 6, 1–8. doi: 10.3389/fpls.2015.00523.
- de Azevedo Souza, C., Li, S., Lin, A. Z., Boutrot, F., Grossmann, G., Zipfel, C., et al. (2017). Cellulose-derived oligomers act as damage-associated molecular patterns and trigger defense-like responses. *Plant Physiol.* 173, 2383–2398. doi: 10.1104/pp.16.01680.
- Decreux, A., Thomas, A., Spies, B., Bresseur, R., Cutsem, P. Van, and Messiaen, J. (2006). In vitro characterization of the homogalacturonan-binding domain of the wall-associated kinase WAK1 using site-directed mutagenesis. *Phytochemistry* 67, 1068–1079. doi: 10.1016/j.phytochem.2006.03.009.
- Delmer, D., Dixon, R. A., Keegstra, K., and Mohnen, D. (2024). The plant cell wall — dynamic, strong, and adaptable — is a natural shapeshifter. 1–55.
- Depuydt, S., Rodriguez-Villalon, A., Santuari, L., Wyser-Rmili, C., Ragni, L., and Hardtke, C. S. (2013). Suppression of Arabidopsis protophloem differentiation and root meristem growth by CLE45 requires the receptor-like kinase BAM3. *Proc. Natl. Acad. Sci. U. S. A.* 110, 7074–7079. doi: 10.1073/pnas.1222314110.
- Derba-Maceluch, M., Awano, T., Takahashi, J., Lucenius, J., Ratke, C., Kontro, I., et al. (2015). Suppression of xylan endotransglycosylase PxtXyn10A affects cellulose microfibril angle in secondary wall in aspen wood. *New Phytol.* 205, 666–681. doi: 10.1111/nph.13099.
- Deslauriers, S. D., and Larsen, P. B. (2010). FERONIA is a key modulator of brassinosteroid and ethylene responsiveness in Arabidopsis hypocotyls. *Mol. Plant* 3, 626–640. doi: 10.1093/mp/ssq015.
- Dewangan, B. P., Gupta, A., Sah, R. K., Das, S., Kumar, S., Bhattacharjee, S., et al.

- (2023). Xylobiose treatment triggers a defense-related response and alters cell wall composition. *Plant Mol. Biol.* 113, 383–400. doi: 10.1007/s11103-023-01391-z.
- Ding, Y., Fromm, M., and Avramova, Z. (2012). Multiple exposures to drought “train” transcriptional responses in Arabidopsis. *Nat. Commun.* 3. doi: 10.1038/ncomms1732.
- Doblas, V. G., Gonneau, M., and Höfte, H. (2018). Cell wall integrity signaling in plants: Malectin-domain kinases and lessons from other kingdoms. *Cell Surf.* 3, 1–11. doi: 10.1016/j.tcs.2018.06.001.
- Donaldson, L. A. (2001). Lignification and lignin topochemistry - An ultrastructural view. *Phytochemistry* 57, 859–873. doi: 10.1016/S0031-9422(01)00049-8.
- Donev, E., Gandla, M. L., Jönsson, L. J., and Mellerowicz, E. J. (2018). Engineering non-cellulosic polysaccharides of wood for the biorefinery. *Front. Plant Sci.* 871. doi: 10.3389/fpls.2018.01537.
- Du, J., Anderson, C. T., and Xiao, C. (2022). Dynamics of pectic homogalacturonan in cellular morphogenesis and adhesion, wall integrity sensing and plant development. *Nat. Plants* 8, 332–340. doi: 10.1038/s41477-022-01120-2.
- Dünser, K., Gupta, S., Herger, A., Feraru, M. I., Ringli, C., and Kleine-Vehn, J. (2019). Extracellular matrix sensing by FERONIA and Leucine-Rich Repeat Extensins controls vacuolar expansion during cellular elongation in Arabidopsis thaliana. *EMBO J.* 38, 1–12. doi: 10.15252/embj.2018100353.
- Ebringerová, A., and Heinze, T. (2000). Xylan and xylan derivatives - Biopolymers with valuable properties, 1: Naturally occurring xylans structures, isolation procedures and properties. *Macromol. Rapid Commun.* 21, 542–556. doi: 10.1002/1521-3927(20000601)21:9<542::AID-MARC542>3.0.CO;2-7.
- Ellis, C., Karafyllidis, I., Wasternack, C., and Turner, J. G. (2002). Erratum: The arabidopsis mutant cev1 links cell wall signaling to jasmonate and ethylene responses (Plant Cell (2002) 14 (1557-1566)). *Plant Cell* 14, 1981. doi: 10.1105/tpc.cor022.
- Ellis, C., and Turner, J. G. (2001). The Arabidopsis mutant cev1 has constitutively active jasmonate and ethylene signal pathways and enhanced resistance to pathogens. *Plant Cell* 13, 1025–1033. doi: 10.1105/tpc.13.5.1025.
- Engelsdorf, T., Gigli-Bisceglia, N., Veerabagu, M., McKenna, J. F., Vaahtera, L., Augstein, F., et al. (2018). The plant cell wall integrity maintenance and immune signaling systems cooperate to control stress responses in Arabidopsis thaliana. *Sci. Signal.* 11. doi: 10.1126/scisignal.aao3070.
- Fangel, J. U., Ulvskov, P., Knox, J. P., Mikkelsen, M. D., Harholt, J., Popper, Z. A., et al. (2012). Cell wall evolution and diversity. *Front. Plant Sci.* 3, 1–8. doi: 10.3389/fpls.2012.00152.
- Faria-Blanc, N., Mortimer, J. C., and Dupree, P. (2018). A transcriptomic analysis of Xylan mutants does not support the existence of a secondary cell wall integrity system in arabidopsis. *Front. Plant Sci.* 9, 1–12. doi: 10.3389/fpls.2018.00384.
- Feng, W., Kita, D., Peaucelle, A., Cartwright, H. N., Doan, V., Duan, Q., et al.

- (2018). The FERONIA Receptor Kinase Maintains Cell-Wall Integrity during Salt Stress through Ca²⁺ Signaling. *Curr. Biol.* 28, 666-675.e5. doi: 10.1016/j.cub.2018.01.023.
- Fichot, R., Barigah, T. S., Chamaillard, S., Le Thiec, D., Laurans, F., Cochard, H., et al. (2010). Common trade-offs between xylem resistance to cavitation and other physiological traits do not hold among unrelated *Populus deltoides* × *Populus nigra* hybrids. *Plant, Cell Environ.* 33, 1553–1568. doi: 10.1111/j.1365-3040.2010.02164.x.
- Franck, C. M., Westermann, J., and Boisson-Dernier, A. (2018). Plant Malectin-Like Receptor Kinases: From Cell Wall Integrity to Immunity and beyond. *Annu. Rev. Plant Biol.* 69, 301–328. doi: 10.1146/annurev-arplant-042817-040557.
- Fujii, H., Chinnusamy, V., Rodrigues, A., Rubio, S., Antoni, R., Park, S. Y., et al. (2009). In vitro reconstitution of an abscisic acid signalling pathway. *Nature* 462, 660–664. doi: 10.1038/nature08599.
- Gallego-Giraldo, L., Liu, C., Pose-Albacete, S., Pattathil, S., Peralta, A. G., Young, J., et al. (2020). ARABIDOPSIS DEHISCENCE ZONE POLYGALACTURONASE 1 (ADPG1) releases latent defense signals in stems with reduced lignin content. *Proc. Natl. Acad. Sci. U. S. A.* 117, 3281–3290. doi: 10.1073/pnas.1914422117.
- Gao, Q., Wang, C., Xi, Y., Shao, Q., Hou, C., Li, L., et al. (2023). RALF signaling pathway activates MLO calcium channels to maintain pollen tube integrity. *Cell Res.* 33, 71–79. doi: 10.1038/s41422-022-00754-3.
- Gao, Q., Wang, C., Xi, Y., Shao, Q., Li, L., and Luan, S. (2022). A receptor–channel trio conducts Ca²⁺ signalling for pollen tube reception. *Nature* 607, 534–539. doi: 10.1038/s41586-022-04923-7.
- Ge, Z., Bergonci, T., Zhao, Y., Zou, Y., Du, S., Liu, M.-C., et al. (2017). Arabidopsis pollen tube integrity and sperm release are regulated by RALF-mediated signaling. *Science* 358, 1596–1600. doi: 10.1126/science.aa03642.
- Geng, P., Zhang, S., Liu, J., Zhao, C., Wu, J., Cao, Y., et al. (2020). MYB20, MYB42, MYB43, and MYB85 regulate phenylalanine and lignin biosynthesis during secondary cell wall formation. *Plant Physiol.* 182, 1272–1283. doi: 10.1104/PP.19.01070.
- Ghosh, R., Barbacci, A., and Leblanc-Fournier, N. (2021). Mechanostimulation: A promising alternative for sustainable agriculture practices. *J. Exp. Bot.* 72, 2877–2888. doi: 10.1093/jxb/erab036.
- Gigli-Bisceglia, N., and Testerink, C. (2021). Fighting salt or enemies: shared perception and signaling strategies. *Curr. Opin. Plant Biol.* 64, 102120. doi: 10.1016/j.pbi.2021.102120.
- Gigli-Bisceglia, N., van Zelm, E., Huo, W., Lamers, J., and Testerink, C. (2022). Arabidopsis root responses to salinity depend on pectin modification and cell wall sensing. *Dev.* 149, 1–13. doi: 10.1242/dev.200363.
- Gille, S., de Souza, A., Xiong, G., Benz, M., Cheng, K., Schultink, A., et al. (2011). O-acetylation of Arabidopsis hemicellulose xyloglucan requires AXY4 or AXY4L, proteins with a TBL and DUF231 domain. *Plant Cell* 23, 4041–4053.

- doi: 10.1105/tpc.111.091728.
- Giummarella, N., and Lawoko, M. (2016). Structural Basis for the Formation and Regulation of Lignin-Xylan Bonds in Birch. *ACS Sustain. Chem. Eng.* 4, 5319–5326. doi: 10.1021/acssuschemeng.6b00911.
- Giummarella, N., Pu, Y., Ragauskas, A. J., and Lawoko, M. (2019). A critical review on the analysis of lignin carbohydrate bonds. *Green Chem.* 21, 1573–1595. doi: 10.1039/c8gc03606c.
- Goh, C. H., Gil Nam, H., and Shin Park, Y. (2003). Stress memory in plants: A negative regulation of stomatal response and transient induction of rd22 gene to light in abscisic acid-entrained Arabidopsis plants. *Plant J.* 36, 240–255. doi: 10.1046/j.1365-313X.2003.01872.x.
- Gonneau, M., Desprez, T., Martin, M., Doblaz, V. G., Bacete, L., Miart, F., et al. (2018). Receptor Kinase THESEUS1 Is a Rapid Alkalinization Factor 34 Receptor in Arabidopsis. *Curr. Biol.* 28, 2452–2458.e4. doi: 10.1016/j.cub.2018.05.075.
- Goujon, T., Minic, Z., El Amrani, A., Lerouxel, O., Aletti, E., Lapierre, C., et al. (2003). AtBXL1, a novel higher plant (*Arabidopsis thaliana*) putative beta-xylosidase gene, is involved in secondary cell wall metabolism and plant development. *Plant J.* 33, 677–690. doi: 10.1046/j.1365-313X.2003.01654.x.
- Grantham, N. J., Wurman-Rodrich, J., Terrett, O. M., Lyczakowski, J. J., Stott, K., Iuga, D., et al. (2017). An even pattern of xylan substitution is critical for interaction with cellulose in plant cell walls. *Nat. Plants* 3, 859–865. doi: 10.1038/s41477-017-0030-8.
- Guedes, F. T. P., Laurans, F., Quemener, B., Assor, C., Lainé-Prade, V., Boizot, N., et al. (2017). Non-cellulosic polysaccharide distribution during G-layer formation in poplar tension wood fibers: abundance of rhamnogalacturonan I and arabinogalactan proteins but no evidence of xyloglucan. *Planta* 246, 857–878. doi: 10.1007/s00425-017-2737-1.
- Guo, H., Li, L., Ye, H., Yu, X., Algreen, A., and Yin, Y. (2009). Three related receptor-like kinases are required for optimal cell elongation in *Arabidopsis thaliana*. *Proc. Natl. Acad. Sci. U. S. A.* 106, 7648–7653. doi: 10.1073/pnas.0812346106.
- Guo, H., Nolan, T. M., Song, G., Liu, S., Xie, Z., Chen, J., et al. (2018). FERONIA Receptor Kinase Contributes to Plant Immunity by Suppressing Jasmonic Acid Signaling in *Arabidopsis thaliana*. *Curr. Biol.* 28, 3316–3324.e6. doi: 10.1016/j.cub.2018.07.078.
- Hamann, T. (2012). Plant cell wall integrity maintenance as an essential component of biotic stress response mechanisms. *Front. Plant Sci.* 3, 1–5. doi: 10.3389/fpls.2012.00077.
- Hamann, T. (2015). The plant cell wall integrity maintenance mechanism - Concepts for organization and mode of action. *Plant Cell Physiol.* 56, 215–223. doi: 10.1093/pcp/pcu164.
- Hamant, O., and Mouliat, B. (2016). How do plants read their own shapes? *New Phytol.* 212, 333–337. doi: 10.1111/nph.14143.

- Hao, Z., Avci, U., Tan, L., Zhu, X., Glushka, J., Pattathil, S., et al. (2014). Loss of arabidopsis GAUT12/IRX8 causes anther indehiscence and leads to reduced G lignin associated with altered matrix polysaccharide deposition. *Front. Plant Sci.* 5, 1–21. doi: 10.3389/fpls.2014.00357.
- Hao, Z., and Mohnen, D. (2014). A review of xylan and lignin biosynthesis: Foundation for studying Arabidopsis irregular xylem mutants with pleiotropic phenotypes. *Crit. Rev. Biochem. Mol. Biol.* 49, 212–241. doi: 10.3109/10409238.2014.889651.
- Haruta, M., Sabat, G., Stecker, K., Minkoff, B. B., and Sussman, M. R. (2014). A peptide hormone and its receptor protein kinase regulate plant cell expansion. *Science (80-)*. 343, 408–411. doi: 10.1126/science.1244454.
- Haswell, E. S., and Verslues, P. E. (2015). The ongoing search for the molecular basis of plant osmosensing. *J. Gen. Physiol.* 145, 389–394. doi: 10.1085/jgp.201411295.
- Hayashi, T. (1989). Xyloglucans in the Primary Cell Wall. *Annu. Rev. Plant Physiol. Plant Mol. Biol.* 40, 139–168. doi: 10.1146/annurev.pp.40.060189.001035.
- Hayashi, T., and Kaida, R. (2011). Functions of xyloglucan in plant cells. *Mol. Plant* 4, 17–24. doi: 10.1093/mp/ssq063.
- Heil, M., and Land, W. G. (2014). Danger signals – Damaged-self recognition across the tree of life. *Front. Plant Sci.* 5, 1–16. doi: 10.3389/fpls.2014.00578.
- Held, M. A., Tan, L., Kamyabi, A., Hare, M., Shpak, E., and Kieliszewski, M. J. (2004). Di-isodityrosine is the intermolecular cross-link of isodityrosine-rich extensin analogs cross-linked in vitro. *J. Biol. Chem.* 279, 55474–55482. doi: 10.1074/jbc.M408396200.
- Hématy, K., Sado, P. E., Van Tuinen, A., Rochange, S., Desnos, T., Balzergue, S., et al. (2007). A Receptor-like Kinase Mediates the Response of Arabidopsis Cells to the Inhibition of Cellulose Synthesis. *Curr. Biol.* 17, 922–931. doi: 10.1016/j.cub.2007.05.018.
- Hernández-Blanco, C., Feng, D. X., Hu, J., Sánchez-Vallet, A., Deslandes, L., Llorente, F., et al. (2007). Impairment of cellulose synthases required for Arabidopsis secondary cell wall formation enhances disease resistance. *Plant Cell* 19, 890–903. doi: 10.1105/tpc.106.048058.
- Hernández-Blanco, C., Feng, D. X., Hu, J., Sánchez-Vallet, A., Deslandes, L., Llorente, F., et al. (2007). Impairment of Cellulose Synthases Required for Arabidopsis Secondary Cell Wall Formation Enhances Disease Resistance. *Plant Cell* 19, 890–903. doi: 10.1105/tpc.106.048058.
- Houtman, C. J., and Atalla, R. H. (1995). Cellulose-lignin interactions: A computational study. *Plant Physiol.* 107, 977–984. doi: 10.1104/pp.107.3.977.
- Huizinga, D. H., Denton, R., Koehler, K. G., Tomasello, A., Wood, L., Sen, S. E., et al. (2010). Farnesylcysteine lyase is involved in negative regulation of abscisic acid signaling in arabidopsis. *Mol. Plant* 3, 143–155. doi: 10.1093/mp/ssp091.
- Iakimova, E. T., and Woltering, E. J. (2017). Xylogenesis in zinnia (*Zinnia elegans*) cell cultures: unravelling the regulatory steps in a complex developmental programmed cell death event. *Planta* 245, 681–705. doi: 10.1007/s00425-017-

2656-1.

- Imamura, T., Watanabe, T., Kuwahara, M., and Koshijima, T. (1994). Ester linkages between lignin and glucuronic acid in lignin-carbohydrate complexes from *Fagus crenata*. *Phytochemistry* 37, 1165–1173. doi: 10.1016/S0031-9422(00)89551-5.
- Isasa, E., Link, R. M., Jansen, S., Tezeh, F. R., Kaack, L., Sarmiento Cabral, J., et al. (2023). Addressing controversies in the xylem embolism resistance–vessel diameter relationship. *New Phytol.* 238, 283–296. doi: 10.1111/nph.18731.
- Jacobsen, A. L., Brandon Pratt, R., Venturas, M. D., and Hacke, U. G. (2019). Large volume vessels are vulnerable to water-stress-induced embolism in stems of poplar. *IAWA J.* 40, 4–22. doi: 10.1163/22941932-40190233.
- Jalakas, P., Merilo, E., Kollist, H., and Brosché, M. (2018). ABA-mediated regulation of stomatal density is OST1-independent. *Plant Direct* 2. doi: 10.1002/pld3.82.
- Jang, G., Chang, S. H., Um, T. Y., Lee, S., Kim, J. K., and Choi, Y. Do (2017). Antagonistic interaction between jasmonic acid and cytokinin in xylem development. *Sci. Rep.* 7, 1–13. doi: 10.1038/s41598-017-10634-1.
- Jang, G., and Choi, Y. Do (2018). Drought stress promotes xylem differentiation by modulating the interaction between cytokinin and jasmonic acid. *Plant Signal. Behav.* 13, e1451707. doi: 10.1080/15592324.2018.1451707.
- Jang, G., Yoon, Y., and Choi, Y. Do (2019). Jasmonic Acid Modulates Xylem Development by Controlling Expression of PIN-FORMED 7. *Plant Signal. Behav.* 14. doi: 10.1080/15592324.2019.1637664.
- Jeong, B. C., Park, S. H., Yoo, K. S., Shin, J. S., and Song, H. K. (2012). Crystal structure of the single cystathionine b-synthase domain-containing protein CBSX1 from *Arabidopsis thaliana*. *Biochem. Biophys. Res. Commun.* doi: 10.1016/j.bbrc.2012.10.139.
- Jing, X. Q., Shalmani, A., Zhou, M. R., Shi, P. T., Muhammad, I., Shi, Y., et al. (2020). Genome-Wide Identification of Malectin/Malectin-Like Domain Containing Protein Family Genes in Rice and Their Expression Regulation Under Various Hormones, Abiotic Stresses, and Heavy Metal Treatments. *J. Plant Growth Regul.* 39, 492–506. doi: 10.1007/s00344-019-09997-8.
- Josè-Estanyol, M., and Puigdomènech, P. (2000). Plant cell wall glycoproteins and their genes. *Plant Physiol. Biochem.* 38, 97–108. doi: 10.1016/S0981-9428(00)00165-0.
- Jose, J., Ghantasala, S., and Choudhury, S. R. (2020). Arabidopsis transmembrane receptor-like kinases (RLKS): A bridge between extracellular signal and intracellular regulatory machinery. *Int. J. Mol. Sci.* 21, 1–29. doi: 10.3390/ijms21114000.
- Kai, D., Tan, M. J., Chee, P. L., Chua, Y. K., Yap, Y. L., and Loh, X. J. (2016). Towards lignin-based functional materials in a sustainable world. *Green Chem.* 18, 1175–1200. doi: 10.1039/c5gc02616d.
- Kamano, S., Kume, S., Iida, K., Lei, K. J., Nakano, M., Nakayama, Y., et al. (2015). Transmembrane Topologies of Ca²⁺-permeable Mechanosensitive Channels

- MCA1 and MCA2 in *Arabidopsis thaliana*. *J. Biol. Chem.* 290, 30901–30909. doi: 10.1074/jbc.M115.692574.
- Kang, X., Kirui, A., Dickwella Widanage, M. C., Mentink-Vigier, F., Cosgrove, D. J., and Wang, T. (2019). Lignin-polysaccharide interactions in plant secondary cell walls revealed by solid-state NMR. *Nat. Commun.* 10, 1–9. doi: 10.1038/s41467-018-08252-0.
- Kanneganti, V., and Gupta, A. K. (2008). Wall associated kinases from plants - An overview. *Physiol. Mol. Biol. Plants* 14, 109–118. doi: 10.1007/s12298-008-0010-6.
- Keegstra, K., Talmadge, K. W., Bauer, W. D., and Albersheim, P. (1973). The Structure of Plant Cell Walls: III. A Model of the Walls of Suspension-cultured Sycamore Cells Based on the Interconnections of the Macromolecular Components. *Plant Physiol.* 51, 188–197. doi: 10.1104/pp.51.1.188.
- Keinath, N. F., Kierszniowska, S., Lorek, J., Bourdais, G., Kessler, S. A., Shimosato-Asano, H., et al. (2010). PAMP (Pathogen-associated Molecular Pattern)-induced changes in plasma membrane compartmentalization reveal novel components of plant immunity. *J. Biol. Chem.* 285, 39140–39149. doi: 10.1074/jbc.M110.160531.
- Keller, B. (1993). Structural cell wall proteins. *Plant Physiol.* 101, 1127–1130. doi: 10.1104/pp.101.4.1127.
- Kepler, B. D., and Showalter, A. M. (2010). IRX14 and IRX14-LIKE, two glycosyl transferases involved in glucuronoxylan biosynthesis and drought tolerance in *Arabidopsis*. *Mol. Plant* 3, 834–841. doi: 10.1093/mp/ssq028.
- Kerchev, P., van der Meer, T., Sujeeth, N., Verlee, A., Stevens, C. V., Van Breusegem, F., et al. (2020). Molecular priming as an approach to induce tolerance against abiotic and oxidative stresses in crop plants. *Biotechnol. Adv.* 40, 107503. doi: 10.1016/j.biotechadv.2019.107503.
- Keynia, S., Jaafar, L., Zhou, Y., Anderson, C. T., and Turner, J. A. (2023). Stomatal opening efficiency is controlled by cell wall organization in *Arabidopsis thaliana*. *PNAS Nexus* 2, 1–10. doi: 10.1093/pnasnexus/pgad294.
- Kim, H. J., Chiang, Y. H., Kieber, J. J., and Schaller, G. E. (2013). SCFKMD controls cytokinin signaling by regulating the degradation of type-B response regulators. *Proc. Natl. Acad. Sci. U. S. A.* 110, 10028–10033. doi: 10.1073/pnas.1300403110.
- Kirui, A., Zhao, W., Deligey, F., Yang, H., Kang, X., Mentink-Vigier, F., et al. (2022). Carbohydrate-aromatic interface and molecular architecture of lignocellulose. *Nat. Commun.* 13, 1–12. doi: 10.1038/s41467-022-28165-3.
- Knogge, W., Lee, J., Rosahl, S., and Scheel, D. (2009). “Signal Perception and Transduction in Plants,” in *The Mycota*, ed. H. B. Deising (Berlin, Heidelberg: Springer Berlin Heidelberg), 337–361. doi: 10.1007/978-3-540-87407-2_17.
- Kohorn, B. D., Johansen, S., Shishido, A., Todorova, T., Martinez, R., Defeo, E., et al. (2009). Pectin activation of MAP kinase and gene expression is WAK2 dependent. *Plant J.* 60, 974–982. doi: 10.1111/j.1365-313X.2009.04016.x.
- Kojima, K., Sunagawa, N., Yoshimi, Y., Tryfona, T., Samejima, M., Dupree, P., et

- al. (2022). Acetylated Xylan Degradation by Glycoside Hydrolase Family 10 and 11 Xylanases from the White-rot Fungus *Phanerochaete chrysosporium*. *J. Appl. Glycosci.* 69, 35–43. doi: 10.5458/jag.jag-2021_0017.
- Kolenová, K., Vršanská, M., and Biely, P. (2006). Mode of action of endo- β -1,4-xylanases of families 10 and 11 on acidic xylooligosaccharides. *J. Biotechnol.* 121, 338–345. doi: 10.1016/j.jbiotec.2005.08.001.
- Kong, Y., Zhou, G., Avci, U., Gu, X., Jones, C., Yin, Y., et al. (2009). Two poplar glycosyltransferase genes, PdGATL1.1 and PdGATL1.2, are functional orthologs to PARVUS/AtGATL1 in Arabidopsis. *Mol. Plant* 2, 1040–1050. doi: 10.1093/mp/ssp068.
- Kouhen, M., Dimitrova, A., Scippa, G. S., and Trupiano, D. (2023). The Course of Mechanical Stress: Types, Perception, and Plant Response. *Biology (Basel)*. 12. doi: 10.3390/biology12020217.
- Kubicki, J. D., Yang, H., Sawada, D., O'Neill, H., Oehme, D., and Cosgrove, D. (2018). The Shape of Native Plant Cellulose Microfibrils. *Sci. Rep.* 8, 4–11. doi: 10.1038/s41598-018-32211-w.
- Kulkarni, A. R., Peña, M. J., Avci, U., Mazumder, K., Urbanowicz, B. R., Pattathil, S., et al. (2012). The ability of land plants to synthesize glucuronoxylans predates the evolution of tracheophytes. *Glycobiology* 22, 439–451. doi: 10.1093/glycob/cwr117.
- Kushwah, S., Banasiak, A., Nishikubo, N., Derba-Maceluch, M., Majda, M., Endo, S., et al. (2020). Arabidopsis XTH4 and XTH9 contribute to wood cell expansion and secondary wall formation1[Open]. *Plant Physiol.* 182, 1946–1965. doi: 10.1104/PP.19.01529.
- Le Gall, H., Philippe, F., Domon, J. M., Gillet, F., Pelloux, J., and Rayon, C. (2015). Cell wall metabolism in response to abiotic stress. *Plants* 4, 112–166. doi: 10.3390/plants4010112.
- Leblanc-Fournier, N., Martin, L., Lenne, C., and Decourteix, M. (2014). To respond or not to respond, the recurring question in plant mechanosensitivity. *Front. Plant Sci.* 5, 1–7. doi: 10.3389/fpls.2014.00401.
- Lee, C., Teng, Q., Huang, W., Zhong, R., and Ye, Z. H. (2009). The F8H glycosyltransferase is a functional paralog of FRA8 involved in glucuronoxylan biosynthesis in arabidopsis. *Plant Cell Physiol.* 50, 812–827. doi: 10.1093/pcp/pcp025.
- Lee, C., Teng, Q., Zhong, R., and Ye, Z. H. (2011). The Four Arabidopsis REDUCED WALL ACETYLATION Genes are expressed in secondary wall-containing cells and required for the acetylation of Xylan. *Plant Cell Physiol.* 52, 1289–1301. doi: 10.1093/pcp/pcr075.
- Lee, C., Teng, Q., Zhong, R., and Ye, Z. H. (2014). Alterations of the degree of xylan acetylation in Arabidopsis xylan mutants. *Plant Signal. Behav.* 9. doi: 10.4161/psb.27797.
- Lee, C., Zhong, R., Richardson, E. A., Himmelsbach, D. S., McPhail, B. T., and Ye, Z. H. (2007). The PARVUS gene is expressed in cells undergoing secondary wall thickening and is essential for glucuronoxylan biosynthesis. *Plant Cell*

- Physiol.* 48, 1659–1672. doi: 10.1093/pcp/pcm155.
- Lee, C., Zhong, R., and Ye, Z. H. (2012). Arabidopsis family GT43 members are xylan xylosyltransferases required for the elongation of the xylan backbone. *Plant Cell Physiol.* 53, 135–143. doi: 10.1093/pcp/pcr158.
- Lee, S., and Park, C. M. (2012). Regulation of reactive oxygen species generation under drought conditions in arabidopsis. *Plant Signal. Behav.* 7, 599–601. doi: 10.4161/psb.19940.
- Lefebvre, V., Fortabat, M. N., Ducamp, A., North, H. M., Maia-Grondard, A., Trouverie, J., et al. (2011). ESKIMO1 disruption in Arabidopsis alters vascular tissue and impairs water transport. *PLoS One* 6. doi: 10.1371/journal.pone.0016645.
- Lens, F., Gleason, S. M., Bortolami, G., Brodersen, C., Delzon, S., and Jansen, S. (2022). Functional xylem characteristics associated with drought-induced embolism in angiosperms. *New Phytol.* 236, 2019–2036. doi: 10.1111/nph.18447.
- Lens, F., Gleason, S. M., Bortolami, G., Brodersen, C., Delzon, S., and Jansen, S. (2023). Comparative anatomy vs mechanistic understanding: how to interpret the diameter-vulnerability link. *IAWA J.* 1, 368–380. doi: 10.1163/22941932-bja10137.
- Leszczuk, A., Kalaitzis, P., Kulik, J., and Zdunek, A. (2023). Review: structure and modifications of arabinogalactan proteins (AGPs). *BMC Plant Biol.* 23, 1–12. doi: 10.1186/s12870-023-04066-5.
- Li, C., Yeh, F. L., Cheung, A. Y., Duan, Q., Kita, D., Liu, M. C., et al. (2015). Glycosylphosphatidylinositol-anchored proteins as chaperones and co-receptors for FERONIA receptor kinase signaling in Arabidopsis. *Elife* 4, 1–21. doi: 10.7554/eLife.06587.
- Li, S., Zhang, Y., Ding, C., Gao, X., Wang, R., Mo, W., et al. (2019). Proline-rich protein gene PdPRP regulates secondary wall formation in poplar. *J. Plant Physiol.* 233, 58–72. doi: 10.1016/j.jplph.2018.12.007.
- Liu, C., Yu, H., Rao, X., Li, L., and Dixon, R. A. (2021). Abscisic acid regulates secondary cell-wall formation and lignin deposition in Arabidopsis thaliana through phosphorylation of NST1. *Proc. Natl. Acad. Sci. U. S. A.* 118, 1–11. doi: 10.1073/pnas.2010911118.
- Liu, C., Yu, H., Voxeur, A., Rao, X., and Dixon, R. A. (2023). FERONIA and wall-associated kinases coordinate defense induced by lignin modification in plant cell walls. *Sci. Adv.* 9, 1–14. doi: 10.1126/sciadv.adf7714.
- Liu, H., Song, S., Zhang, H., Li, Y., Niu, L., Zhang, J., et al. (2022). Signaling Transduction of ABA, ROS, and Ca²⁺ in Plant Stomatal Closure in Response to Drought. *Int. J. Mol. Sci.* 23. doi: 10.3390/ijms232314824.
- Lotze, M. T., Zeh, H. J., Rubartelli, A., Sparvero, L. J., Amoscato, A. A., Washburn, N. R., et al. (2007). The grateful dead: Damage-associated molecular pattern molecules and reduction/oxidation regulate immunity. *Immunol. Rev.* 220, 60–81. doi: 10.1111/j.1600-065X.2007.00579.x.
- Loveys, B., and Kriedemann, P. (1974). Internal Control of Stomatal Physiology and

- Photosynthesis. I. Stomatal Regulation and Associated Changes in Endogenous Levels of Abscisic and Phaseic Acids. *Funct. Plant Biol.* 1, 407. doi: 10.1071/pp9740407.
- Lovisolò, C., and Schubert, A. (1998). Effects of water stress on vessel size and xylem hydraulic conductivity in *Vitis vinifera* L. *J. Exp. Bot.* 49, 693–700. doi: 10.1093/jxb/49.321.693.
- Lyczakowski, J. J., Bourdon, M., Terrett, O. M., Helariutta, Y., Wightman, R., and Dupree, P. (2019). Structural Imaging of Native Cryo-Preserved Secondary Cell Walls Reveals the Presence of Macrofibrils and Their Formation Requires Normal Cellulose, Lignin and Xylan Biosynthesis. *Front. Plant Sci.* 10, 1–14. doi: 10.3389/fpls.2019.01398.
- Lyczakowski, J. J., Wicher, K. B., Terrett, O. M., Faria-Blanc, N., Yu, X., Brown, D., et al. (2017). Removal of glucuronic acid from xylan is a strategy to improve the conversion of plant biomass to sugars for bioenergy. *Biotechnol. Biofuels* 10, 1–11. doi: 10.1186/s13068-017-0902-1.
- Ma, L., Cheng, K., Li, J., Deng, Z., Zhang, C., and Zhu, H. (2021). Roles of plant glycine-rich rna-binding proteins in development and stress responses. *Int. J. Mol. Sci.* 22. doi: 10.3390/ijms22115849.
- Ma, Y., MacMillan, C. P., de Vries, L., Mansfield, S. D., Hao, P., Ratcliffe, J., et al. (2022). FLA11 and FLA12 glycoproteins fine-tune stem secondary wall properties in response to mechanical stresses. *New Phytol.* 233, 1750–1767. doi: 10.1111/nph.17898.
- Ma, Y., Ratcliffe, J., Bacic, A., and Johnson, K. L. (2023). Promoter and domain structures regulate FLA12 function during *Arabidopsis* secondary wall development. *Front. Plant Sci.* 14, 1–11. doi: 10.3389/fpls.2023.1275983.
- Malivert, A., Erguvan, Ö., Chevallier, A., Dehem, A., Friaud, R., Liu, M., et al. (2021). FERONIA and microtubules independently contribute to mechanical integrity in the *Arabidopsis* shoot. *PLoS Biol.* 19, 1–22. doi: 10.1371/journal.pbio.3001454.
- Manabe, Y., Nafisi, M., Verhertbruggen, Y., Orfila, C., Gille, S., Rautengarten, C., et al. (2011). Loss-of-function mutation of REDUCED WALL ACETYLATION2 in *Arabidopsis* leads to reduced cell wall acetylation and increased resistance to *Botrytis cinerea*. *Plant Physiol.* 155, 1068–1078. doi: 10.1104/pp.110.168989.
- Mang, H., Feng, B., Hu, Z., Boisson-Dernier, A., Franck, C. M., Meng, X., et al. (2017). Differential regulation of two-tiered plant immunity and sexual reproduction by ANXUR receptor-like kinases. *Plant Cell* 29, 3140–3156. doi: 10.1105/tpc.17.00464.
- Marriott, P. E., Gómez, L. D., and Mcqueen-Mason, S. J. (2016). Unlocking the potential of lignocellulosic biomass through plant science. *New Phytol.* 209, 1366–1381. doi: 10.1111/nph.13684.
- Marshall, A., Aalen, R. B., Audenaert, D., Beeckman, T., Broadley, M. R., Butenko, M. A., et al. (2012). Tackling drought stress: RECEPTOR-LIKE KINASES present new approaches. *Plant Cell* 24, 2262–2278. doi:

- 10.1105/tpc.112.096677.
- Martínez-Abad, A., Berglund, J., Toriz, G., Gatenholm, P., Henriksson, G., Lindström, M., et al. (2017). Regular motifs in xylan modulate molecular flexibility and interactions with cellulose surfaces. *Plant Physiol.* 175, 1579–1592. doi: 10.1104/pp.17.01184.
- Martínez-Abad, A., Giummarella, N., Lawoko, M., and Vilaplana, F. (2018). Differences in extractability under subcritical water reveal interconnected hemicellulose and lignin recalcitrance in birch hardwoods. *Green Chem.* 20, 2534–2546. doi: 10.1039/c8gc00385h.
- Martorell, S., Diaz-Espejo, A., Medrano, H., Ball, M. C., and Choat, B. (2014). Rapid hydraulic recovery in *Eucalyptus pauciflora* after drought: Linkages between stem hydraulics and leaf gas exchange. *Plant, Cell Environ.* 37, 617–626. doi: 10.1111/pce.12182.
- McDougall, G. J., Morrison, I. M., Stewart, D., Weyers, J. D. B., and Hillman, J. R. (1993). Plant fibres: Botany, chemistry and processing for industrial use. *J. Sci. Food Agric.* 62, 1–20. doi: 10.1002/jsfa.2740620102.
- Mélida, H., Bacete, L., Ruprecht, C., Rebaque, D., del Hierro, I., López, G., et al. (2020). Arabinoxylan-Oligosaccharides Act as Damage Associated Molecular Patterns in Plants Regulating Disease Resistance. *Front. Plant Sci.* 11, 1–16. doi: 10.3389/fpls.2020.01210.
- Mellerowicz, E. J., Baucher, M., Sundberg, B., and Boerjan, W. (2001). Unravelling cell wall formation in the woody dicot stem. *Plant Mol. Biol.* 47, 239–274. doi: 10.1023/A:1010699919325.
- Mellerowicz, E. J., and Gorshkova, T. A. (2012). Tensional stress generation in gelatinous fibres: A review and possible mechanism based on cell-wall structure and composition. *J. Exp. Bot.* 63, 551–565. doi: 10.1093/jxb/err339.
- Melnyk, C. W., Gabel, A., Hardcastle, T. J., Robinson, S., Miyashima, S., Grosse, I., et al. (2018). Transcriptome dynamics at Arabidopsis graft junctions reveal an intertissue recognition mechanism that activates vascular regeneration. *Proc. Natl. Acad. Sci. U. S. A.* 115, E2447–E2456. doi: 10.1073/pnas.1718263115.
- Mikkelsen, D., Flanagan, B. M., Wilson, S. M., Bacic, A., and Gidley, M. J. (2015). Interactions of Arabinoxylan and (1,3)(1,4)- β -Glucan with Cellulose Networks. *Biomacromolecules* 16, 1232–1239. doi: 10.1021/acs.biomac.5b00009.
- Monshausen, G. B., and Haswell, E. S. (2013). A force of nature: Molecular mechanisms of mechanoperception in plants. *J. Exp. Bot.* 64, 4663–4680. doi: 10.1093/jxb/ert204.
- Morato do Canto, A., Ceciliato, P. H. O., Ribeiro, B., Ortiz Morea, F. A., Franco Garcia, A. A., Silva-Filho, M. C., et al. (2014). Biological activity of nine recombinant AtRALF peptides: Implications for their perception and function in Arabidopsis. *Plant Physiol. Biochem.* 75, 45–54. doi: 10.1016/j.plaphy.2013.12.005.
- Mortimer, J. C., Faria-Blanc, N., Yu, X., Tryfona, T., Sorieul, M., Ng, Y. Z., et al.

- (2015). An unusual xylan in *Arabidopsis* primary cell walls is synthesised by GUX3, IRX9L, IRX10L and IRX14. *Plant J.* 83, 413–426. doi: 10.1111/tbj.12898.
- Mortimer, J. C., Miles, G. P., Brown, D. M., Zhang, Z., Segura, M. P., Weimar, T., et al. (2010). Absence of branches from xylan in *Arabidopsis* gux mutants reveals potential for simplification of lignocellulosic biomass. *Proc. Natl. Acad. Sci. U. S. A.* 107, 17409–17414. doi: 10.1073/pnas.1005456107.
- Moussu, S., Augustin, S., Roman, A. O., Broyart, C., and Santiago, J. (2018). Crystal structures of two tandem malectin-like receptor kinases involved in plant reproduction. *Acta Crystallogr. Sect. D Struct. Biol.* 74, 671–680. doi: 10.1107/S205979831800774X.
- Müller, M., and Munné-Bosch, S. (2015). Ethylene response factors: A key regulatory hub in hormone and stress signaling. *Plant Physiol.* 169, 32–41. doi: 10.1104/pp.15.00677.
- Murphy, E., Vu, L. D., Van Den Broeck, L., Lin, Z., Ramakrishna, P., Van De Cotte, B., et al. (2016). RALFL34 regulates formative cell divisions in *Arabidopsis* pericycle during lateral root initiation. *J. Exp. Bot.* 67, 4863–4875. doi: 10.1093/jxb/erw281.
- Mustilli, A. C., Merlot, S., Vavasseur, A., Fenzi, F., and Giraudat, J. (2002). *Arabidopsis* OST1 protein kinase mediates the regulation of stomatal aperture by abscisic acid and acts upstream of reactive oxygen species production. *Plant Cell* 14, 3089–3099. doi: 10.1105/tpc.007906.
- Nakagawa, Y., Katagiri, T., Shinozaki, K., Qi, Z., Tatsumi, H., Furuichi, T., et al. (2007). *Arabidopsis* plasma membrane protein crucial for Ca²⁺ influx and touch sensing in roots. *Proc. Natl. Acad. Sci. U. S. A.* 104, 3639–3644. doi: 10.1073/pnas.0607703104.
- Nguyen, K. H., Ha, C. Van, Nishiyama, R., Watanabe, Y., Leyva-González, M. A., Fujita, Y., et al. (2016). *Arabidopsis* type B cytokinin response regulators ARR1, ARR10, and ARR12 negatively regulate plant responses to drought. *Proc. Natl. Acad. Sci. U. S. A.* 113, 3090–3095. doi: 10.1073/pnas.1600399113.
- Nieminen, K., Robischon, M., Immanen, J., and Helariutta, Y. (2012). Towards optimizing wood development in bioenergy trees. *New Phytol.* 194, 46–53. doi: 10.1111/j.1469-8137.2011.04011.x.
- NIKLAS, K. J. (2004). The Cell Walls that Bind the Tree of Life. *Bioscience* 54, 831. doi: 10.1641/0006-3568(2004)054[0831:tcwtbt]2.0.co;2.
- Nishikubo, N., Awano, T., Banasiak, A., Bourquin, V., Ibatullin, F., Funada, R., et al. (2007). Xyloglucan endo-transglycosylase (XET) functions in gelatinous layers of tension wood fibers in poplar - A glimpse into the mechanism of the balancing act of trees. *Plant Cell Physiol.* 48, 843–855. doi: 10.1093/pcp/pcm055.
- Nishimura, H. (2022). Direct evidence of α ester linkages between lignin and glucuronoxylan that reveal the robust heteropolymeric complex in plant cell walls.

- Novaković, L., Guo, T., Bacic, A., Sampathkumar, A., and Johnson, K. L. (2018). Hitting the wall—sensing and signaling pathways involved in plant cell wall remodeling in response to abiotic stress. *Plants* 7, 1–25. doi: 10.3390/plants7040089.
- Nunez, A., Fishman, M. L., Fortis, L. L., Cooke, P. H., and Hotchkiss, A. T. (2009). Identification of extensin protein associated with sugar beet pectin. *J. Agric. Food Chem.* 57, 10951–10958. doi: 10.1021/jf902162t.
- O'NEILL, M., ALBERSHEIM, P., and DARVILL, A. (1990). “12 - The Pectic Polysaccharides of Primary Cell Walls,” in *Carbohydrates Methods in Plant Biochemistry.*, ed. P. M. DEY (Academic Press), 415–441. doi: <https://doi.org/10.1016/B978-0-12-461012-5.50018-5>.
- Oliveira, D. M. (2023). Glucuronic acid: not just another brick in the cell wall. *New Phytol.* 238, 8–10. doi: 10.1111/nph.18804.
- Oliveira, D. M., Mota, T. R., Salatta, F. V., Marchiosi, R., Gomez, L. D., McQueen-Mason, S. J., et al. (2019). Designing xylan for improved sustainable biofuel production. *Plant Biotechnol. J.* 17, 2225–2227. doi: 10.1111/pbi.13150.
- Panshin, A. J., and De Zeeuw, C. (1980). *Textbook of Wood Technology: Structure, Identification, Properties, and Uses of the Commercial Woods of the United States and Canada.* McGraw-Hill Available at: <https://books.google.se/books?id=B1HxAAAAMAAJ>.
- Park, A. R., Cho, S. K., Yun, U. J., Jin, M. Y., Lee, S. H., Sachetto-Martins, G., et al. (2001). Interaction of the Arabidopsis Receptor Protein Kinase Wak1 with a Glycine-rich Protein, AtGRP-3. *J. Biol. Chem.* 276, 26688–26693. doi: 10.1074/jbc.M101283200.
- Park, Y. B., and Cosgrove, D. J. (2015). Xyloglucan and its interactions with other components of the growing cell wall. *Plant Cell Physiol.* 56, 180–194. doi: 10.1093/pcp/pcu204.
- Pawar, P. M. A., Derba-Maceluch, M., Chong, S. L., Gómez, L. D., Miedes, E., Banasiak, A., et al. (2016). Expression of fungal acetyl xylan esterase in Arabidopsis thaliana improves saccharification of stem lignocellulose. *Plant Biotechnol. J.* 14, 387–397. doi: 10.1111/pbi.12393.
- Pawar, P. M. A., Koutaniemi, S., Tenkanen, M., and Mellerowicz, E. J. (2013). Acetylation of woody lignocellulose: Significance and regulation. *Front. Plant Sci.* 4, 1–8. doi: 10.3389/fpls.2013.00118.
- Pawar, P. M. A., Ratke, C., Balasubramanian, V. K., Chong, S. L., Gandla, M. L., Adriasola, M., et al. (2017). Downregulation of RWA genes in hybrid aspen affects xylan acetylation and wood saccharification. *New Phytol.* 214, 1491–1505. doi: 10.1111/nph.14489.
- Pearce, G., Moura, D. S., Stratmann, J., and Ryan, C. A. (2001). RALF, a 5-kDa ubiquitous polypeptide in plants, arrests root growth and development. *Proc. Natl. Acad. Sci. U. S. A.* 98, 12843–12847. doi: 10.1073/pnas.201416998.
- Pei, S., Liu, Y., Li, W., Krichilsky, B., Dai, S., Wang, Y., et al. (2022). OSCA1 is an osmotic specific sensor: a method to distinguish Ca²⁺-mediated osmotic and ionic perception. *New Phytol.* 235, 1665–1678. doi: 10.1111/nph.18217.

- Pell, G., Taylor, E. J., Gloster, T. M., Turkenburg, J. P., Fontes, C. M. G. A., Ferreira, L. M. A., et al. (2004). The Mechanisms by Which Family 10 Glycoside Hydrolases Bind Decorated Substrates. *J. Biol. Chem.* 279, 9597–9605. doi: 10.1074/jbc.M312278200.
- Peña, M. J., Zhong, R., Zhou, G. K., Richardson, E. A., O’Neill, M. A., Darvill, A. G., et al. (2007). Arabidopsis irregular xylem8 and irregular xylem9: Implications for the complexity of glucuronoxylan biosynthesis. *Plant Cell* 19, 549–563. doi: 10.1105/tpc.106.049320.
- Persson, S., Caffall, K. H., Freshour, G., Hilley, M. T., Bauer, S., Poindexter, P., et al. (2007). The Arabidopsis irregular xylem8 mutant is deficient in glucuronoxylan and homogalacturonan, which are essential for secondary cell wall integrity. *Plant Cell* 19, 237–255. doi: 10.1105/tpc.106.047720.
- Pesquet, E., Zhang, B., Gorzsás, A., Puhakainen, T., Serk, H., Escamez, S., et al. (2013). Non-cell-autonomous postmortem lignification of tracheary elements in *Zinnia elegans*. *Plant Cell* 25, 1314–1328. doi: 10.1105/tpc.113.110593.
- Pinheiro, C., and Chaves, M. M. (2011). Photosynthesis and drought: Can we make metabolic connections from available data? *J. Exp. Bot.* 62, 869–882. doi: 10.1093/jxb/erq340.
- Plett, J. M., Mathur, J., and Regan, S. (2009). Ethylene receptor ETR2 controls trichome branching by regulating microtubule assembly in arabidopsis thaliana. *J. Exp. Bot.* 60, 3923–3933. doi: 10.1093/jxb/erp228.
- Pontiggia, D., Benedetti, M., Costantini, S., De Lorenzo, G., and Cervone, F. (2020). Dampening the DAMPs: How Plants Maintain the Homeostasis of Cell Wall Molecular Patterns and Avoid Hyper-Immunity. *Front. Plant Sci.* 11. doi: 10.3389/fpls.2020.613259.
- Popa, V. I. (2017). Hemicelluloses. *Polysaccharides Med. Appl.*, 107–124. doi: 10.1201/9780203742815.
- Popper, Z. A., Michel, G., Hervé, C., Domozych, D. S., Willats, W. G. T., Tuohy, M. G., et al. (2011). Evolution and diversity of plant cell walls: From algae to flowering plants. *Annu. Rev. Plant Biol.* 62, 567–590. doi: 10.1146/annurev-arplant-042110-103809.
- Pramod, S., Gandla, M. L., Derba-Maceluch, M., Jönsson, L. J., Mellerowicz, E. J., and Winestrand, S. (2021). Saccharification Potential of Transgenic Greenhouse- and Field-Grown Aspen Engineered for Reduced Xylan Acetylation. *Front. Plant Sci.* 12. doi: 10.3389/fpls.2021.704960.
- Puijalón, S., Bouma, T. J., Douady, C. J., van Groenendael, J., Anten, N. P. R., Martel, E., et al. (2011). Plant resistance to mechanical stress: Evidence of an avoidance-tolerance trade-off. *New Phytol.* 191, 1141–1149. doi: 10.1111/j.1469-8137.2011.03763.x.
- Qaseem, M. F., and Wu, A. M. (2020). Balanced xylan acetylation is the key regulator of plant growth and development, and cell wall structure and for industrial utilization. *Int. J. Mol. Sci.* 21, 1–21. doi: 10.3390/ijms21217875.
- Qi, X., Behrens, B. X., West, P. R., and Mort, A. J. (1995). Solubilization and partial characterization of extensin fragments from cell walls of cotton suspension

- cultures: Evidence for a covalent cross-link between extensin and pectin. *Plant Physiol.* 108, 1691–1701. doi: 10.1104/pp.108.4.1691.
- Qin, X., and Zeevaart, J. A. D. (1999). The 9-cis-epoxycarotenoid cleavage reaction is the key regulatory step of abscisic acid biosynthesis in water-stressed bean. *Proc. Natl. Acad. Sci. U. S. A.* 96, 15354–15361. doi: 10.1073/pnas.96.26.15354.
- Qin, Y. C., Lee, W. C., Choi, Y. C., and Kim, T. W. (2003). Biochemical and physiological changes in plants as a result of different sonic exposures. *Ultrasonics* 41, 407–411. doi: 10.1016/S0041-624X(03)00103-3.
- Ramírez, V., and Pauly, M. (2019). Genetic dissection of cell wall defects and the strigolactone pathway in Arabidopsis. *Plant Direct* 3, 1–11. doi: 10.1002/pld3.149.
- Ramírez, V., Xiong, G., Mashiguchi, K., Yamaguchi, S., and Pauly, M. (2018). Growth- and stress-related defects associated with wall hypoacetylation are strigolactone-dependent. *Plant Direct* 2, e00062. doi: 10.1002/pld3.62.
- Rastogi, L., Chaudhari, A. A., Sharma, R., and Pawar, P. A. M. (2022). Arabidopsis GELP7 functions as a plasma membrane-localized acetyl xylan esterase, and its overexpression improves saccharification efficiency. *Plant Mol. Biol.* 109, 781–797. doi: 10.1007/s11103-022-01275-8.
- Ratke, C., Pawar, P. M. A., Balasubramanian, V. K., Naumann, M., Duncranz, M. L., Derba-Maceluch, M., et al. (2015). Populus GT43 family members group into distinct sets required for primary and secondary wall xylan biosynthesis and include useful promoters for wood modification. *Plant Biotechnol. J.* 13, 26–37. doi: 10.1111/pbi.12232.
- Ratke, C., Terebieniec, B. K., Winstrand, S., Derba-Maceluch, M., Grahm, T., Schiffthaler, B., et al. (2018). Downregulating aspen xylan biosynthetic GT43 genes in developing wood stimulates growth via reprogramming of the transcriptome. *New Phytol.* 219, 230–245. doi: 10.1111/nph.15160.
- Raza, A., Mubarak, M. S., Sharif, R., Habib, M., Jabeen, W., Zhang, C., et al. (2023). Developing drought-smart, ready-to-grow future crops. *Plant Genome* 16, 1–37. doi: 10.1002/tpg2.20279.
- Rennie, E. A., Hansen, S. F., Baidoo, E. E. K., Hadi, M. Z., Keasling, J. D., and Scheller, H. V. (2012). Three members of the Arabidopsis glycosyltransferase family 8 are xylan glucuronosyltransferases. *Plant Physiol.* 159, 1408–1417. doi: 10.1104/pp.112.200964.
- Rennie, E. A., and Scheller, H. V. (2014). Xylan biosynthesis. *Curr. Opin. Biotechnol.* 26, 100–107. doi: 10.1016/j.copbio.2013.11.013.
- Rinaldi, R., Jastrzebski, R., Clough, M. T., Ralph, J., Kennema, M., Bruijninx, P. C. A., et al. (2016). Paving the Way for Lignin Valorisation: Recent Advances in Bioengineering, Biorefining and Catalysis. *Angew. Chemie - Int. Ed.* 55, 8164–8215. doi: 10.1002/anie.201510351.
- Ringli, C., Keller, B., and Ryser, U. (2001). Glycine-rich proteins as structural components of plant cell walls. *Cell. Mol. Life Sci.* 58, 1430–1441. doi: 10.1007/PL00000786.

- Roignant, J., Badel, É., Leblanc-Fournier, N., Brunel-Michac, N., Ruelle, J., Moulia, B., et al. (2018). Feeling stretched or compressed? the multiple mechanosensitive responses of wood formation to bending. *Ann. Bot.* 121, 1151–1161. doi: 10.1093/aob/mcx211.
- Ros Barceló, A. (1997). Lignification in plant cell walls. *Int. Rev. Cytol.* 176, 87–132. doi: 10.1016/s0074-7696(08)61609-5.
- Rui, Y., Chen, Y., Kandemir, B., Yi, H., Wang, J. Z., Puri, V. M., et al. (2018). Balancing strength and flexibility: how the synthesis, organization, and modification of guard cell walls govern stomatal development and dynamics. *Front. Plant Sci.* 9, 1–11. doi: 10.3389/fpls.2018.01202.
- Rui, Y., and Dinneny, J. R. (2020). A wall with integrity: surveillance and maintenance of the plant cell wall under stress. *New Phytol.* 225, 1428–1439. doi: 10.1111/nph.16166.
- Savatin, D. V., Gramegna, G., Modesti, V., and Cervone, F. (2014). Wounding in the plant tissue: The defense of a dangerous passage. *Front. Plant Sci.* 5, 1–11. doi: 10.3389/fpls.2014.00470.
- Schallus, T., Jaeckh, C., Fehér, K., Palma, A. S., Liu, Y., Simpson, J. C., et al. (2008). Malectin: a novel carbohydrate-binding protein of the endoplasmic reticulum and a candidate player in the early steps of protein N-glycosylation. *Mol. Biol. Cell* 19, 3404–3414. doi: 10.1091/mbc.e08-04-0354.
- Scheller, H. V., and Ulvskov, P. (2010). Hemicelluloses. *Annu. Rev. Plant Biol.* 61, 263–289. doi: 10.1146/annurev-arplant-042809-112315.
- Schindler, T., Bergfeld, R., and Schopfer, P. (1995). Arabinogalactan proteins in maize coleoptiles: developmental relationship to cell death during xylem differentiation but not to extension growth †. *Plant J.* 7, 25–36. doi: 10.1046/j.1365-313x.1995.07010025.x.
- Schoenaers, S., Lee, H. K., Gonneau, M., Faucher, E., Levasseur, T., Akary, E., et al. (2024). Rapid alkalization factor 22 has a structural and signalling role in root hair cell wall assembly. doi: 10.1038/s41477-024-01637-8.
- Schultink, A., Naylor, D., Dama, M., and Pauly, M. (2015). The role of the plant-specific altered xyloglucan9 protein in arabidopsis cell wall polysaccharide o-acetylation. *Plant Physiol.* 167, 1271–1283. doi: 10.1104/pp.114.256479.
- Schulze-Muth, P., Irmeler, S., Schröder, G., and Schröder, J. (1996). Novel type of receptor-like protein kinase from a higher plant (*Catharanthus roseus*): cDNA, gene, intramolecular autophosphorylation, and identification of a threonine important for auto- and substrate phosphorylation. *J. Biol. Chem.* 271, 26684–26689. doi: 10.1074/jbc.271.43.26684.
- Seybold, H., Trempel, F., Ranf, S., Scheel, D., Romeis, T., and Lee, J. (2014). Ca²⁺ signalling in plant immune response: From pattern recognition receptors to Ca²⁺ decoding mechanisms. *New Phytol.* 204, 782–790. doi: 10.1111/nph.13031.
- Shahzad, R., Jamil, S., Ahmad, S., Nisar, A., Amina, Z., Saleem, S., et al. (2021). Harnessing the potential of plant transcription factors in developing climate resilient crops to improve global food security: Current and future

- perspectives. *Saudi J. Biol. Sci.* 28, 2323–2341. doi: 10.1016/j.sjbs.2021.01.028.
- Shani, Z., Dekel, M., Roiz, L., Horowitz, M., Kolosovski, N., Lapidot, S., et al. (2006). Expression of endo-1,4- β -glucanase (cell1) in *Arabidopsis thaliana* is associated with plant growth, xylem development and cell wall thickening. *Plant Cell Rep.* 25, 1067–1074. doi: 10.1007/s00299-006-0167-9.
- Sherwin, H. W., Pammenter, N. W., February, E., Vander Willigen, C., and Farrant, J. M. (1998). Xylem hydraulic characteristics, water relations and wood anatomy of the resurrection plant *Myrothamnus flabellifolius* Welw. *Ann. Bot.* 81, 567–575. doi: 10.1006/anbo.1998.0590.
- Shih, H. W., Depew, C. L., Miller, N. D., and Monshausen, G. B. (2015). The cyclic nucleotide-gated channel CNGC14 regulates root gravitropism in *Arabidopsis thaliana*. *Curr. Biol.* 25, 3119–3125. doi: 10.1016/j.cub.2015.10.025.
- Shih, H. W., Miller, N. D., Dai, C., Spalding, E. P., and Monshausen, G. B. (2014). The receptor-like kinase FERONIA is required for mechanical signal transduction in *Arabidopsis* seedlings. *Curr. Biol.* 24, 1887–1892. doi: 10.1016/j.cub.2014.06.064.
- Showalter, A. M. (2001). Arabinogalactan-proteins: Structure, expression and function. *Cell. Mol. Life Sci.* 58, 1399–1417. doi: 10.1007/PL00000784.
- Simson, B. W., and Timell, T. E. (1978). Polysaccharides in cambial tissues of *Populus tremuloides* and *Tilia americana*. *Cellul. Chem. Technol.* 12, 39. Available at: <https://api.semanticscholar.org/CorpusID:92742027>.
- Singh, R., Parihar, P., Singh, S., Mishra, R. K., Singh, V. P., and Prasad, S. M. (2017). Reactive oxygen species signaling and stomatal movement: Current updates and future perspectives. *Redox Biol.* 11, 213–218. doi: 10.1016/j.redox.2016.11.006.
- Sivan, P., Vilaplana, F., and Mellerowicz, E. J. (2023). Cell Wall Polysaccharide Matrix Dynamics during Wood Development. *Plant Cell Walls Res. Milestones Concept. Insights*, 412–440. doi: 10.1201/9781003178309-21.
- Smith, P. J., Wang, H. T., York, W. S., Peña, M. J., and Urbanowicz, B. R. (2017). Designer biomass for next-generation biorefineries: Leveraging recent insights into xylan structure and biosynthesis. *Biotechnol. Biofuels* 10, 1–14. doi: 10.1186/s13068-017-0973-z.
- Stegmann, M., Monaghan, J., Smakowska-Luzan, E., Rovenich, H., Lehner, A., Holton, N., et al. (2017). The receptor kinase FER is a RALF-regulated scaffold controlling plant immune signaling. *Science (80-.).* 355, 287–289. doi: 10.1126/science.aal2541.
- Sterling, J. D., Atmodjo, M. A., Inwood, S. E., Kolli, V. S. K., Quigley, H. F., Hahn, M. G., et al. (2006). Functional identification of an *Arabidopsis* pectin biosynthetic homogalacturonan galacturonosyltransferase. *Proc. Natl. Acad. Sci. U. S. A.* 103, 5236–5241. doi: 10.1073/pnas.0600120103.
- Stiller, V. (2009). Soil salinity and drought alter wood density and vulnerability to xylem cavitation of baldcypress (*Taxodium distichum* (L.) Rich.) seedlings. *Environ. Exp. Bot.* 67, 164–171. doi: 10.1016/j.envexpbot.2009.03.012.

- Sultana, M. M., Hachiya, T., Dutta, A. K., Nishimura, K., Suzuki, T., Tanaka, A., et al. (2020). Expression analysis of genes encoding malectin-like domain (MLD)- And leucine-rich repeat (LRR)- containing proteins in *Arabidopsis thaliana*. *Biosci. Biotechnol. Biochem.* 84, 154–158. doi: 10.1080/09168451.2019.1661769.
- Suzuki, M., Kato, A., Nagata, N., and Komeda, Y. (2002). A xylanase, AtXyn1, is predominantly expressed in vascular bundles, and four putative xylanase genes were identified in the *Arabidopsis thaliana* genome. *Plant Cell Physiol.* 43, 759–767. doi: 10.1093/pcp/pcf088.
- Swaminathan, S., Lionetti, V., and Zobotina, O. A. (2022). Plant Cell Wall Integrity Perturbations and Priming for Defense. *Plants* 11, 1–26. doi: 10.3390/plants11243539.
- Takahashi, N., and Koshijima, T. (1988). Ester linkages between lignin and glucuronoxylan in a lignin-carbohydrate complex from beech (*Fagus crenata*) wood. *Wood Sci. Technol.* 22, 231–241. doi: 10.1007/BF00386018.
- Tan, L., Eberhard, S., Pattathil, S., Warder, C., Glushka, J., Yuan, C., et al. (2013). An *Arabidopsis* cell wall proteoglycan consists of pectin and arabinoxylan covalently linked to an arabinogalactan protein. *Plant Cell* 25, 270–287. doi: 10.1105/tpc.112.107334.
- Tan, L., Tees, D., Qian, J., Kareem, S., and Kieliszewski, M. J. (2018). Intermolecular interactions between glycomodules of plant cell wall arabinogalactan-proteins and extensins. *Cell Surf.* 1, 25–33. doi: 10.1016/j.tcs.2018.03.001.
- Tanaka, Y., Nose, T., Jikumaru, Y., and Kamiya, Y. (2013). ABA inhibits entry into stomatal-lineage development in *Arabidopsis* leaves. *Plant J.* 74, 448–457. doi: 10.1111/tpj.12136.
- Tee, E. E., Fairweather, S. J., Vo, H. M., Zhao, C., Breakspear, A., Kimura, S., et al. (2023). Cell-specialized chloroplast signaling orchestrates photosynthetic and extracellular reactive oxygen species for stress responses. *bioRxiv*, 2023.08.02.551742. Available at: <https://www.biorxiv.org/content/10.1101/2023.08.02.551742v1%0Ahttps://www.biorxiv.org/content/10.1101/2023.08.02.551742v1.abstract>.
- Terashima, N., Kitano, K., Kojima, M., Yoshida, M., Yamamoto, H., and Westermark, U. (2009). Nanostructural assembly of cellulose, hemicellulose, and lignin in the middle layer of secondary wall of ginkgo tracheid. *J. Wood Sci.* 55, 409–416. doi: 10.1007/s10086-009-1049-x.
- Thompson, J. E., and Fry, S. C. (2001). Restructuring of wall-bound xyloglucan by transglycosylation in living plant cells. *Plant J.* 26, 23–34. doi: 10.1046/j.1365-313X.2001.01005.x.
- Toyota, M., Spencer, D., Sawai-Toyota, S., Jiaqi, W., Zhang, T., Koo, A. J., et al. (2018). Glutamate triggers long-distance, calcium-based plant defense signaling. *Science (80-.)*. 361, 1112–1115. doi: 10.1126/science.aat7744.
- Trache, D., Tarchoun, A. F., Derradji, M., Hamidon, T. S., Masruchin, N., Brosse, N., et al. (2020). *Nanocellulose: From Fundamentals to Advanced*

- Applications*. doi: 10.3389/fchem.2020.00392.
- Tsabary, G., Shani, Z., Roiz, L., Levy, I., Riov, J., and Shoseyov, O. (2003). Abnormal “wrinkled” cell walls and retarded development of transgenic *Arabidopsis thaliana* plants expressing endo-1,4- β -glucanase (cell1) antisense. *Plant Mol. Biol.* 51, 213–224. doi: 10.1023/A:1021162321527.
- Tsang, D. L., Edmond, C., Harrington, J. L., and Nühse, T. S. (2011). Cell wall integrity controls root elongation via a general 1-aminocyclopropane-1-carboxylic acid-dependent, ethylene-independent pathway. *Plant Physiol.* 156, 596–604. doi: 10.1104/pp.111.175372.
- Tunc-Ozdemir, M., Rato, C., Brown, E., Rogers, S., Mooneyham, A., Frietsch, S., et al. (2013). Cyclic Nucleotide Gated Channels 7 and 8 Are Essential for Male Reproductive Fertility. *PLoS One* 8. doi: 10.1371/journal.pone.0055277.
- Turner, S. R., and Somerville, C. R. (1997). Collapsed xylem phenotype of *Arabidopsis* identifies mutants deficient in cellulose deposition in the secondary cell wall. *Plant Cell* 9, 689–701. doi: 10.1105/tpc.9.5.689.
- Urbanowicz, B. R., Peña, M. J., Moniz, H. A., Moremen, K. W., and York, W. S. (2014). Two *Arabidopsis* proteins synthesize acetylated xylan in vitro. *Plant J.* 80, 197–206. doi: 10.1111/tpj.12643.
- Urbanowicz, B. R., Peña, M. J., Ratnaparkhe, S., Avci, U., Backe, J., Steet, H. F., et al. (2012). 4-O-methylation of glucuronic acid in *Arabidopsis* glucuronoxylan is catalyzed by a domain of unknown function family 579 protein. *Proc. Natl. Acad. Sci. U. S. A.* 109, 14253–14258. doi: 10.1073/pnas.1208097109.
- Vaahtera, L., Schulz, J., and Hamann, T. (2019). Cell wall integrity maintenance during plant development and interaction with the environment. *Nat. Plants* 5, 924–932. doi: 10.1038/s41477-019-0502-0.
- Vanholme, R., De Meester, B., Ralph, J., and Boerjan, W. (2019). Lignin biosynthesis and its integration into metabolism. *Curr. Opin. Biotechnol.* 56, 230–239. doi: 10.1016/j.copbio.2019.02.018.
- Vanholme, R., Demedts, B., Morreel, K., Ralph, J., and Boerjan, W. (2010). Lignin biosynthesis and structure. *Plant Physiol.* 153, 895–905. doi: 10.1104/pp.110.155119.
- Vardakou, M., Dumon, C., Murray, J. W., Christakopoulos, P., Weiner, D. P., Juge, N., et al. (2008). Understanding the Structural Basis for Substrate and Inhibitor Recognition in Eukaryotic GH11 Xylanases. *J. Mol. Biol.* 375, 1293–1305. doi: 10.1016/j.jmb.2007.11.007.
- Verica, J. A., and He, Z. H. (2002). The cell wall-associated kinase (WAK) and WAK-like kinase gene family. *Plant Physiol.* 129, 455–459. doi: 10.1104/pp.011028.
- Vijayaraghavareddy, P., Lekshmy, S. V., Struik, P. C., Makarla, U., Yin, X., and Sreeman, S. (2022). Production and scavenging of reactive oxygen species confer to differential sensitivity of rice and wheat to drought stress. *Crop Environ.* 1, 15–23. doi: 10.1016/j.crope.2022.03.010.
- Virilouvet, L., and Fromm, M. (2015). Physiological and transcriptional memory in guard cells during repetitive dehydration stress. *New Phytol.* 205, 596–607.

- doi: 10.1111/nph.13080.
- Wang, L., Ma, C., Wang, S., Yang, F., Sun, Y., Tang, J., et al. (2024). Ethylene and jasmonate signaling converge on gibberellin catabolism during thigmomorphogenesis in Arabidopsis. *Plant Physiol.* 194, 758–773. doi: 10.1093/plphys/kiad556.
- Wang, L., Wang, L., Yang, T., Wang, B., Lin, Q., Zhu, S., et al. (2020). RALF1-FERONIA complex affects splicing dynamics to modulate stress responses and growth in plants. *Sci. Adv.* 6, 1–13. doi: 10.1126/sciadv.aaz1622.
- Wanke, A., Rovenich, H., Schwanke, F., Velte, S., Becker, S., Hehemann, J. H., et al. (2020). Plant species-specific recognition of long and short β -1,3-linked glucans is mediated by different receptor systems. *Plant J.* 102, 1142–1156. doi: 10.1111/tpj.14688.
- Watanabe, T., Ohnishi, L., Yamasaki, Y., Kaizu, S., and Koshijima, T. (1989). Binding-site analysis of the ether linkages between lignin and hemicelluloses in lignin-carbohydrate complexes by ddq-oxidation. *Agric. Biol. Chem.* 53, 2233–2252. doi: 10.1080/00021369.1989.10869603.
- Weng, J. K., and Chapple, C. (2010). The origin and evolution of lignin biosynthesis. *New Phytol.* 187, 273–285. doi: 10.1111/j.1469-8137.2010.03327.x.
- Wilson, R. L., Kim, H., Bakshi, A., and Binder, B. M. (2014). The ethylene receptors ethylene response1 and ethylene response2 have contrasting roles in seed germination of Arabidopsis during salt stress. *Plant Physiol.* 165, 1353–1356. doi: 10.1104/pp.114.241695.
- Wisniewski, M., and Davis, G. (1989). Evidence for the involvement of a specific cell wall layer in regulation of deep supercooling of xylem parenchyma. *Plant Physiol.* 91, 151–156. doi: 10.1104/pp.91.1.151.
- Wolf, S. (2022). Cell Wall Signaling in Plant Development and Defense. *Annu. Rev. Plant Biol.* 73, 323–353. doi: 10.1146/annurev-arplant-102820-095312.
- Wolf, S., Hématy, K., and Höfte, H. (2012). Growth control and cell wall signaling in plants. *Annu. Rev. Plant Biol.* 63, 381–407. doi: 10.1146/annurev-arplant-042811-105449.
- Wu, A. M., Rihouey, C., Seveno, M., Hörnblad, E., Singh, S. K., Matsunaga, T., et al. (2009). The Arabidopsis IRX10 and IRX10-LIKE glycosyltransferases are critical for glucuronoxylan biosynthesis during secondary cell wall formation. *Plant J.* 57, 718–731. doi: 10.1111/j.1365-313X.2008.03724.x.
- Xia, J., Yuan, W., Wang, Y. P., and Zhang, Q. (2017). Adaptive Carbon Allocation by Plants Enhances the Terrestrial Carbon Sink. *Sci. Rep.* 7, 1–11. doi: 10.1038/s41598-017-03574-3.
- Xie, Y., Sun, P., Li, Z., Zhang, F., You, C., and Zhang, Z. (2022). FERONIA Receptor Kinase Integrates with Hormone Signaling to Regulate Plant Growth, Development, and Responses to Environmental Stimuli. *Int. J. Mol. Sci.* 23. doi: 10.3390/ijms23073730.
- Xin, Z., and Browse, J. (1998). eskimo1 mutants of Arabidopsis are constitutively freezing-tolerant. *Proc. Natl. Acad. Sci. U. S. A.* 95, 7799–7804. doi: 10.1073/pnas.95.13.7799.

- Xin, Z., Mandaokar, A., Chen, J., Last, R. L., and Browse, J. (2007). Arabidopsis ESK1 encodes a novel regulator of freezing tolerance. *Plant J.* 49, 786–799. doi: 10.1111/j.1365-313X.2006.02994.x.
- Xiong, G., Dama, M., and Pauly, M. (2015). Glucuronic Acid Moieties on Xylan Are Functionally Equivalent to O-Acetyl-Substituents. *Mol. Plant* 8, 1119–1121. doi: 10.1016/j.molp.2015.02.013.
- Xu, C., Xia, C., Xia, Z., Zhou, X., Huang, J., Huang, Z., et al. (2018). Physiological and transcriptomic responses of reproductive stage soybean to drought stress. *Plant Cell Rep.* 37, 1611–1624. doi: 10.1007/s00299-018-2332-3.
- Xu, Y., Liu, K., Yang, Y., Kim, M. S., Lee, C. H., Zhang, R., et al. (2023). Hemicellulose-based hydrogels for advanced applications. *Front. Bioeng. Biotechnol.* 10, 1–18. doi: 10.3389/fbioe.2022.1110004.
- Yan, J., Aznar, A., Chalvin, C., Birdseye, D. S., Baidoo, E. E. K., Eudes, A., et al. (2018). Increased drought tolerance in plants engineered for low lignin and low xylan content. *Biotechnol. Biofuels* 11, 1–11. doi: 10.1186/s13068-018-1196-7.
- Yang, H., Wang, D., Guo, L., Pan, H., Yvon, R., Garman, S., et al. (2021). Malectin/Malectin-like domain-containing proteins: A repertoire of cell surface molecules with broad functional potential. *Cell Surf.* 7, 100056. doi: 10.1016/j.tcs.2021.100056.
- Yi, H., Chen, Y., and Anderson, C. T. (2022). Turgor pressure change in stomatal guard cells arises from interactions between water influx and mechanical responses of their cell walls. *Quant. Plant Biol.* 3. doi: 10.1017/qpb.2022.8.
- York, W. S., and O’Neill, M. A. (2008). Biochemical control of xylan biosynthesis - which end is up? *Curr. Opin. Plant Biol.* 11, 258–265. doi: 10.1016/j.pbi.2008.02.007.
- Yoshida, K., Sakamoto, S., and Mitsuda, N. (2021). In Planta Cell Wall Engineering: From Mutants to Artificial Cell Walls. *Plant Cell Physiol.* 62, 1813–1827. doi: 10.1093/pcp/pcab157.
- Yu, F., Qian, L., Nibau, C., Duan, Q., Kita, D., Levasseur, K., et al. (2012). FERONIA receptor kinase pathway suppresses abscisic acid signaling in Arabidopsis by activating ABI2 phosphatase. *Proc. Natl. Acad. Sci. U. S. A.* 109, 14693–14698. doi: 10.1073/pnas.1212547109.
- Yu, L., Yoshimi, Y., Cresswell, R., Wightman, R., Lyczakowski, J. J., Wilson, L. F. L., et al. (2022). Eudicot primary cell wall glucomannan is related in synthesis, structure, and function to xyloglucan. *Plant Cell* 34, 4600–4622. doi: 10.1093/plcell/koac238.
- Yuan, F., Yang, H., Xue, Y., Kong, D., Ye, R., Li, C., et al. (2014a). OSCA1 mediates osmotic-stress-evoked Ca²⁺ increases vital for osmosensing in Arabidopsis. *Nature* 514, 367–371. doi: 10.1038/nature13593.
- Yuan, Y., Teng, Q., Lee, C., Zhong, R., and Ye, Z. H. (2014b). Modification of the degree of 4-O-methylation of secondary wall glucuronoxylan. *Plant Sci.* 219–220, 42–50. doi: 10.1016/j.plantsci.2014.01.005.
- Yuan, Y., Teng, Q., Zhong, R., and Ye, Z. H. (2013). The arabidopsis DUF231

- domain-containing protein ESK1 mediates 2-o- and 3-o-acetylation of xylosyl residues in xylan. *Plant Cell Physiol.* 54, 1186–1199. doi: 10.1093/pcp/pct070.
- Yuan, Y., Teng, Q., Zhong, R., and Ye, Z. H. (2016). TBL3 and TBL31, Two Arabidopsis DUF231 domain proteins, are required for 3-O-monoacetylation of xylan. *Plant Cell Physiol.* 57, 35–45. doi: 10.1093/pcp/pcv172.
- Yue, Z. L., Liu, N., Deng, Z. P., Zhang, Y., Wu, Z. M., Zhao, J. L., et al. (2022). The receptor kinase OsWAK11 monitors cell wall pectin changes to fine-tune brassinosteroid signaling and regulate cell elongation in rice. *Curr. Biol.* 32, 2454–2466.e7. doi: 10.1016/j.cub.2022.04.028.
- Zabackis, E., Huang, J., Müller, B., Darvill, A. G., and Albersheim, P. (1995). Characterization of the cell-wall polysaccharides of Arabidopsis thaliana leaves. *Plant Physiol.* 107, 1129–1138. doi: 10.1104/pp.107.4.1129.
- Zeng, W., Jiang, N., Nadella, R., Killen, T. L., Nadella, V., and Faik, A. (2010). A Glucurono(arabino)xylan synthase complex from wheat contains members of the GT43, GT47, and GT75 families and functions cooperatively. *Plant Physiol.* 154, 78–97. doi: 10.1104/pp.110.159749.
- Zeng, W., Lampugnani, E. R., Picard, K. L., Song, L., Wu, A. M., Farion, I. M., et al. (2016). Asparagus IRX9, IRX10, and IRX14A are components of an active xylan backbone synthase complex that forms in the Golgi apparatus. *Plant Physiol.* 171, 93–109. doi: 10.1104/pp.15.01919.
- Zhang, B., Zhang, L., Li, F., Zhang, D., Liu, X., Wang, H., et al. (2017). Control of secondary cell wall patterning involves xylan deacetylation by a GDSE esterase. *Nat. Plants* 3, 1–9. doi: 10.1038/nplants.2017.17.
- Zhang, Q., Jia, M., Xing, Y., Qin, L., Li, B., and Jia, W. (2016). Genome-wide identification and expression analysis of MRLK family genes associated with strawberry (*Fragaria vesca*) fruit ripening and abiotic stress responses. *PLoS One* 11, 1–19. doi: 10.1371/journal.pone.0163647.
- Zhang, R., Shi, P. T., Zhou, M., Liu, H. Z., Xu, X. J., Liu, W. T., et al. (2023). Rapid alkalization factor: function, regulation, and potential applications in agriculture. *Stress Biol.* 3. doi: 10.1007/s44154-023-00093-2.
- Zhao, C., Jiang, W., Zayed, O., Liu, X., Tang, K., Nie, W., et al. (2021). The LRXS-RALFs-FER module controls plant growth and salt stress responses by modulating multiple plant hormones. *Natl. Sci. Rev.* 8. doi: 10.1093/nsr/nwaa149.
- Zhao, Y., Song, D., Sun, J., and Li, L. (2013). Populus endo-beta-mannanase PtrMAN6 plays a role in coordinating cell wall remodeling with suppression of secondary wall thickening through generation of oligosaccharide signals. *Plant J.* 74, 473–485. doi: 10.1111/tpj.12137.
- Zhong, R., Cui, D., and Ye, Z. H. (2017). Regiospecific acetylation of xylan is mediated by a group of DUF231-containing O-acetyltransferases. *Plant Cell Physiol.* 58, 2126–2138. doi: 10.1093/pcp/pcx147.
- Zhong, R., Lee, C., Zhou, J., McCarthy, R. L., and Ye, Z. H. (2008). A battery of transcription factors involved in the regulation of secondary cell wall

- biosynthesis in Arabidopsis. *Plant Cell* 20, 2763–2782. doi: 10.1105/tpc.108.061325.
- Zhong, R., Peña, M. J., Zhou, G. K., Nairn, C. J., Wood-Jones, A., Richardson, E. A., et al. (2005). Arabidopsis fragile fiber8, which encodes a putative glucuronyltransferase, is essential for normal secondary wall synthesis. *Plant Cell* 17, 3390–3406. doi: 10.1105/tpc.105.035501.
- Zhong, R., Phillips, D. R., Adams, E. R., and Ye, Z. H. (2023). An Arabidopsis family GT106 glycosyltransferase is essential for xylan biosynthesis and secondary wall deposition. *Planta* 257, 1–14. doi: 10.1007/s00425-023-04077-4.
- Zhu, J. K. (2016). Abiotic Stress Signaling and Responses in Plants. *Cell* 167, 313–324. doi: 10.1016/j.cell.2016.08.029.
- Zhu, L., Zhang, X. Q., Ye, D., and Chen, L. Q. (2021). The mildew resistance locus o 4 interacts with cam/cml and is involved in root gravity response. *Int. J. Mol. Sci.* 22. doi: 10.3390/ijms22115962.
- Zhu, X. F., Wan, J. X., Sun, Y., Shi, Y. Z., Braam, J., Li, G. X., et al. (2014). Xyloglucan endotransglucosylase-hydrolase17 interacts with xyloglucan endotransglucosylase-hydrolase31 to confer xyloglucan endotransglucosylase action and affect aluminum sensitivity in arabidopsis. *Plant Physiol.* 165, 1566–1574. doi: 10.1104/pp.114.243790.
- Zinkgraf, M., Gerttula, S., Zhao, S., Filkov, V., and Groover, A. (2018). Transcriptional and temporal response of Populus stems to gravi-stimulation. *J. Integr. Plant Biol.* 60, 578–590. doi: 10.1111/jipb.12645.
- Zipfel, C. (2009). Early molecular events in PAMP-triggered immunity. *Curr. Opin. Plant Biol.* 12, 414–420. doi: 10.1016/j.pbi.2009.06.003.
- Zwack, P. J., Compton, M. A., Adams, C. I., and Rashotte, A. M. (2016). Cytokinin response factor 4 (CRF4) is induced by cold and involved in freezing tolerance. *Plant Cell Rep.* 35, 573–584. doi: 10.1007/s00299-015-1904-8.

Popular science summary

Trees form vast forest ecosystems thanks to their mechanical strength largely determined by the cell walls of their wood tissue. Xylan, one of main cell wall components, plays a significant role in reinforcing cell walls in broad-leaf tree species like aspen and the model herbaceous plant *Arabidopsis*.

This thesis investigated how xylan contributes to the structural integrity of cell walls and how the loss of this integrity affects plant physiology and the ability of plants to withstand environmental stresses. Studies in *Arabidopsis* and aspen were included to compare different strategies of herbaceous and woody plants.

This work advances our understanding of plant biology and supports the development of innovative strategies for enhancing plant resilience. Such advances are critical for improving the productivity of trees and crops when facing climatic challenges and for the development of sustainable feedstocks for the production of bioenergy and biomaterials.

Populärvetenskaplig sammanfattning

Träd bildar omfattande skogsekosystem tack vare deras mekaniska styrka, som till stor del bestäms av cellväggarna i deras trävävnad. Xylan, en av huvudkomponenterna i cellväggarna, spelar en betydande roll för att förstärka cellväggarna hos lövträd såsom asp och den örtartade modellväxten *Arabidopsis*.

Denna avhandling undersökte hur xylan bidrar till cellväggarnas strukturella integritet och hur förlusten av denna integritet påverkar växternas fysiologi och deras förmåga att stå emot miljömässiga påfrestningar.

Studier på *Arabidopsis* och asp inkluderades för att jämföra olika strategier hos örtartade och vedartade växter. Arbetet främjar vår förståelse av växtbiologi och stödjer utvecklingen av innovativa strategier för att förbättra växternas motståndskraft. Sådana framsteg är avgörande för att förbättra produktiviteten hos träd och grödor inför klimatutmaningar samt för utvecklingen av hållbara råvaror för produktion av bioenergi och biomaterial.

Acknowledgements

First and foremost, I extend my deepest gratitude to my supervisor and mentor, **Ewa Mellerowicz**, whose expertise, understanding, and patience added considerably to my doctoral experience. Her guidance was invaluable in formulating the research questions and framework, and her insights and support helped me to coordinate my project and bring it to a successful completion. Her willingness to give her time so generously has been very much appreciated.

Many thanks to my advisory committee for their support and challenging questions: **Totte Niittylä**, **Stéphane Verger**, and **Catherine Bellini**.

I am sincerely thankful to **all my colleagues** for their camaraderie and support throughout my research, especially those who worked directly on aspects of the projects discussed in this thesis. Special thanks to **Evgeniy**, who was not only a close colleague but also a friend. I extend heartfelt thanks to the other past and current members of the Ewa Mellerowicz group, Janos, Vikash, Sunita, Marta, Madhusree, Garima, and Pramod, for their significant contributions and support.

I particularly appreciated the collaborations with **Laurent Gutierrez** and **Emilie Cavel** for phenotyping *Arabidopsis* in Amiens, as well as **Ioanna Gaboreanu** for collaboration with aspen phenotyping at UPSC. Their contributions were vital to the success of these projects. I am grateful to my master's student intern, **Yamin Lebsir**, whose enthusiasm and efforts in our joint projects have been really appreciated.

Many thanks go to all my childhood friends, **Kennedy**, and **Benjamin**, who contributed directly to my research through their expertise in graphic production and bioinformatics, respectively. Their work has improved the quality and presentation of my findings.

My sincere appreciation also goes to my partner, whose love and support have been unwavering throughout this journey. I must express my very profound gratitude to **my family** in France for providing me with unfailing support and continuous encouragement throughout my years of study. This accomplishment would not have been possible without them. Thank you.

Thank you to all who have guided, encouraged, and inspired me.



Genome-Wide Identification of *Populus* Malectin/Malectin-Like Domain-Containing Proteins and Expression Analyses Reveal Novel Candidates for Signaling and Regulation of Wood Development

Vikash Kumar¹, Evgeniy N. Donev¹, Félix R. Barbut¹, Sunita Kushwah¹, Chanaka Mannapperuma², János Urbancsok^{1*} and Ewa J. Mellerowicz¹

OPEN ACCESS

Edited by:

Seonghoe Jang,
World Vegetable Center Korea,
South Korea

Reviewed by:

Hanyao Zhang,
Southwest Forestry University, China
Melis Kucukoglu,
University of Helsinki, Finland
Nathalie Leblanc-Fournier,
Université Clermont Auvergne, France

*Correspondence:

János Urbancsok
janos.urbancsok@slu.se

Specialty section:

This article was submitted to
Plant Development and EvoDevo,
a section of the journal
Frontiers in Plant Science

Received: 11 August 2020

Accepted: 18 November 2020

Published: 22 December 2020

Citation:

Kumar V, Donev EN, Barbut FR,
Kushwah S, Mannapperuma C,
Urbancsok J and Mellerowicz EJ
(2020) Genome-Wide Identification of
Populus Malectin/Malectin-Like
Domain-Containing Proteins
and Expression Analyses Reveal
Novel Candidates for Signaling
and Regulation of Wood
Development.
Front. Plant Sci. 11:588846.
doi: 10.3389/fpls.2020.588846

¹ Department of Forest Genetics and Plant Physiology, Umeå Plant Science Centre, Swedish University of Agricultural Sciences, Umeå, Sweden, ² Department of Plant Physiology, Umeå Plant Science Centre, Umeå University, Umeå, Sweden

Malectin domain (MD) is a ligand-binding protein motif of pro- and eukaryotes. It is particularly abundant in Viridiplantae, where it occurs as either a single (MD, PF11721) or tandemly duplicated domain (PF12819) called malectin-like domain (MLD). In herbaceous plants, MD- or MLD-containing proteins (MD proteins) are known to regulate development, reproduction, and resistance to various stresses. However, their functions in woody plants have not yet been studied. To unravel their potential role in wood development, we carried out genome-wide identification of MD proteins in the model tree species black cottonwood (*Populus trichocarpa*), and analyzed their expression and co-expression networks. *P. trichocarpa* had 146 MD genes assigned to 14 different clades, two of which were specific to the genus *Populus*. 87% of these genes were located on chromosomes, the rest being associated with scaffolds. Based on their protein domain organization, and in agreement with the exon-intron structures, the MD genes identified here could be classified into five superclades having the following domains: leucine-rich repeat (LRR)-MD-protein kinase (PK), MLD-LRR-PK, MLD-PK (CrRLK1L), MLD-LRR, and MD-Kinesin. Whereas the majority of MD genes were highly expressed in leaves, particularly under stress conditions, eighteen showed a peak of expression during secondary wall formation in the xylem and their co-expression networks suggested signaling functions in cell wall integrity, pathogen-associated molecular patterns, calcium, ROS, and hormone pathways. Thus, *P. trichocarpa* MD genes having different domain organizations comprise many genes with putative foliar defense functions, some of which could be specific to *Populus* and related species, as well as genes with potential involvement in signaling pathways in other tissues including developing wood.

Keywords: *Populus*, cell wall integrity, malectin domain, malectin-like domain, CBM57, receptor-like protein kinases, CrRLK1L

INTRODUCTION

Plant cells are surrounded by cell walls made of cellulose, hemicelluloses, pectins and structural proteins, with lignin being present in cell types specialized for mechanical support (sclerenchyma) and water transport (xylem). Cell wall biosynthesis needs to be regulated so that its mechanical properties can be adapted to different circumstances according to the signals perceived. It is becoming generally accepted that there is constant feedback from the wall to the protoplast, mediated by different molecular pathways commonly termed cell wall integrity (CWI) signaling (Hématy et al., 2007; reviewed by Wolf and Höfte, 2014; Hamann, 2015; Voxeur and Höfte, 2016; Wolf, 2017; Rui and Dinneny, 2020). Perception of signals external to the protoplast is usually mediated by plasmalemma-localized proteins with various ectodomains. One large group of ectodomain-containing proteins is the receptor-like kinases (RLKs) that allow the plant cells to perceive external cues and transduce them, using a phosphorylation relay, into signals to initiate cellular responses (Gish and Clark, 2011; Engelsdorf and Hamann, 2014). Plant RLKs belong to the RLK/Pelle kinase family, one of the largest gene families in plants with more than 600 members in *Arabidopsis* (Shiu and Bleecker, 2001, 2003). It comprises both RLKs and receptor-like cytoplasmic kinases (RLCKs), and has been divided into 45 subfamilies, including wall-associated kinases, extensin-like RLKs, lectin RLKs, and leucine-rich repeat RLKs. RLCKs are cytoplasmic kinases without a transmembrane domain (TMD) and they recognize signaling molecules intracellularly. The RLKs usually function as heterodimers: one subunit with a large extracellular domain interacts with a ligand, and the other, which has a smaller extracellular domain, stabilizes this interaction and enhances signal transduction (Xi et al., 2019).

Among the different clades of plant RLKs, the *Catharanthus roseus* receptor-like kinase 1-like proteins (*CrRLK1Ls*) have received significant attention as mediators of CWI (reviewed by Wolf and Höfte, 2014; Li et al., 2016; Franck et al., 2018). The family is conserved in all Streptophytes analyzed so far, including moss and liverwort, indicating its ancient origin (Galindo-Trigo et al., 2016). *CrRLK1Ls* are characterized by two malectin ectodomains (MDs) forming a malectin-like domain (MLD), a transmembrane helix and a C-terminal intracellular Ser and Thr kinase domain. The *Arabidopsis* genome contains 17 *CrRLK1L* genes and the majority of them have been functionally analyzed. THESEUS1 (THE1) was the first member to be identified as a mediator of dwarfism and ectopic lignification induced by defects in cellulose biosynthesis (Hématy et al., 2007; Merz et al., 2017). Other members of *CrRLK1L* family including CURVY1 (CVY1), FERONIA (FER) and ANXUR1 (ANX1) are required for polar cell growth in different cell types. FER, ANX1/2 and BUDDHA'S PAPER SEAL1 and 2 (BUPS1 and 2) participate in sexual reproduction. FER mediates signaling by reactive oxygen species (ROS) and Ca²⁺ during pollen tube reception at the filiform apparatus (Escobar-Restrepo et al., 2007), whereas ANX1/2 together with BUPS1/2 form a receptor complex for RAPID ALKALINIZATION FACTOR (RALF) 4 or 19 in the growing tip of pollen tube and regulate ROS and Ca²⁺ gradients essential for its growth and CWI (Ge et al., 2017). In

addition, *CrRLK1L* proteins are involved in immune responses. FER positively regulates pathogen-associated molecular pattern (PAMP)-triggered immunity (PTI) by facilitating the formation of a receptor complex composed of BAK1-FLS2-FER or BAK1-EFR-FER (Stegmann et al., 2017), whereas ANX1 functions antagonistically in PTI and inhibits effector-triggered immunity (ETI) (Mang et al., 2017). The downstream responses of *CrRLK1Ls* are diverse and include Rho-GTPases activating NADPH oxidases involved in the production of apoplastic ROS (Foreman et al., 2003; Duan et al., 2010; Denness et al., 2011; Boisson-Dernier et al., 2013), RLCKs (Boisson-Dernier et al., 2015; Du et al., 2016), inhibition of the proton pump AHA1 (Haruta et al., 2014), Ca²⁺ signaling mediated by MLO proteins (Kessler et al., 2010; Meng et al., 2020), as yet unknown Ca²⁺ channels and a signaling cascade via intracellular kinases that eventually activate or repress gene transcription (Franck et al., 2018).

The MLD, which is characteristic of *CrRLK1L* proteins, and the MD are also found in other types of plant RLKs (Zhang et al., 2016; Bellande et al., 2017). The MD was first identified in the protein called malectin residing in the endoplasmic reticulum of *Xenopus laevis* and other animals, where it monitors protein glycosylation by binding diglucose motifs with α -1,4-, α -1,3- and α -1,2-linkage in glycosylated proteins (Schallus et al., 2008, 2010). However, the crystal structure of MLD in ANX1, ANX2, and FER indicated an absence of the aromatic residues that interact with diglucosides in animal MDs, and suggested different ligand specificities and/or functions of the MLDs in these proteins (Du et al., 2018; Moussu et al., 2018; Xiao et al., 2019). Several peptides from the RALF family have been demonstrated to bind to ectodomains of *CrRLK1L* proteins in *Arabidopsis*: RALF34 to THE1 (Gonneau et al., 2018), RALF1/17/23/32/33 to FER (Haruta et al., 2014; Stegmann et al., 2017), and RALF4/19 to the ANX1/2-BUPS1/2 receptor complex (Ge et al., 2017). Recently it has been shown that the binding of RALF23 to FER is stabilized by interaction with LORELEI-like-GPI-ANCHORED PROTEINS (LLGs) and the formation of such a heterocomplex is required for PTI signaling (Xiao et al., 2019). Moreover, the ectodomain of FER has been shown to bind to the leucine-rich repeat (LRR) domain of LRR-extensin 1 (LRX1) (Dünser et al., 2019) and to pectin (Feng et al., 2018).

Malectin domain is classified as CBM57 in the CAZY database¹. Interestingly, the CBM57 family is greatly expanded in the model tree species *Populus trichocarpa* compared to the herbaceous model plant *Arabidopsis thaliana* (Kumar et al., 2019). Moreover, transcript of the CBM57 family members are highly upregulated in developing wood tissues of *Populus tremula* (Kumar et al., 2019) and *Eucalyptus grandis* (Pinard et al., 2015). These data suggest that MD/MLD-containing proteins (subsequently called MD proteins) have important functions in trees. We hypothesize that MD proteins are involved in the regulation of cell wall formation during secondary growth via pathways analogous to those reported for primary growth (Wolf and Höfte, 2014; Hamann, 2015; Li et al., 2016; Wolf, 2017), and that they participate in signaling cascades related to stress responses and developmental processes in trees. To

¹<http://www.cazy.org/>

find candidates for receptors active during secondary growth, we first carried out genome-wide identification of *P. trichocarpa* genes with predicted MD and MLD. Second, we used expression datasets from different organs (Sundell et al., 2015; Immanen et al., 2016) and high-resolution expression data for wood developmental zones in *P. tremula* (Sundell et al., 2017) to identify those MD proteins that are expressed during wood biosynthesis, and to classify them according to expression at specific stages of xylogenesis. Finally, we identified co-expression networks for the MD proteins expressed during secondary wall deposition, which include their putative interactors. Our analyses provide a framework to identify CWI monitoring, stress response, and other signaling pathways operating during wood development.

MATERIALS AND METHODS

Identification of *P. trichocarpa* Proteins With Malectin and Malectin-Like Domains

The MD proteins of black cottonwood (*P. trichocarpa* Torr. and A. Gray) were identified by Basic Local Alignment Search Tool (BLAST) (Altschul et al., 1990) searches in the genome browser of the PopGenIE database² containing *P. trichocarpa* genome assembly v3.0, using as baits the *P. trichocarpa* proteins containing Pfam domains 11721 and 12819, corresponding to MD and MLD, respectively, retrieved from the Pfam database³ (El-Gebali et al., 2019). The same approach was applied to *A. thaliana* using the TAIR database (v10.0) for BLAST searches⁴. The BLASTP tool of a high-performance sequence aligner DIAMOND was used in -unal 0, -evaluate 1e-05, -max-target-seqs 4000, and -more-sensitive mode, other parameters were kept as default (Buchfink et al., 2015). All other web-based tools were used in default mode as per developers' recommendations. The presence of MDs/MLDs in the proteins selected for both *P. trichocarpa* and *A. thaliana* was confirmed using the CDvst web tool⁵ (Adebali et al., 2015), which also served to identify other conserved domains in these proteins. The amino acid sequence lengths, molecular weights, isoelectric points and indices of protein stability of the putative proteins were calculated using the ProtParam tool provided on the Expasy website⁶. The presence of signal peptides and subcellular localization were predicted with the SignalP 4.1 server⁷ (Petersen et al., 2011) and DeepLoc-1.0 server⁸ (Armenteros et al., 2017), respectively. The exon-intron organization of the *PtMD* genes was determined using the PopGenIE GBrowse tool⁹ and their localization was

mapped to *P. trichocarpa* chromosomes using the chromosome-diagram tool¹⁰. Assignment of a gene to a gene cluster on each chromosome was based on the definition of Holub (2001).

Phylogenetic Analysis and Classification of the MD Proteins of *P. trichocarpa*

All *PtMD* proteins identified were classified into clades based on phylogenetic analysis with *A. thaliana*. The amino acid sequences were aligned by MUSCLE¹¹ and phylogenetic trees were constructed using the neighbor-joining (NJ) method in the MEGA7 software package with a bootstrap test with 1000 replicates (Kumar et al., 2016).

To identify the conserved residues in MD and MLD regions of poplar MD proteins, these regions were aligned with reference sequences using Jalview Version 2 (Waterhouse et al., 2009) with the MAFFT option (Katoh et al., 2005).

To evaluate evolutionary conservation of MD genes across tree species, we have extracted protein sequences for *Eucalyptus grandis* v2.0, *Malus domestica* v1.0, *Salix purpurea* v1.0, *Theobroma cacao* v2.1, *Citrus sinensis* v1.1, *Prunus persica* v1.0 and *Betula pendula* v1.0 from Phytozome genome portal¹² using BLAST (with same parameters as stated in the section above) and *PtMDs* as query sequences. The protein sequences of resulting hits and the MD proteins of *P. trichocarpa* and *A. thaliana* were used to generate a phylogenetic tree using one click method described in <https://ngphylogeny.fr> (Lemoine et al., 2019). The phylogenetic tree and other detailed method descriptions can be found at <ftp://plantgenie.org/Publications/Kumar2020/Phylogeny>.

Expression Analysis of *PtMDs* in Developing Leaves and Wood

Developing leaves (leaf number 8, 11, 21 and 23) and developing wood including cambium/phloem and xylem depositing secondary walls were collected from 10 weeks old hybrid aspen (*Populus tremula* L. x *tremuloides* Michx.) grown in the greenhouse. The cultivation conditions and RNA extraction protocols were as described in Ratke et al. (2018). Between five and ten biological replicates of each sample were sequenced using Illumina HiSeq-PE150 platforms of Novogene Bioinformatics Technology Co., Ltd. (Beijing). Quality control and mapping to *P. trichocarpa* transcriptome v3.0 of leaf 8 and 11 samples were performed by Novogene. Other samples had RNA-Seq raw data filtered using FastQC (v0.10.1¹³). rRNA reads were removed using SortMeRNA v1.8 (Kopylova et al., 2012). Low-quality reads were removed using Trimmomatic v0.27 (Lohse et al., 2012) with a sliding window of 5 bp, minimum quality score of 20, minimum read length of 50 bp, minimum leading read quality of 20 and a custom clipping file containing all Illumina adapters. The preprocessed reads were mapped to v3.0 of the *P. trichocarpa* transcriptome (retrieved from PopGenIE see

²<http://popgenie.org>

³<https://pfam.xfam.org>

⁴<http://www.arabidopsis.org/>

⁵<http://cdvst.zhulinlab.org>

⁶<https://web.expasy.org/protparam/>

⁷<http://www.cbs.dtu.dk/services/SignalP/>

⁸<http://www.cbs.dtu.dk/services/DeepLoc/>

⁹<http://popgenie.org/gbrowse>

¹⁰<http://popgenie.org/chromosome-diagram>

¹¹<http://phylogeny.lirmm.fr/phylo.cgi/index.cgi>

¹²<https://genome.jgi.doe.gov/portal/pages/dynamicOrganismDownload.jsf?organism=Phytozome>

¹³www.bioinformatics.babraham.ac.uk/projects/fastqc/

footnote 2) using Kallisto (v0.43.1) with default parameters (Bray et al., 2016). The raw counts were normalized separately for each experiment using Variance Stabilizing Transformation (VST) in R (v3.4.0; R Core Team, 2014) using the Bioconductor (v3.4; Gentleman et al., 2004) DESeq2 package (v1.16.1; Love et al., 2014). Then the VST data were merged together using a sample-based median centering approach as described by Kumar et al. (2019); the R scripts are available at <https://github.com/UPSCb/UPSCb/tree/master/manuscripts/Kumar2018>. Mean VST data for *PtMDs* were displayed using ComplexHeatmap with default parameters and using the tissue with a peak of expression for each gene as a categorical variable for clustering (Gu et al., 2016). The tissue/organ specificity score *tau* - a score ranging from 0 (ubiquitous expression) to 1 (tissue/organ specific expression), as detailed in Yanai et al. (2005) was calculated for each *PtMD* gene. The customized R scripts used to calculate *tau* are available at <https://github.com/UPSCb/UPSCb/tree/master/manuscripts/Kumar2018>. The raw RNA-Seq data for this study have been deposited in the European Nucleotide Archive (ENA) at EMBL-EBI under accession number PRJEB41170¹⁴.

Expression of *PtMDs* in Different Organs of *Populus*

RNA-Seq datasets of expression values in different tissues/organs of outdoor and greenhouse grown aspen (*P. tremula* L.) and hybrid aspen (*P. tremula* L. x *tremuloides* Michx., clone T89) are available from the PlantGenIE website (Sundell et al., 2015). Data for secondary tissues of greenhouse grown T89 hybrid aspen are detailed by Immanen et al. (2016). Raw data for all biological replicates of each sample (min. = 3) were preprocessed as described in the section above except that the reads were aligned to the *Populus trichocarpa* genome using STAR and quantified using HTSeq. Other steps of quality assessment and filtering are explained above and available at: <http://www.epigenesys.eu/en/protocols/bio-informatics/1283-guidelines-for-rna-seq-data-analysis>. The VST values were median-centered for each sample, and means for all biological replicates were used for hierarchical clustering and calculating the *tau* tissue/organ specificity score, as described above.

PtMDs Involved in Wood Biosynthesis

The AspWood high-spatial-resolution RNA-Seq dataset (Sundell et al., 2017) was used for analysis of expression of *PtMDs* during wood biosynthesis. The database provides VST expression values for four trees. Identity of wood developmental zones was based on the expression of marker genes (Sundell et al., 2017). A heatmap of *PtMD* expression in wood developmental zones was constructed for one representative tree (tree 1) using the AspWood server¹⁵.

Co-expression Analysis

PtMD genes from the selected expression clusters were used as 'Guide Genes' to obtain co-expression networks for developing secondary tissues, using the AspWood program (see text footnote

14). The AspWood calculates co-expression networks utilizing mutual information and context likelihood of relatedness as explained by Sundell et al. (2017). The corresponding GraphML files were generated using the ExNet tool¹⁶ with a Z-score threshold of 5.0, and visualized using Cytoscape 3.4.0 (Shannon et al., 2003).

RESULTS AND DISCUSSION

Identification of MD Proteins in *P. trichocarpa* and Their Classification

Searches of the *P. trichocarpa* and *A. thaliana* genomes for MD proteins resulted in the identification of 146 and 87 gene models, respectively (Supplementary Tables 1, 2). Previous analyses identified 62 MD genes in strawberry (Zhang et al., 2016), 74 in *A. thaliana* (Bellande et al., 2017; Sultana et al., 2020), and 84 in rice (Jing et al., 2020).

The *P. trichocarpa* proteins identified were analyzed for sequence similarity using protein sequence alignment and phylogenetic analysis, revealing the presence of 12 clades supported by at least 87 % of bootstrap replicates, and three ungrouped sequences, two of which had orthologous sequences in *A. thaliana*, and were therefore considered to be two single member clades III and XI (Figures 1, 2). The sequences were numbered *PtMD1* to *PtMD146* according to their sequential appearance in the intraspecific phylogenetic tree (Figure 1). The predicted protein properties and probable subcellular localizations of *PtMD* proteins are listed in Supplementary Table 1. The deduced sequence lengths ranged from 274 to 1192 amino acids, and isoelectric points (pIs) ranged from 4.55 to 9.49. Seventy-six out of the 146 *PtMD* proteins had a signal peptide (SP) cleavage site. The SP was not found in any members of clades I and XIV. Thirteen of the *PtMDs* were predicted to be soluble proteins, with the predicted localization of six of them being extracellular, six - including all members of clade XIV - being cytoplasmic and one being peroxisomal. Out of 133 membrane proteins, one was predicted to localize in the endoplasmic reticulum.

Domain analysis (Figure 1 and Supplementary Table 1) revealed the presence of two major groups, one with MD (clades I–VIII, and XIV) and the other with MLD (clades IX to XIII). There was relatively little conservation in the amino acid sequence between the two domains (Figure 3), and in many cases, the proteins having MLD were not classified as members of the CBM57 family (Supplementary Table 1; Kumar et al., 2019). Nevertheless, similarity between MD and each of the two sub-domains of MLD has previously been shown by comparisons of their 3D structures (Moussu et al., 2018). Among the conserved residues of MD, which were proposed to interact with diglucose in *Xenopus laevis* malectin (Y67, Y89, Y116, F117, and D186) (Schallus et al., 2008, 2010), only Y67 and F117 were conserved in poplar MD (Figure 3 and Supplementary Figure 1). In contrast, the residues proposed to interact with ligands in the MLD of ANX1, Y77, R102, E150, E182, R215, L232, and R234 (Moussu et al., 2018) were to a large

¹⁴<https://www.ebi.ac.uk/ena/browser/view/PRJEB41170>

¹⁵<http://aspwood.popgenie.org/aspwood-v3.0/>

¹⁶<http://popgenie.org/exnet>

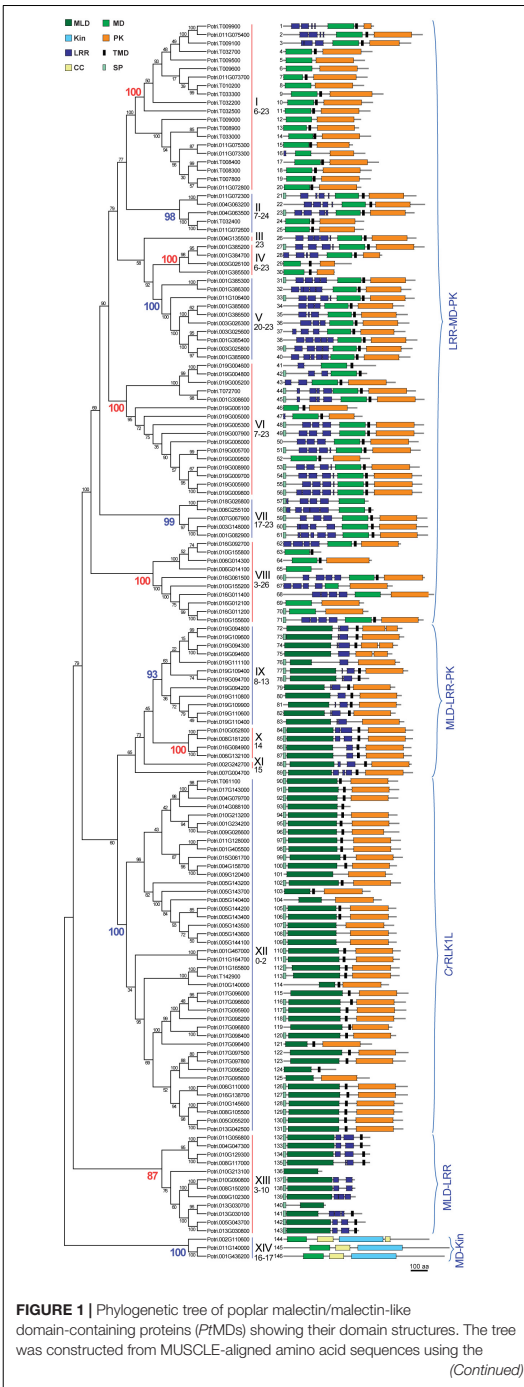


FIGURE 1 | Continued neighbor-joining method in MEGA 7.0 with 1000 bootstrap replicates and bootstrap support is displayed beside the nodes as percentages. *PtMDs* are identified by the number shown next to each protein structure. Domain abbreviations are: CC, coiled coil; Kin, kinesin; LRR, leucine-rich repeat; MD, malectin domain; MLD, malectin-like domain; PK, protein kinase; SP, signal peptide; TMD, transmembrane domain. Main clades are numbered with Roman numerals and their corresponding bootstrap values are colored in the phylogenetic tree. Numbers below the Roman numerals correspond to the number of introns observed within a clade. Five groups containing clades with similar protein domain structures are identified by the blue brackets: LRR-MD-PK (also known as poplar LRR-RLK XII; Zan et al., 2013), MLD-LRR-PK (known as poplar LRR-RLK I; Zan et al., 2013), CrRLK1L, MLD-LRR, and MD-Kin.

extent conserved in poplar MLD (Figure 3 and Supplementary Figures 2A,B).

Clades I-XII had MD or MLD followed by a transmembrane helix preceding the protein kinase domain, in agreement with the typical topology of RLKs (Figure 1 and Supplementary Table 1). Protein kinase domains were frequently of the Tyr kinase type. Some MD proteins with a kinase domain had extracellular localization predicted for this domain (Supplementary Table 1). Clade V was the only one in which all kinase domains were predicted to be intracellular. Extracellular kinase domains were also predicted for the majority of G- and L-type lectin RLKs in poplar (Yang et al., 2016) but experimental validation of such predictions is currently lacking.

In all clades but XII and XIV, several LRR domains were found in tandem repeats. The LRR domain forms a horseshoe-like structure that functions in protein-protein or protein-ligand interactions (Bella et al., 2008). LRRs are known to occur in LRR-RLKs, receptor-like proteins (RLPs), resistance (R) proteins, LRR extensins (LRX), and other families (Wang et al., 2008; Draeger et al., 2015; Choi et al., 2016; Song et al., 2018). Poplar MD proteins had various types of LRR domains, most frequently LRR_4 and LRR_8 (Supplementary Table 1). The proteins from clade XIII had unique combinations of LRR domains; *PtMD134* and *PtMD135* had the sd00031 LRR domain, *PtMD141* had the LRR_1 domain, and *PtMD137*, -138, and -139 had the LRRNT2 domain. The LRR domains found in the poplar MD family either preceded MD (clades I-VIII) or followed MLD (clades IX-XI and XIII) (Figure 1). Thus, the placement of LRR domains correlated with the presence of either MD or MLD. In clades with members containing LRRs, there were also several members devoid of any LRRs. This probably indicates domain loss due to unequal crossing over. A previous study on poplar LRR-RLKs (Zan et al., 2013) identified and classified some of the MD proteins studied here; MD clades I-VIII were previously classified as LRR-RLK group XIII, and MD clades IX-XI as LRR-RLK group I (Supplementary Table 1).

Clade XI and clade XII members exhibited an unusual TMD, CD12087, which is typical of epidermal growth factor receptors of animals where it functions in receptor dimerization (Mineev et al., 2010). Whether it can carry out such a function in plant MD proteins remains to be investigated.

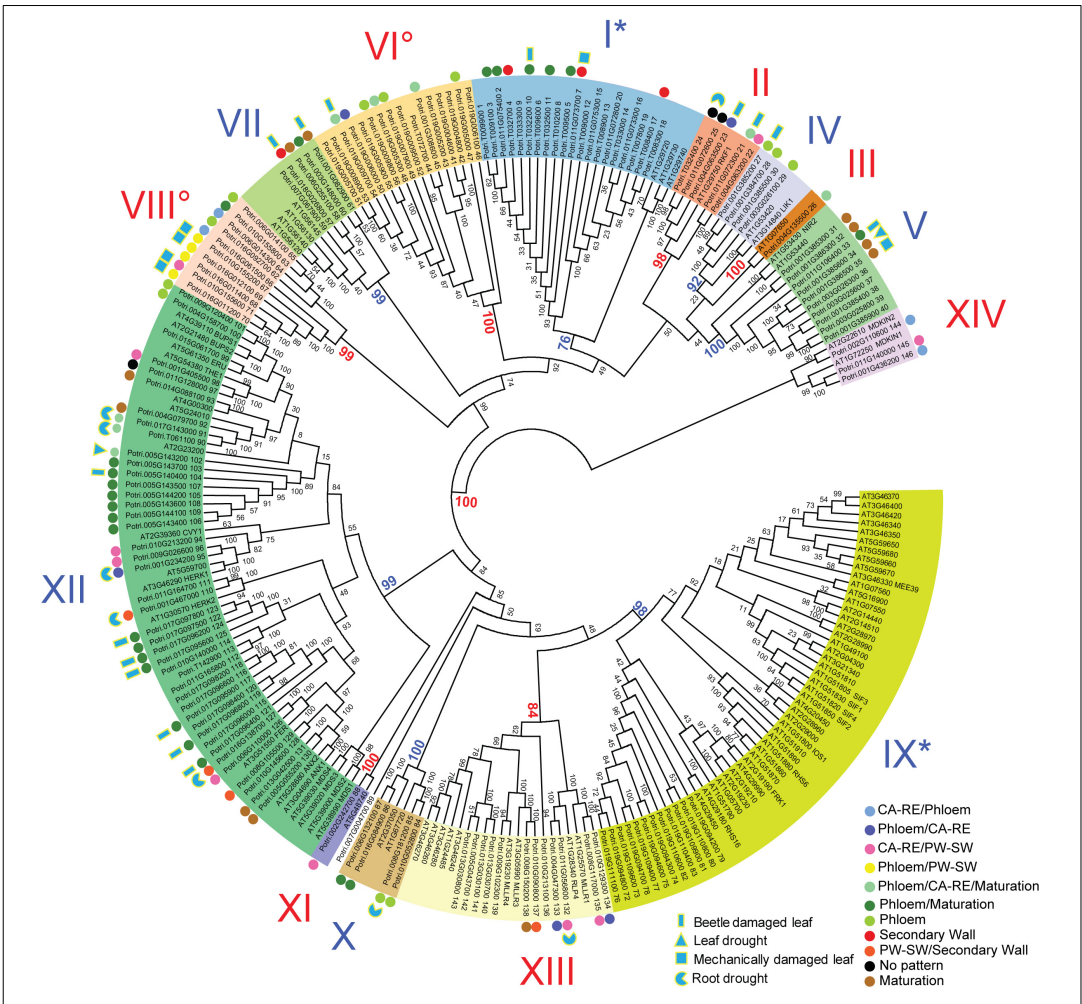
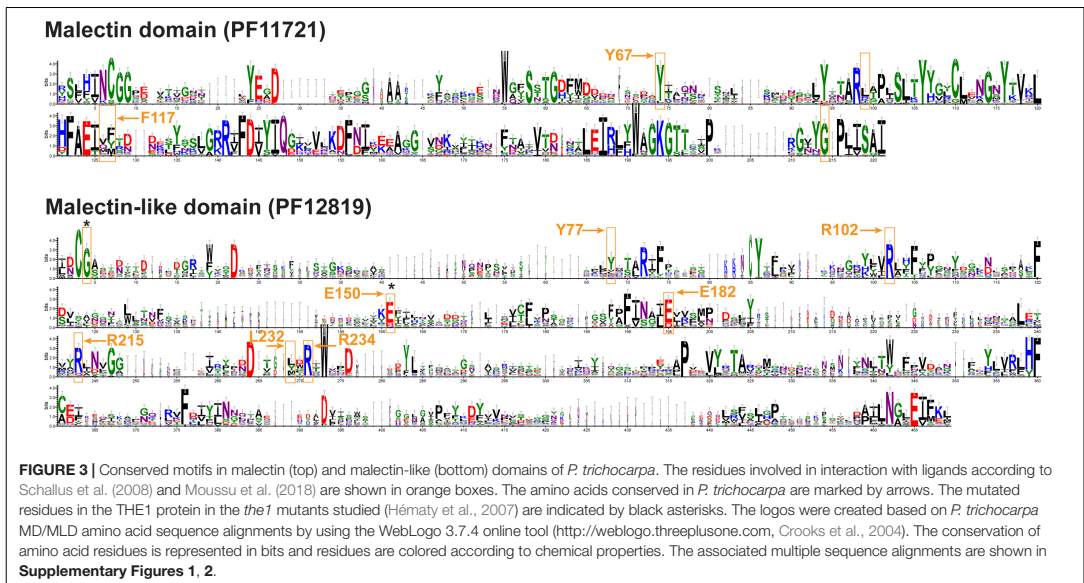


FIGURE 2 | Phylogenetic tree of malectin/malectin-like domain-containing proteins in *P. trichocarpa* and *A. thaliana*. Each protein ID is followed by the name (*A. thaliana*) or PtMD tree number (*P. trichocarpa*). The phylogenetic tree was constructed based on MUSCLE-aligned amino acid sequences using the neighbor-joining method in MEGA 7.0 using 1000 bootstrap replicates, and the bootstrap support is displayed in percentages. Main clades are numbered with Roman numerals, and their supporting bootstrap values are shown in color. Colored dots beside PtMDs identify genes expressed in secondary vascular tissues based on the AspWood (<http://aspwood.poggenie.org/aspwood-v3.0/>) database and showing maximum expression in different developmental zones as indicated by colors. CA-RE, cambium-radial expansion zone; PW-SW, primary to secondary wall transition zone. Asteric shapes with yellow outlines show stress-related expression based on the aspen expression atlas available at <http://popgenie.org>. Degree symbols and asterisks beside Roman numerals indicate clades that are represented by only one species or are significantly expanded in one species (χ^2 -test, $P \leq 0.05$), respectively.

Clade XIV domain structure and topology was unique in having a kinesin domain (Kin) along with an N-terminal MD (Figure 1). This clade has not been previously included in the surveys of MD genes in *A. thaliana* (Bellande et al., 2017) or rice (Jing et al., 2020). Recently, one of the *A. thaliana* clade XIV members, MDKIN2, was found to function in pollen and seed development (Galindo-Trigo et al., 2020).

Orthologs of the clade XIV genes could be identified in many species of Viridiplantae, including moss, lower vascular plants, dicots and monocots.

Based on domain composition and domain order, poplar MD gene clades could be grouped into a higher order organization with five superclades characterized by the following domain patterns: 1) LRR-MD-PK (LRR-RLK group XIII, Zan et al., 2013),



2) MLD-LRR-PK (LRR-RLK group I, Zan et al., 2013), 3) MLD-PK (CrRLK1L), 4) MLD-LRR (RLPs) and 5) MD-Kin (Figure 1).

Chromosomal Distribution of MD Genes in *P. trichocarpa*

127 out of the 146 poplar MD gene models were mapped to chromosomes, while 19 gene models were located on five different scaffolds (Figure 4). The majority of chromosomal genes (79) were present in clusters comprising between two and eleven genes (Figure 4 and Supplementary Table 3). Clusters were also present on the scaffolds. The clusters consisted of tandem repeats having the same or reverse orientations. This large number of tandem duplications strongly suggests that the main mechanism of MD family expansion in *P. trichocarpa* is via local gene duplication, rather than whole genome duplications. Gene multiplication at a given locus could occur via an unequal crossing over mechanism, which after multiple rounds would result in large numbers of tandemly repeated sequences. Such a mechanism was proposed as featuring particularly in various LRR gene families (Schaper and Anisimova, 2015) including LRR-RLK (Shiu and Bleecker, 2001; Zan et al., 2013; Zulawski et al., 2014; Zhang et al., 2016; Wang et al., 2019) and R genes (Choi et al., 2016). Indeed, 11 out of our 16 clusters of *PtMD* genes had members with LRR domain(s) (Supplementary Table 3).

Tandem duplications allow rapid gene family expansion and the creation of novel alleles are thought to be particularly important for the co-evolution of R and Avr genes in hosts and their parasites (Holub, 2001; Choi et al., 2016). Partial duplications with omission of some domains form a key mechanism for neofunctionalization. Such a process apparently characterized the poplar MD family, since there were seven out

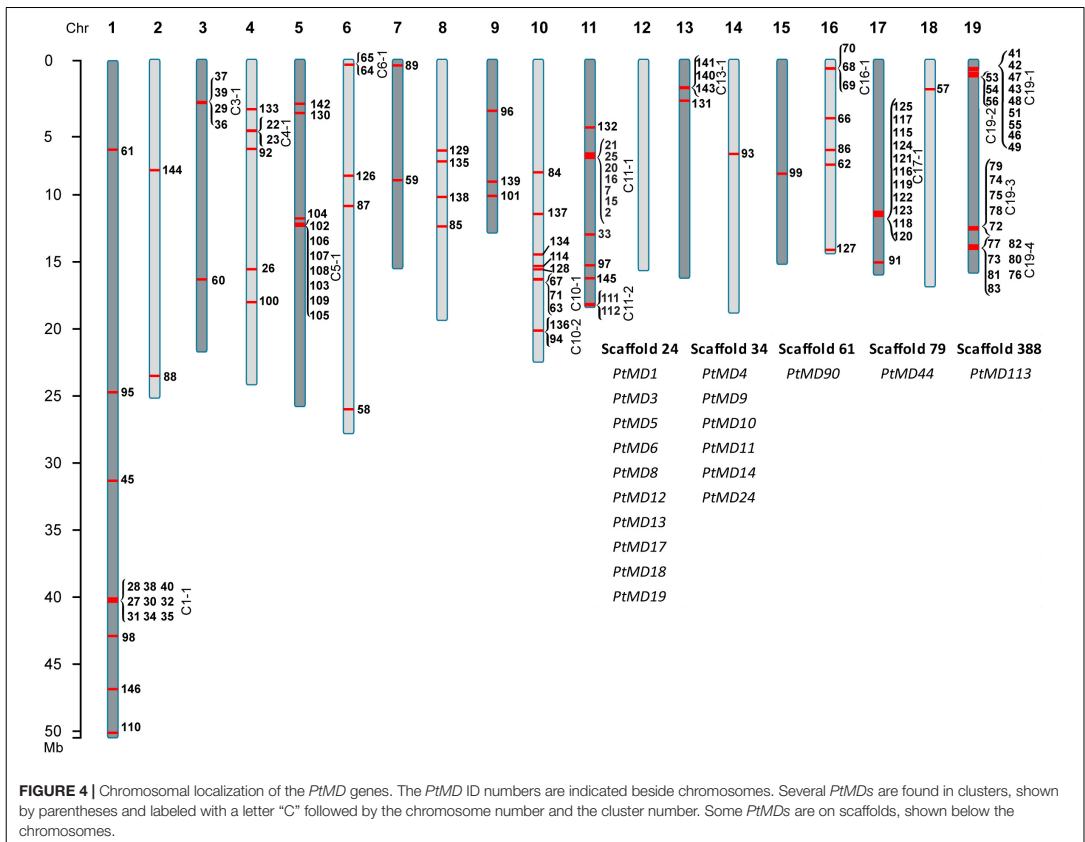
of 16 clusters that included genes with LRR and kinase domains along with closely related members without LRR domains (Figure 4 and Supplementary Table 3).

Analysis of Exon-Intron Structures of *PtMD* Genes

Exon-intron structure reflects the evolutionary history of genes; hence we analyzed the exon-intron organization of *PtMDs*. Although the majority of clades displayed very diverse numbers of introns (Supplementary Table 4 and Figure 1), the maximum number of introns for clades within a superclade was similar. The superclade LRR-MD-PK, comprising clades I-VIII, had genes with very large numbers of introns (maximum between 23 and 26); superclade MLD-LRR-PK (clades IX-XI) had at most 15 introns; superclade MLD-PK (clade XII or the CrRLK1L group) contained genes with up to two, but typically without any introns; and superclades MLD-LRR (clade XIII) and MD-Kin (clade XIV) had at most 10 and 17 introns, respectively (Supplementary Table 4 and Figure 1). Lack, or low frequency, of introns in CrRLK1L genes has also been observed in other species including strawberry, *Arabidopsis* and rice (Zhang et al., 2016; Bellande et al., 2017; Jing et al., 2020). Thus, the exon-intron organization of poplar MD genes supported their grouping into superclades, which represent ancestral diversification of plant MD genes.

Comparison of *P. trichocarpa* and *A. thaliana* MD Proteins

The phylogenetic tree of MD proteins was generally consistent between *P. trichocarpa* and *A. thaliana* with bootstrap values of greater than 76 % for the main clades (Figure 2). Three exceptions were noted, however: one orphan protein *PtMD89*,



clade VI that included *PtMD41-PtMD56*, and clade VIII with *PtMD62-PtMD71*. These poplar genes apparently did not have orthologs in *A. thaliana*. To address a hypothesis that these genes represent tree-specific functions, we analyzed the MD gene families in other tree species with the whole genome data available (Supplementary Figure 3). Close homologs to *PtMD89* were found in other tree species including *Salix purpurea*, *Eucalyptus grandis*, *Theobroma cacao*, *Malus domestica*, *Prunus persica*, and *Citrus sinensis* (Supplementary Figure 3). Each of these species had only one putative *PtMD89* ortholog indicating that *PtMD89* function is conserved in angiosperm trees belonging to different families. Clades VI and VIII include tandemly repeated genes and were not well resolved by the phylogenetic analysis (Figure 4 and Supplementary Table 3). The clear homologs to *P. trichocarpa* tandemly replicated genes of clade VI were present in *Salix purpurea* although we cannot exclude that genes with less supported association to clade VI are present in *Prunus persica*, *Malus domestica*, *Theobroma cacao* and *Betula pendula* (Supplementary Figure 3). Clade VIII included only *P. trichocarpa* and *Salix purpurea* genes, but this clade had a

weak bootstrap support (Supplementary Figure 3). Thus, the genes of clades VI and VIII had undergone recent tandem duplication in the *P. trichocarpa* lineage after its separation from that of *A. thaliana* that could be conserved in other members of Salicaceae. It is therefore possible that they represent specialized genes, such as R genes important for immunity, that co-evolved with poplar symbionts and/or pathogens of the Salicaceae family (Holub, 2001).

Besides identifying clades not represented in *Arabidopsis*, we found that the relative clade sizes (number of genes per clade relative to genome size) show some differences between the two species (Figure 2). Clade IX was expanded in *A. thaliana*, whereas clade I was expanded in *P. trichocarpa* (χ^2 -test at $P \leq 0.05$). The phylogenetic analysis of MD genes including different tree species confirmed the expansion of clade IX in *A. thaliana* and clade I in *P. trichocarpa* (Supplementary Figure 3).

Domain composition and organization were consistent between *P. trichocarpa* and *A. thaliana* in clades present in both species (Supplementary Tables 1, 2). Previous studies in *A. thaliana* classified LRR-RLKs (Shiu and Bleecker, 2001) and

assigned them putative receptor or co-receptor functions based on the sizes of ectodomains (Xi et al., 2019). Many MD proteins identified in the current study were among the previously classified LRR-RLKs (Supplementary Table 2). The group of clades I–VIII, except for clades VI and VIII, which were not represented in *A. thaliana*, have been classified as being of the LRR-VIII-2 class (Shiu and Bleecker, 2001). This group had large ectodomains including several LRR motifs followed by MD, TMD and internal kinase domains (LRR-MD-PK) (Supplementary Table 2 and Figure 1). *A. thaliana* proteins of clades IX–XI belong to class LRR-I (Shiu and Bleecker, 2001), having a large MLD ectodomain terminated with a short LRR repeat, TMD, and an internal protein kinase domain (MLD-LRR-PK), as was observed for poplar (Supplementary Table 2 and Figure 1). *A. thaliana* clade XII proteins correspond to the CrRLK1L group, which is characterized by a large MLD ectodomain followed by TMD and the internal protein kinase domain, whereas clade XIII in *A. thaliana*, as in *P. trichocarpa*, was characterized by a large ectodomain including MLD and LRR domains. Such proteins are classified as RLPs (Wang et al., 2008).

Only four out of the 14 clades identified contained members that have been functionally analyzed in *A. thaliana*. In addition to clade XII (CrRLK1L), which has been the most extensively studied, with members involved in CWI sensing, polar growth, fertilization, and immune responses (Franck et al., 2018), the members of clades IV, V, and IX have been functionally characterized. Clade IV includes LYSM RLK1-INTERACTING KINASE 1 (LIK1), an RLK interacting with the chitin receptor formed by the CERK1-LYSM RLK1 complex, which signals the presence of chitin and activates PTI (Le et al., 2014). Clade IX includes several RLKs involved in both immunity and development. For example, IMPAIRED OOMYCETE SUSCEPTIBILITY 1 (IOS1) acts as a co-receptor of flagellin, EF-Tu and chitin, interacting with FLS2, EFR, and CERK1, respectively (Yeh et al., 2016). STRESS INDUCED FACTORS 1–4 (SIF1, SIF2, SIF3 and SIF4) have been characterized as RLKs involved in biotic and abiotic stress responses (Yuan et al., 2018). SIF2 was found to interact with BAK1 and mediate PTI during pathogen attack. *FLG22-INDUCED RECEPTOR-LIKE KINASE 1* (*FRK1*) is known to be an early-induced PTI gene (Asai et al., 2002). *ROOT HAIR SPECIFIC 6* and *16* (*RHS6* and *RHS16*) were found to be specifically expressed in root hairs and *RHS16* overexpression dramatically altered root hair morphology, indicating an important function in root hair growth (Won et al., 2009), whereas MATERNAL EFFECT EMBRYO ARREST 39 (*MEE39*) was found to be essential for embryo development based on the mutant phenotype (Pagnussat et al., 2005).

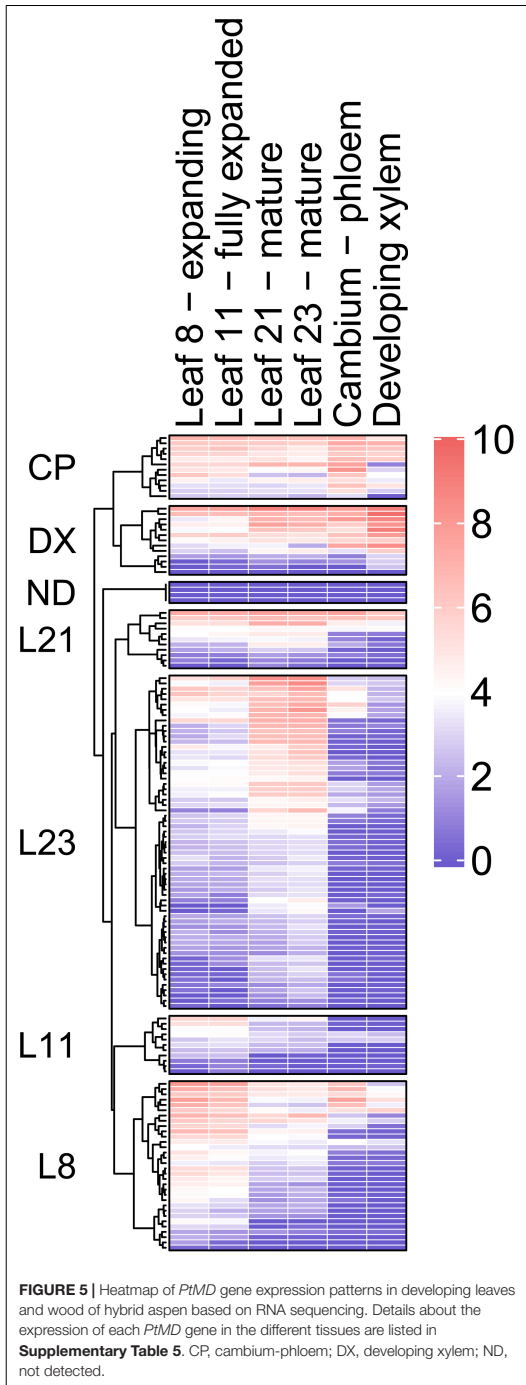
Expression of *PtMDs* in Different Organs of *Populus*

RNA sequencing strategy was adopted to examine the expression of 146 *PtMD* genes in developing leaves and wood tissues (Figure 5 and Supplementary Table 5). Datasets were centered by median expression in each sample and the variance-stabilized transformation (VST) expression values were clustered

considering the tissue with maximum expression as a covariate. Majority of *PtMD* genes had the highest expression in the leaves, especially the fully mature ones (leaf 23). Relatively large number of *PtMD* genes was highly expressed in expanding leaves (leaf 8), and many of these genes were also highly expressed in the cambium. There were 12 and 13 *PtMD* genes with maximum expression in the cambium-phloem and developing xylem tissues, respectively. Majority of these genes showed generally high expression in leaves.

High expression in mature leaves suggests function in foliar defenses and homeostasis for majority of the *PtMD* genes. To investigate it, we also examined the RNA sequencing datasets available for different organs and tissues subjected to variety of stress and growth conditions in the greenhouse and in the field, and calculated VST expression values (Figure 6 and Supplementary Table 6) using the same approach as used for our leaf and wood developmental series. Considering all datasets examined (Figures 5, 6 and Supplementary Tables 5, 6), out of the 146 genes, 145 were expressed at least in one of the organs and tissues tested. Similar to our datasets, the majority of *PtMD* genes (99) showed maximum expression in leaves, especially the mature ones. Moreover, many of them (51) showed the highest expression in leaves exposed to abiotic/biotic stress, such as beetle, drought or mechanical damage. The genes highly expressed in mature and stress-exposed leaves usually exhibited high expression specificity as determined by the *tau* specificity score (Supplementary Table 6). Interestingly, genes belonging to the clades missing in *Arabidopsis* (VI and VIII) were found expressed, indicating that they are functional, and many of them showed a peak of expression in the mature and beetle or mechanically damaged leaves (Figure 2 and Supplementary Tables 5, 6) pointing to their involvement in stress responses. These observations support an important role of the leaf-expressed *PtMD* genes in foliar defense responses, some of which could be species-specific, as suggested by the phylogenetic analyses revealing differences in the presence and size of certain clades of *MD* genes (Figure 2 and Supplementary Figure 3) as well as by the expression analyses in different species. For example, almost all *MD* genes of strawberry (*Fragaria vesca*) were upregulated upon exposure to low temperature or drought stress (Zhang et al., 2016), whereas in rice (*Oryza sativa*), the expression levels of many *MD* genes greatly increased upon salt and drought stress, but not in response to low temperature (Jing et al., 2020).

Twenty *PtMD* genes were most highly expressed in roots of which nine showed highest expression in roots exposed to drought. Genes with maximal expression values detected in stressed organs were distributed among clades I, II, IV, V, VI, VII, VIII, X, XII, and XIII (Figure 2), suggesting stress response functions for these clades. Interestingly, no gene that was maximally expressed in stressed organs was found in clades III, IX, XI or XIV, suggesting their involvement in other types of signaling. Several *PtMD* genes were most highly expressed in the vegetative growing organs: young roots or leaves (Figures 5, 6 and Supplementary Tables 5, 6). Eight genes, all from clades XII and XIII, were most highly expressed in female flowers at various developmental stages, and four in mature seeds. The genes highly expressed in expanding female flower buds or in mature seeds



were in many cases also highly expressed in developing secondary tissues, vascular cambium or developing secondary xylem and phloem (**Figure 6** and **Supplementary Table 6**).

PtMDs Involved in Wood Biosynthesis

Since many *PtMD* genes were found expressed in developing wood (**Figure 5** and **Supplementary Table 5**), we wanted to determine at which wood developmental stage these genes are active. For that, we used the AspWood database (see text footnote 14), which provides data on high-spatial-resolution transcript abundance in developing secondary xylem and phloem tissues of aspen (Sundell et al., 2017). Only 89 *PtMDs* (61%) were found to be expressed in developing secondary vascular tissues (**Supplementary Table 7**), with the majority exhibiting distinct patterns of expression, clustering in ten expression groups (**Supplementary Table 7** and **Figure 7**). This clustering indicates that certain sets of *PtMDs* have specific functions at certain stages of secondary vascular development. Some of the *PtMD* genes expressed in secondary vascular tissue also exhibited high expression under diverse stress conditions in leaves or roots (**Supplementary Table 6** and **Figure 2**).

The largest group of *PtMD* genes (50) that were expressed in secondary vascular tissue showed a peak of expression in the phloem (**Supplementary Table 7** and **Figure 7**). These genes were mostly from superclades LRR-MD-PK including many members of clade VI and VIII without orthologs in *Arabidopsis*, MLD-PK (*CrRLK1L*), and MLD-LRR-PK. Cambium and radial expansion zones were the zones characterized by the greatest variety of *PtMD* transcripts including members of superclades MD-Kin, LRR-MD-PK, MLD-LRR, and MLD-PK (*CrRLK1L*). In contrast, *PtMD* genes having a peak of expression at the transition between primary and secondary wall deposition were mostly from the MLD-PK (*CrRLK1L*) group. Intriguingly, the genes with maximum expression during secondary wall deposition were expressed at relatively low levels and many of them belonged to clade I of *PtMDs*, which lacks LRR. *PtMD* genes with the highest expression in the maturation zone were mostly from clades V and XII.

Networks of Xylogenes-Related *PtMD* Genes

To find putative partners involved in signaling pathways together with the xylogenes-related *PtMD* genes, we analyzed co-expression networks of *PtMD* genes identified as being expressed during xylogenesis. Ten *PtMD* genes forming two clusters with a peak of expression in the cambium-radial expansion zone and primary to secondary transition zone (CA-RE/PW-SW), and eight genes from clusters PW-SW/Secondary Wall and Secondary Wall (**Figure 7** and **Supplementary Table 7**), representing, respectively, the early and main stages of secondary wall deposition were used as baits for network analyses.

The baits for the CA-RE/PW-SW zones formed five separate networks (**Figure 8A** and **Supplementary Table 8**), the largest being that of *PtMD126* -one of the two poplar orthologs of *AtFER*. It included several candidates for functioning in signaling by phosphorylation relay and ROS, and for regulation of cell

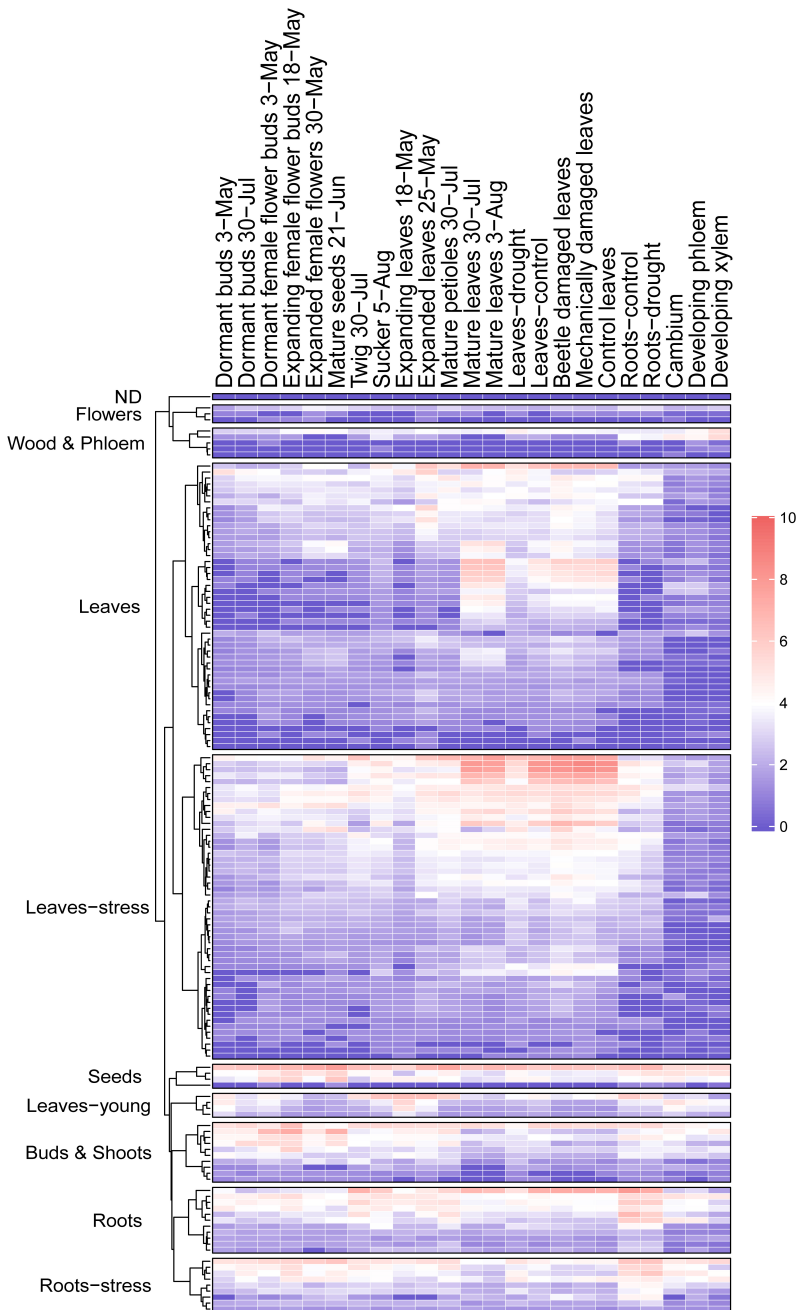


FIGURE 6 | Heatmap of *PtMD* gene expression patterns in different organs of aspen. Data were retrieved from repositories described by Sundell et al. (2015) and Immanen et al. (2016), and normalized expression values are listed in **Supplementary Table 6**.

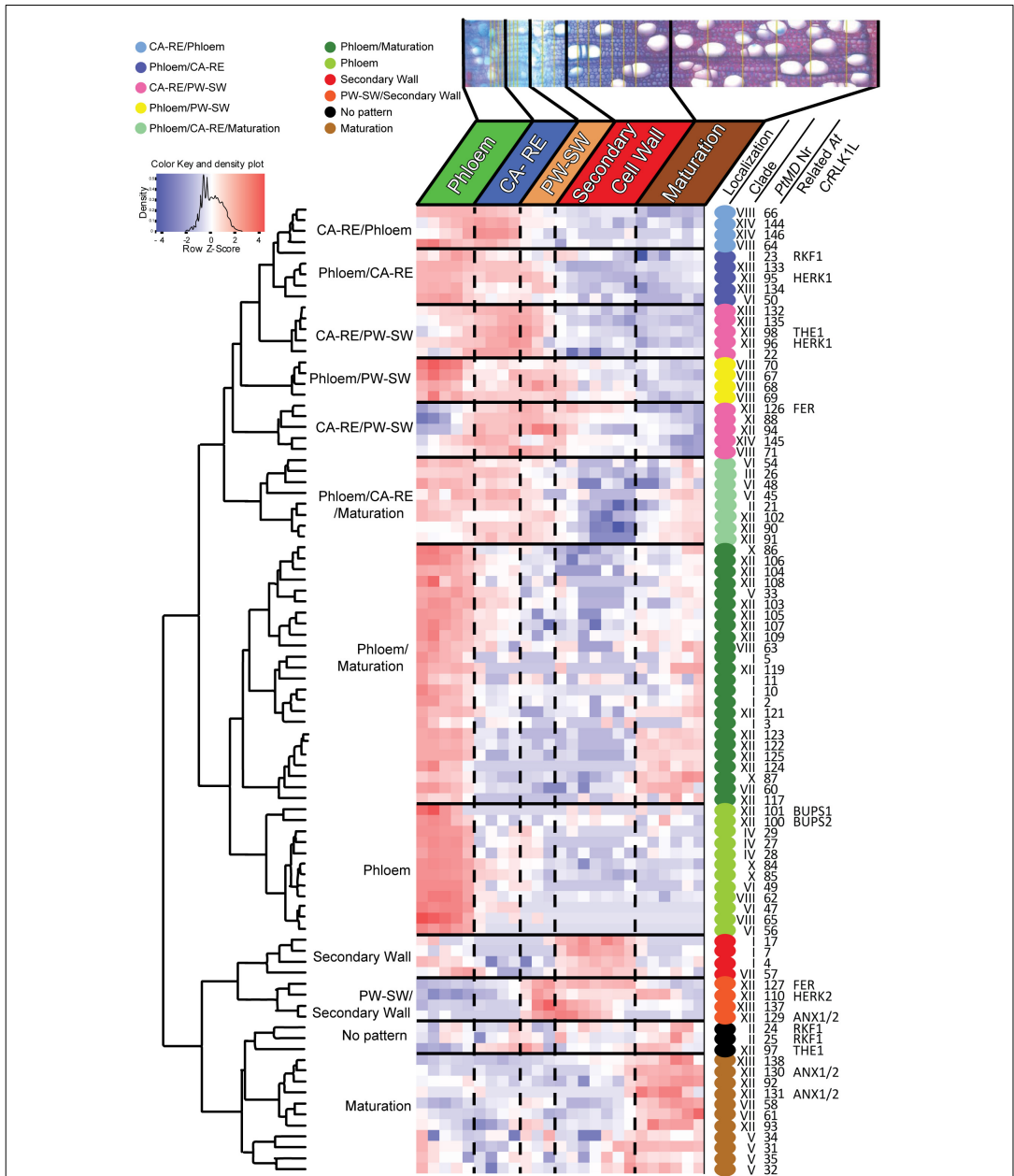
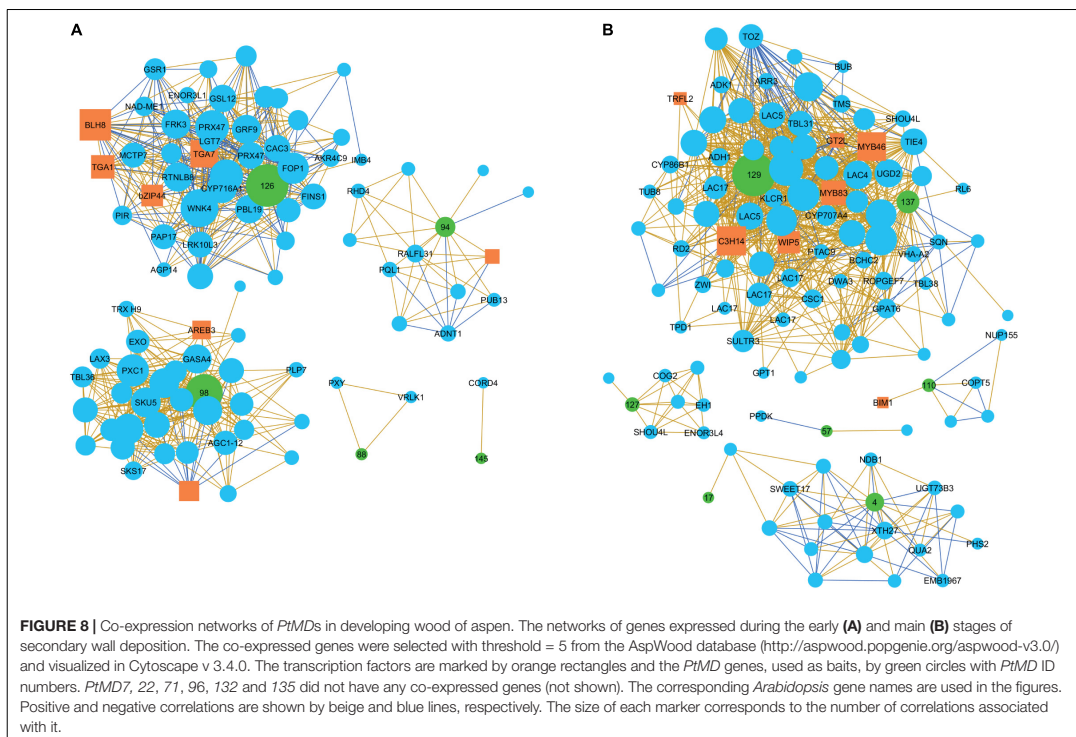


FIGURE 7 | Heatmap of scaled *PtMD* expression patterns in developing secondary vascular tissues based on the AspWood database (<http://aspwood.poggenie.org/aspwood-v3.0/>). The majority of *PtMD* genes show maximum expression in the phloem and in the cambium-radial expansion zone (CA-RE). Smaller clusters of genes are expressed in the developing xylem including the secondary wall formation zone, the transition between the primary and secondary wall zone (PW-SW), or the maturation zone. Specific wood developmental stages are defined based on the patterns of expression of marker genes (Sundell et al., 2017). Colored dots beside *PtMDs* identify groups with maximum expression in different developmental zones.



wall development. Apoplastic ROS in wood forming tissues could have a double role, in signaling and in regulation of lignin polymerization. Thus, the *PtMD126* network included a homolog of *PBS1-LIKE 19* (*AtPBL19*), encoding a RLCK of subfamily VII-4, which signals a response to chitin perceived by CHITIN ELICITOR RECEPTOR KINASE 1 (*AtCERK1*) through a phosphorylation relay (Bi et al., 2018), and ROS production (Rao et al., 2018). Homologs of *AtTGA1* and *AtTGA7*, which encode basic leucine zipper transcription factors involved in oxidative stress-mediated responses to biotrophic and necrotrophic pathogens (reviewed by Gatz, 2013), were, respectively, positively and negatively correlated with *PtMD126* (Figure 8A and Table 1). The oxidation state of *AtTGA1* is regulated by a glutaredoxin, *AtROXY19* (Li et al., 2019), the homolog of which has been found to respond to altered secondary wall xylan in aspen (Ratke et al., 2018), suggesting that the *PtMD126* network might include candidates for sensing secondary wall integrity. *AtTGA1* interacts with the BLADE-ON-PETIOLE 1 and 2 (*AtBOP1/2*) transcription factors (Wang et al., 2019), which are known to regulate xylem fiber differentiation (Liesch et al., 2014). Moreover, the network includes a homolog of the BEL1-LIKE HOMEODOMAIN 8 (*AtBLH8*) transcription factor, which controls expression of BOP1 (Khan et al., 2015; Figure 8A and Table 1). The network also includes a homolog of the gene encoding GROWTH-REGULATING FACTOR

9 (*AtGRF9*), a 14-3-3 protein that regulates developmental programs and stress signaling by binding phosphoproteins and regulating their activities (Mayfield et al., 2007; Liu et al., 2014; Omidbakhshfar et al., 2018). The presence of a homolog of IMPORTIN-BETA 4 (*AtIMB4*), which is required to transport GRF-INTERACTING FACTOR 1 (*AtGIF1*) to the nucleus (Liu et al., 2019; Figure 8A and Table 1) further supports the involvement of *GRF/14-3-3* genes in the *PtMD126* network.

A separate large network was formed by neighbors of *PtMD98* -one of the two poplar orthologs of *AtTHE1* (Figure 8A, Table 1 and Supplementary Table 8). This network comprised genes related to hormonal signaling by IAA and GA, and to the regulation of xylogenesis. One example is a homolog of *AtLAX3*, which encodes an auxin influx carrier (Swarup et al., 2008). Another is a homolog of *AtAGC1-12*, encoding a kinase phosphorylating the auxin efflux carrier *AtPIN1* (Haga et al., 2018). We have also identified a homolog of *AtGASA4* involved in GA responses and redox regulation (Rubinovich and Weiss, 2010). It is noteworthy that GA responses and *GASA* genes were also found to be upregulated in response to a secondary wall xylan defect in aspen (Ratke et al., 2018). Moreover, the co-expression network included an LRR-RLK homologous to *AtPXY-CORRELATED 1* (*AtPXC1*), which is required for secondary wall deposition (Wang et al., 2013).

TABLE 1 | Genes co-regulated with poplar *MD* genes expressed during secondary wall formation that were discussed in the text.

First neighbors	Poplar name	Best BLAST Agl codes	Ath-names	Baits							Ath short description	Pathway/process
				MD126 (Potl.006G110000)	MD94 (Potl.010G213200)	MD98 (Potl.001G405500)	MD88 (Potl.002G242700)	MD129 (Potl.008G105500)	MD137 (Potl.010G090800)	MD110 (Potl.001G467000)		
Potri.014G062700	AT5G47070	PBL19	+							PBS1-LIKE 19 - a RLOK phosphorylating MAPKKK5 and MEKK1 in response to chitin	PAMP, ROS, P, JA, and BR signaling, BOP1/2	
Potri.002G090700	AT5G66210	TGA1	+							TGA-BINDING 1 - a bZIP TF, a redox-controlled regulator of SAR and development	PAMP, ROS, P, JA, and BR signaling, BOP1/2	
Potri.005G170500	AT1G77920	TGA7	-							TGA-BINDING 7 - a bZIP TF, a redox-controlled regulator of SAR and development	PAMP, ROS, P, JA, and BR signaling, BOP1/2	
Potri.004G213300	AT2G27990	BLH8	+							BEL1-like TF, regulating BOP1 and integrating stress signaling via JA	PAMP, ROS, P, JA, and BR signaling, BOP1/2	
Potri.001G392200	AT2G42590	GRF9	+							GROWTH-REGULATING FACTOR 9, 14-3-3 gene. Binds Ca ²⁺ and regulates development.	Ca ²⁺ and P signaling and regulation	
Potri.010G169800	AT4G27640	IMB4	+							IMPORTIN-BETA 4 transporting GRF-interacting factor 1 (GIF1) to nucleus	Ca ²⁺ and P signaling and regulation	
Potri.009G029600	AT3G46510	PUB13	+	+						PLANT U-BOX 13, an E3 ubiquitin ligase involved in ubiquitination of receptor FLS2.	PAMP signaling	
Potri.005G100500	AT3G51460	RHD4	+	+						ROOT HAIR DEFECTIVE4, a phosphatidylinositol-4-P phosphatase required by root hairs	P signaling and regulation	
Potri.015G108700	AT5G61820	RALFL31	+	+						Stress up-regulated Nod 19 protein;	Ca ²⁺ and P signaling and regulation	
Potri.017G059500	AT4G13950	RALFL31	+	+						RAPID ALKALINIZATION FACTOR LIKE 31 - peptide hormone	Ca ²⁺ and P signaling and regulation	
Potri.005G174000	AT1G77690	LAX3	+		+					Auxin influx carrier LAX3 (Like Aux1)	Auxin signaling	
Potri.010G236200	AT3G44610	AGC1-12	+		+					Kinase involved in phototropism and gravitropism. Phosphorylates PIN1	Auxin signaling	
Potri.017G083000	AT5G15230	GASA4	+		+					Encodes GA-regulated protein GASA4. Promotes GA responses and exhibits redox activity.	GA signaling	
Potri.006G117200	AT2G36570	PXC1	+							Leucine-rich repeat protein kinase family protein	Xylogenesis and SW formation	
Potri.001G057800	AT1G67310		-							Calmodulin-binding TF	Ca ²⁺ -related signaling	

(Continued)

TABLE 1 | Continued

First neighbors	Poplar name	Best BLAST Agl codes	Ath-names	Baits							Ath short description	Pathway/process
				MD126 (Pofr:006G11000)	MD94 (Pofr:010G21320)	MD98 (Pofr:001G40550)	MD88 (Pofr:002G24270)	MD129 (Pofr:008G10550)	MD137 (Pofr:010G90800)	MD110 (Pofr:001G46700)		
Pofr:001G126100		AT5G61480	PXY				+				PHLOEM INTERCALATED WITH XYLEM - α LRR-RLK receptor of TDIF regulating xylem cell fate	Xylogenesis and SW formation
Pofr:006G114400		AT1G79620	VRLK1				+				VASCULAR-RELATED RLK1 - α LRR kinase regulating onset of secondary cell wall thickening.	Xylogenesis and SW formation
Pofr:009G063900	MYB021	AT5G12870	MYB46					+			Master secondary wall TF MYB46	Xylogenesis and SW formation
Pofr:001G018900		AT1G61220	WIP5					+			WIP domain 5. Target of WRKY53, involved cell fate determination in response to auxin via MP.	Auxin signaling
Pofr:008G105600		AT4G24972	TPD1					+			TAPETUM DETERMINANT 1, peptide hormone perceived by EMS1-SERK1	P signaling and regulation
Pofr:001G267300	MYB3	AT3G08500	MYB83					+			Master secondary wall TF MYB83	Xylogenesis and SW formation
Pofr:016G104400		AT5G02010	ROGEE7						+		ROP (RHO OF PLANTS) GUANINE NUCLEOTIDE EXCHANGE FACTOR 7	CPLK1L -mediated signaling
Pofr:005G135500		AT2G15790	SQN						-		SQUINT - homolog of cyclophilin 40, involved in miRNA regulation	miRNA regulation
Pofr:004G005900		AT4G22120	CSC1						+		CALCIUM PERMEABLE STRESS-GATED CATION CHANNEL 1 - stretch activated cation channel.	Ca ²⁺ -related signaling
Pofr:005G051700		AT5G28300	GT2L								GT2-LIKE PROTEIN - α CaM-binding protein involved in cold stress signaling	Transcriptional regulation
Pofr:001G295100		AT3G19590	BUB3.1						-		BUDDING UNINHIBITED BY BENZYMIDAZOL 3.1 - spindle assembly.	Cell division
Pofr:001G394200		AT4G20010	PTAC9						-		PLASTID TRANSCRIPTIONALLY ACTIVE 9- α single-stranded DNA binding protein.	Cell division
Pofr:013G079600		AT5G16750	TOZ						-		TORMOZ -RNA processing required for cell division	Cell division
Pofr:015G048000		AT5G08130	BIM1							+	BES1-INTERACTING MYC-LIKE 1- α BHLH TF involved in brassinosteroid signaling	BR signaling

All genes from network analyses are listed in **Supplementary Tables 8, 9.**

The network of *PtMD94* -the clade XII member related to *AtHERK1* and *AtCVY1* -included a homolog of *AtRALFL31* (Figure 8A, Table 1 and Supplementary Table 8). *RALF* genes encode hormone peptides that signal developmental processes and stress responses by interacting with *CrRLK1Ls*. *AtRALFL31* belongs to subfamily IIIA which includes as yet uncharacterized members, but both *AtRALFL31* and *Potri.017G059500* have the conserved YISY motif essential for interaction with *AtFER* (Campbell and Turner, 2017). Thus, *Potri.017G059500* could potentially encode a peptide hormone recognized by *PtMD94*. The *PtMD94* network also included other candidates for signaling. For example, there was a homolog of *PLANT U-BOX 13* (*AtPUB13*), which encodes an E3 ligase involved in signal-activated ubiquitination and subsequent degradation of different receptors including ABA INSENSITIVE 1 (*AtABI1*) (Kong et al., 2015), BRASSINOSTEROID INSENSITIVE 1 (*AtBRI1*) (Zhou et al., 2018), LYSM-CONTAINING RECEPTOR-LIKE KINASE 5 (*AtLYK5*) (Liao et al., 2017), and FLAGELLIN-SENSITIVE 2 (*AtFLS2*) (Liu et al., 2012; Antignani et al., 2015). The ubiquitination of flg22-bound *AtFLS2* by *AtPUB13* depends on its interactor protein RAB GTPASE HOMOLOG A 4B (*AtRABA4B*) (Antignani et al., 2015). Interestingly, a homolog to another *PtMD94* network member encodes ROOT HAIR DEFECTIVE 4 (*AtRHD4*) which mediates polar localization of *AtRABA4B* (Thole et al., 2008). Consequently, it seems likely that these *PtMD94* network members are indeed functionally linked within the same network.

Two other *PtMD* genes expressed during early secondary wall biosynthesis, *PtMD88* and *PtMD145*, formed small networks, which included important regulatory genes in xylem cell differentiation (Figure 8A, Table 1 and Supplementary Table 8). One of them was the homolog of the master spatial regulator of vascular differentiation, *PHLOEM INTERCALATED WITH XYLEM* (*AtPXY*), encoding an LRR-RLK that promotes cell division in the cambium upon binding the small CLE peptide *AtTDIF*, which is essential for xylem differentiation (Fisher and Turner, 2007). The other was a homolog of *VASCULAR-RELATED RECEPTOR-LIKE KINASE 1* (*AtVRLK1*) (Huang et al., 2018) which is probably responsible for the switch between xylem cell expansion and secondary wall deposition.

The late secondary wall-expressed baits formed five networks (Figure 8B, Table 1 and Supplementary Table 9). The largest of these was associated with two *PtMD* genes, *PtMD129*, a clade XII member related to *AtANX1* and *AtANX2*, and *PtMD137*, which encodes an LRR-RLK, from clade XIII. Orthologs of key signaling-related genes were included within this network. One of them was *CALCIUM PERMEABLE STRESS-GATED CATION CHANNEL 1* (*AtCSC1*). Stretch-activated Ca^{2+} channels have been predicted to be important players in CWI (Engelsdorf and Hamann, 2014). *AtCSC1* belongs to a newly characterized family of stretch-activated Ca^{2+} channels conserved in eukaryotes (Hou et al., 2014; Liu et al., 2018). In addition, we found *Potri.015G108700/AT5G61820*, encoding an uncharacterized NOD19-like protein, which has been implicated in responses to cold stress downstream of mechanosensitive Ca^{2+} channels (Mori et al., 2018). The aspen homolog of *AtCSC1* is thus a promising candidate for a secondary wall damage sensor.

Another important signaling-related homolog is *TAPETUM DETERMINANT 1* (*AtTPD1*), which encodes a small peptide hormone that is recognized by an RLK complex consisting of *AtEMS1* and *AtSERK1/2* to activate transcription factors of the BES1 family (Chen et al., 2019). Moreover, a homolog of *Arabidopsis ROP* (*RHO OF PLANTS*) *GUANINE NUCLEOTIDE EXCHANGE FACTOR 7* (*AtROPGEF7*) was among the hits for *PtMD137*. *AtROPGEF7* interacts with the kinase domain of *AtFER*, mediating downstream NADPH oxidase-dependent ROS signaling which is needed for polarized cell growth (Duan et al., 2010). Finally, we identified a homolog of *Arabidopsis GT-LIKE PROTEIN* (*AtGT2L*), which encodes a Ca^{2+} -dependent calmodulin (CaM)-binding trihelix transcription factor involved in plant abiotic stress signaling (Xi et al., 2012). In addition to signaling-related genes, the *PtMD129-PtMD137* network included some key cell fate regulator proteins (Figure 8B, Table 1 and Supplementary Table 9). One of these was the homolog of *WIP DOMAIN PROTEIN 5* (*AtWIP5*), which encodes a zinc-finger protein involved in root patterning downstream of auxin (Crawford et al., 2015) and ROS signaling (Miao et al., 2004). Another was a homolog of *Arabidopsis SQUINT* (*AtSQN*), which encodes a cyclophilin 40-like protein that promotes the accumulation of miRNAs miR156 and miR172, targeting master regulatory genes in organ development (Smith et al., 2009; Prunet et al., 2015). The network also included orthologs of two genes encoding master transcriptional regulators, *AtMYB46* and *AtMYB83*, which activate the secondary wall program (Zhong and Ye, 2012). Both these genes showed positive correlation with *PtMD129*. In contrast, orthologs of three genes with roles in cell division were negatively correlated with *PtMD129* (Table 1). This supports the hypothesis that secondary wall integrity signaling results in coordination between cell division and secondary wall formation activities in developing wood (Ratke et al., 2018).

The network for *PtMD110*, which together with *PtMD111* forms a pair orthologous to *AtHERK2*, included a homolog of the *Arabidopsis* gene encoding the transcription factor BES1-INTERACTING MYC-LIKE1 (*AtBIM1*) (Figure 8B, Table 1 and Supplementary Table 9), which mediates brassinosteroid signaling (Chandler et al., 2009). Several other genes discussed above can be linked to BR-dependent or BES-related BR-independent signaling (Table 1). Intriguingly, a secondary wall xylan defect induced transcriptionomic changes suggesting stimulation of BR signaling in aspen (Ratke et al., 2018), supporting the involvement of the *AtBIM1* homolog in sensing secondary wall integrity.

CONCLUSION

Malectin and malectin-like domains (MD/MLD) are lectin-like motifs found in proteins (MD proteins) of pro- and eukaryotes; they are particularly abundant in plants, where they carry out essential signaling functions in defense and development (Bellande et al., 2017; Franck et al., 2018). This has been shown by studies on *MD* genes from herbaceous plants such as *Arabidopsis* (Bellande et al., 2017; Sultana et al., 2020), strawberry (Zhang et al., 2016) and rice (Jing et al., 2020). However, no such

comprehensive study has been available for *MD* genes in trees. Here we carried out a census of *MD* genes in the model woody species *P. trichocarpa* (Supplementary Table 1) and expanded the set for *A. thaliana* (Supplementary Table 2).

In total, 146 *MD* genes were found in *P. trichocarpa* and they were assigned to fourteen clades based on sequence similarity, and to five superclades based on predicted protein domain organization and intron-exon structures (Figures 1, 2). The variety of *MD* protein structures reflects their range of different functions in plants.

Additional genome-wide analysis by using available sequence data from different woody species revealed, that certain *MD* genes appeared to be specific either to trees or to the *Populus* lineage and absent from *Arabidopsis* (Supplementary Figure 3). The prevalence of tandem duplications within the *MD* gene family, which apparently led to family expansion, may have created conditions conducive to gene neofunctionalization and rapid evolution (Schaper and Anisimova, 2015; Choi et al., 2016).

The majority of the poplar *MD* genes were found to be highly expressed in mature leaves, particularly those subjected to biotic and abiotic stress conditions (Figure 6), supporting their role in stress signaling. Detailed analysis of expression in wood forming tissues revealed subsets upregulated in xylem cells during secondary wall deposition (Figure 7). These genes, not unexpectedly, include candidates for the sensing of cell wall integrity. We identified their co-expression networks revealing potential molecular pathways in which these *MD* genes might participate to ensure the coordination of secondary wall formation (Table 1).

The current study provides an extensive analysis of *Populus MD* genes and opens the possibility to better understand their role in essential physiological pathways related to stress signaling and the regulation of wood formation in trees.

DATA AVAILABILITY STATEMENT

The datasets presented in this study can be found in online repositories. The names of the repository/repositories

and accession number(s) can be found in the article/Supplementary Material.

AUTHOR CONTRIBUTIONS

VK identified *MD* genes and their chromosomal clustering, and wrote the first draft. VK and FB identified protein domains and the main clades of *MD* genes. VK and SK analyzed exon-intron structures. ED analyzed gene expression in leaves and wood. VK and ED analyzed *in silico* gene expression in different organs. ED, JU, and VK analyzed conserved regions in MD and MLD of poplar. VK and FB analyzed co-expression networks. VK and CM analyzed the phylogeny across the tree species. EM conceived and coordinated the project, and finalized the manuscript with contributions from all authors. All authors contributed to the article and approved the submitted version.

FUNDING

This work was supported by Swedish Research Council, the Kempe Foundation, the Knut and Alice Wallenberg Foundation, and the SSF program ValueTree RBP14-0011.

ACKNOWLEDGMENTS

We thank Dr. Nicolas Delhomme and the Bioinformatics Facility at UPSC for allowing us to use their server during the work. This manuscript has been released as a pre-print at Research Square, Kumar et al. (2020).

SUPPLEMENTARY MATERIAL

The Supplementary Material for this article can be found online at: <https://www.frontiersin.org/articles/10.3389/fpls.2020.588846/full#supplementary-material>

REFERENCES

Adebali, O., Ortega, D. R., and Zhulin, I. B. (2015). CDvist: a webserver for identification and visualization of conserved domains in protein sequences. *Bioinformatics* 31, 1475–1477. doi: 10.1093/bioinformatics/btu836

Altschul, S. F., Gish, W., Miller, W., Myers, E. W., and Lipman, D. J. (1990). Basic local alignment search tool. *J. Mol. Biol.* 215, 403–410. doi: 10.1016/S0022-2836(05)80360-2

Antignani, V., Klocko, A. L., Bak, G., Chandrasekaran, S. D., Dunivin, T., and Nielsen, E. (2015). Recruitment of PLANT U-BOX13 and the PI4K β 1/ β 2 phosphatidylinositol-4 kinases by the small GTPase Raba4B plays important roles during salicylic acid-mediated plant defense signaling in *Arabidopsis*. *Plant Cell* 27, 243–261. doi: 10.1105/tpc.114.134262

Armenteros, A. J. J., Sønderby, C. K., Sønderby, S. K., Nielsen, H., and Winther, O. (2017). DeepLoc: prediction of protein subcellular localization using deep learning. *Bioinformatics* 33, 3387–3395. doi: 10.1093/bioinformatics/btx431

Asai, T., Tena, G., Plotnikova, J., Willmann, M. R., Chiu, W.-L., Gomez-Gomez, L., et al. (2002). MAP kinase signalling cascade in *Arabidopsis* innate immunity. *Nature* 415, 977–983. doi: 10.1038/415977a

Bella, J., Hindle, K. L., McEwan, P. A., and Lovell, S. C. (2008). The leucine-rich repeat structure. *Cell. Mol. Life Sci.* 65, 2307–2333. doi: 10.1007/s00018-008-8019-0

Bellande, K., Bono, J.-J., Savelli, B., Jamet, E., and Canut, H. (2017). Plant lectins and lectin receptor-like kinases: how do they sense the outside? *Intern. J. Mol. Sci.* 18:1164. doi: 10.3390/ijms18061164

Bi, G., Zhou, Z., Wang, W., Li, L., Rao, S., Wu, Y., et al. (2018). Receptor-like cytoplasmic kinases directly link diverse pattern recognition receptors to the activation of mitogen-activated protein kinase cascades in *Arabidopsis*. *Plant Cell* 30, 1543–1561. doi: 10.1105/tpc.17.00981

Boisson-Dernier, A., Franck, C. M., Lituiev, D. S., and Grossniklaus, U. (2015). Receptor-like cytoplasmic kinase MARIS functions downstream of CrRLK1L-dependent signaling during tip growth. *Proc. Natl. Acad. Sci. U.S.A.* 112, 12211–12216. doi: 10.1073/pnas.1512375112

Boisson-Dernier, A., Lituiev, D. S., Nestorova, A., Franck, C. M., Thirugnanarajah, S., and Grossniklaus, U. (2013). ANXUR receptor-like kinases coordinate cell wall integrity with growth at the pollen tube tip via NADPH oxidases. *PLoS Biol.* 11:e1001719. doi: 10.1371/journal.pbio.1001719

Bray, N. L., Pimentel, H., Melsted, P., and Pachter, L. (2016). Near-optimal probabilistic RNA-seq quantification. *Nat. Biotechnol.* 34, 525–527. doi: 10.1038/nbt.3519

Buchfink, B., Xie, C., and Huson, D. H. (2015). Fast and sensitive protein alignment using DIAMOND. *Nat. Methods* 12, 59–60. doi: 10.1038/nmeth.3176

Campbell, L., and Turner, S. R. (2017). A comprehensive analysis of RALF proteins in green plants suggests there are two distinct functional groups. *Front. Plant Sci.* 8:37. doi: 10.3389/fpls.2017.00037

Chandler, J. W., Cole, M., Flier, A., and Werr, W. (2009). BIM1, a bHLH protein involved in brassinosteroid signalling, controls *Arabidopsis* embryonic patterning via interaction with DORNROSCHEN and DORNROSCHEN-LIKE. *Plant Mol. Biol.* 69, 57–68. doi: 10.1007/s11103-008-9405-6

Chen, W., Lv, M., Wang, Y., Wang, P.-A., Cui, Y., Li, M., et al. (2019). BES1 is activated by EMS1-TPD1-SERK1/2-mediated signaling to control tapetum development in *Arabidopsis thaliana*. *Nat. Commun.* 10:4164. doi: 10.1038/s41467-019-12118-4

Choi, K., Reinhard, C., Serra, H., Ziolkowski, P. A., Underwood, C. J., Zhao, X., et al. (2016). Recombination rate heterogeneity within *Arabidopsis* disease resistance genes. *PLoS Genet.* 12:e1006179. doi: 10.1371/journal.pgen.1006179

Crawford, B. C. W., Sewell, J., Golembeski, G., Roshan, C., Long, J. A., and Yanofsky, M. F. (2015). Genetic control of distal stem cell fate within root and embryonic meristems. *Science* 347, 655–659. doi: 10.1126/science.aaa0196

Crooks, G. E., Hon, G., Chandonia, J.-M., and Brenner, S. E. (2004). WebLogo: a sequence logo generator. *Genome Res.* 14, 1188–1190. doi: 10.1101/gr.849004

Denness, L., McKenna, S. F., Segonzac, C., Wormit, A., Madhou, P., Bennett, M., et al. (2011). Cell wall damage-induced lignin biosynthesis is regulated by a reactive oxygen species- and jasmonic acid-dependent process in *Arabidopsis*. *Plant Physiol.* 156, 1364–1374. doi: 10.1104/pp.111.175737

Draeger, C., Ndiyanka Fabrice, T., Gineau, E., Mouille, G., Kuhn, B. M., Moller, I., et al. (2015). *Arabidopsis* leucine-rich repeat extensin (LRX) proteins modify cell wall composition and influence plant growth. *BMC Plant Biol.* 15:155. doi: 10.1186/s12870-015-0548-8

Du, C., Li, X., Chen, J., Chen, W., Li, B., Li, C., et al. (2016). Receptor kinase complex transmits RALF peptide signal to inhibit root growth in *Arabidopsis*. *Proc. Natl. Acad. Sci. U.S.A.* 113, E8326–E8334. doi: 10.1073/pnas.1609626113

Du, S., Qu, L.-J., and Xiao, J. (2018). Crystal structures of the extracellular domains of the CrRLK1L receptor-like kinases ANXUR1 and ANXUR2. *Protein Sci.* 27, 886–892. doi: 10.1002/pro.3381

Duan, Q., Kita, D., Li, C., Cheung, A. Y., and Wu, H.-M. (2010). FERONIA receptor-like kinase regulates RHO GTPase signaling of root hair development. *Proc. Natl. Acad. Sci. U.S.A.* 107, 17821–17826. doi: 10.1073/pnas.1005366107

Dünser, K., Gupta, S., Herger, A., Feraru, M. I., Ringli, C., and Kleine-Vehn, J. (2019). Extracellular matrix sensing by FERONIA and leucine-rich repeat extensins controls vacuolar expansion during cellular elongation in *Arabidopsis thaliana*. *EMBO J.* 38:e100353. doi: 10.15252/embj.2018100353

El-Gebali, S., Mistry, J., Bateman, A., Eddy, S. R., Luciani, A., Potter, S. C., et al. (2019). The Pfam protein families database in 2019. *Nucleic Acids Res.* 47, D427–D432. doi: 10.1093/nar/gky995

Engelsdorf, T., and Hamann, T. (2014). An update on receptor-like kinase involvement in the maintenance of plant cell wall integrity. *Ann. Bot.* 114, 1339–1347. doi: 10.1093/aob/mcu043

Escobar-Restrepo, J.-M., Huck, N., Kessler, S., Gagliardini, V., Gheyselinck, J., Yang, W.-C., et al. (2007). The FERONIA receptor-like kinase mediates male-female interactions during pollen tube reception. *Science* 317, 656–660. doi: 10.1126/science.1143562

Feng, W., Kita, D., Peaucelle, A., Cartwright, H. N., Doan, V., Duan, Q., et al. (2018). The FERONIA receptor kinase maintains cell-wall integrity during salt stress through Ca²⁺ signaling. *Curr. Biol.* 28, 666–675.e665. doi: 10.1016/j.cub.2018.01.023

Fisher, K., and Turner, S. (2007). PXY, a receptor-like kinase essential for maintaining polarity during plant vascular-tissue development. *Curr. Biol.* 17, 1061–1066. doi: 10.1016/j.cub.2007.05.049

Foreman, J., Demidchik, V., Bothwell, J. H. F., Mylona, P., Miedema, H., Torres, M. A., et al. (2003). Reactive oxygen species produced by NADPH oxidase regulate plant cell growth. *Nature* 422, 442–446. doi: 10.1038/nature01485

Franck, C. M., Westermann, J., and Boisson-Dernier, A. (2018). Plant malectin-like receptor kinases: from cell wall integrity to immunity and beyond. *Ann. Rev. Plant Biol.* 69, 301–328. doi: 10.1146/annurev-arplant-042817-40557

Galindo-Trigo, S., Grand, T. M., Voigt, C. A., and Smith, L. M. (2020). A malectin domain kinesin functions in pollen and seed development in *Arabidopsis*. *J. Exper. Bot.* 71, 1828–1841. doi: 10.1093/jxb/eraa023

Galindo-Trigo, S., Gray, J. E., and Smith, L. M. (2016). Conserved roles of CrRLK1L receptor-like kinases in cell expansion and reproduction from algae to angiosperms. *Front. Plant Sci.* 7:1269. doi: 10.3389/fpls.2016.01269

Gatz, C. (2013). From pioneers to team players: TGA transcription factors provide a molecular link between different stress pathways. *Mol. Plant Microb. Interact.* 26, 151–159. doi: 10.1094/mpmi-04-12-0078-ia

Ge, Z., Bergonci, T., Zhao, Y., Zou, Y., Du, S., Liu, M.-C., et al. (2017). *Arabidopsis* pollen tube integrity and sperm release are regulated by RALF-mediated signaling. *Science* 358, 1596–1600. doi: 10.1126/science.aaa3642

Gentleman, R. C., Carey, V. J., Bates, D. M., Bolstad, B., Dettling, M., Dudoit, S., et al. (2004). Bioconductor: open software development for computational biology and bioinformatics. *Genome Biol.* 5:R80. doi: 10.1186/gb-2004-5-10-r80

Gish, L. A., and Clark, S. E. (2011). The RLK/Pelle family of kinases. *Plant J.* 66, 117–127. doi: 10.1111/j.1365-3113X.2011.04518.x

Gonneau, M., Desprez, T., Martin, M., Doblas, V. G., Bacete, L., Miart, F., et al. (2018). Receptor kinase THESEUS1 is a rapid alkalization factor 34 receptor in *Arabidopsis*. *Curr. Biol.* 28, 2452–2458.e2454. doi: 10.1016/j.cub.2018.05.075

Gu, Z., Eils, R., and Schlesner, M. (2016). Complex heatmaps reveal patterns and correlations in multidimensional genomic data. *Bioinformatics* 32, 2847–2849. doi: 10.1093/bioinformatics/btw313

Haga, K., Frank, L., Kimura, T., Schwechheimer, C., and Sakai, T. (2018). Roles of AGCVIII kinases in the hypocotyl phototropism of *Arabidopsis* seedlings. *Plant Cell Physiol.* 59, 1060–1071. doi: 10.1093/pcp/pcy048

Hamann, T. (2015). The plant cell wall integrity maintenance mechanism - A case study of a cell wall plasma membrane signaling network. *Phytochemistry* 112, 100–109. doi: 10.1016/j.phytochem.2014.09.019

Haruta, M., Sabat, G., Stecker, K., Minkoff, B. B., and Sussman, M. R. (2014). A peptide hormone and its receptor protein kinase regulate plant cell expansion. *Science* 343, 408–411. doi: 10.1126/science.1244454

Hématy, K., Sado, P.-E., Van Tuinen, A., Rochange, S., Desnos, T., Balzergue, S., et al. (2007). A receptor-like kinase mediates the response of *Arabidopsis* cells to the inhibition of cellulose synthesis. *Curr. Biol.* 17, 922–931. doi: 10.1016/j.cub.2007.05.018

Holub, E. B. (2001). The arms race is ancient history in *Arabidopsis*, the wildflower. *Nat. Rev. Genet.* 2, 516–527. doi: 10.1038/35080508

Hou, C., Tian, W., Kleist, T., He, K., Garcia, V., Bai, F., et al. (2014). DUF221 proteins are a family of osmosensitive calcium-permeable cation channels conserved across eukaryotes. *Cell Res.* 24, 632–635. doi: 10.1038/cr.2014.14

Huang, C., Zhang, R., Gui, J., Zhong, Y., and Li, L. (2018). The receptor-like kinase AtVRLK1 regulates secondary cell wall thickening. *Plant Physiol.* 177, 671–683. doi: 10.1104/pp.17.01279

Immanen, J., Nieminen, K., Smolander, O.-P., Kojima, M., Alonso Serra, J., Koskinen, P., et al. (2016). Cytokinin and auxin display distinct but interconnected distribution and signaling profiles to stimulate cambial activity. *Curr. Biol.* 26, 1990–1997. doi: 10.1016/j.cub.2016.05.053

Jing, X.-Q., Shalmani, A., Zhou, M.-R., Shi, P.-T., Muhammad, I., Shi, Y., et al. (2020). Genome-wide identification of malectin/malectin-like domain containing protein family genes in rice and their expression regulation under various hormones, abiotic stresses, and heavy metal treatments. *J. Plant Growth Regul.* 39, 492–506. doi: 10.1007/s00344-019-09977-8

Katoh, K., Kuma, K.-I., Toh, H., and Miyata, T. (2005). MAFFT version 5: improvement in accuracy of multiple sequence alignment. *Nucleic Acids Res.* 33, 511–518. doi: 10.1093/nar/gki198

Kessler, S. A., Shimosato-Asano, H., Keinath, N. F., Wuest, S. E., Ingram, G., Panstruga, R., et al. (2010). Conserved molecular components for pollen tube reception and fungal invasion. *Science* 330, 968–971. doi: 10.1126/science.1195211

Khan, M., Ragni, L., Tabb, P., Salasini, B. C., Chatfield, S., Datla, R., et al. (2015). Repression of lateral organ boundary genes by PENNYWISE and POUND-FOOLISH is essential for meristem maintenance and flowering in *Arabidopsis*. *Plant Physiol.* 169, 2166–2186. doi: 10.1104/pp.15.00915

Kong, L., Cheng, J., Zhu, Y., Ding, Y., Meng, J., Chen, Z., et al. (2015). Degradation of the ABA co-receptor AB11 by PUB12/13 U-box E3 ligases. *Nat. Commun.* 6:8630. doi: 10.1038/ncomms9630

Kopylova, E., Noé, L., and Touzet, H. (2012). SortMeRNA: fast and accurate filtering of ribosomal RNAs in metatranscriptomic data. *Bioinformatics* 28, 3211–3217. doi: 10.1093/bioinformatics/bts611

Kumar, S., Stecher, G., and Tamura, K. (2016). MEGA7: molecular evolutionary genetics analysis version 7.0 for bigger datasets. *Mol. Biol. Evol.* 33, 1870–1874. doi: 10.1093/molbev/msw054

Kumar, V., Barbut, F., Kushwah, S., Donev, E. N., Urbancsok, J., and Mellerowicz, E. J. (2020). Genome-wide identification of poplar malectin/malectin-like domain-containing proteins and *in-silico* expression analyses find novel candidates for signaling and regulation of wood development. *Research Square* [Preprint]. doi: 10.21203/rs.3.rs-28356/v1

Kumar, V., Hainaut, M., Delhomme, N., Mannapperuma, C., Immerzeel, P., Street, N. R., et al. (2019). Poplar carbohydrate-active enzymes: whole-genome annotation and functional analyses based on RNA expression data. *Plant J.* 99, 589–609. doi: 10.1111/tpj.14417

Le, M. H., Cao, Y., Zhang, X.-C., and Stacey, G. (2014). LIK1, a CERK1-interacting kinase, regulates plant immune responses in *Arabidopsis*. *PLoS One* 9:e102245. doi: 10.1371/journal.pone.0102245

Lemoine, F., Correia, D., Lefort, V., Doppelt-Azeroual, O., Mareuil, F., Cohen-Boulakia, S., et al. (2019). NGPhylogeny.fr: new generation phylogenetic services for non-specialists. *Nucleic Acids Res.* 47, W260–W265. doi: 10.1093/nar/gkz303

Li, C., Wu, H.-M., and Cheung, A. Y. (2016). FERONIA and her pals: functions and mechanisms. *Plant Physiol.* 171, 2379–2392. doi: 10.1104/pp.16.00667

Li, N., Muthreich, M., Huang, L.-J., Thurov, C., Sun, T., Zhang, Y., et al. (2019). TGACC-BINDING FACTORS (TGAs) and TGA-interacting CC-type glutaredoxins modulate hyponastic growth in *Arabidopsis thaliana*. *New Phytol.* 221, 1906–1918. doi: 10.1111/nph.15496

Liao, D., Cao, Y., Sun, X., Espinoza, C., Nguyen, C. T., Liang, Y., et al. (2017). *Arabidopsis* E3 ubiquitin ligase PLANT U-BOX13 (PUB13) regulates chitin receptor LYSIN MOTIF RECEPTOR KINASE5 (LYK5) protein abundance. *New Phytol.* 214, 1646–1656. doi: 10.1111/nph.14472

Liebsch, D., Sunaryo, W., Holmlund, M., Norberg, M., Zhang, J., Hall, H. C., et al. (2014). Class I KNOX transcription factors promote differentiation of cambial derivatives into xylem fibers in the *Arabidopsis* hypocotyl. *Development* 141, 4311–4319. doi: 10.1242/dev.111369

Liu, H.-H., Xiong, F., Duan, C.-Y., Wu, Y.-N., Zhang, Y., and Li, S. (2019). Importin $\beta 4$ mediates nuclear import of GRF-interacting factors to control ovule development in *Arabidopsis*. *Plant Physiol.* 179, 1080–1092. doi: 10.1104/pp.18.01135

Liu, J., Li, W., Ning, Y., Shirsekar, G., Cai, Y., Wang, X., et al. (2012). The U-Box E3 ligase SPL11/PUB13 is a convergence point of defense and flowering signaling in plants. *Plant Physiol.* 160, 28–37. doi: 10.1104/pp.112.199430

Liu, J., Rice, J. H., Chen, N., Baum, T. J., and Hewezi, T. (2014). Synchronization of developmental processes and defense signaling by growth regulating transcription factors. *PLoS One* 9:e98477. doi: 10.1371/journal.pone.0098477

Liu, X., Wang, J., and Sun, L. (2018). Structure of the hyperosmolality-gated calcium-permeable channel OSCA1.2. *Nat. Commun.* 9:5060. doi: 10.1038/s41467-018-07564-5

Lohse, M., Bolger, A. M., Nagel, A., Fernie, A. R., Lunn, J. E., Stitt, M., et al. (2012). RobiNA: a user-friendly, integrated software solution for RNA-seq-based transcriptomics. *Nucleic Acids Res.* 40, W622–W627. doi: 10.1093/nar/gks540

Love, M. I., Huber, W., and Anders, S. (2014). Moderated estimation of fold change and dispersion for RNA-seq data with DESeq2. *Genome Biol.* 15:550. doi: 10.1186/s13059-014-0550-8

Mang, H., Feng, B., Hu, Z., Boisson-Dernier, A., Franck, C. M., Meng, X., et al. (2017). Differential regulation of two-tiered plant immunity and sexual reproduction by ANXUR receptor-like kinases. *Plant Cell* 29, 3140–3156. doi: 10.1105/tpc.17.00464

Mayfield, J. D., Folta, K. M., Paul, A.-L., and Ferl, R. J. (2007). The 14-3-3 proteins μ and ν influence transition to flowering and early phytochrome response. *Plant Physiol.* 145, 1692–1702. doi: 10.1104/pp.107.108654

Meng, J.-G., Liang, L., Jia, P.-F., Wang, Y.-C., Li, H.-J., and Yang, W.-C. (2020). Integration of ovular signals and exocytosis of a Ca^{2+} channel by MLOs in pollen tube guidance. *Nat. Plants* 6, 143–153. doi: 10.1038/s41477-020-0599-1

Merz, D., Richter, J., Gonneau, M., Sanchez-Rodriguez, C., Eder, T., Sormani, R., et al. (2017). T-DNA alleles of the receptor kinase THESEUS1 with opposing effects on cell wall integrity signaling. *J. Exper. Bot.* 68, 4583–4593. doi: 10.1093/jxb/erx263

Miao, Y., Laun, T., Zimmermann, P., and Zentgraf, U. (2004). Targets of the WRKY53 transcription factor and its role during leaf senescence in *Arabidopsis*. *Plant Mol. Biol.* 55, 853–867. doi: 10.1007/s11003-004-2142-6

Mineev, K. S., Bocharov, E. V., Pustovalova, Y. E., Bocharova, O. V., Chupin, V. V., and Arseniev, A. S. (2010). Spatial structure of the transmembrane domain heterodimer of ErbB1 and ErbB2 receptor tyrosine kinases. *J. Mol. Biol.* 400, 231–243. doi: 10.1016/j.jmb.2010.05.016

Mori, K., Renhu, N., Naito, M., Nakamura, A., Shiba, H., Yamamoto, T., et al. (2018). Ca^{2+} -permeable mechanosensitive channels MCA1 and MCA2 mediate cold-induced cytosolic Ca^{2+} increase and cold tolerance in *Arabidopsis*. *Sci. Rep.* 8:550. doi: 10.1038/s41598-017-17483-y

Moussu, S., Augustin, S., Roman, A. O., Broyard, C., and Santiago, J. (2018). Crystal structures of two tandem malectin-like receptor kinases involved in plant reproduction. *Acta Crystallogr.* 74(Pt 7), 671–680. doi: 10.1107/s205979831800774x

Omidbakhshfar, M. A., Fujikura, U., Olas, J. J., Xue, G.-P., Balazadeh, S., and Mueller-Roeber, B. (2018). GROWTH-REGULATING FACTOR 9 negatively regulates *Arabidopsis* leaf growth by controlling ORG3 and restricting cell proliferation in leaf primordia. *PLoS Genet.* 14:e1007484. doi: 10.1371/journal.pgen.1007484

Pagnussat, G. C., Yu, H.-J., Ngo, Q. A., Rajani, S., Mayalagu, S., Johnson, C. S., et al. (2005). Genetic and molecular identification of genes required for female gametophyte development and function in *Arabidopsis*. *Development* 132, 603–614. doi: 10.1242/dev.01595

Petersen, T. N., Brunak, S., von Heijne, G., and Nielsen, H. (2011). SignalP 4.0: discriminating signal peptides from transmembrane regions. *Nat. Methods* 8, 785–786. doi: 10.1038/nmeth.1701

Pinard, D., Mizrahi, E., Hefer, C. A., Kersting, A. R., Joubert, F., Douglas, C. J., et al. (2015). Comparative analysis of plant carbohydrate active enzymes and their role in xylogenesis. *BMC Genom.* 16:402. doi: 10.1186/s12864-015-1571-8

Prunet, N., Morel, P., Champelovier, P., Thierry, A.-M., Negruțiu, I., Jack, T., et al. (2015). SQUINT promotes stem cell homeostasis and floral meristem termination in *Arabidopsis* through APETALA2 and CLAVATA signalling. *J. Exper. Bot.* 66, 6905–6916. doi: 10.1093/jxb/erv394

R Core Team (2014). *R: A Language and Environment for Statistical Computing*. Vienna: R Foundation for Statistical Computing.

Rao, S., Zhou, Z., Miao, P., Bi, G., Hu, M., Wu, Y., et al. (2018). Roles of receptor-like cytoplasmic kinase VII members in pattern-triggered immune signaling. *Plant Physiol.* 177, 1679–1690. doi: 10.1104/pp.18.00486

Ratke, C., Terebieniec, B. K., Winestrand, S., Derba-Maceluch, M., Grahn, T., Schiffthaler, B., et al. (2018). Downregulating aspen xylan biosynthetic GT43 genes in developing wood stimulates growth via reprogramming of the transcriptome. *New Phytol.* 219, 230–245. doi: 10.1111/nph.15160

Rubinovich, L., and Weiss, D. (2010). The *Arabidopsis* cysteine-rich protein GASA4 promotes GA responses and exhibits redox activity in bacteria and in plants. *Plant J.* 64, 1018–1027. doi: 10.1111/j.1365-313X.2010.04390.x

Rui, Y., and Dinnyen, J. R. (2020). A wall with integrity: surveillance and maintenance of the plant cell wall under stress. *New Phytol.* 225, 1428–1439. doi: 10.1111/nph.16166

Schallus, T., Fehér, K., Sternberg, U., Rybin, V., and Muhle-Goll, C. (2010). Analysis of the specific interactions between the lectin domain of malectin and diglucosides. *Glycobiology* 20, 1010–1020. doi: 10.1093/glycob/cwq059

Schallus, T., Jaekch, C., Fehér, K., Palma, A. S., Liu, Y., Simpson, J. C., et al. (2008). Malectin: a novel carbohydrate-binding protein of the endoplasmic reticulum and a candidate player in the early steps of protein N-glycosylation. *Mol. Biol. Cell* 19, 3404–3414. doi: 10.1091/mbc.08-04-0354

Schaper, E., and Anisimova, M. (2015). The evolution and function of protein tandem repeats in plants. *New Phytol.* 206, 397–410. doi: 10.1111/nph.13184

Shannon, P., Markiel, A., Ozier, O., Baliga, N. S., Wang, J. T., Ramage, D., et al. (2003). Cytoscape: a software environment for integrated models of biomolecular interaction networks. *Genome Res.* 13, 2498–2504. doi: 10.1101/gr.1239303

Shiu, S.-H., and Bleecker, A. B. (2001). Receptor-like kinases from *Arabidopsis* form a monophyletic gene family related to animal receptor kinases. *Proc. Natl. Acad. Sci. U.S.A.* 98, 10763–10768. doi: 10.1073/pnas.181141598

- Shiu, S.-H., and Bleecker, A. B. (2003). Expansion of the receptor-like kinase/Pelle gene family and receptor-like proteins in *Arabidopsis*. *Plant Physiol.* 132, 530–543. doi: 10.1104/pp.103.021964
- Smith, M. R., Willmann, M. R., Wu, G., Berardini, T. Z., Möller, B., Weijers, D., et al. (2009). Cyclophilin 40 is required for microRNA activity in *Arabidopsis*. *Proc. Natl. Acad. Sci. U.S.A.* 106, 5424–5429. doi: 10.1073/pnas.0812729106
- Song, H., Guo, Z., Chen, T., Sun, J., and Yang, G. (2018). Genome-wide identification of LRR-containing sequences and the response of these sequences to nematode infection in *Arachis duranensis*. *BMC Plant Biol.* 18:279. doi: 10.1186/s12870-018-1508-x
- Stegmann, M., Monaghan, J., Smakowska-Luzan, E., Rovenich, H., Lehner, A., Holton, N., et al. (2017). The receptor kinase FER is a RALF-regulated scaffold controlling plant immune signaling. *Science* 355, 287–289. doi: 10.1126/science.aal2541
- Sultana, M. M., Hachiya, T., Dutta, A. K., Nishimura, K., Suzuki, T., Tanaka, A., et al. (2020). Expression analysis of genes encoding malectin-like domain (MLD)- and leucine-rich repeat (LRR)-containing proteins in *Arabidopsis thaliana*. *Biosci. Biotechnol. Biochem.* 84, 154–158. doi: 10.1080/09168451.2019.1661769
- Sundell, D., Mannapperuma, C., Netotea, S., Delhomme, N., Lin, Y.-C., Sjödin, A., et al. (2015). The plant genome integrative explorer resource: plantGenIE.org. *New Phytol.* 208, 1149–1156. doi: 10.1111/nph.13557
- Sundell, D., Street, N. R., Kumar, M., Mellerowicz, E. J., Kucukoglu, M., Johnsson, C., et al. (2017). AspWood: high-spatial-resolution transcriptome profiles reveal uncharacterized modularity of wood formation in *Populus tremula*. *Plant Cell* 29, 1585–1604. doi: 10.1105/tpc.17.00153
- Swarup, K., Benková, E., Swarup, R., Casimiro, I., Péret, B., Yang, Y., et al. (2008). The auxin influx carrier LAX3 promotes lateral root emergence. *Nat. Cell Biol.* 10, 946–954. doi: 10.1038/ncb1754
- Thole, J. M., Vermeer, J. E. M., Zhang, Y., Gadella, T. W. J., and Nielsen, E. (2008). ROOT HAIR DEFECTIVE4 encodes a phosphatidylinositol-4-phosphate phosphatase required for proper root hair development in *Arabidopsis thaliana*. *Plant Cell* 20, 381–395. doi: 10.1105/tpc.107.054304
- Voxeur, A., and Höfte, H. (2016). Cell wall integrity signaling in plants: “To grow or not to grow that’s the question”. *Glycobiology* 26, 950–960. doi: 10.1093/glycob/cww029
- Wang, G., Ellendorff, U., Kemp, B., Mansfield, J. W., Forsyth, A., Mitchell, K., et al. (2008). A genome-wide functional investigation into the roles of receptor-like proteins in *Arabidopsis*. *Plant Physiol.* 147, 503–517. doi: 10.1104/pp.108.119487
- Wang, J., Kucukoglu, M., Zhang, L., Chen, P., Decker, D., Nilsson, O., et al. (2013). The *Arabidopsis* LRR-RLK, PXC1, is a regulator of secondary wall formation correlated with the TDIF-PXY/TDR-WOX4 signaling pathway. *BMC Plant Biol.* 13:94. doi: 10.1186/1471-2229-13-94
- Wang, Y., Salasini, B. C., Khan, M., Devi, B., Bush, M., Subramaniam, R., et al. (2019). Clade I TGACG-motif binding basic leucine zipper transcription factors mediate BLADE-ON-PETIOLE-dependent regulation of development. *Plant Physiol.* 180, 937–951. doi: 10.1104/pp.18.00805
- Wang, J., Hu, T., Wang, W., Hu, H., Wei, Q., and Bao, C. (2019). Investigation of evolutionary and expression relationships in the function of the leucine-rich repeat receptor-like protein kinase gene family (LRR-RLK) in the radish (*Raphanus sativus* L.). *Sci. Rep.* 9:6937. doi: 10.1038/s41598-019-43516-9
- Waterhouse, A. M., Procter, J. B., Martin, D. M. A., Clamp, M., and Barton, G. J. (2009). Jalview Version 2 - a multiple sequence alignment editor and analysis workbench. *Bioinformatics* 25, 1189–1191. doi: 10.1093/bioinformatics/btp033
- Wolf, S. (2017). Plant cell wall signalling and receptor-like kinases. *Biochem. J.* 474, 471–492. doi: 10.1042/bcj20160238
- Wolf, S., and Höfte, H. (2014). Growth control: a saga of cell walls, ROS, and peptide receptors. *Plant Cell* 26, 1848–1856. doi: 10.1105/tpc.114.125518
- Won, S.-K., Lee, Y.-J., Lee, H.-Y., Heo, Y.-K., Cho, M., and Cho, H.-T. (2009). cis-Element- and transcriptome-based screening of root hair-specific genes and their functional characterization in *Arabidopsis*. *Plant Physiol.* 150, 1459–1473. doi: 10.1104/pp.109.140905
- Xi, J., Qiu, Y., Du, L., and Poovaliah, B. W. (2012). Plant-specific trihelix transcription factor *AGT2L* interacts with calcium/calmodulin and responds to cold and salt stresses. *Plant Sci.* 185–186, 274–280. doi: 10.1016/j.plantsci.2011.11.013
- Xi, L., Wu, X. N., Gilbert, M., and Schulze, W. X. (2019). Classification and interactions of LRR receptors and co-receptors within the *Arabidopsis* plasma membrane - an overview. *Front. Plant Sci.* 10:472. doi: 10.3389/fpls.2019.00472
- Xiao, Y., Stegmann, M., Han, Z., DeFalco, T. A., Parys, K., Xu, L., et al. (2019). Mechanisms of RALF peptide perception by a heterotypic receptor complex. *Nature* 572, 270–274. doi: 10.1038/s41586-019-1409-7
- Yanai, I., Benjamin, H., Shmoish, M., Chalifa-Caspi, V., Shklar, M., Ophir, R., et al. (2005). Genome-wide midrange transcription profiles reveal expression level relationships in human tissue specification. *Bioinformatics* 21, 650–659. doi: 10.1093/bioinformatics/bti042
- Yang, Y., Labbé, J., Muchero, W., Yang, X., Jawdy, S. S., Kennedy, M., et al. (2016). Genome-wide analysis of lectin receptor-like kinases in *Populus*. *BMC Genom.* 17:699. doi: 10.1186/s12864-016-3026-2
- Yeh, Y.-H., Panzeri, D., Kadota, Y., Huang, Y.-C., Huang, P.-Y., Tao, C.-N., et al. (2016). The *Arabidopsis* malectin-like/LRR-RLK IOS1 is critical for BAK1-dependent and BAK1-independent pattern-triggered immunity. *Plant Cell* 28, 1701–1721. doi: 10.1105/tpc.16.00313
- Yuan, N., Yuan, S., Li, Z., Zhou, M., Wu, P., Hu, Q., et al. (2018). STRESS INDUCED FACTOR 2, a leucine-rich repeat kinase regulates basal plant pathogen defense. *Plant Physiol.* 176, 3062–3080. doi: 10.1104/pp.17.01266
- Zan, Y., Ji, Y., Zhang, Y., Yang, S., Song, Y., and Wang, J. (2013). Genome-wide identification, characterization and expression analysis of *Populus* leucine-rich repeat receptor-like protein kinase genes. *BMC Genom.* 14:318. doi: 10.1186/1471-2164-14-318
- Zhang, Q., Jia, M., Xing, Y., Qin, L., Li, B., and Jia, W. (2016). Genome-wide identification and expression analysis of MRLK family genes associated with strawberry (*Fragaria vesca*) fruit ripening and abiotic stress responses. *PLoS One* 11:e0163647. doi: 10.1371/journal.pone.0163647
- Zhong, R., and Ye, Z.-H. (2012). MYB46 and MYB83 bind to the SMRE sites and directly activate a suite of transcription factors and secondary wall biosynthetic genes. *Plant Cell Physiol.* 53, 368–380. doi: 10.1093/pcp/pcr185
- Zhou, J., Liu, D., Wang, P., Ma, X., Lin, W., Chen, S., et al. (2018). Regulation of *Arabidopsis* brassinosteroid receptor BRI1 endocytosis and degradation by plant U-box PUB12/PUB13-mediated ubiquitination. *Proc. Natl. Acad. Sci. U.S.A.* 115, E1906–E1915. doi: 10.1073/pnas.1712251115
- Zulawski, M., Schulze, G., Braginets, R., Hartmann, S., and Schulze, W. X. (2014). The *Arabidopsis* kinome: phylogeny and evolutionary insights into functional diversification. *BMC Genom.* 15:548. doi: 10.1186/1471-2164-15-548

Conflict of Interest: The authors declare that the research was conducted in the absence of any commercial or financial relationships that could be construed as a potential conflict of interest.

Copyright © 2020 Kumar, Donev, Barbut, Kushwah, Mannapperuma, Urbancsok and Mellerowicz. This is an open-access article distributed under the terms of the Creative Commons Attribution License (CC BY). The use, distribution or reproduction in other forums is permitted, provided the original author(s) and the copyright owner(s) are credited and that the original publication in this journal is cited, in accordance with accepted academic practice. No use, distribution or reproduction is permitted which does not comply with these terms.

Flexure wood formation via growth reprogramming in hybrid aspen involves jasmonates and polyamines and transcriptional changes resembling tension wood development

János Urbancsik^{1*} , Evgeniy N. Donev^{1*} , Pramod Sivan¹ , Elena van Zalen² , Félix R. Barbut¹ , Marta Derba-Maceluch¹ , Jan Šimura¹ , Zakiya Yassin³ , Madhavi L. Gandla⁴ , Michal Karady⁵ , Karin Ljung¹ , Sandra Winstrand⁴ , Leif J. Jönsson⁴ , Gerhard Scheepers³ , Nicolas Delhomme¹ , Nathaniel R. Street^{2,6}  and Ewa J. Mellerowicz¹ 

¹Umeå Plant Science Centre (UPSC), Department of Forest Genetics and Plant Physiology, Swedish University of Agricultural Sciences, 90183, Umeå, Sweden; ²Umeå Plant Science Centre (UPSC), Department of Plant Physiology, Umeå University, 90187, Umeå, Sweden; ³RISE Research Institutes of Sweden, Drottning Kristinas väg 61, 11428, Stockholm, Sweden;

⁴Department of Chemistry, Umeå University, 90187, Umeå, Sweden; ⁵Laboratory of Growth Regulators, Institute of Experimental Botany of the Czech Academy of Sciences and Faculty of Science of Palacký University, 78371, Olomouc, Czech Republic; ⁶SciLifeLab, Umeå University, 90187, Umeå, Sweden

Summary

Author for correspondence:
Ewa J. Mellerowicz
Email: ewa.mellerowicz@slu.se

Received: 11 July 2023
Accepted: 19 September 2023

New Phytologist (2023) **240**: 2312–2334
doi: 10.1111/nph.19307

Key words: flexure wood, jasmonic acid signaling, mechanostimulation, polyamines, *Populus tremula* × *tremuloides*, saccharification, thigmomorphogenesis, wood development.

- Stem bending in trees induces flexure wood but its properties and development are poorly understood. Here, we investigated the effects of low-intensity multidirectional stem flexing on growth and wood properties of hybrid aspen, and on its transcriptomic and hormonal responses.
- Glasshouse-grown trees were either kept stationary or subjected to several daily shakes for 5 wk, after which the transcriptomes and hormones were analyzed in the cambial region and developing wood tissues, and the wood properties were analyzed by physical, chemical and microscopy techniques.
- Shaking increased primary and secondary growth and altered wood differentiation by stimulating gelatinous-fiber formation, reducing secondary wall thickness, changing matrix polysaccharides and increasing cellulose, G- and H-lignin contents, cell wall porosity and saccharification yields. Wood-forming tissues exhibited elevated jasmonate, polyamine, ethylene and brassinosteroids and reduced abscisic acid and gibberellin signaling. Transcriptional responses resembled those during tension wood formation but not opposite wood formation and revealed several thigmomorphogenesis-related genes as well as novel gene networks including *FLA* and *XTH* genes encoding plasma membrane-bound proteins.
- Low-intensity stem flexing stimulates growth and induces wood having improved biorefinery properties through molecular and hormonal pathways similar to thigmomorphogenesis in herbaceous plants and largely overlapping with the tension wood program of hardwoods.

Introduction

The ever-changing environment represents a constant challenge to all living organisms, hence proper perception and response to diverse external stimuli is crucial for their survival. These abilities are particularly important for sessile organisms such as plants. Plants evolved in environments rich in diverse mechanical stimuli whose perception and subsequent adjustment of growth and development is called thigmomorphogenesis (Jaffe, 1973; Chehab *et al.*, 2009; Telewski, 2021; Brenya *et al.*, 2022). It involves growth redistribution resulting in more compact form and expanded root system (Jaffe, 1973; Telewski & Jaffe, 1986a,b;

Braam & Davis, 1990; Gartner, 1994; Telewski & Pruyn, 1998; Pruyn *et al.*, 2000; Braam, 2005; Kern *et al.*, 2005; Coutand *et al.*, 2008; Coutand, 2010; Wu *et al.*, 2016). It can also delay vegetative to reproductive phase transition (Chehab *et al.*, 2012). Mild mechanostimulation has been shown to increase the growth and resilience of plants to various abiotic/biotic factors in different crops, hence it has been proposed as a potential sustainable agricultural practice (Ghosh *et al.*, 2021).

Mechanostimulated plants also modify cell walls, as evidenced by upregulation of xyloglucan-, cellulose- and lignin-related genes, and genes encoding fasciclin-like arabinogalactan proteins (FLAs) in *Arabidopsis thaliana* (Xu *et al.*, 1995, 2019; Lee *et al.*, 2005; Saidi *et al.*, 2010). Trees exposed to mechanical disturbance develop a special kind of wood, called flexure wood

*These authors contributed equally to this work.

(Telewski, 1989, 2016). Development of flexure wood involves increased radial growth, especially in the direction of mechanical stress, which can lead to stem ovality, thickened cell walls, increased cellulose microfibril angle (MFA), reduced diameter and length of tracheary elements, and in the case of angiosperms, reduced frequency of vessel elements relative to fibers compared with normal wood. Xyloglucan deposition was recorded in the wood formed during seismic activity in hardwoods (Kaida *et al.*, 2020). Flexure wood increases mechanical resilience of hardwood and softwood trees (Telewski & Jaffe, 1986b; Niez *et al.*, 2020), which could impact timber quality for solid wood products. However, its effect on wood biorefinery-related properties has not been investigated.

In addition to flexure wood, woody plants can develop reaction wood (tension wood in case of hardwoods or compression wood in case of softwoods) to gravitropically bend secondarily thickened stems (Groover, 2016). The structure and composition of cell walls in tension and compression wood are modified. Tension wood fibers in many hardwoods reduce deposition of secondary wall layers and instead produce a thick, unlignified tertiary cell wall layer called gelatinous layer, which contains high amounts of axially oriented cellulose, and low amounts of matrix polysaccharides, primarily β -1,4-galactan. By contrast, the compression wood tracheids of softwoods modify their S2 layer by producing helically oriented cellulose and increasing lignification, and by adding an inner S2 layer with helical thickenings that contain β -1,4-galactan and deposit callose between the thickenings. These modifications of tension and compression wood induce longitudinal tension and compression in the wood, respectively, driving stem bending.

The mechanisms of mechanoperception and subsequent growth reprogramming are complex and poorly understood (Telewski, 2021; Brenya *et al.*, 2022). Mechanoresponses are triggered within seconds and involve the cell wall, plasma membrane, cytosol and mitochondria (Baluška *et al.*, 2003; Xu *et al.*, 2019), followed by systemic reaction (Toyota *et al.*, 2018) and changes in chromatin responsible for stress acclimation (Coutand, 2010). Structural changes in the cell wall and plasma membrane are thought to activate different mechanosensitive ion channels responsible for converting the mechanical cues to essential ion fluxes, in particular Ca^{2+} (Nakagawa *et al.*, 2007; Monshausen & Haswell, 2013; Basu & Haswell, 2017) and plasma membrane-localized receptor-like kinases that transduce signals via mitogen-activated protein (MAP) kinase cascades and other protein phosphorylation relays (Wang *et al.*, 2018a). The elevated intracellular Ca^{2+} concentration is sensed mainly by calmodulin and calmodulin-like (CML) proteins, mRNAs of which are highly represented among the early touch-response transcripts (Braam & Davis, 1990; Lee *et al.*, 2005). Ca^{2+} signaling was reported to induce production of reactive oxygen species (ROS; Benikhlef *et al.*, 2013), and these pathways possibly overlap with cell wall integrity maintenance mechanisms (Bacete & Hamann, 2020). Downstream signals involve the crosstalk of jasmonates and gibberellins (GAs; Brenya *et al.*, 2020, 2022), when jasmonic acid (JA) via MYC2/3/4 (Chehab *et al.*, 2012; Van Moerkercke *et al.*, 2019) and GA catabolism mediated by

gibberellin 2-oxidases (Lange & Lange, 2015) are responsible for inhibition of stem elongation.

Even though a growing body of evidence indicates that mechanical stimuli can alter tree growth and induce flexure wood formation, there are few detailed descriptions of the properties of flexure wood and tree trunk thigmomorphogenesis, especially for hardwood species (Telewski, 2016). Moreover, the hormonal responses to stem bending and the molecular mechanisms of mechanoperception and signal transduction events that lead to flexure wood formation are poorly understood, although a pioneering transcriptome analysis following single stem bending (Pomiès *et al.*, 2017) suggested some similarities with the general thigmomorphogenesis program in herbaceous plants. An early woody stem thigmomorphogenesis marker was identified as a Cys2/His2-type zinc finger transcription factor (TF) ZFP2 (Leblanc-Fournier *et al.*, 2008; Martin *et al.*, 2009, 2014), which is induced within minutes by a single stem bending (Coutand *et al.*, 2009) and could be involved in suppressing mechanoresponses as part of the de-sensitizing mechanism (Martin *et al.*, 2014). In the current study, we characterized hybrid aspen (*Populus tremula* L. \times *tremuloides* Michx.) growth responses to repeated low-intensity multidirectional flexures, especially their effects in developing wood, including changes in wood structure, chemistry, transcriptome and hormonal profiles. We also tested whether flexure wood has improved saccharification properties.

Materials and Methods

Plant material and growth conditions

Hybrid aspen (*Populus tremula* L. \times *tremuloides* Michx., clone T89) was micropropagated *in vitro*, transferred to soil and grown in the glasshouse as described in detail in Supporting Information Methods S1. For the first 2 wk, all trees were grown under stationary conditions. From the third week, a set of 13 trees (flexure set) were subjected to two series of *c.* 50–60 sudden accelerations and stops per day with pot rotations on a conveyor belt resulting in stem swaying movements (Video S1). The ultimate speed of the belt was 0.2 m s^{-1} , and it was reached in at most 1.5 s as could be seen on the video, which would result in acceleration of at least 0.13 m s^{-2} . The maximum angle from the vertical recorded with a digital camera at two consecutive stops for nine trees was $3.7^\circ \pm 0.12$ (SE). The accelerations and stops also caused vibration of the stems. The other set of 13 trees were kept on the immobile belt (stationary set) throughout the growth period.

Assessment of growth

Stem height and diameter at the stem base were measured with a measuring tape and caliper, respectively. The aboveground biomass was recorded by weighing freshly cut shoots. Developing leaves, starting from leaf 8 (which was the first unfolded leaf from the apex) and ending at leaf 22, were collected and digitalized using a scanner followed by the calculation of their leaf area by IMAGEJ (Schneider *et al.*, 2012). The average internode length

was determined for internodes 35–55. Belowground biomass was determined by weighing cleaned and air-dried roots.

Wood microscopy analysis

Wood samples of internodes 36–37 were fixed in FAA (4% formaldehyde, 5% acetic acid and 50% ethanol). Transverse 40–50 μm -thick sections were prepared with a vibratome (VT1000S; Leica Biosystems, Nussloch, Germany) and stained with a solution of one volume of 1% (w/v) Safranin O (CAS 477-73-6; Sigma-Aldrich) in 50% ethanol and two volumes of 1% aqueous (w/v) Alcian Blue (CAS 123439-83-8; Sigma-Aldrich). Images were acquired using a Leica DMI8 microscope (Leica Biosystems) and analyzed with IMAGEJ. Tension wood was identified by the presence of gelatinous fibers (G-fibers).

Cell wall chemical analyses

Forty centimeter-long stem segments below internode 37 from seven trees per set were debarked and freeze-dried for 48 h. Wood powder from individual trees for Py-GC/MS and trimethylsilyl (TMS) analyses was obtained with a file and sieved with Retsch AS 200 analytical sieve shaker (Retsch GmbH, Haan, Germany) to isolate 50–100 μm -particles. Fifty micrograms ($\pm 10 \mu\text{g}$) of this powder was pyrolyzed in a pyrolyser equipped with an auto-sampler (PY-2020iD and AS-1020E; Frontier Lab, Koriyama, Japan) connected to a GC/MS (7890A/5975C; Agilent Technologies Inc., Santa Clara, CA, USA) and analyzed according to Gerber *et al.* (2012). Alcohol-insoluble residue (AIR) was generated as described by Gandla *et al.* (2015) and enzymatically destarched as described by Pramod *et al.* (2021). Portions of 500 μg ($\pm 10\%$) of destarched AIR were acid-methanolized and derivatized by TMS procedure; then, the silylated monosaccharides were separated by GC/MS (7890A/5975C; Agilent Technologies Inc.) according to Gandla *et al.* (2015). Raw data MS files were converted to CDF format in Agilent Chemstation Data Analysis (v.E.02.00.493) and processed in R (v.4.1.3; R Core Team, 2022) for peak identification. 4-*O*-methylglucuronic acid was identified according to Chong *et al.* (2013). Destarched AIR of seven trees per set was pooled and five portions of 3 mg were used for cellulose analysis by the Updegraff method (Updegraff, 1969), followed by glucose content determination with the anthrone method (Scott & Melvin, 1953).

Saccharification assay and nanoporosity analysis

Freeze-dried stem segments of seven trees per set had their pith removed and were ground using Retsch Ultra Centrifugal Mill ZM 200 (Retsch GmbH) equipped with a 0.5 mm ring sieve and sieved with a Retsch AS 200 vibratory sieve shaker to obtain particle size of 100–500 μm . Analytical-scale saccharification (Gandla *et al.*, 2021) was performed using five portions, each consisting of 50 mg of dry material pooled from seven trees per set, either pretreated in 1% (w/w) sulfuric acid (based on mass of reaction mixture) at 165°C for 10 min in an initiator single-mode microwave instrument (Biotage Sweden AB, Uppsala,

Sweden) followed by enzymatic hydrolysis or used directly for the enzymatic hydrolysis at 45°C using 4 mg of the liquid enzyme mixture Cellic CTec2 (cat. nr. SAE0020; Sigma-Aldrich). Samples were analyzed for Glc production rate at 2 h by using an Accu-Chek[®] Aviva glucometer (Roche Diagnostics Scandinavia AB, Solna, Sweden). After 72 h of incubation, the yield of monosaccharides (Ara, Gal, Glc, Xyl and Man) was determined using a high-performance anion-exchange chromatography (HPAEC) system with pulsed amperometric detection method (Ion Chromatography System ICS-5000 by Dionex, Sunnyvale, CA, USA; Wang *et al.*, 2018b).

The surface area of wood powder was analyzed by using the Brunauer–Emmett–Teller (BET) method (Brunauer *et al.*, 1938) in a single-point BET automated gas adsorption analyzer (Tristar 3000 BET analyzer by Micromeritics, Norcross, GA, USA) using five technical replicates of pooled material (particle size of 100–500 μm) from seven trees per set. Nonspecific adsorbents were removed from samples by a 3 h degassing procedure using a SmartPrep Degasser (Micromeritics) before analysis.

SilviScan analysis

A SilviScan instrument (RISE, Stockholm, Sweden) was used for determining wood and fiber properties at the base of the stem for seven trees per set. Radial bark-to-bark stem sections having 2 mm tangential width and 7 mm height were prepared and equilibrated at 23°C and 43% relative humidity before the measurements. Wood density along the radius was determined using X-ray transmission whereas MFA was estimated by X-ray diffraction (Evans *et al.*, 1996; Evans & Ilic, 2001). The average density of each section was determined by measuring its volume and weight.

RNA extraction and transcriptomics

Developing xylem and cambium tissues were scrapped from the frozen debarked wood surface or from the inner surface of the corresponding bark, respectively, of *c.* 30 cm-long stem segments above internode 35. Total RNA was isolated according to Chang *et al.* (1993) and was subsequently purified using an RNeasy Plant Mini Kit (Qiagen GmbH, Hilden, Germany). RNA quantity and quality were determined by NanoDrop 2000 (Thermo Fisher Scientific, Waltham, MA, USA) and Agilent 2100 Bioanalyzer (Agilent Technologies Inc.), respectively. cDNA libraries were prepared and sequenced using NovaSeq 6000 PE150 at Novogene Co., Ltd (Cambridge, UK). Raw sequence data preprocessing and quality assessment are described in Methods S1. The reads were aligned to the *P. tremula* genome assembly (v.2.2) retrieved from the PlantGenIE (<https://plantgenie.org>; Sundell *et al.*, 2015). Putative orthologs in *Populus trichocarpa* (v.3.1) and *Arabidopsis thaliana* (v.11.0) were retrieved from PlantGenIE or, for selected gene families, were determined by phylogenetic analyses at PlantGenIE. Gene Ontology (GO) enrichment analysis, co-expression networks and heatmaps were obtained using PlantGenIE tools. The networks were visualized by CYTOSCAPE (v.3.6.0, Shannon *et al.*, 2003) and the heatmaps with COMPLEXHEATMAP (Gu *et al.*, 2016).

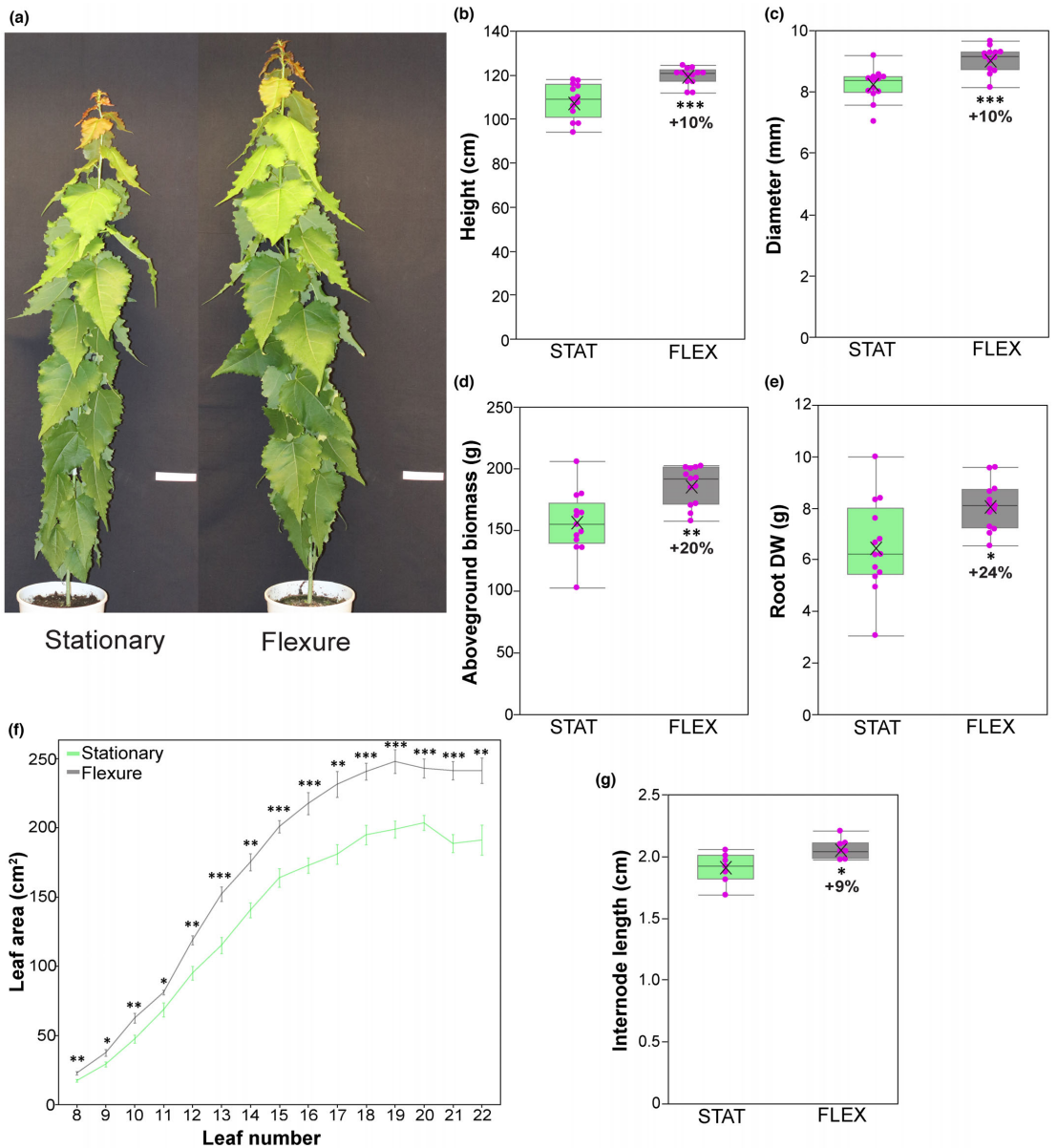


Fig. 1 Effects of hybrid aspen (*Populus tremula* × *tremuloides*) stem flexing on growth. (a) Representative individuals of aspen grown either in the stationary condition (STAT) or subjected to regular low-intensity multidirectional stem flexing (FLEX; as shown in Supporting Information Video S1). Bars, 10 cm. Stem height (b) and diameter (c), aboveground biomass (d), air-dried root biomass (e), leaf area (f) and internode length (g) were measured after five and a half weeks of growth under contrasting conditions. The data are means (\pm SE), $n = 13$ (b–e) or 7 (f–g). Asterisks denote significance assessed by Student's *t*-test for comparison between flexure and stationary set (*, $P < 0.05$; **, $P < 0.01$; ***, $P < 0.001$). Box plots show interquartile ranges (IQRs) as boxes, medians as horizontal lines, means as crosses, data points as dots, and ranges of all data points as whiskers, except for outliers (points further from the box than 1.5 times IQR).

Hormone analyses

Cambium and developing xylem tissues (the same as used for RNA analyses) were subjected to hormone profiling using

methods described by Šimura *et al.* (2018), with modifications described in Methods S1.

ACC quantification was performed in multiple reaction monitoring (MRM) mode employing an LC-MS/MS 1260 Infinity II

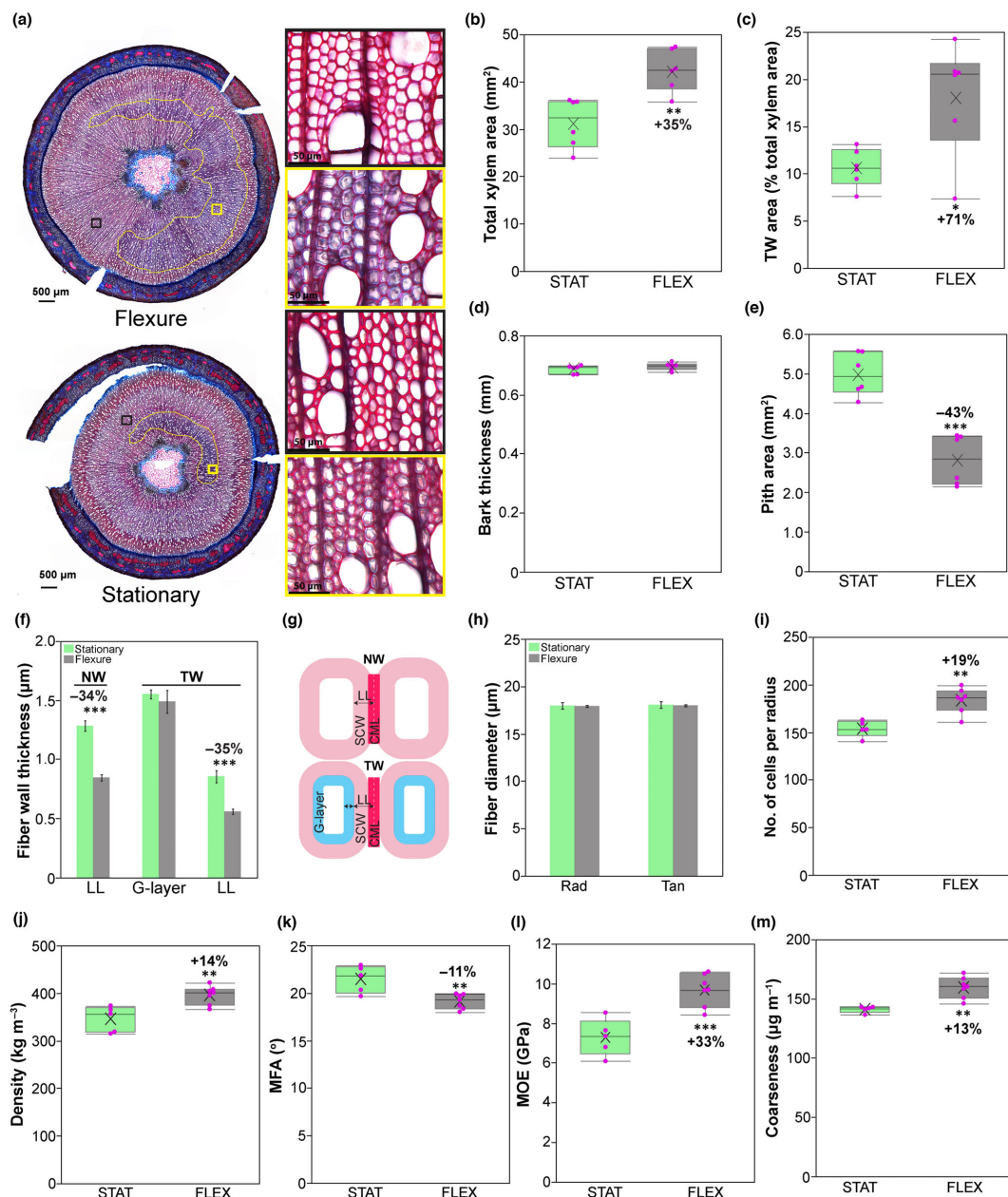


Fig. 2 Effects of hybrid aspen (*Populus tremula* × *tremuloides*) stem flexing on wood anatomy and other wood traits determined by SilviScan analyses. (a) Representative transverse stem sections stained by Safranin O and Alcian Blue from flexed and stationary trees. The yellow lines mark the tension wood area and the yellow or black rectangles depict tension or normal wood areas shown in the magnified images. Xylem area (b), tension wood area relative to the total xylem area (c), bark thickness (d) and pith area (e) for six trees from each growth condition. (f) Thickness of different cell wall layers in normal and tension wood fibers (G, gelatinous layer; LL, lignified layer, including secondary cell wall and compound middle lamella layers corresponding to one cell) obtained from measurements of 10 randomly selected fibers in cross-sections from each of six trees per set. (g) Schematic illustration of fiber cells in normal and tension wood indicating the different cell wall layers used for fiber wall thickness measurements. Various wood traits including fiber radial and tangential diameters (h), number of xylem cells per radius (i), wood density (j), MFA (k), MOE (l) and coarseness (m) determined by SilviScan analysis at radial resolution of 25 µm. Data are means (±SE), $n = 5$ (stationary) or 7 (flexure) trees. Asterisks show the significance levels assessed by Student's *t*-test for comparison between flexure and stationary set (*, $P < 0.05$; **, $P < 0.01$; ***, $P < 0.001$). Box plots show interquartile ranges (IQRs) as boxes, medians as horizontal lines, means as crosses, data points as dots, and ranges of all data points as whiskers, except for outliers (points further from the box than 1.5 times IQR). MFA, microfibril angle; MOE, modulus of elasticity; NW, normal wood; TW, tension wood.

LC System with Kinetex Polar C18 column (150 × 2.1 mm, 2.6 µm; Phenomenex Inc., Torrance, CA, USA) coupled to a 6495 Triple Quad LC/MS System with a Jet Stream and Dual Ion Funnel technologies (Agilent Technologies Inc.).

Polyamines (PAs) were extracted with methanol: chloroform: water (60 : 20 : 20; v/v/v), derivatized by AccQ-Tag™ (Waters, Milford, MA, USA) and analyzed by LC-ESI-MS/MS as described in Methods S1.

Results

Enhanced tree growth and altered stem anatomy in response to low-intensity flexure

The trees exposed to low-intensity stem flexures grew faster than trees maintained in stationary conditions (Figs 1a–g, S1). After five and a half weeks of flexure treatment, stem height and diameter were increased by 10%, internode length by 9%, above-ground biomass by 20%, root biomass by 24% and mature leaf size (leaf 22) by 32% compared with the control trees.

The nature of the increase in stem diameter of the flexure trees was further investigated by microscopy analysis (Fig. 2a–e). This revealed a 35% increment in wood area and a 43% decrease in pith area but no change in bark thickness, demonstrating that trees exposed to flexure produced more secondary xylem. Even though all trees, regardless of the presence of mechanical stimulus, developed tension wood characterized by the presence of G-fibers, exposure to regular flexure almost doubled the proportion of tension wood area relative to the total wood area.

Further assessment revealed differences in fiber cell walls when the two growth conditions were compared (Fig. 2f,g). In G-fibers, no change was observed for the thickness of the G-layer; however, the thickness of lignified cell wall layers (LL in Fig. 2g), including secondary cell wall and a half of the compound middle lamella, was *c.* 35% reduced in flexed compared with stationary trees. A similar reduction in thickness of lignified wall layers was observed in normal wood fibers. These data indicate that the flexure treatment stimulated secondary xylem formation, promoted G-fiber fate and inhibited secondary cell wall formation in both normal wood fibers and G-fibers.

SilviScan analysis (Fig. 2h–m; Table S1) showed that radial and tangential fiber diameters remained unaffected by flexure treatments, and that diameters of vessels or the frequency of vessels did not change significantly when comparing the two growth

conditions. However, a 19% increase in the number of xylem cells produced by one fusiform initial was recorded in trees exposed to mechanical stimulation, providing evidence that the wider stem diameters and the larger total xylem areas of flexure-treated stems were caused by an increased rate of xylem cell production by the vascular cambium. Furthermore, SilviScan analysis revealed an increase in wood density and decrease in MFA, and consequently, the estimated modulus of elasticity (MOE), and fiber coarseness were increased in trees subjected to flexures.

Flexure altered wood cell wall chemistry, nanoporosity and saccharification yield

Analysis of the wood by Py-GC/MS indicated elevated G- and H-lignin contents in the flexure set by *c.* 6% and 23%, respectively, resulting in a decrease in the S/G ratio, whereas total carbohydrate and lignin contents were not affected (Fig. 3a). The glycosyl unit composition of the matrix polysaccharides analyzed by acid methanolysis-TMS found that Ara, Xyl and GlcA contents were reduced whereas the contents of Gal, Glc and Man were increased in the flexed trees (Fig. 3b). Moreover, the crystalline cellulose content determined by the Updegraff method showed a 16% increase in flexed compared with stationary trees (Fig. 3c). Intriguingly, when nanoporosity of cell wall material was assayed by BET, a significantly greater (by 24%) specific surface area was observed for flexed trees (Fig. 3d).

To determine whether these changes had any effects on biomass recalcitrance to saccharification, we performed two analytical saccharification experiments on biomass without and with acidic pretreatment (Figs 4a–d, S2). Glc production rate was 21% higher in the flexure set compared with stationary set for the untreated biomass but it was not affected by growth condition for the pretreated biomass. The enzymatic hydrolysis yields from the untreated material indicated significantly increased yields for Glc (+16%) and Gal (+25%; Fig. 4b). Acid hydrolysis liberated more Gal (+40%) and Man (+18%) from flexure than normal wood (Fig. 4c), which was more than expected based on their higher content in flexure wood, whereas the yield of Xyl was not affected by flexure treatment despite the treatment causing a significant decrease in Xyl content. This indicates that matrix polysaccharides from flexure wood are easier to hydrolyze by acid compared with normal wood. The enzymatic hydrolysate after acid pretreatment contained mainly Glc and its yields did not show any significant alterations between the two growth

conditions (Fig. S2). The total Glc and Xyl yields (i.e. the sum of pretreatment liquid and enzymatic hydrolysis fractions) were not affected by the growth conditions (Fig. 4d).

Low-intensity stem flexing alters the hormone profiles of tree stems

To gain insight into changes in hormonal profiles of trees exposed to regular low-intensity stem flexures relative to the stationary trees, we performed general hormonomics analysis in cambial region tissues (denoted ‘cambium’) and developing xylem tissues (denoted ‘xylem’), which targeted different forms of cytokinins (CKs), auxins, jasmonates, as well as salicylic acid (SA), abscisic acid (ABA) and the ethylene precursor 1-aminocyclopropane-1-carboxylic acid (ACC) and PAs with their precursors (for list see Table S2). In the cambium, many CK forms were decreased by flexing, whereas in the developing xylem, some forms were increased while others decreased (Fig. 5a,b). Among the auxins, the only significant change upon flexure was a 26% reduction in oxIAA – an IAA catabolite in the xylem. By contrast, distinct changes were detected in hormones mediating abiotic and biotic stresses. Approximately 20% less ABA and SA were detected in the cambium and in the xylem, respectively, and ACC was reduced by c. 38% in both tissues when the trees were exposed to stem flexures. However, the most striking alterations in hormone levels were observed for the jasmonates and PAs. The content of *cis*-12-oxophytodienoic acid (*cis*OPDA), a precursor for JA, was strongly reduced in the cambium and xylem (by 50% and 71%, respectively), whereas that of JA was massively increased (by 266% and 572%, respectively) in flexed trees. Moreover, the content of the biologically active JA-Ile was increased by nearly 50% in the xylem upon mechanical stimuli. These data indicate a metabolic conversion of *cis*OPDA toward JA and the active JA-Ile in the developing xylem in response to the mechanical treatment. In the case of PAs, we found strong decreases in their early precursors, arginine (Arg) in the cambium and glutamic acid (Glu) in the xylem, and an over twofold increase in their downstream precursor – ornithine (Orn) – and in active form – spermidine (Spd), in the xylem, indicating that stem flexing increases PA signaling in the developing xylem.

Complex transcriptional changes in aspen tree stems subjected to flexure

RNA-Seq analysis identified 167 and 219 differentially expressed genes (DEGs) uniquely affected by flexure in the cambium and in the developing xylem, respectively, and 27 genes commonly affected in both tissues (Fig. 6a; Tables S3, S4). In the cambium, the majority of DEGs (75%) were downregulated by the flexing treatment, whereas in the xylem there were similar numbers of up- and downregulated genes. The most strongly affected genes are listed in Table 1.

Gene Ontology enrichment analysis of DEGs in the cambium revealed changes in categories ‘generation of precursor metabolites and energy’, ‘photosynthesis’ and closely related categories with the majority of corresponding genes downregulated

(Fig. S3; Tables S3, S5). Reduction in expression of photosynthesis-related genes was also reported following a single stem bending in poplar (Pomiès *et al.*, 2017).

In the xylem, GO categories related to cell wall organization and biosynthesis were most highly affected, with the majority of corresponding genes upregulated (Tables 2, S4–S7; Fig. S3). Stem flexure stimulated expression of primary wall CesAs *PtCESA6-A* and *PtCESA6-F* (Fig. S4; Suzuki *et al.*, 2006; Desprez *et al.*, 2007; Kumar *et al.*, 2009; Hu *et al.*, 2018; Zhang *et al.*, 2018) and genes involved in microtubule organization, such as *PtMAP20* (Rajagam *et al.*, 2008). Noteworthy, primary wall CesAs were reported in developing wood cells depositing secondary cell walls (Song *et al.*, 2010). Elevated transcript levels were observed for genes encoding pectin acetyltransferases homologous to *AtPAE8* and *AtPAE12* (de Souza *et al.*, 2014), and pectin methylesterases (PMEs) homologous to *AtPME41* and *AtPMEI-PME20*, whereas a homolog of *AtPMEI-PME18* along with two polygalacturonase-encoding genes, *PtPG28* and *PtPG41*, were downregulated in the xylem. Interestingly, *AtPMEI-PME18* is the main PME downregulated under microgravity (Xu *et al.*, 2022). Several xyloglucan transglycosidases/hydrolases (XTH) were upregulated by flexure, in agreement with the proposed role of this family in touch responses in *Arabidopsis* (Xu *et al.*, 1995; Lee *et al.*, 2005). One of them, *PtXTH37* (*AtXTH23*; Fig. S5), was among the most highly upregulated genes in the cambium (Table 1) and 2 h after a single stem bending (Pomiès *et al.*, 2017). Several genes encoding xylan *O*-acetyltransferases known to be involved in regio-specific *O*-acetylation of xylan (Zhong *et al.*, 2017, 2018) were upregulated in the xylem by stem flexing, including *PtXOAT1* (*AtESK1/TBL29*), *PtXOAT7* (*AtTBL3*) and *PtXOAT8* (*AtTBL31*). In addition, a putative xylan acetyltransferase of the CE6 family showed upregulation upon stem flexure in the xylem, as was also seen during tension wood formation (Andersson-Gunnerås *et al.*, 2006). However, among other xylan biosynthetic genes, only *PtGATL2-A* (*AtGATL1/PARVUS*) involved in reducing sequence biosynthesis (Lee *et al.*, 2007, 2009) and *PtGXM3* (*AtGXMT1*) involved in glucuronosyl methylation (Urbanowicz *et al.*, 2012; Yuan *et al.*, 2014) were slightly upregulated. These changes suggest alteration in xylan acetylation in both flexure and tension wood compared with normal wood. Four out of 17 genes of clade *AtFLA11/FLA12* (Zang *et al.*, 2015) were upregulated by flexure in the xylem, including *PtFLA6*, which has been implicated in tension wood formation (Wang *et al.*, 2017). This clade is involved in G-layer biosynthesis (Lafarguette *et al.*, 2004; Andersson-Gunnerås *et al.*, 2006), and it was also reported to be upregulated after single stem bending (Pomiès *et al.*, 2017). Genes encoding laccases *PtLAC21* and *PtLAC49* (*AtLAC4*), *PtLAC12* (*AtLAC17*; Berther *et al.*, 2011; Lu *et al.*, 2013; Kumar *et al.*, 2019) and a class III peroxidase *PtPRX67* (Ren *et al.*, 2014) likely involved in lignin polymerization, and genes involved in monolignol metabolism and transport were also upregulated in either xylem or cambium of flexed trees (Franke *et al.*, 2002; Kaneda *et al.*, 2011; Lin *et al.*, 2016; Table 2). By contrast, the genes encoding three other class III peroxidases, including a homolog of *AtPRX72* responsible for lignification in *Arabidopsis* stems (Fernández-Pérez *et al.*, 2015; Hoffmann *et al.*, 2020), were strongly downregulated. These peroxidases, however, were

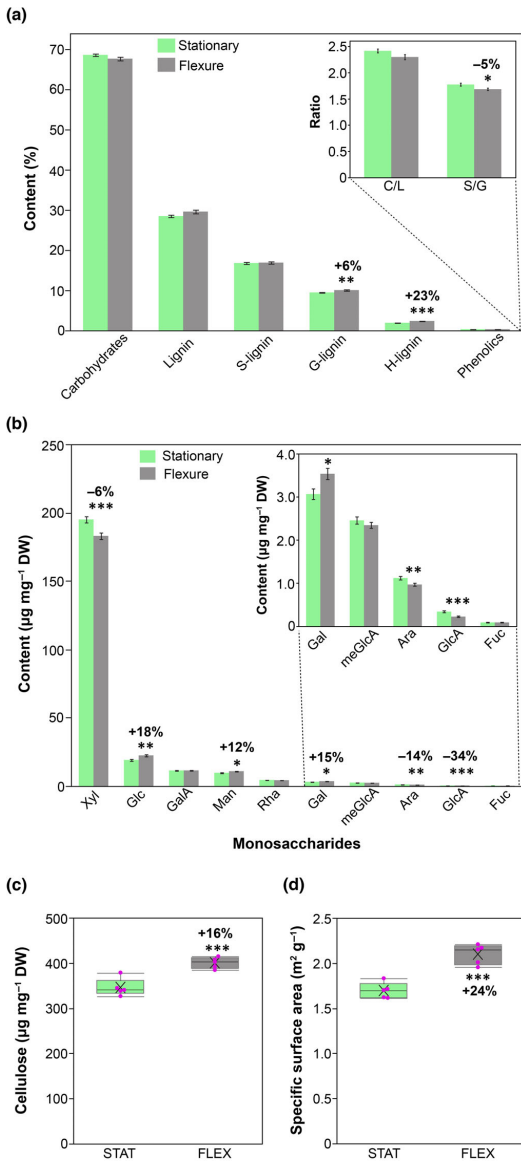


Fig. 3 Effects of hybrid aspen (*Populus tremula* × *tremuloides*) stem flexing on wood chemistry. (a) Py-GC/MS results reveal changes in wood chemical composition according to the different identified compounds present in the material. Carbohydrates to lignin as well as S-lignin to G-lignin ratios are presented in the top right corner of the chart. (b) Monosaccharide (anhydrous form) composition by TMS analysis of aspen wood material. The bars representing the sugars with relatively low amounts are shown in the inset. Data in (a) and (b) are means (±SE), $n = 7$ biological replicates. (c) Crystalline cellulose content measured by the Updegraff method. (d) Specific surface area (SSA) determined by BET nanoporosity assay. Data in (c) and (d) are means (±SE) of $n = 5$ technical replicates from pooled wood material from seven trees. Asterisks show the significance of the differences between growth conditions assessed by Student's *t*-test (*, $P < 0.05$; **, $P < 0.01$; ***, $P < 0.001$). Box plots show interquartile ranges (IQRs) as boxes, medians as horizontal lines, means as crosses, data points as dots, and ranges of all data points as whiskers, except for outliers (points further than the box than 1.5 times IQR). Ara, arabinose; Fuc, fucose; Gal, galactose; GalA, galacturonic acid; Glc, glucose; GlcA, glucuronic acid; Man, mannose; meGlcA, methylglucuronic acid; Rha, rhamnose; Xyl, xylose.

(Fig. S3). In the cambium, there was significant enrichment of GO terms including thermospermine synthase activity, and general processes like protein or DNA binding and response to abiotic stimulus, whereas in the xylem, there was enrichment for processes related to auxin, GAs, jasmonates and the osmosensor activity. Some of the most highly affected genes were within these categories. In the cambium, a homolog of *AtACL5* encoding a thermospermine synthase in the PA biosynthetic pathway (Kakehi *et al.*, 2008; Muñiz *et al.*, 2008) exhibited higher expression upon stem flexures whereas an arginine decarboxylase (*AtADC1*) was *de novo* induced in the xylem along with downregulation of a PA oxidase (*AtPAOI*). These changes suggest increased PA levels in flexed stems. Furthermore, reduced expression in the xylem was observed for the homolog of the type-B response regulator *AtRR12* mediating CK responses (Yokoyama *et al.*, 2007), suggesting suppressed CK signaling upon stem flexures, which is in agreement with the general decrease in CKs observed in the cambium (Fig. 5a). Reductions in transcripts encoding several ABA biosynthetic enzymes were observed in both tissues (Table 3), including a homolog of *AtNCED3* (Iuchi *et al.*, 2001), and an increase in transcripts related to ABA catabolism homologous to *AtCYP707A4* (Kushiro *et al.*, 2004) in the xylem, indicating reduced ABA levels, which was in agreement with the hormonics results (Fig. 5b). Moreover, several ABA-related TFs and signaling components such as homolog of *AtRD26* (Jiang *et al.*, 2019) were downregulated in the cambium (Tables 1, 3, S6). By contrast, genes related to BR biosynthesis and regulation were upregulated including a homolog of *AtDWF4/CYP90B1* (Fujita *et al.*, 2006), *AtEXO* and *AtEXL5* (Schröder *et al.*, 2009). In the xylem, a homolog of *AtBARK1/TMK4* encoding a kinase negatively regulating auxin biosynthesis (Wang *et al.*, 2020a) was one of the most upregulated genes by stem flexing and homologs of different auxin transporters *AtPIN1*, *AtLAX3* and *AtAUX1* were affected whereas in the cambium, increased transcript levels of phosphatidylinositol transfer patellins involved in *AtPIN1* relocation (Tejos *et al.*, 2018) indicated changes in auxin transport upon stem flexures. Ethylene

relatively lowly expressed in aspen wood-forming tissues. This indicates that flexure activates lignification using specific sets of enzymes. In general, the changes in gene expression point to increased cellulose biosynthesis, modified pectin esterification, increased xylan acetylation and lignification.

Both cambium and xylem tissues showed significantly enriched GO terms related to transcriptional and hormonal regulation, but with different specificities (Tables 1, 3, S3–S7;

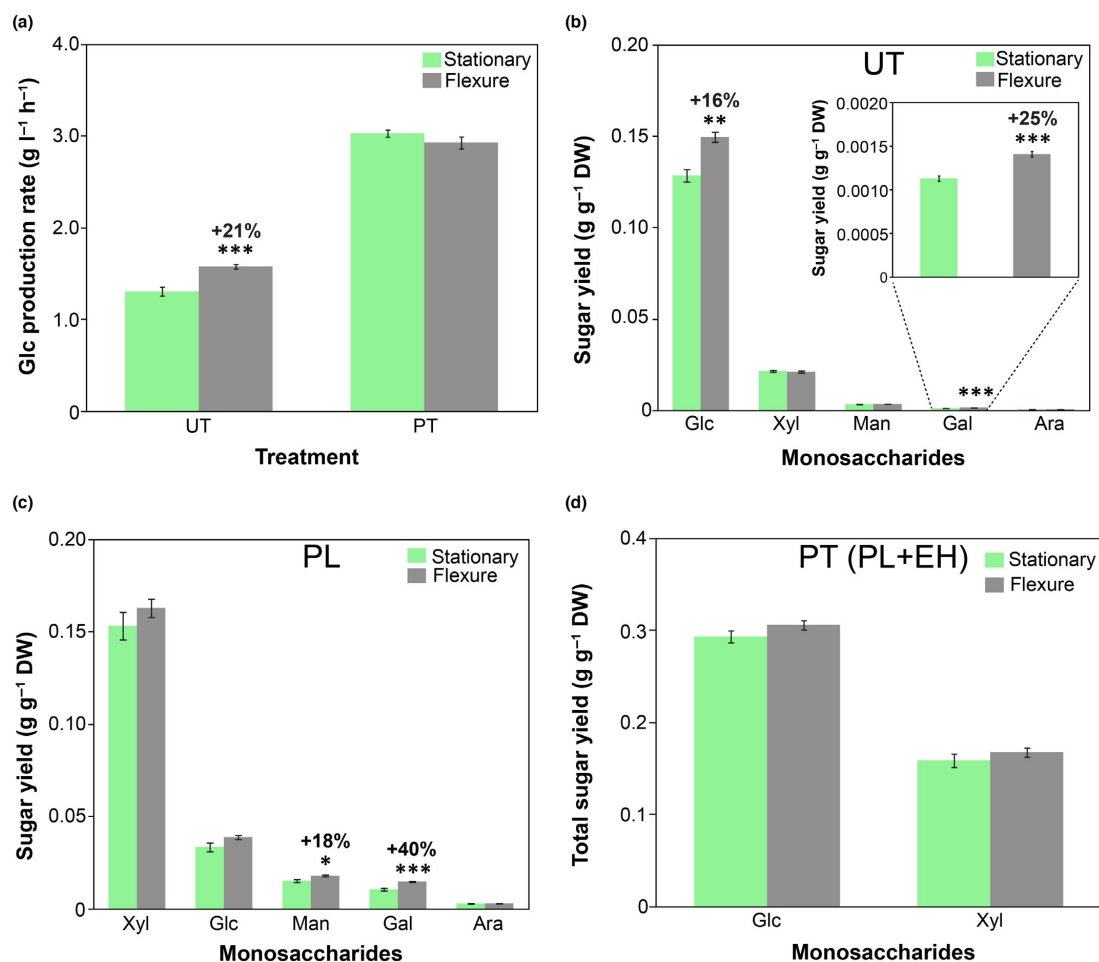


Fig. 4 Effects of hybrid aspen (*Populus tremula* × *tremuloides*) stem flexing on wood recalcitrance. Glc production rates for saccharification without pretreatment (a, left) and with acidic pretreatment (a, right). (b) Sugar yield of biomass in enzymatic hydrolysate following saccharification assay of untreated wood. The significant change in Gal yield is shown in the inset for better interpretation. (c) Sugar yield of biomass in pretreatment liquid fraction following thermochemical hydrolysis of wood during acidic pretreatment. (d) Total sugar yield of biomass for Glc and Xyl after acidic pretreatment. Data are means (±SE) of $n = 5$ technical replicates from pooled wood material from seven trees. Asterisks show the significance of the differences between growth conditions assessed by Student's *t*-test (*, $P < 0.05$; **, $P < 0.01$; ***, $P < 0.001$). Ara, arabinose; EH, enzymatic hydrolysate; Gal, galactose; Glc, glucose; Man, mannose; PL, pretreatment liquid; PT, pretreated; UT, untreated; Xyl, xylose.

biosynthesis and signaling appeared to be stimulated by the mechanical stimuli since transcripts encoding ACC oxidase – the key ethylene biosynthetic gene – homologous to *AtACO4/EFE* were among the most upregulated in the xylem whereas some negative regulators of ethylene signaling, such as homologs of *AtEBF2* and *AtERF4* (Yang *et al.*, 2005; Li *et al.*, 2015), were downregulated in the cambium. Altered GA signaling in the xylem of flexed stems was evidenced by strong upregulation of aspen homologs of gibberellin 2-oxidase *AtGA2OX6* involved in GA catabolism (Lange & Lange, 2015) and GA-stimulated protein *AtGASAI4*. Despite the remarkable increase in JA and JA-Ile

content upon stem flexures (Fig. 5), we did not find a significant upregulation of transcripts in the jasmonate biosynthesis pathway. Homologs of *AtJARI* involved in the formation of biologically active JA-Ile (Staswick & Tiryaki, 2004) and *AtJAZ3* (*Potra2n10c21496*) mediating downstream jasmonate responses (Liu *et al.*, 2021) exhibited decreased expression in the xylem (Table 3).

Mechanical stimuli also caused alterations in transcript levels of genes involved in Ca²⁺, G-protein and receptor-like kinase (RLK) signaling (Table 3). For instance, the *CML* gene homologous to *AtCML5/MSS3*, which is induced by touch in

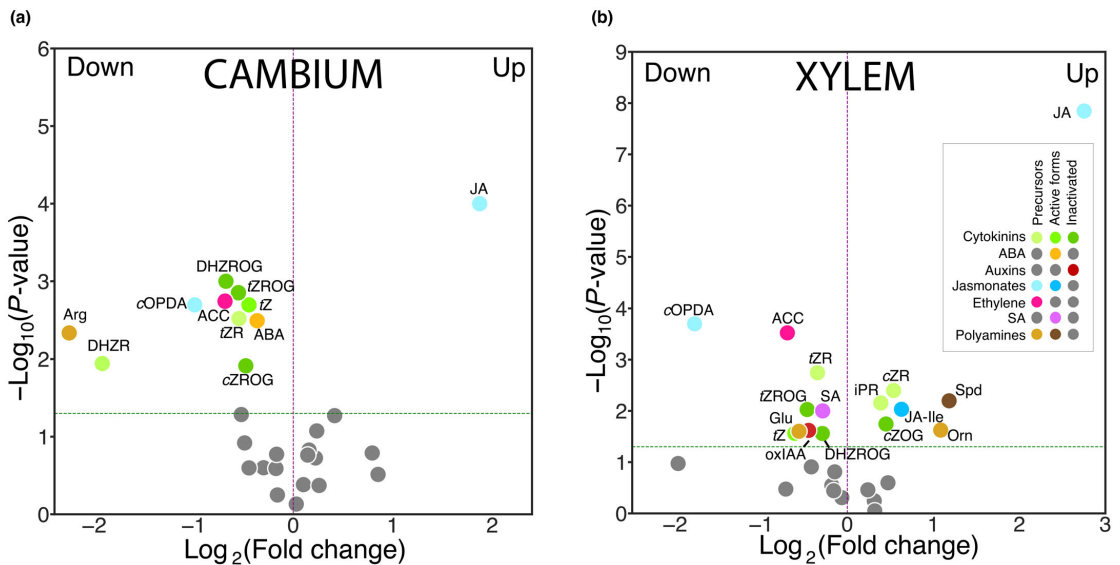


Fig. 5 Hormonal alterations in hybrid aspen (*Populus tremula* × *tremuloides*) upon regular stem flexures. Volcano plots depict the changes in the mean ($n = 5$ for polyamines or 4 for remaining compounds) hormone concentrations (pmol g^{-1} FW) of the different targeted compounds analyzed in the cambial region tissues (cambium) (a) and developing xylem tissues (xylem) (b) in the flexure-treated trees as compared with the stationary trees. Gray dots without labels represent the detected compounds that did not meet the significance criteria ($P < 0.05$, Student's t -test). Colored dots with names show the hormones that were either significantly increased ('Up') or reduced ('Down') in the flexure set compared with the stationary trees. ABA, abscisic acid (active); ACC, 1-aminocyclopropane-1-carboxylic acid (precursor); Arg, arginine (precursor); cOPDA, *cis*-12-oxophytodienoic acid (precursor); cZOG, *cis*-zeatin-O-glucoside (inactivated); cZR, *cis*-zeatin riboside (precursor); cZROG, *cis*-zeatin riboside-O-glucoside (inactivated); DHZR, dihydrozeatin riboside (precursor); DHZROG, dihydrozeatin riboside-O-glucoside (inactivated); Glu, glutamic acid (precursor); iPR, N^6 -isopentenyladenine riboside (precursor); JA, jasmonate (precursor); JA-Ile, jasmonate-isoleucine conjugate (active); Orn, ornithine (precursor); oxIAA, 2-oxoindole-3-acetic acid (inactivated); SA, salicylic acid (active); Spd, spermidine (active); *tZ*, *trans*-zeatin (active); *tZR*, *trans*-zeatin riboside (precursor); *tZROG*, *trans*-zeatin riboside-O-glucoside (inactivated).

Arabidopsis (Lee *et al.*, 2005), had greater expression in the cambium of flexed vs stationary stems. An aspen homolog of a leucine-rich repeat RLK *AtXIP1/CEPR1*, a receptor of C-terminally encoded peptides involved in vascular development (Bryan *et al.*, 2012), exhibited almost a six-fold downregulation in the xylem, whereas a homolog of *AtRLK902* encoding a RLK mediating BR responses (Zhao *et al.*, 2019) was upregulated. In the cambium of flexed stems, several genes related to cell division and growth were upregulated such as homologs of *AtCYCP32* – a cyclin regulating cell division cycle (Torres Acosta *et al.*, 2004), and *AtWLIM1* (Table S3) from the LIM family involved in cytoskeleton organization and known to be involved in tension wood formation (Arnaud *et al.*, 2007).

Among the TFs with altered expression in the xylem (Table S6), the simultaneous upregulation of homologs of *AtMYB52*, *AtKNAT3*, as well as the tandem CCCH zinc finger transcriptional activators *AtC3H14* and *AtC3H15/CDM1* that regulate secondary cell wall formation in the xylem (Zhong *et al.*, 2008; Zhong & Ye, 2012; Cassan-Wang *et al.*, 2013; Kim *et al.*, 2013; Chai *et al.*, 2015; Wang *et al.*, 2020b), further indicate sophisticated control over secondary cell wall deposition during mechanical stimuli in aspen. Three genes encoding C2H2-type zinc finger proteins were also affected by flexure in

the xylem, including a homolog of *AtZAT5* related to the previously identified stem bending marker *ZFP2* (Fig. S6; Leblanc-Fournier *et al.*, 2008; Martin *et al.*, 2009).

Differentially expressed genes in stems subjected to flexure form co-expression networks in stems of field-grown trees

To reveal the co-expression networks among the genes differentially expressed in the wood-forming tissues of flexed stems, we analyzed their networks within the developing wood of field-grown aspen naturally exposed to stem flexures using the AspWood database (Sundell *et al.*, 2017). Five and three clusters of co-expressed genes were found for the cambium and xylem DEGs, respectively, and their expression patterns were shown as heatmaps (Fig. 6a–c; Table S8). Xylem cluster 1 and cambium cluster 5 included genes that were upregulated by flexing while the remaining clusters included downregulated genes, identifying candidates for positive or negative regulators of flexure wood formation, respectively. Xylem cluster 1 included genes expressed at the onset of secondary wall formation. It contained several TFs, notably zinc finger TFs such as homologs of the putative mechanoperception regulator *AtZAT5* and secondary cell wall biosynthesis regulators *AtC3H14* and *AtC3H15*. It also contained

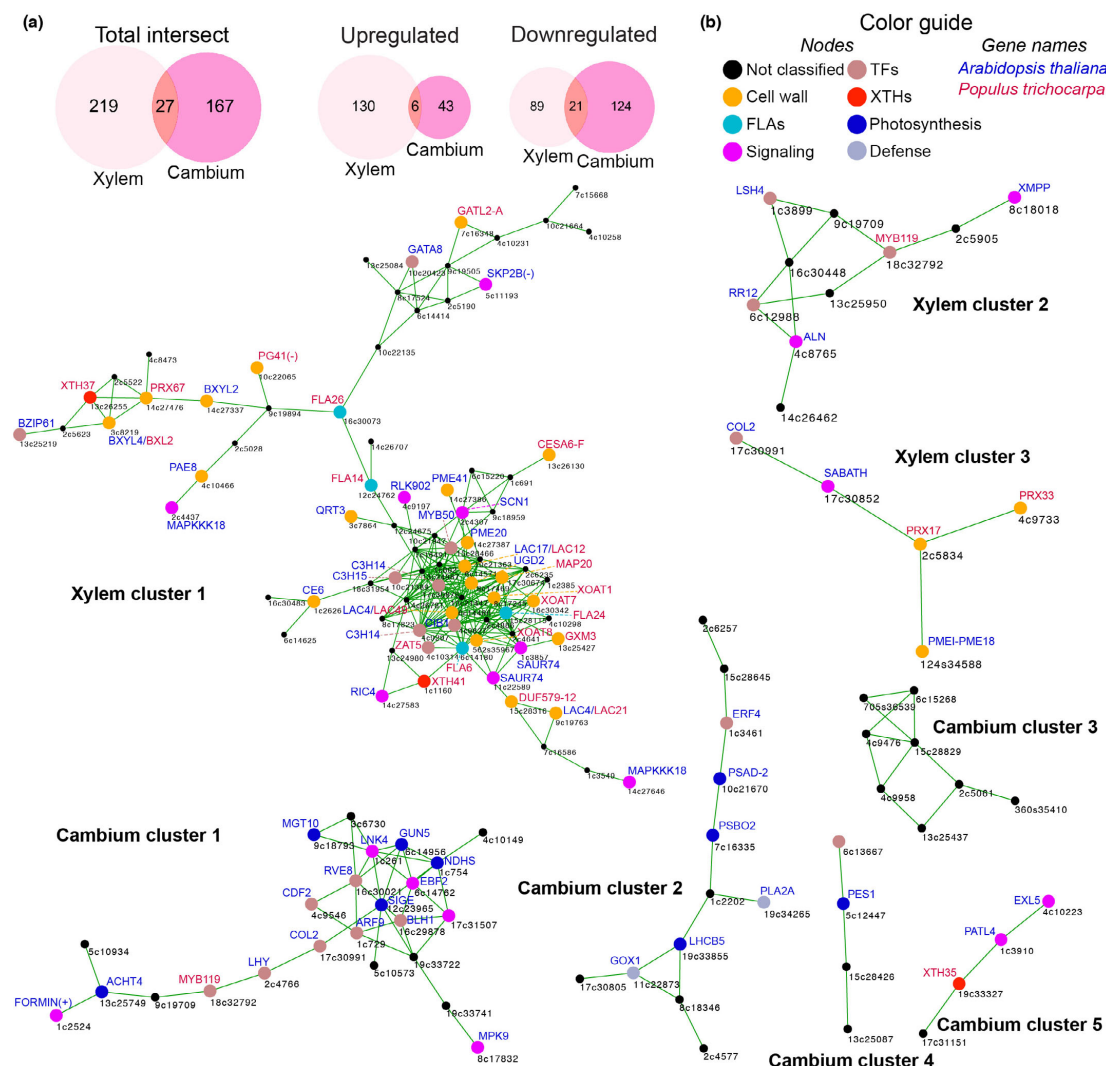


Fig. 6 Transcriptional changes in hybrid aspen (*Populus tremula* × *tremuloides*) stems in response to flexure. (a) Venn diagrams represent the total number of differentially expressed genes (DEGs, $FC \geq 1.5$) in the xylem and cambium from aspen stems subjected to low-intensity stem flexures relative to the stationary stems. (b) Co-expression clusters, based on the AspWood database (Sundell *et al.*, 2017) of DEGs in xylem and cambium tissues. The gene names are shown for *Arabidopsis thaliana* (blue) and/or *Populus trichocarpa* (red), also the color guide explains the differently colored nodes indicating various categories the DEGs were assigned to. Codes beside the nodes correspond to Potra2n gene ID. (c) Heatmaps indicating the AspWood expression patterns of the genes from the clusters shown in (b). Ca, cambium and radial expansion zone; PCD, lignification and programmed cell death; Ph, phloem; PW-SW, primary to secondary wall transition zone; SW, secondary wall deposition zone; numbers 01–25 above the heatmaps correspond to the sample number for tree 1 in AspWood; genes are identified by their Potra2n IDs on the right.

signaling-related genes such as homologs of *AtSKP2B* and *AtRLK902*, four *AtFLA11/FLA12* homologs, *PxXTH37* and *41*, as well as xylan and pectin acetylation-related genes. Remarkably, the expression pattern of *SKP2B* in developing wood was opposite to other genes of this cluster and this gene was negatively

regulated by flexing. Its product functions as a part of E3 ubiquitin ligase SCF complex negatively regulating the level of E2FC TF, which is a key regulator of cambial cell division and secondary cell wall formation in *Arabidopsis* (Manzano *et al.*, 2012; Taylor-Teeples *et al.*, 2015). Xylem cluster 2 included genes

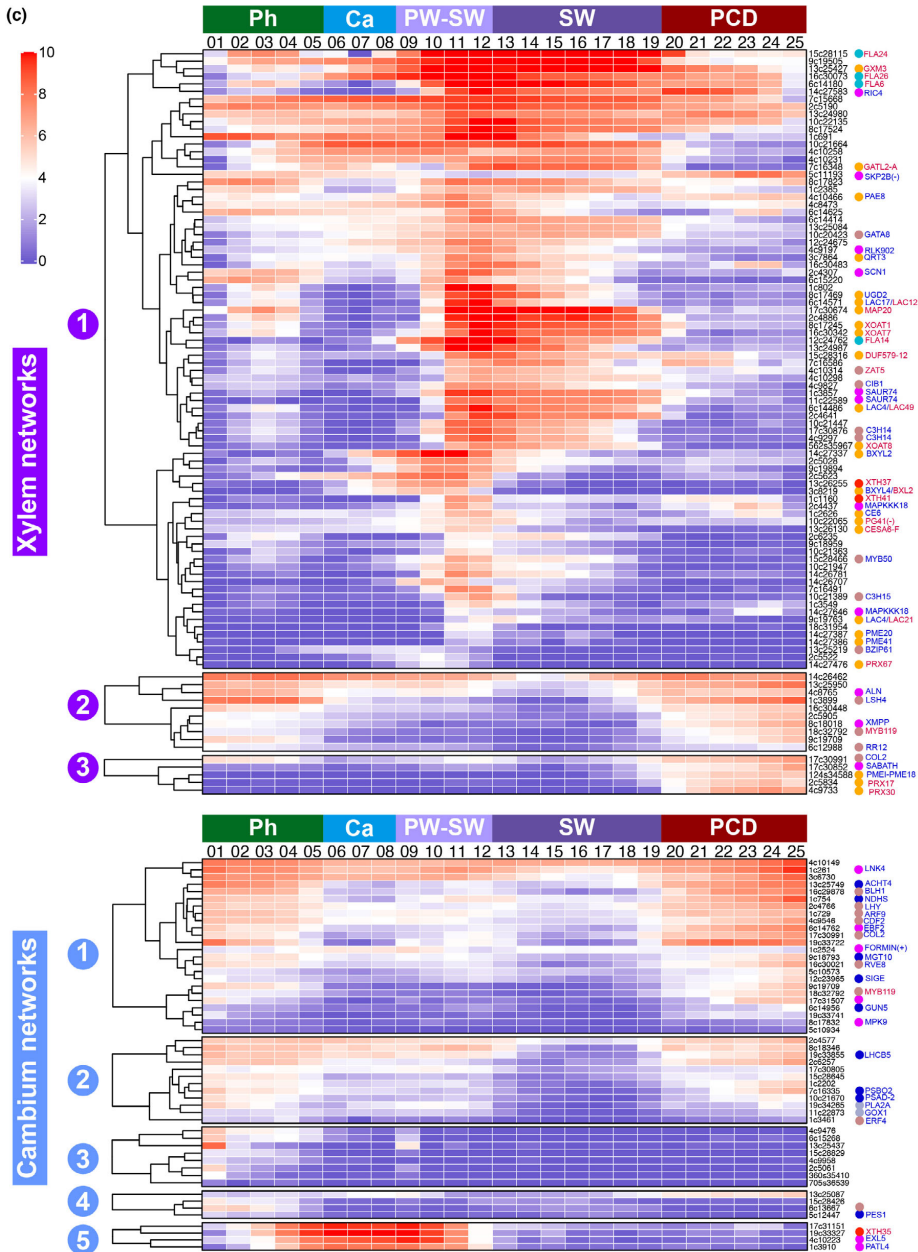


Fig. 6 (Continued)

expressed in the phloem and in the xylem programmed cell death (PCD) zone, comprising the CK regulator *AtRR12* and homologs of genes encoding enzymes related to purine catabolism, *AtXMPP*

(Heinemann *et al.*, 2021) and *AtALN* (Takagi *et al.*, 2016), regulating the steady-state of allantoin, a stress-related metabolite that activates JA signaling. Xylem cluster 3 included genes expressed

Table 1 List of the five most up- and downregulated differentially expressed genes (DEGs; $P \leq 0.05$ and fold change expression ≥ 1.5) in the cambium and xylem tissues of mechanically stimulated hybrid aspen (*Populus tremula* \times *tremuloides*) stems compared with the stationary set.

Potra v.2.2 gene ID*	Log ₂ FC	Potri v.3.1 gene ID**	Populus name***	CAZY****	AGI gene ID****	AGI gene name	Description (TAIR, www.arabidopsis.org/)
Cambium							
Potra2n14c27099	1.5	Potri.014G096000		GT1	AT4G01070	UGT72B1	UDP-glucosyltransferase
Potra2n12c24367	1.4	Potri.002G022500			AT5G14920	GASA14	Gibberellin-stimulated protein
Potra2n5c11397	1.3	Potri.002G098800			AT4G08950	EXO	Exordium
Potra2n1c2524	1.2	Potri.001G288900			AT1G10020		Formin-like protein (DUF1005)
Potra2n13c26255	1.1	Potri.013G005700	XTH37	GH16	AT4G25810	XTH23/XTR6	XTH
Potra2n11c22767	-3.0	Potri.011G123300			AT4G27410	RD26/ ANAC72	NAC transcription factor
Potra2n4c9958	-3.0	Potri.004G172300			AT2G17880	DJC24	Chaperone DNAJ-domain protein
Potra2n13c25439	-3.2	Potri.013G100800			AT4G24350		Phosphorylase family protein
Potra2n13c25212	-3.6	Potri.013G125300			AT3G25180	CYP82G1	Cytochrome P450 monooxygenase
Potra2n13c25437	-4.7	Potri.013G100800			AT4G24340		Phosphorylase family protein
Xylem							
Potra2n1022s36932	9.2	Potri.004G163300			AT2G16500	ADC1	Arginine decarboxylase
Potra2n13c25987	1.8	Potri.013G035900			AT3G23750	BARK1/ TMK4	Receptor-like kinase
Potra2n747s36676	1.6	Potri.002G224100			AT1G05010	ACO4/EFE	ACC oxidase
Potra2n12c24367	1.5	Potri.002G022500			AT5G14920	GASA14	Gibberellin-stimulated protein
Potra2n14c27286	1.4	Potri.014G117300			AT1G02400	GA2OX6	Gibberellin 2-oxidase
Potra2n2c5061	-3.9	Potri.002G150400			AT2G45550	CYP76C4	Geraniol 9- or 8-hydroxylase
Potra2n2c6318	-4.3	Potri.002G015100			AT3G03190	GSTF11	Glutathione S-transferase
Potra2n2c4331	-4.4	Potri.002G233200			AT5G16740		Amino acid transporter
Potra2n7c16468	-4.5	Potri.005G118700			AT5G66390	PRX72	Peroxidase
Potra2n1398s37044	-5.4	Potri.011G016400			AT3G18670		Ankyrin repeat family protein

**Populus tremula* v.2.2 gene ID.

**Best DIAMOND Potri gene ID based on Potra v.2.2 gene ID.

***CAZy, carbohydrate-active enzymes and gene name (Kumar *et al.*, 2019).

****Best DIAMOND AGI gene ID based on Potra v.2.2 gene ID; FC, fold change (flexure/stationary expression).

in the PCD zone where stress-related peroxidases and a homolog of *AtPMEI-PME18* were suppressed by flexing. Cambium clusters 1 and 2 exhibited upregulation in the phloem and PCD zone, similar to xylem cluster 2. Functionally however, these clusters differed by having large numbers of photosynthesis-related genes. Cambium cluster 1 also included genes encoding TFs and signaling proteins related to ABA (similar to *AtBLH1* and *AtMPK9*), auxin (similar to *AtARF9*), CK (similar to *AtCOL2*) and ethylene (similar to *AtEBF2*) responses. Cambium cluster 5 was distinct by including genes highly and specifically expressed in the cambium and radial expansion zone that were upregulated by flexing. They included a homolog of *AtPATL4* involved in PIN1 relocation and genes encoding cell wall-localized proteins involved in cell proliferation and growth, such as a homolog of *AtEXL5* involved in BR responses and *PtXTH35* (*AtXTH9*), the most abundant XTH in wood-forming tissues mediating xylem cell size (Kushwah *et al.*, 2020).

Discussion

Plants perceive both internal and external mechanical cues to adjust their growth and development (Alonso-Serra *et al.*, 2020; Moulia *et al.*, 2021). Low-intensity stem flexure stress induced by wind is an everyday mechanical perturbation encountered by young trees. In the present study, we investigated the effects of multiple low-intensity stem flexures mimicking wind sway in

aspen to advance our understanding of tree growth, and to reveal possible signaling pathways involved in these responses.

Low-intensity stem flexing increases growth

We found that gentle stem flexure led to an overall increase in growth (Fig. 1). Root biomass showed the highest increase, indicating augmented biomass allocation to the root, although there was also a prominent increase in leaf size, which largely contributed to the higher aboveground biomass of the flexed trees. Increased stem radial expansion and root growth but reduced stem elongation and leaf growth were reported in mechanically perturbed plants (Telewski & Jaffe, 1986a,b; Telewski & Pruyn, 1998; Coutand *et al.*, 2000, 2008, 2009; Kern *et al.*, 2005; Wu *et al.*, 2016), but this phenotype was not always observed in all studied genotypes (Jaffe, 1973; Telewski & Jaffe, 1986b; Wu *et al.*, 2016; Roignant *et al.*, 2018) or in all types of experiments (Paul-Victor & Rowe, 2011). Stem elongation was shown to be inhibited shortly after mechanical stimulation, followed by growth recovery and/or growth stimulation (Jaffe *et al.*, 1980; Coutand *et al.*, 2000, 2009); thus, the observed growth effect can vary depending on the time the observations are made. Moreover, the extent of plant responses to stem bending has been shown to be correlated with the number of flexures applied, the magnitude of stem longitudinal strain or the bending angle (Jaffe *et al.*, 1980; Telewski & Pruyn, 1998; Coutand *et al.*, 2009). The swaying angle in our experiment was

Table 2 Differentially expressed genes (DEGs; $P \leq 0.05$ and fold change expression ≥ 1.5) related to cell wall biosynthesis and modification in the cambium and xylem tissues of mechanically stimulated hybrid aspen (*Populus tremula* × *tremuloides*) stems and their transcriptional behavior (up- or downregulation) relative to the stationary set.

Potra v.2.2 gene ID*	Log ₂ FC	Potri v.3.1 gene ID**	Populus name***	CAZY****	AGI gene ID****	AGI gene name	Description (TAIR, www.arabidopsis.org/)
Cambium							
Potra2n13c26255	1.1	Potri.013G005700	XTH37	GH16	AT4G25810	XTH23/XTR6	XTH
Potra2n19c33327	0.6	Potri.019G125000	XTH35	GH16	AT4G03210	XTH9	XTH
Potra2n9c18880	1.0	Potri.007G083400	EXPLA2	EXPN	AT4G38400	EXLA1, EXLA2	Expansin-like
Potra2n14c27766	0.8	Potri.014G168100			AT4G12730	FLA2	Fasciclin-like arabinogalactan protein
Potra2n10c22065	-1.1	Potri.010G042100	PG41	GH28	AT1G10640		Polygalacturonase
Potra2n10c22100	0.7	Potri.010G038300	GATL8-B	GT8	AT1G70090	GATL9	Galacturonosyltransferase-like protein
Potra2n16c29485	-1.3	Potra2n16c29485			AT2G40890	REF8	Coumarate 3-hydrolase
Potra2n14c27099	1.5	Potri.014G096000		GT1	AT4G01070	UGT72B1	UDP-glucosyltransferase
Xylem							
Potra2n13c26130	0.8	Potri.013G019800	CesA6-F	GT2	AT5G64740	CESA6/IXR2	Primary wall cellulose synthase
Potra2n5c12058	0.7	Potri.005G087500	CesA6-A	GT2	AT4G39350	CESA2	Primary wall cellulose synthase
Potra2n1c1160	1.0	Potri.001G136100	XTH41	GH16	AT1G32170	XTH30/XTR4	XTH
Potra2n13c26255	0.7	Potri.013G005700	XTH37	GH16	AT4G25810	XTH23/XTR6	XTH
Potra2n5c12814	0.6	Potri.005G001500		CE13	AT3G05910	PAE12	Pectin acetyltransferase
Potra2n4c10466	0.6	Potri.004G234100		CE13	AT4G19420	PAE8	Pectin acetyltransferase
Potra2n14c27387	1.3	Potri.014G127000		CE8	AT2G47550	PME1-PME20	Pectin methylesterase inhibitor-PME
Potra2n14c27386	1.0	Potri.014G127000		CE8	AT4G02330	PME41	PME
Potra2n10c22100	0.8	Potri.010G038300	GATL8-B	GT8	AT1G70090	GATL9	Galacturonosyltransferase-like protein
Potra2n8c17469	0.6	Potri.008G094300			AT3G29360	UGD2	UDP-glucose dehydrogenase
Potra2n124s34588	-1.9	Potri.011G025400		CE8	AT1G11580	PME1-PME18	Pectin methylesterase inhibitor-PME
Potra2n8c17528	-1.5	Potri.008G100500	PG28	GH28	AT1G48100	PGX3	Polygalacturonase
Potra2n3c7864	0.6	Potri.003G074600			AT4G20050	QRT3/PGF11	Polygalacturonase
Potra2n10c22065	-1.0	Potri.010G042100	PG41	GH28	AT1G10640		Polygalacturonase
Potra2n3c8219	0.7	Potri.003G022900	BXL2	GH3	AT5G64570	XYL4	β-D-xylosidase
Potra2n14c27337	0.6	Potri.014G122200		GH3	AT1G02640	BXL2	β-D-xylosidase
Potra2n16c30342	0.6	Potri.016G119100	XOAT7/TBL59		AT5G01360	TBL3	Xylan O-acetyltransferase
Potra2n56s235967	0.8	Potri.001G376700	XOAT8/TBL60		AT1G73140	TBL31	Xylan O-acetyltransferase
Potra2n5c12326	0.7	Potri.005G060800	TBL27		AT1G48880	TBL7	Likely xylan O-acetyltransferase
Potra2n8c17245	0.6	Potri.008G069900	XOAT1/TBL51		AT3G55990	ESK1/TBL29	Xylan O-acetyltransferase
Potra2n1c2626	0.6	Potri.009G096400		CE6	AT4G34215		SGNH-hydrolase family protein
Potra2n7c16348	0.7	Potri.007G031700	GATL2-A	GT8	AT1G19300	PARVUS/GATL1	Galacturonosyltransferase-like
Potra2n13c25427	0.7	Potri.013G102200	GXM3		AT1G33800	GXM1	Glucuronoxylan 4-O-methyltransferase
Potra2n15c28316	0.6	Potri.015G096900			AT4G24910		Glucuronoxylan 4-O-methyltransferase-like
Potra2n16c30073	0.7	Potri.016G088700	FLA26		AT5G03170	FLA11	Fasciclin-like arabinogalactan protein
Potra2n6c14180	0.6	Potri.006G129200	FLA6		AT5G03170	FLA11	Fasciclin-like arabinogalactan protein
Potra2n12c24762	0.8	Potri.012G127900	FLA14		AT5G60490	FLA12	Fasciclin-like arabinogalactan protein
Potra2n15c28115	0.6	Potri.015G129400	FLA24		AT5G60490	FLA12	Fasciclin-like arabinogalactan protein
Potra2n9c19763	0.8	Potri.009G042500	LAC21	AA1	AT2G38080	LAC4/IRX12	Laccase
Potra2n6c14486	0.6	Potri.006G097100	LAC49	AA1	AT2G38080	LAC4/IRX12	Laccase
Potra2n6c14571	0.8	Potri.006G087500	LAC12	AA1	AT5G60020	LAC17	Laccase
Potra2n14c27476	1.1	Potri.012G042800	PRX67		AT2G39040	PER24	Class III peroxidase****
Potra2n2c5834	-1.9	Potri.002G065300	PRX17		AT1G71695	PRX12	Class III peroxidase****
Potra2n4c9733	-2.3	Potri.004G144600	PRX30		AT1G49570	PRX10	Class III peroxidase****
Potra2n7c16468	-4.5	Potri.005G118700	PRX34		AT5G66390	PRX72	Class III peroxidase****
Potra2n14c27252	1.0	Potri.014G113100			AT1G02520	ABCB11	ABC transporter
Potra2n9c19878	-1.5	Potri.009G028800		GH152	AT2G28790		Thaumatococcus family protein

**Populus tremula* v.2.2 gene ID.

**Best DIAMOND or phylogenetic tree-deduced assignment for homologous Potri gene ID based on Potra v.2.2 gene ID (for full annotation cf Supporting Information Tables S3 and S4).

***CAZy, carbohydrate-active enzyme family and gene name (Kumar *et al.*, 2019).

****Best DIAMOND AGI gene ID based on Potra v.2.2 gene ID or phylogenetic tree-deduced assignment for homologous Ath based on Potri ID.

******Populus* peroxidase names are according to Ren *et al.* (2014); FC, fold change (flexure/stationary expression).

Table 3 List of selected differentially expressed genes (DEGs; fold change ≥ 1.5) including Ca^{2+} -, G-protein- and receptor-like kinase-mediated signaling as well as hormone-related transcripts in the cambium and xylem tissues of mechanically stimulated hybrid aspen (*Populus tremula* \times *tremuloides*) stems relative to the stationary set.

Potra v.2.2 gene ID*	Log ₂ FC	Potri v.3.1 gene ID**	AGI gene ID***	AGI gene name (TAIR)	Description (TAIR, https://www.arabidopsis.org/)
Cambium					
Potra2n8c18019	0.9	Potri.008G151800	AT5G19530	ACL5	Thermospermine synthase
Potra2n1c2524	1.2	Potri.001G288900	AT1G10020		Formin-like protein (DUF1005)
Potra2n14c26822	0.7	Potri.014G066400	AT3G60550	CYP3;2	Cyclin p interacting with cyclin-dependent protein kinase
Potra2n12c24367	1.4	Potri.002G022500	AT5G14920	GASA14	Gibberellin-stimulated protein
Potra2n15c28577	0.9	Potri.T155100	AT5G14920	GASA14	Gibberellin-stimulated protein
Potra2n7c16398	0.8	Potri.005G124000	AT3G50660	DWF4/CYP90B1	C22 alpha hydroxylase
Potra2n7c15551	0.7	Potri.007G128600	AT2G43290	MSS3/CML5	Calmodulin-like protein
Potra2n1c3910	0.7	Potri.001G461400	AT1G30690	PATL4	Sec14p-like phosphatidylinositol transfer protein
Potra2n13c25391	0.6	Potri.019G079500	AT1G72160	PATL3	Sec14p-like phosphatidylinositol transfer protein
Potra2n1c3437	-1.7	Potri.011G112400	AT3G14440	NCED3	9- <i>cis</i> -epoxycarotenoid dioxygenase
Potra2n6c14762	-0.8	Potri.006G068500	AT5G25350	EBF2	EIN3-binding F-box protein
Potra2n18c32128	-0.9	Potri.018G130800	AT5G25350	EBF2	EIN3-binding F-box protein
Potra2n12c24080	-1.5	Potri.012G043200	AT1G73500	MKK9	Mitogen-activated protein kinase kinase
Potra2n16c30484	-1.5	Potri.016G134600	AT5G58350	WNK4	With no lysine (K) kinase
Potra2n8c17488	-1.5	Potri.008G096500	AT1G13740	AFP2	ABI five binding protein
Potra2n8c17832	-0.7	Potri.010G112200	AT3G18040	MPK9	Mitogen-activated protein kinase
Potra2n13c25835	-1.2	Potri.013G051300	AT5G63930		Leucine-rich repeat protein kinase
Potra2n15c28419	-1.2	Potri.015G086800	AT2G31880	SOBIR1	Leucine-rich repeat receptor-like kinase
Xylem					
Potra2n12c23757	0.7	Potri.012G007600	AT5G54130		Ca^{2+} -binding protein
Potra2n11c23262	0.7	Potri.011G063200	AT3G15050	IQD10	Calmodulin-binding protein
Potra2n16c29614	-3.1	Potri.006G046500	AT2G41560	ACA4	Calmodulin-regulated Ca^{2+} -ATPase
Potra2n2c4307	0.7	Potri.002G234600	AT3G07880	SCN1	RhoGTPase GDP dissociation inhibitor
Potra2n14c27583	0.6	Potri.014G147000	AT5G16490	RIC4	ROP-interactive CRIB motif-containing protein
Potra2n4c9197	0.6	Potri.004G086100	AT3G17840	RLK902	Receptor-like kinase
Potra2n2c4437	0.6	Potri.002G228200	AT1G05100	MAPKKK18	Mitogen-activated protein kinase kinase kinase
Potra2n14c27646	0.6	Potri.014G155000	AT1G05100	MAPKKK18	Mitogen-activated protein kinase kinase kinase
Potra2n7c16491	0.8	Potri.007G016800	AT5G66330		Leucine-rich repeat protein kinase
Potra2n2c5402	-2.5	Potri.002G111700	AT5G49660	XIP1/CEPR1	Leucine-rich repeat receptor kinase
Potra2n13c25987	1.8	Potri.013G035900	AT3G23750	BARK1/TMK4	Leucine-rich repeat receptor-like kinase
Potra2n6c14169	0.7	Potri.016G087800	AT3G53380	LECRK-VIII.1	L-type lectin receptor kinase
Potra2n8c17630	-2.0	Potri.008G110300	AT5G16000	NIK1	Leucine-rich repeat receptor-like kinase
Potra2n11c22876	-1.9	Potri.011G112400	AT3G14440	NCED3	9- <i>cis</i> -epoxycarotenoid dioxygenase
Potra2n1c3437	-1.9	Potri.011G112400	AT3G14440	NCED3	9- <i>cis</i> -epoxycarotenoid dioxygenase
Potra2n2c5263	0.9	Potri.002G126100	AT3G19270	CYP707A4	ABA 8'-hydroxylase
Potra2n14c27095	-0.8	Potri.014G095500	AT2G46370	JAR1	Jasmonate-amido synthetase
Potra2n10c21496	-0.7	Potri.010G108200	AT3G17860	JAZ3	Jasmonate-ZIM-domain protein 3
Potra2n747s36676	1.6	Potri.002G224100	AT1G05010	ACC04/EFE	ACC oxidase
Potra2n12c24119	-0.7	Potri.015G038700	AT1G73590	PIN1	Auxin efflux carrier
Potra2n2c5623	0.7	Potri.002G087000	AT1G77690	LAX3	Auxin influx carrier
Potra2n6c14477	-0.6	Potri.006G098300	AT2G38120	AUX1	Auxin influx carrier
Potra2n11c22589	0.8	Potri.001G458000	AT3G12955	SAUR74	SAUR-like auxin-responsive protein
Potra2n1c3857	0.7	Potri.001G458000	AT3G12955	SAUR74	SAUR-like auxin-responsive protein
Potra2n12c24367	1.5	Potri.002G022500	AT5G14920	GASA14	Gibberellin-stimulated protein
Potra2n14c27286	1.4	Potri.014G117300	AT1G02400	GA2OX6	Gibberellin 2-oxidase
Potra2n7c16146	-1.3	Potri.005G111700	AT2G17820	AHK1	Histidine kinase
Potra2n15c28548	-1.4	Potri.015G074600	AT5G13700	PAO1	Polyamine oxidase
Potra2n1022s36932	9.2	Potri.004G163300	AT2G16500	ADC1	Arginine decarboxylase
Potra2n5c11193	-1.3	Potri.005G185700	AT1G77000	SKP2B	Protein of E3 ubiquitin ligase SCF complex

**Populus tremula* genome assembly v.2.2 gene ID.

**Best DIAMOND Potri gene ID based on Potra v.2.2 gene ID.

***Best DIAMOND AGI gene ID based on Potra v.2.2 gene ID; FC, fold change (flexure/stationary expression).

relatively low (4°), compared with angles used in some other studies ($30\text{--}45^\circ$) reporting inhibition of stem and leaf elongation (Prunyn *et al.*, 2000; Kern *et al.*, 2005). Our treatment also differed from

plant rubbing used for herbaceous plants (Jaffe *et al.*, 1980; Saidi *et al.*, 2010; Chehab *et al.*, 2012) or stem bending as it was applied in the previous above-mentioned studies, since the stem in our

experiment was allowed to vibrate after each acceleration/deceleration (Video S1). Interestingly, sound vibrations have been shown to induce overall growth in many species (Jung *et al.*, 2018) and to induce responses at a distance (Appel & Crocroft, 2014).

Properties of flexure wood induced by low-intensity stem flexing

Detailed anatomical investigations revealed that flexed aspen formed significantly more secondary xylem compared with the stationary trees due to an increased number of xylem descendants of each fusiform initial (Fig. 2). This was supported by increased expression of cyclin *CYCP3;2* in the cambium and decreased expression of the negative regulator of cell cycle *SKP2B* in the xylem (Table 3), suggesting that the population of dividing xylem mother cells was increased by mechanical stress. These data support and extend the conclusions from many other reports (Pruyn *et al.*, 2000; Kern *et al.*, 2005; Coutand *et al.*, 2008; Telewski, 2016; Roignant *et al.*, 2018).

Stem flexing also strongly affected xylem cell differentiation. The most striking change was the induction of G-fiber biosynthesis, resulting in overall phenotypical changes typical of tension wood (Fagerstedt *et al.*, 2014), such as decreased MFA and xylan content, increased cell wall thickness, wood density, fiber coarseness, nanoporosity, crystalline cellulose and galactan contents as well as yields of sugars from enzymatic saccharification of wood without pretreatment (Figs 2–4). Despite decreased xylan content, several genes encoding xylan acetyltransferases were upregulated in flexure wood (Table 2; Fig. S7), suggesting increased xylan acetylation, which would affect xylan interaction with cellulose (Grantham *et al.*, 2017) and lignin (Giummarella & Lawoko, 2016), and would thus mediate mechanical properties of flexure wood (Niez *et al.*, 2020).

Unilateral stem bending for 5 s also induced G-fibers but only on the tensile/upper side of the bent stems (Roignant *et al.*, 2018), indicating that G-fibers can be induced after much shorter stimulation times than previously anticipated (Jourez & Avella-Shaw, 2003; Coutand, 2010) and their molecular triggers could be similar for flexure and tension wood. Reports of reduced vessel frequency and diameter in poplar flexure wood (Kern *et al.*, 2005; Roignant *et al.*, 2018) and other hardwood species (Telewski, 2016) could also reflect activation of the tension wood program by stem bending, although we did not detect such changes in this study. Whether the triggers of flexure wood G-fibers respond to stem stretching or to gravity vector deflection, as in tension wood (Groover, 2016), remains to be established.

Flexure wood shares developmental program with tension wood but not with opposite wood

As each stem flexure induces tensional strain together with gravistimulation inducing tension wood and compression strain together with gravistimulation inducing opposite wood, the multiple flexures in different planes induce all these stresses alternately. To reveal the common response between flexure treatment and gravitationally induced tension and opposite

wood, we compared the DEGs from our study with 8000 DEGs between tension and opposite wood in gravistimulated stems for different durations (2 h to 14 d; Zinkgraf *et al.*, 2018). Approximately 40% of flexure-affected genes were also differentially expressed between gravitropically induced tension and opposite wood (Tables S3, S4). Remarkably, almost all of them (97%) reacted the same way as in tension wood. This indicates that flexure wood shares the molecular program with gravitationally induced tension wood rather than opposite wood. Approximately 60% of DEGs in both cambium and xylem were not affected by gravitational stimuli and potentially reflect compression and/or tensional strain signaling. Interestingly, *KNAT3* and *MYB52* were among these genes and could regulate the secondary cell wall biosynthetic program contributing to decreased wall thickness in response to mechanical stress.

Membrane-attached proteins as putative mechanical stress sensors in flexure wood

Among different candidates for perception of mechanical disturbance (Frulieux *et al.*, 2019), we found several genes encoding proteins linking the cell wall with plasma membrane that were upregulated in flexure wood. *FLA11/FLA12s* are examples of such genes and were recently shown to control secondary cell wall thickening and lignification in Arabidopsis (Ma *et al.*, 2022). Other candidates are *XTHs* encoding XET, which are well-known touch- and bending-responsive genes (Lee *et al.*, 2005; Pomiès *et al.*, 2017). Some of the encoded XETs, including *PtXTH41* (*AtXTH30*), have plasma membrane localization (Ndamukong *et al.*, 2009; Witasari *et al.*, 2019; Yan *et al.*, 2019); others could be associated with the plasma membrane via another XTH protein (Zhu *et al.*, 2014). Since the active site of XETs is covalently binding xyloglucan in cell walls, these proteins are good candidates for sensing mechanical stresses. In support, overexpression of *AtTCH4/XTH22* in Arabidopsis resulted in increased cell wall porosity (Zhang *et al.*, 2022), reminiscent of changes in flexure wood (Fig. 3d), whereas mutations in *xtb4* and *xtb9* resulted in changes in secondary cell wall layers and lignification with the activation of cell wall integrity-related genes (Kushwah *et al.*, 2020). Formins were also proposed as proteins involved in mechanical stress perception (Baluska *et al.*, 2003). How these plasma membrane-attached proteins could be involved in perception of mechanical stress is a matter of conjecture. The general belief is that they could provide a means for transferring mechanical strains of cell walls to the plasma membrane activating other sensors located there, such as stretch-activated ion channels, or that they could provide a physical link between the cell wall and actin filaments (with participation of other proteins) generating cell wall – plasma membrane – cytoskeleton continuity (Baluska *et al.*, 2003; Telewski, 2021).

Hormones involved in flexure wood formation

Our hormonomics and transcriptomics analyses provided evidence for the hormonal signaling during flexure wood formation, which is summarized in Fig. 7.

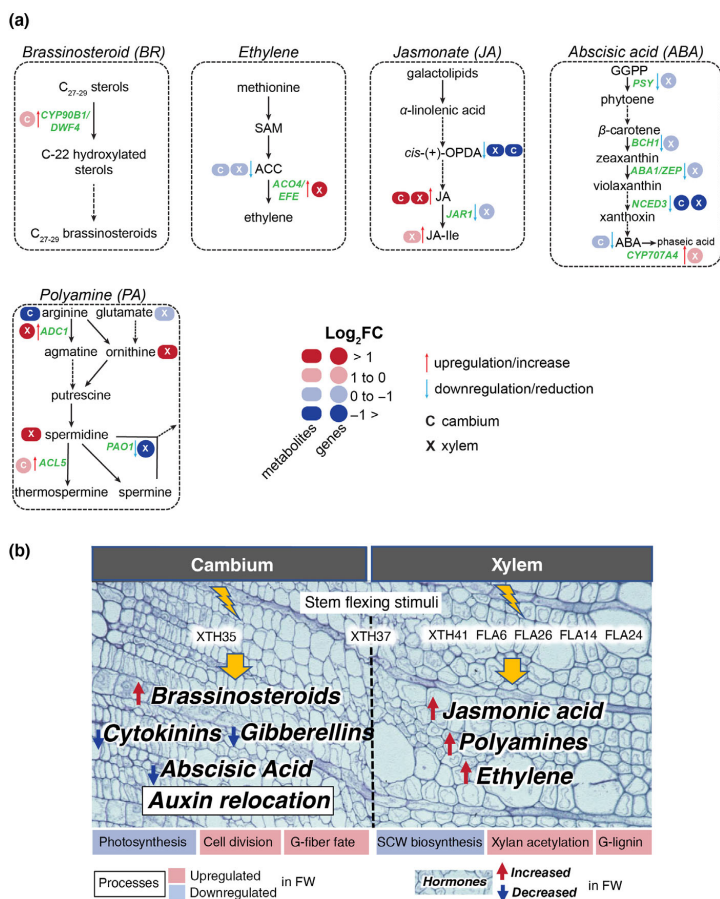


Fig. 7 Summary of main results from transcriptomics and hormonal analyses in flexure wood highlighting main changes in hormones and processes affected in the cambium and xylem tissues of hybrid aspen (*Populus tremula* × *tremuloides*). (a) Changes in brassinosteroid, ethylene, jasmonate, abscisic acid and polyamine biosynthesis. Continuous arrows depict single enzymatic steps, whereas dashed arrows indicate the involvement of multiple enzymes and intermediates. Gene names are shown in green and are according to the *Arabidopsis* nomenclature. (b) Graphical summary highlighting main processes and hormonal changes identified in the cambial region tissues (cambium) and developing xylem (xylem) tissues. The background micrograph represents the analyzed tissues. Proteins listed in the upper part of the diagram represent main candidates for the perception of mechanical stimuli identified by transcriptomics. Red boxes, ovals and arrows indicate upregulated processes, genes, metabolites and hormonal pathways/signaling; blue boxes, circles, ovals and arrows indicate downregulated processes, genes, metabolites and hormonal pathways/signaling. FW, flexure wood.

Prominent changes in PA metabolism are indicative of increased levels of PA signaling during flexure wood formation, which have not been previously observed in gravitropically or mechanically stimulated plants. Our findings, along with the report in Chinese cabbage on increased PAs in plants exposed to sound vibration (Qin *et al.*, 2003), suggest that PAs could be involved in mechanoresponses.

The substantial changes in jasmonate levels observed in flexed stems (Fig. 7) mimic those in mechanostimulated *Arabidopsis* leaves (Chehab *et al.*, 2012) and could be responsible for increased xylem production (Sehr *et al.*, 2010). These prominent metabolic changes in developing flexure wood were not reflected in transcriptomes (Table 3). The jasmonate-related genes are considered as early touch-responsive genes (Van Moerkercke *et al.*, 2019). They were shown to be upregulated only shortly after a single stem bending in poplar but not after subsequent bending (Pomiès *et al.*, 2017). Thus, the jasmonate-related transcriptome could be dampened upon repetitive

mechanostimulations during flexure wood formation, as was observed for other touch genes in poplar stems subjected to repetitive bending (Martin *et al.*, 2010).

There was a coordinate downregulation of the ABA biosynthetic pathway along with decreased ABA levels during the flexure wood response (Fig. 7). Decreased ABA was reported in different mechanically stressed plants (Ishihara *et al.*, 2017; Van Moerkercke *et al.*, 2019; Li *et al.*, 2023), suggesting that it might be a general mechanical stress response. Catabolism of GA also appears to be similar between flexure wood and touch response, with common upregulation of *GA2OX6* (Table 3; Lange & Lange, 2015). Although GAs are positive regulators of tension wood (Funada *et al.*, 2008; Gerttula *et al.*, 2015; Wang *et al.*, 2017), our findings suggest that this pathway is not used for G-fiber induction in flexure wood. By contrast, we find support for the involvement of ethylene in flexure wood, which could be responsible for G-fiber induction and increased growth, similar to its role in tension wood (Andersson-Gunnerås

et al., 2006; Love *et al.*, 2009; Felten *et al.*, 2018). Ethylene signaling is also involved in thigmomorphogenesis in other plant species that do not form G-fibers (Telewski, 2021; Brenya *et al.*, 2022). Our transcriptome data provide some evidence for involvement of BRs during flexure wood induction (Table 3; Fig. 7), in agreement with their positive role in xylem proliferation and G-fiber production (Du *et al.*, 2020; Jin *et al.*, 2020). The BRs are part of early touch responses along with jasmonates, ethylene and auxins (Brenya *et al.*, 2022). In flexure wood, there was indication of a change in auxin transport, which is a key response during gravitropically induced tension wood (Gerttula *et al.*, 2015), based on altered expression of different auxin transporters (Table 3). Thus, this analysis of flexure wood formation in aspen supports a novel involvement of PAs, as well as involvement of jasmonate, ethylene, BR, ABA, GA and auxin signaling, which are also known to be implicated in other mechanoreponses of plants.

In conclusion, this study provides evidence of overall growth stimulation in aspen subjected to multidirectional low-intensity stem flexures, and the formation of flexure wood that exhibited altered cell wall structure, composition and nanoporosity, resulting in improved saccharification properties. The transcriptional program of flexure wood partially overlapped the tension wood program but not the opposite wood program. Induction of different membrane-attached proteins that could be connected to cell wall components, such as FLAs and XTHs, supports the idea that they could act as mechanosensors of flexure wood (Fig. 7b). Changes in transcripts and hormone levels in the cambium and developing xylem of flexed trees provided evidence for increased PAs, JA ethylene, auxin and BR signaling, and decreased ABA and GA signaling in flexure wood formation. Many of these pathways are also known to be involved in thigmomorphogenesis in other plant tissues and some are shared with tension wood responses. These findings contribute to the emerging picture of transcriptional and hormonal control of flexure and tension wood formation in poplar (Gerttula *et al.*, 2015; Pomiès *et al.*, 2017; Zinkgraf *et al.*, 2018; Lopez *et al.*, 2021), improving our understanding on how gravitational and/or mechanical stimulation influence secondary growth in woody species.

Acknowledgements

We acknowledge the Bioinformatics Facility at UPSC for bioinformatic analyses, Dr Junko Takahashi-Schmidt and the Biopolymer Analytical Platform (BAP) at UPSC for the help with cell wall chemistry analyses, the UPSC Microscopy Facility for help with wood anatomy analyses and the Swedish Metabolomics Centre in Umeå for carrying out metabolite analyses. The work was funded by the Knut and Alice Wallenberg (KAW) Foundation, VR, Bio4Energy and T4F programs. M.K. was supported by a junior grant (20-25948Y) from the Czech Science Foundation (GACR).

Competing interests

None declared.

Author contributions

JU analyzed the data and wrote the manuscript. END performed growth phenotyping and RNA analyses and analyzed transcriptomics data. PS analyzed wood chemical composition and carried out light microscopy analyses. EvZ, ND and NRS carried out comparative transcriptome analyses. FRB and MD-M helped with setting up the experiment. JŠ, MK and KL analyzed hormones. ZY and GS carried out wood SilviScan analyses. MLG, SW and LJJ analyzed saccharification potential, microporosity and cellulose content. EJM designed and coordinated experimental work and finalized the manuscript with contributions from all authors. JU and END contributed equally to this work.

ORCID

Félix R. Barbut  <https://orcid.org/0000-0001-5395-6776>
Nicolas Delhomme  <https://orcid.org/0000-0002-3053-0796>
Marta Derba-Maceluch  <https://orcid.org/0000-0002-8034-3630>
Evgeniy N. Donev  <https://orcid.org/0000-0002-7279-0481>
Madhavi L. Gandla  <https://orcid.org/0000-0003-2798-6298>
Leif J. Jönsson  <https://orcid.org/0000-0003-3866-0111>
Michal Karady  <https://orcid.org/0000-0002-5603-706X>
Karin Ljung  <https://orcid.org/0000-0003-2901-189X>
Ewa J. Mellerowicz  <https://orcid.org/0000-0001-6817-1031>
Gerhard Scheepers  <https://orcid.org/0000-0002-5630-1377>
Jan Šimura  <https://orcid.org/0000-0002-1567-2278>
Pramod Sivan  <https://orcid.org/0000-0001-5297-2221>
Nathaniel R. Street  <https://orcid.org/0000-0001-6031-005X>
János Urbancsok  <https://orcid.org/0000-0003-3237-6806>
Sandra Winstrand  <https://orcid.org/0000-0001-8784-9696>
Zakiya Yassin  <https://orcid.org/0000-0001-6878-3361>
Elena van Zalen  <https://orcid.org/0000-0003-1621-3222>

Data availability

The raw RNA-Seq data that support the findings of this study are openly available in the European Nucleotide Archive (ENA) at EMBL-EBI (<https://www.ebi.ac.uk/ena/browser/home>), under accession no. PRJEB61635.

References

- Alonso-Serra J, Shi X, Peaucelle A, Rastas P, Bourdon M, Immanuel J, Takahashi J, Koivula H, Eswaran G, Muranen S *et al.* 2020. *ELIMÁKI* locus is required for vertical proprioceptive response in birch trees. *Current Biology* 30: 589–599.
- Andersson-Gunnerås S, Mellerowicz EJ, Love J, Segerman B, Ohmija Y, Coutinho PM, Nilsson P, Henrissat B, Moritz T, Sundberg B. 2006. Biosynthesis of cellulose-enriched tension wood in *Populus*: global analysis of transcripts and metabolites identifies biochemical and developmental regulators in secondary wall biosynthesis. *The Plant Journal* 45: 144–165.
- Appel HM, Cocroft RB. 2014. Plants respond to leaf vibrations caused by insect herbivore chewing. *Oecologia* 175: 1257–1266.
- Arnaud D, Déjardin A, Leplé J-C, Lesage-Descauses M-C, Pilate G. 2007. Genome-wide analysis of LIM gene family in *Populus trichocarpa*, *Arabidopsis thaliana*, and *Oryza sativa*. *DNA Research* 14: 103–116.

- Bacete L, Hamann T. 2020. The role of mechanoperception in plant cell wall integrity maintenance. *Plants* 9: 574.
- Baluška F, Šamaj J, Wojtaszek P, Volkmann D, Menzel D. 2003. Cytoskeleton-plasma membrane-cell wall continuum in plants. Emerging links revisited. *Plant Physiology* 133: 483–491.
- Basu D, Haswell ES. 2017. Plant mechanosensitive ion channels: an ocean of possibilities. *Current Opinion in Plant Biology* 40: 43–48.
- Benikhlef L, L'Haridon F, Abou-Mansour E, Serrano M, Binda M, Costa A, Lehmann S, Métraux J-P. 2013. Perception of soft mechanical stress in *Arabidopsis* leaves activates disease resistance. *BMC Plant Biology* 13: 133.
- Berthet S, Demont-Caulet N, Pollet B, Bidzinski P, Cézard L, Le Bris P, Borrega N, Hervé J, Blondet E, Balzergue S *et al.* 2011. Disruption of LACCASE4 and 17 results in tissue-specific alterations to lignification of *Arabidopsis thaliana* stems. *Plant Cell* 23: 1124–1137.
- Braam J. 2005. In touch: plant responses to mechanical stimuli. *New Phytologist* 165: 373–389.
- Braam J, Davis RW. 1990. Rain-, wind- and touch-induced expression of calmodulin and calmodulin-related genes in *Arabidopsis*. *Cell* 60: 357–364.
- Brenya E, Chen Z-H, Tissue D, Papanicolaou A, Cazzonelli CI. 2020. Prior exposure of *Arabidopsis* seedlings to mechanical stress heightens jasmonic acid-mediated defense against necrotrophic pathogens. *BMC Plant Biology* 20: 548.
- Brenya E, Pervin M, Chen ZH, Tissue DT, Johnson S, Braam J, Cazzonelli CI. 2022. Mechanical stress acclimation in plants: linking hormones and somatic memory to thigmomorphogenesis. *Plant, Cell & Environment* 45: 989–1010.
- Brunauer S, Emmett PH, Teller E. 1938. Adsorption of gases in multimolecular layers. *Journal of the American Chemical Society* 60: 309–319.
- Bryan AC, Obaidi A, Wierzbza M, Tax FE. 2012. XYLEM INTERMIXED WITH PHLOEM1, a leucine-rich repeat receptor-like kinase required for stem growth and vascular development in *Arabidopsis thaliana*. *Planta* 235: 111–122.
- Cassan-Wang H, Goué N, Saidi M, Legay S, Sivadon P, Goffner D, Grima-Pettenati J. 2013. Identification of novel transcription factors regulating secondary cell wall formation in *Arabidopsis*. *Frontiers in Plant Science* 4: 189.
- Chai G, Kong Y, Zhu M, Yu L, Qi G, Tang X, Wang Z, Cao Y, Yu C, Zhou G. 2015. *Arabidopsis* C3H14 and C3H15 have overlapping roles in the regulation of secondary wall thickening and anther development. *Journal of Experimental Botany* 66: 2595–2609.
- Chang S, Puryear J, Cairney J. 1993. A simple and efficient method for isolating RNA from pine trees. *Plant Molecular Biology Reporter* 11: 113–116.
- Chehab EW, Eich E, Braam J. 2009. Thigmomorphogenesis: a complex plant response to mechano-stimulation. *Journal of Experimental Botany* 60: 43–56.
- Chehab EW, Yao C, Henderson Z, Kim S, Braam J. 2012. *Arabidopsis* touch-induced morphogenesis is jasmonate mediated and protects against pests. *Current Biology* 22: 701–706.
- Chong S-L, Koutaniemi S, Virkki L, Pynnönen H, Tuomainen P, Tenkanen M. 2013. Quantitation of 4-O-methylglucuronic acid from plant cell walls. *Carbohydrate Polymers* 91: 626–630.
- Coutand C. 2010. Mechanosensing and thigmomorphogenesis, a physiological and biomechanical point of view. *Plant Science* 179: 168–182.
- Coutand C, Julien JL, Moulia B, Mauget JC, Guitard D. 2000. Biomechanical study of the effect of a controlled bending on tomato stem elongation: global mechanical analysis. *J Exp Bot.* 51:1813–24.
- Coutand C, Dupraz C, Jaouen G, Ploquin S, Adam B. 2008. Mechanical stimuli regulate the allocation of biomass in trees: demonstration with young *Prunus avium* trees. *Annals of Botany* 101: 1421–1432.
- Coutand C, Julien JL, Moulia B, Mauget JC, Guitard D. 2000. Biomechanical study of the effect of a controlled bending on tomato stem elongation: global mechanical analysis. *Journal of Experimental Botany* 51: 1813–1824.
- Coutand C, Martin L, Leblanc-Fournier N, Decourteix ML, Julien J-L, Moulia B. 2009. Strain mechanosensing quantitatively controls diameter growth and *PtaZFP2* gene expression in poplar. *Plant Physiology* 151: 223–232.
- Desprez T, Juraniec M, Crowell EF, Jouy H, Pochylova Z, Parcy F, Höfte H, Gonneau M, Vernhettes S. 2007. Organization of cellulose synthase complexes involved in primary cell wall synthesis in *Arabidopsis thaliana*. *Proceedings of the National Academy of Sciences, USA* 104: 15572–15577.
- Du J, Gerttula S, Li Z, Zhao S-T, Liu Y-L, Liu Y, Lu M-Z, Groover AT. 2020. Brassinosteroid regulation of wood formation in poplar. *New Phytologist* 225: 1516–1530.
- Evans R, Ilic J. 2001. Rapid prediction of wood stiffness from microfibril angle and density. *Forest Products Journal* 51: 53–57.
- Evans R, Stuart SA, Van Der Touw J. 1996. Microfibril angle scanning of increment cores by X-ray densitometry. *Appita Journal* 49: 411–414.
- Fagerstedt KV, Mellerowicz E, Gorshkova T, Ruel K, Joseleau J-P. 2014. Cell wall polymers in reaction wood. In: Gardiner B, Barnett J, Saranpää P, Gril J, eds. *The biology of reaction wood*. Berlin, Germany: Springer, 37–106.
- Felten J, Vahala J, Love J, Gorzsás A, Rüggeberg M, Delhomme N, Lesniewska J, Kangasjärvi J, Hvidsten TR, Mellerowicz EJ *et al.* 2018. Ethylene signaling induces gelatinous layers with typical features of tension wood in hybrid aspen. *New Phytologist* 218: 999–1014.
- Fernández-Pérez F, Pomar F, Pedreño MA, Novo-Uzal E. 2015. Suppression of *Arabidopsis* peroxidase 72 alters cell wall and phenylpropanoid metabolism. *Plant Science* 239: 192–199.
- Frankie R, Humphreys JM, Hemm MR, Denault JW, Ruegger MO, Cusumano JC, Chapple C. 2002. The *Arabidopsis* REF8 gene encodes the 3-hydroxylase of phenylpropanoid metabolism. *The Plant Journal* 30: 33–45.
- Fruleux A, Verger S, Boudaoud A. 2019. Feeling stressed or strained? A biophysical model for cell wall mechanosensing in plants. *Frontiers in Plant Science* 10: 757.
- Fujita S, Ohnishi T, Watanabe Y, Yokota T, Takatsuto S, Fujioka S, Yoshida S, Sakata K, Mizutani M. 2006. *Arabidopsis* CYP90B1 catalyses the early C-22 hydroxylation of C27, C28 and C29 sterols. *The Plant Journal* 45: 765–774.
- Funada R, Miura T, Shimizu Y, Kinase T, Nakaba S, Kubo T, Sano Y. 2008. Gibberellin-induced formation of tension wood in angiosperm trees. *Planta* 227: 1409–1414.
- Gandla ML, Derba-Maceluch M, Liu X, Gerber L, Master ER, Mellerowicz EJ, Jönsson LJ. 2015. Expression of a fungal glucuronoyl esterase in *Populus*: effects on wood properties and saccharification efficiency. *Phytochemistry* 112: 210–220.
- Gandla ML, Mähler N, Escamez S, Skotare T, Obudulu O, Möller L, Abreu IN, Bygdell J, Hertzberg M, Hvidsten TR *et al.* 2021. Overexpression of vesicle-associated membrane protein PttVAP27-17 as a tool to improve biomass production and the overall saccharification yields in *Populus* trees. *Biotechnology for Biofuels* 14: 43.
- Gartner BL. 1994. Root biomechanics and whole-plant allocation patterns: responses of tomato plants to stem flexure. *Journal of Experimental Botany* 45: 1647–1654.
- Gerber L, Eliasson M, Trygg J, Moritz T, Sundberg B. 2012. Multivariate curve resolution provides a high-throughput data processing pipeline for pyrolysis-gas chromatography/mass spectrometry. *Journal of Analytical and Applied Pyrolysis* 95: 95–100.
- Gerttula S, Zinkgraf M, Muday GK, Lewis DR, Ibatullin FM, Brumer H, Hart F, Mansfield SD, Filkov V, Groover A. 2015. Transcriptional and hormonal regulation of gravitropism of woody stems in *Populus*. *Plant Cell* 27: 2800–2813.
- Ghosh R, Barbacci A, Leblanc-Fournier N. 2021. Mechanostimulation: a promising alternative for sustainable agriculture practices. *Journal of Experimental Botany* 72: 2877–2888.
- Giummarella N, Lawoko M. 2016. Structural basis for the formation and regulation of lignin-xylan bonds in birch. *ACS Sustainable Chemistry & Engineering* 4: 5319–5326.
- Grantham NJ, Wurman-Rodrich J, Terrett OM, Lyczakowski JJ, Stott K, Iuga D, Simmons TJ, Durand-Tardif M, Brown SP, Dupree R *et al.* 2017. An even pattern of xylan substitution is critical for interaction with cellulose in plant cell walls. *Nature Plants* 3: 859–865.
- Groover A. 2016. Gravitropisms and reaction woods of forest trees – evolution, functions and mechanisms. *New Phytologist* 211: 790–802.
- Gu Z, Eils R, Schlesner M. 2016. Complex heatmaps reveal patterns and correlations in multidimensional genomic data. *Bioinformatics* 32: 2847–2849.
- Heinemann KJ, Yang S-Y, Straube H, Medina-Escobar N, Varbanova-Herde M, Herde M, Rhee S, Witte C-P. 2021. Initiation of cytosolic plant purine

- nucleotide catabolism involves a monospecific xanthosine monophosphate phosphatase. *Nature Communications* 12: 6846.
- Hoffmann N, Benske A, Betz H, Schuetz M, Samuels AL. 2020. Laccases and peroxidases co-localize in lignified secondary cell walls throughout stem development. *Plant Physiology* 184: 806–822.
- Hu H, Zhang R, Feng S, Wang Y, Wang Y, Fan C, Li Y, Liu Z, Schneider R, Xia T *et al.* 2018. Three AtCesA6-like members enhance biomass production by distinctively promoting cell growth in *Arabidopsis*. *Plant Biotechnology Journal* 16: 976–988.
- Ishihara KL, Lee EKW, Borthakur D. 2017. Thigmomorphogenesis: changes in morphology, biochemistry, and levels of transcription in response to mechanical stress in *Acacia koa*. *Canadian Journal of Forest Research* 47: 583–593.
- Iuchi S, Kobayashi M, Tajiri T, Naramoto M, Seki M, Kato T, Tabata S, Kakubari Y, Yamaguchi-Shinozaki K, Shinozaki K. 2001. Regulation of drought tolerance by gene manipulation of 9-cis-epoxycarotenoid dioxygenase, a key enzyme in abscisic acid biosynthesis in *Arabidopsis*. *The Plant Journal* 27: 325–333.
- Jaffe MJ. 1973. Thigmomorphogenesis: the response of plant growth and development to mechanical stimulation. *Planta* 114: 143–157.
- Jaffe MJ, Biro R, Bridle K. 1980. Thigmomorphogenesis: calibration of the parameters of the sensory function in beans. *Physiologia Plantarum* 49: 410–416.
- Jiang H, Tang B, Xie Z, Nolan T, Ye H, Song G-Y, Walley J, Yin Y. 2019. GSK3-like kinase BIN2 phosphorylates RD26 to potentiate drought signaling in *Arabidopsis*. *The Plant Journal* 100: 923–937.
- Jin Y, Yu C, Jiang C, Guo X, Li B, Wang C, Kong F, Zhang H, Wang H. 2020. *PtiCYP85A3*, a BR C-6 oxidase gene, plays a critical role in brassinosteroid-mediated tension wood formation in poplar. *Frontiers in Plant Science* 11: 468.
- Jourez B, Avella-Shaw T. 2003. Effet de la durée d'application d'un stimulus gravitationnel sur la formation de bois de tension et de bois opposé dans de jeunes pousses de peuplier (*Populus euramericana* cv 'Ghoy'). *Annals of Forest Science* 60: 31–41.
- Jung J, Kim S-K, Kim JY, Jeong M-J, Ryu C-M. 2018. Beyond chemical triggers: evidence for sound-evoked physiological reactions in plants. *Frontiers in Plant Science* 9: 25.
- Kaida R, Sasaki Y, Ozaki K, Ki B, Momoi T, Ohbayashi H, Tajiri T, Sakata Y, Hayashi T. 2020. Intake of radionuclides in the trees of Fukushima forests 5. Earthquake could have caused an increase in xyloglucan in trees. *Forests* 11: 966.
- Kakehi J-I, Kuwashiro Y, Niitsu M, Takahashi T. 2008. Thermopermine is required for stem elongation in *Arabidopsis thaliana*. *Plant and Cell Physiology* 49: 1342–1349.
- Kaneda M, Schuetz M, Lin BSP, Chanis C, Hamberger B, Western TL, Ehrling J, Samuels AL. 2011. ABC transporters coordinately expressed during lignification of *Arabidopsis* stems include a set of ABCBs associated with auxin transport. *Journal of Experimental Botany* 62: 2063–2077.
- Kern KA, Ewers FW, Telewski FW, Koehler L. 2005. Mechanical perturbation affects conductivity, mechanical properties and aboveground biomass of hybrid poplars. *Tree Physiology* 25: 1243–1251.
- Kim D, Cho Y-h, Ryu H, Kim Y, Kim T-H, Hwang I. 2013. BLH1 and KNAT3 modulate ABA responses during germination and early seedling development in *Arabidopsis*. *The Plant Journal* 75: 755–766.
- Kumar M, Thammannagowda S, Bulone V, Chiang V, Han K-H, Joshi CP, Mansfield SD, Mellerowicz E, Sundberg B, Teeri T *et al.* 2009. An update on the nomenclature for the cellulose synthase genes in *Populus*. *Trends in Plant Science* 14: 248–254.
- Kumar V, Hainaut M, Delhomme N, Mannapperuma C, Immerzeel P, Street NR, Henrisat B, Mellerowicz EJ. 2019. Poplar carbohydrate-active enzymes: whole-genome annotation and functional analyses based on RNA expression data. *The Plant Journal* 99: 589–609.
- Kushiro T, Okamoto M, Nakabayashi K, Yamagishi K, Kitamura S, Asami T, Hirai N, Koshiba T, Kamiya Y, Nambara E. 2004. The *Arabidopsis* cytochrome P450 CYP707A encodes ABA 8'-hydroxylases: key enzymes in ABA catabolism. *EMBO Journal* 23: 1647–1656.
- Kushwah S, Banasiak A, Nishikubo N, Derba-Maceluch M, Majda M, Endo S, Kumar V, Gomez L, Gorzras A, McQueen-Mason S *et al.* 2020. *Arabidopsis XTH4* and *XTH9* contribute to wood cell expansion and secondary wall formation. *Plant Physiology* 182: 1946–1965.
- Lafarguette F, Leplé J-C, Déjardin A, Laurans F, Costa G, Lesage-Descauses M-C, Pilate G. 2004. Poplar genes encoding fasciclin-like arabinogalactan proteins are highly expressed in tension wood. *New Phytologist* 164: 107–121.
- Lange MJP, Lange T. 2015. Touch-induced changes in *Arabidopsis* morphology dependent on gibberellin breakdown. *Nature Plants* 1: 14025.
- Leblanc-Fournier N, Coutand C, Crouzet J, Brunel N, Lenne C, Mouliat B, Julien J-L. 2008. *Jr-ZFP2*, encoding a Cys2/His2-type transcription factor, is involved in the early stages of the mechano-perception pathway and specifically expressed in mechanically stimulated tissues in woody plants. *Plant, Cell & Environment* 31: 715–726.
- Lee C, Teng Q, Huang W, Zhong R, Ye Z-H. 2009. The poplar GT8E and GT8F glycosyltransferases are functional orthologs of *Arabidopsis* PARVUS involved in glucuronoxylan biosynthesis. *Plant and Cell Physiology* 50: 1982–1987.
- Lee C, Zhong R, Richardson EA, Himmelsbach DS, McPhail BT, Ye Z-H. 2007. The *PARVUS* Gene is expressed in cells undergoing secondary wall thickening and is essential for glucuronoxylan biosynthesis. *Plant and Cell Physiology* 48: 1659–1672.
- Lee D, Polisenky DH, Braam J. 2005. Genome-wide identification of touch- and darkness-regulated *Arabidopsis* genes: a focus on calmodulin-like and XTH genes. *New Phytologist* 165: 429–444.
- Li Q, Zargar O, Park S, Pharr M, Muliiana A, Finlayson SA. 2023. Mechanical stimulation reprograms the sorghum internode transcriptome and broadly alters hormone homeostasis. *Plant Science* 327: 111555.
- Li W, Ma M, Feng Y, Li H, Wang Y, Ma Y, Li M, An F, Guo H. 2015. EIN2-directed translational regulation of ethylene signaling in *Arabidopsis*. *Cell* 163: 670–683.
- Lin C-Y, Li Q, Tunlaya-Anukit S, Shi R, Sun Y-H, Wang JP, Liu J, Loziuk P, Edmunds CW, Miller ZD *et al.* 2016. A cell wall-bound anionic peroxidase, PtrPO21, is involved in lignin polymerization in *Populus trichocarpa*. *Tree Genetics & Genomes* 12: 22.
- Liu B, Seong K, Pang S, Song J, Gao H, Wang C, Zhai J, Zhang Y, Gao S, Li X *et al.* 2021. Functional specificity, diversity, and redundancy of *Arabidopsis* JAZ family repressors in jasmonate and COI1-regulated growth, development, and defense. *New Phytologist* 231: 1525–1545.
- Lopez D, Franchel J, Venisse J-S, Drevet JR, Label P, Coutand C, Roeckel-Drevet P. 2021. Early transcriptional response to gravistimulation in poplar without phototropic confounding factors. *AOB Plants* 13: pla071.
- Love J, Björklund S, Vahala J, Hertzberg M, Kangasjärvi J, Sundberg B. 2009. Ethylene is an endogenous stimulator of cell division in the cambial meristem of *Populus*. *Proceedings of the National Academy of Sciences, USA* 106: 5984–5989.
- Lu S, Li Q, Wei H, Chang M-J, Tunlaya-Anukit S, Kim H, Liu J, Song J, Sun Y-H, Yuan L *et al.* 2013. Ptr-miR397a is a negative regulator of laccase genes affecting lignin content in *Populus trichocarpa*. *Proceedings of the National Academy of Sciences, USA* 110: 10848–10853.
- Ma Y, MacMillan CP, de Vries L, Mansfield SD, Hao P, Ratcliffe J, Bacic A, Johnson KL. 2022. FLA11 and FLA12 glycoproteins fine-tune stem secondary wall properties in response to mechanical stresses. *New Phytologist* 233: 1750–1767.
- Manzano C, Ramirez-Parra E, Casimiro I, Otero S, Desvoyes B, De Rybel B, Beeckman T, Casero P, Gutierrez C, del Pozo JC. 2012. Auxin and epigenetic regulation of SKP2B, an F-box that represses lateral root formation. *Plant Physiology* 160: 749–762.
- Martin L, Decourteix M, Badel E, Huguet S, Mouliat B, Julien J-L, Leblanc-Fournier N. 2014. The zinc finger protein PtaZFP2 negatively controls stem growth and gene expression responsiveness to external mechanical loads in poplar. *New Phytologist* 203: 168–181.
- Martin L, Leblanc-Fournier N, Azri W, Lenne C, Henry C, Coutand C, Julien J-L. 2009. Characterization and expression analysis under bending and other abiotic factors of PtaZFP2, a poplar gene encoding a Cys2/His2 zinc finger protein. *Tree Physiology* 29: 125–136.
- Martin L, Leblanc-Fournier N, Julien J-L, Mouliat B, Coutand C. 2010. Acclimation kinetics of physiological and molecular responses of plants to multiple mechanical loadings. *Journal of Experimental Botany* 61: 2403–2412.

- Monshausen GB, Haswell ES. 2013. A force of nature: molecular mechanisms of mechanoperception in plants. *Journal of Experimental Botany* 64: 4663–4680.
- Moulija B, Douady S, Hamant O. 2021. Fluctuations shape plants through proprioception. *Science* 372: eabc6868.
- Muñiz L, Minguet EG, Singh SK, Pesquet E, Vera-Sirera F, Moreau-Courtois CL, Carbonell J, Blázquez MA, Tuominen H. 2008. ACAULIS5 controls *Arabidopsis* xylem specification through the prevention of premature cell death. *Development* 135: 2573–2582.
- Nakagawa Y, Katagiri T, Shinozaki K, Qi Z, Tatsumi H, Furuichi T, Kishigami A, Sokabe M, Kojima I, Sato S *et al.* 2007. *Arabidopsis* plasma membrane protein crucial for Ca²⁺ influx and touch sensing in roots. *Proceedings of the National Academy of Sciences, USA* 104: 3639–3644.
- Ndamukong I, Chetram A, Saleh A, Avramova Z. 2009. Wall-modifying genes regulated by the *Arabidopsis* homolog of trithorax, ATX1: repression of the *XTH33* gene as a test case. *The Plant Journal* 58: 541–553.
- Niez B, Dlouha J, Gril J, Ruelle J, Toussaint E, Moulija B, Badel E. 2020. Mechanical properties of “flexure wood”: compressive stresses in living trees improve the mechanical resilience of wood and its resistance to damage. *Annals of Forest Science* 77: 17.
- Paul-Victor C, Rowe N. 2011. Effect of mechanical perturbation on the biomechanics, primary growth and secondary tissue development of inflorescence stems of *Arabidopsis thaliana*. *Annals of Botany* 107: 209–218.
- Pomiès L, Decourteix M, Franchel J, Moulija B, Leblanc-Fournier N. 2017. Poplar stem transcriptome is massively remodelled in response to single or repeated mechanical stimuli. *BMC Genomics* 18: 300.
- Pramod S, Gandia ML, Derba-Maceluch M, Jönsson LJ, Mellerowicz EJ, Winstrand S. 2021. Saccharification potential of transgenic greenhouse- and field-grown aspen engineered for reduced xylan acetylation. *Frontiers in Plant Science* 12: 704960.
- Pruyn ML, Ewers BJ III, Telewski FW. 2000. Thigmomorphogenesis: changes in the morphology and mechanical properties of two *Populus* hybrids in response to mechanical perturbation. *Tree Physiology* 20: 535–540.
- Qin Y-C, Lee W-C, Choi Y-C, Kim T-W. 2003. Biochemical and physiological changes in plants as a result of different sonic exposures. *Ultrasonics* 41: 407–411.
- R Core Team. 2022. *R: A language and environment for statistical computing*. Vienna, Austria: R Foundation for Statistical Computing. [WWW document] URL <https://www.R-project.org> [accessed 10 October 2023].
- Rajangas AS, Kumar M, Aspeborg H, Guerriero G, Arvestad L, Pansri P, Brown CJ-L, Hober S, Blomqvist K, Divne C *et al.* 2008. MAP20, a microtubule-associated protein in the secondary cell walls of hybrid aspen, is a target of the cellulose synthesis inhibitor 2,6-dichlorobenzonitrile. *Plant Physiology* 148: 1283–1294.
- Ren L-L, Liu Y-J, Liu H-J, Qian T-T, Qi L-W, Wang X-R, Zeng Q-Y. 2014. Subcellular relocalization and positive selection play key roles in the retention of duplicate genes of *Populus* class III peroxidase family. *Plant Cell* 26: 2404–2419.
- Roignant J, Badel É, Leblanc-Fournier N, Brunel-Michac N, Ruelle J, Moulija B, Decourteix M. 2018. Feeling stretched or compressed? The multiple mechanosensory responses of wood formation to bending. *Annals of Botany* 121: 1151–1161.
- Saidi I, Ammar S, Demont-Caulet Saïda N, Thévenin J, Lapierre C, Bouzid S, Jouanin L. 2010. Thigmomorphogenesis in *Solanum lycopersicum*. *Plant Signaling & Behavior* 5: 122–125.
- Schneider CA, Rasband WS, Eliceiri KW. 2012. NIH Image to IMAGEJ: 25 years of image analysis. *Nature Methods* 9: 671–675.
- Schröder F, Liso J, Lange P, Müssig C. 2009. The extracellular EXO protein mediates cell expansion in *Arabidopsis* leaves. *BMC Plant Biology* 9: 20.
- Scott TA, Melvin EH. 1953. Determination of dextran with anthrone. *Analytical Chemistry* 25: 1656–1661.
- Sehr EM, Agusti J, Lehner R, Farmer EE, Schwarz M, Greb T. 2010. Analysis of secondary growth in the *Arabidopsis* shoot reveals a positive role of jasmonate signalling in cambium formation. *The Plant Journal* 63: 811–822.
- Shannon P, Markiel A, Ozier O, Baliga NS, Wang JT, Ramage D, Amin N, Schwikowski B, Ideker T. 2003. CYTOSCAPE: a software environment for integrated models of biomolecular interaction networks. *Genome Research* 13: 2498–2504.
- Šimura J, Antoniadis I, Široká J, Tarkovská D, Strnad M, Ljung K, Novák O. 2018. Plant hormones: multiple phytohormone profiling by targeted metabolomics. *Plant Physiology* 177: 476–489.
- Song D, Shen J, Li L. 2010. Characterization of cellulose synthase complexes in *Populus* xylem differentiation. *New Phytologist* 187: 777–790.
- de Souza A, Hull PA, Gille S, Pauly M. 2014. Identification and functional characterization of the distinct plant pectin esterases PAE8 and PAE9 and their deletion mutants. *Planta* 240: 1123–1138.
- Staswick PE, Tiryaki I. 2004. The oxylipin signal jasmonic acid is activated by an enzyme that conjugates it to isoleucine in *Arabidopsis*. *Plant Cell* 16: 2117–2127.
- Sundell D, Mannapperuma C, Netotea S, Delhomme N, Lin YC, Sjödin A, Van de Peer Y, Jansson S, Hvidsten TR, Street NR. 2015. The plant genome integrative explorer resource: PlantGenIE.org. *New Phytologist* 208: 1149–1156.
- Sundell D, Street NR, Kumar M, Mellerowicz EJ, Kucukoglu M, Johansson C, Kumar V, Mannapperuma C, Delhomme N, Nilsson O *et al.* 2017. AspWood: high-spatial-resolution transcriptome profiles reveal uncharacterized modularity of wood formation in *Populus tremula*. *Plant Cell* 29: 1585–1604.
- Suzuki S, Li L, Sun Y-H, Chiang VL. 2006. The cellulose synthase gene superfamily and biochemical functions of xylem-specific cellulose synthase-like genes in *Populus trichocarpa*. *Plant Physiology* 142: 1233–1245.
- Takagi H, Ishiga Y, Watanabe S, Konishi T, Egusa M, Akiyoshi N, Matsuura T, Mori IC, Hirayama T, Kaminaka H *et al.* 2016. Allantoin, a stress-related purine metabolite, can activate jasmonate signaling in a MYC2-regulated and abscisic acid-dependent manner. *Journal of Experimental Botany* 67: 2519–2532.
- Taylor-Teeples M, Lin L, de Lucas M, Turco G, Toal TW, Gaudinier A, Young NF, Trabucco GM, Veling MT, Lamothe R *et al.* 2015. An *Arabidopsis* gene regulatory network for secondary cell wall synthesis. *Nature* 517: 571–575.
- Tejos R, Rodriguez-Furlán C, Adamowski M, Sauer M, Norambuena L, Friml J. 2018. PATELLINS are regulators of auxin-mediated PIN1 relocation and plant development in *Arabidopsis thaliana*. *Journal of Cell Science* 131: jcs204198.
- Telewski FW. 1989. Structure and function of flexure wood in *Abies fraseri*. *Tree Physiology* 5: 113–121.
- Telewski FW. 2016. Flexure wood: mechanical stress induced secondary xylem formation. In: Kim YS, Funada R, Singh AP, eds. *Secondary xylem biology*. Boston, MA, USA: Academic Press, 73–91.
- Telewski FW. 2021. Mechanosensing and plant growth regulators elicited during the thigmomorphogenetic response. *Frontiers in Forests and Global Change* 3: 574096.
- Telewski FW, Jaffe MJ. 1986a. Thigmomorphogenesis: field and laboratory studies of *Abies fraseri* in response to wind or mechanical perturbation. *Physiologia Plantarum* 66: 211–218.
- Telewski FW, Jaffe MJ. 1986b. Thigmomorphogenesis: anatomical, morphological and mechanical analysis of genetically different sibs of *Pinus taeda* in response to mechanical perturbation. *Physiologia Plantarum* 66: 219–226.
- Telewski FW, Pruyn ML. 1998. Thigmomorphogenesis: a dose response to flexing in *Ulmus americana* seedlings. *Tree Physiology* 18: 65–68.
- Torres Acosta JA, de Almeida Engler J, Raes J, Magyar Z, De Groot R, Inzé D, De Veylder L. 2004. Molecular characterization of *Arabidopsis* PHO80-like proteins, a novel class of CDKA1-interacting cyclins. *Cellular and Molecular Life Sciences* 61: 1485–1497.
- Toyota M, Spencer D, Sawai-Toyota S, Jiaqi W, Zhang T, Koo AJ, Howe GA, Gilroy S. 2018. Glutamate triggers long-distance, calcium-based plant defense signaling. *Science* 361: 1112–1115.
- Updegraff DM. 1969. Semimicro determination of cellulose in biological materials. *Analytical Biochemistry* 32: 420–424.
- Urbanowicz BR, Peña MJ, Ratnaparkhe S, Avci U, Backe J, Steet HF, Foston M, Li H, O'Neill MA, Ragauskas AJ *et al.* 2012. 4-O-methylation of glucuronic acid in *Arabidopsis* glucuronoxylan is catalyzed by a domain of unknown function family 579 protein. *Proceedings of the National Academy of Sciences, USA* 109: 14253–14258.
- Van Moerkercke A, Duncan O, Zander M, Šimura J, Broda M, Bossche RV, Lewsey MG, Lama S, Singh KB, Ljung K *et al.* 2019. A MYC2/MYC3/

- MYC4-dependent transcription factor network regulates water spray-responsive gene expression and jasmonate levels. *Proceedings of the National Academy of Sciences, USA* 116: 23345–23356.
- Wang H, Jin Y, Wang C, Li B, Jiang C, Sun Z, Zhang Z, Kong F, Zhang H. 2017. Fasciclin-like arabinogalactan proteins, pFLAs, play important roles in GA-mediated tension wood formation in *Populus*. *Scientific Reports* 7: 6182.
- Wang K, Yang Z, Qing D, Ren F, Liu S, Zheng Q, Liu J, Zhang W, Dai C, Wu M *et al.* 2018a. Quantitative and functional posttranslational modification proteomics reveals that TREP1 plays a role in plant touch-delayed bolting. *Proceedings of the National Academy of Sciences, USA* 115: E10265–E10274.
- Wang Q, Qin G, Cao M, Chen R, He Y, Yang L, Zeng Z, Yu Y, Gu Y, Xing W *et al.* 2020a. A phosphorylation-based switch controls TAA1-mediated auxin biosynthesis in plants. *Nature Communications* 11: 679.
- Wang S, Yamaguchi M, Grienenberger E, Martone PT, Samuels AL, Mansfield SD. 2020b. The Class II KNOX genes KNA13 and KNA17 work cooperatively to influence deposition of secondary cell walls that provide mechanical support to *Arabidopsis* stems. *The Plant Journal* 101: 293–309.
- Wang Z, Winestrand S, Gillgren T, Jönsson LJ. 2018b. Chemical and structural factors influencing enzymatic saccharification of wood from aspen, birch and spruce. *Biomass and Bioenergy* 109: 125–134.
- Witasari LD, Huang F-C, Hoffmann T, Rozhon W, Fry SC, Schwab W. 2019. Higher expression of the strawberry xyloglucan endotransglucosylase/hydrolase genes FvXTH9 and FvXTH6 accelerates fruit ripening. *The Plant Journal* 100: 1237–1253.
- Wu T, Zhang P, Zhang L, Wang GG, Yu M. 2016. Morphological response of eight *Quercus* species to simulated wind load. *PLoS ONE* 11: e0163613.
- Xu P, Chen H, Hu J, Pang X, Jin J, Cai W. 2022. Pectin methyltransferase gene *AtPMEPCRA* contributes to physiological adaptation to simulated and spaceflight microgravity in *Arabidopsis*. *iScience* 25: 104331.
- Xu W, Purugganan MM, Polisenky DH, Antosiewicz DM, Fry SC, Braam J. 1995. *Arabidopsis* TCH4, regulated by hormones and the environment, encodes a xyloglucan endotransglucosylase. *Plant Cell* 7: 1555–1567.
- Xu Y, Berkowitz O, Narsari R, De Clercq I, Hooi M, Bulone V, Van Breusegem F, Whelan J, Wang Y. 2019. Mitochondrial function modulates touch signalling in *Arabidopsis thaliana*. *The Plant Journal* 97: 623–645.
- Yan J, Huang Y, He H, Han T, Di P, Sechet J, Fang L, Liang Y, Scheller HV, Mortimer JC *et al.* 2019. Xyloglucan endotransglucosylase-hydrolase30 negatively affects salt tolerance in *Arabidopsis*. *Journal of Experimental Botany* 70: 5495–5506.
- Yang Z, Tian L, Latoszek-Green M, Brown D, Wu K. 2005. *Arabidopsis* ERF4 is a transcriptional repressor capable of modulating ethylene and abscisic acid responses. *Plant Molecular Biology* 58: 585–596.
- Yokoyama A, Yamashino T, Amano Y-I, Tajima Y, Imamura A, Sakakibara H, Mizuno T. 2007. Type-B ARR transcription factors, ARR10 and ARR12, are implicated in cytokinin-mediated regulation of protoxylem differentiation in roots of *Arabidopsis thaliana*. *Plant and Cell Physiology* 48: 84–96.
- Yuan Y, Teng Q, Zhong R, Ye Z-H. 2014. Identification and biochemical characterization of four wood-associated glucuronoxylan methyltransferases in *Populus*. *PLoS ONE* 9: e87370.
- Zang L, Zheng T, Chu Y, Ding C, Zhang W, Huang Q, Su X. 2015. Genome-wide analysis of the fasciclin-like arabinogalactan protein gene family reveals differential expression patterns, localization, and salt stress response in *Populus*. *Frontiers in Plant Science* 6: 1140.
- Zhang C, He M, Jiang Z, Liu L, Pu J, Zhang W, Wang S, Xu F. 2022. The xyloglucan endotransglucosylase/hydrolase gene *XTH22/TCH4* regulates plant growth by disrupting the cell wall homeostasis in *Arabidopsis* under boron deficiency. *International Journal of Molecular Sciences* 23: 1250.
- Zhang X, Dominguez PG, Kumar M, Bygdell J, Miroshnichenko S, Sundberg B, Wingsle G, Niittylä T. 2018. Cellulose synthase stoichiometry in aspen differs from *Arabidopsis* and Norway spruce. *Plant Physiology* 177: 1096–1107.
- Zhao Y, Wu G, Shi H, Tang D. 2019. RECEPTOR-LIKE KINASE 902 associates with and phosphorylates BRASSINOSTEROID-SIGNALING KINASE1 to regulate plant immunity. *Molecular Plant* 12: 59–70.
- Zhong R, Cui D, Ye Z-H. 2017. Regiospecific acetylation of xylan is mediated by a group of DUF231-containing O-acetyltransferases. *Plant and Cell Physiology* 58: 2126–2138.
- Zhong R, Cui D, Ye Z-H. 2018. A group of *Populus trichocarpa* DUF231 proteins exhibit differential O-acetyltransferase activities toward xylan. *PLoS ONE* 13: e0194532.
- Zhong R, Lee C, Zhou J, McCarthy RL, Ye ZH. 2008. A battery of transcription factors involved in the regulation of secondary cell wall biosynthesis in *Arabidopsis*. *Plant Cell* 20: 2763–2782.
- Zhong R, Ye Z-H. 2012. MYB46 and MYB83 bind to the SMRE sites and directly activate a suite of transcription factors and secondary wall biosynthetic genes. *Plant and Cell Physiology* 53: 368–380.
- Zhu XF, Wan JX, Sun Y, Shi YZ, Braam J, Li GX, Zheng SJ. 2014. Xyloglucan endotransglucosylase-hydrolase17 interacts with xyloglucan endotransglucosylase-hydrolase31 to confer xyloglucan endotransglucosylase action and affect aluminum sensitivity in *Arabidopsis*. *Plant Physiology* 165: 1566–1574.
- Zinkgraf M, Gerttula S, Zhao S, Filkov V, Groover A. 2018. Transcriptional and temporal response of *Populus* stems to gravi-stimulation. *Journal of Integrative Plant Biology* 60: 578–590.

Supporting Information

Additional Supporting Information may be found online in the Supporting Information section at the end of the article.

Fig. S1 Effects of hybrid aspen (*Populus tremula* × *tremuloides*) stem flexing on tree growth kinetics.

Fig. S2 Effects of hybrid aspen (*Populus tremula* × *tremuloides*) stem flexing on sugar yield in enzymatic hydrolysates following acid pretreatment.

Fig. S3 Transcriptional changes in hybrid aspen (*Populus tremula* × *tremuloides*) trees in response to mechanical stimuli analyzed by GO enrichment.

Fig. S4 Phylogenetic tree of *CesA* gene family in *Arabidopsis thaliana*, *Populus trichocarpa* and *P. tremula*.

Fig. S5 Phylogenetic tree of *XTH* gene family in *Arabidopsis thaliana*, *Populus trichocarpa* and *P. tremula*.

Fig. S6 Phylogenetic tree of *ZAT* gene family in *Arabidopsis thaliana*, *Populus trichocarpa* and *P. tremula*.

Fig. S7 Phylogenetic tree of *TBL* gene family in *Arabidopsis thaliana*, *Populus trichocarpa* and *P. tremula*.

Methods S1 Detailed description of plant growing conditions, bioinformatic procedures, hormone analyses and statistical analyses.

Table S1 Hybrid aspen (*Populus tremula* × *tremuloides*) wood properties determined by SilviScan analysis at either 25 μm or 2 mm resolution.

Table S2 List of targeted compounds during general hormone profiling (shown also on Fig. 5).

Table S3 Differentially expressed genes ($P \leq 0.05$ and fold change (FC) ≥ 1.5) in the cambium tissue of flexed hybrid aspen

(*Populus tremula* × *tremuloides*) stems relative to the stationary stems.

Table S4 Differentially expressed genes ($P \leq 0.05$ and fold change (FC) ≥ 1.5) in the xylem tissue of flexed hybrid aspen (*Populus tremula* × *tremuloides*) stems relative to the stationary stems.

Table S5 Gene Ontology enrichment analysis on the differentially expressed genes identified in the cambium tissue of flexed hybrid aspen (*Populus tremula* × *tremuloides*) stems relative to the stationary stems.

Table S6 List of transcription factors selected among the differentially expressed genes ($P \leq 0.05$ and fold change expression ≥ 1.5) in the cambium and xylem tissues of mechanically stimulated hybrid aspen (*Populus tremula* × *tremuloides*) stems compared with the stationary set.

Table S7 Gene Ontology Enrichment Analysis on the differentially expressed genes identified in the xylem tissue of flexed hybrid aspen (*Populus tremula* × *tremuloides*) stems relative to the stationary stems.

Table S8 List of genes from the co-expression clusters shown in Fig. 6(b).

Video S1 Representative hybrid aspen trees subjected to low-intensity stem flexures during their movement by the conveyor belt system in the phenotyping facility.

Please note: Wiley is not responsible for the content or functionality of any Supporting Information supplied by the authors. Any queries (other than missing material) should be directed to the *New Phytologist* Central Office.

Xylan glucuronic acid side chains fix suberin-like aliphatic compounds to wood cell walls

Marta Derba-Maceluch¹ , Madhusree Mitra¹ , Mattias Hedenström² , Xiaokun Liu¹ ,
Madhavi L. Gandla² , Félix R. Barbut¹ , Ilka N. Abreu¹ , Evgeniy N. Donev¹ , János Urbancsok¹ ,
Thomas Moritz¹ , Leif J. Jönsson² , Adrian Tsang³ , Justin Powlowski^{3†}, Emma R. Master⁴  and
Ewa J. Mellerowicz¹ 

¹Department of Forest Genetics and Plant Physiology, Umeå Plant Science Centre, Swedish University of Agricultural Sciences, 901 83 Umeå, Sweden; ²Department of Chemistry, Umeå University, 901 87 Umeå, Sweden; ³Centre for Structural and Functional Genomics, Concordia University, Montreal, QC H4B 1R6, Canada; ⁴Department of Chemical Engineering and Applied Chemistry, University of Toronto, 200 College Street, Toronto, ON M5S 3E5, Canada

Summary

Author for correspondence:

Ewa J. Mellerowicz

Email: ewa.mellerowicz@slu.se

Received: 10 October 2022

Accepted: 30 November 2022

New Phytologist (2023) 238: 297–312

doi: 10.1111/nph.18712

Key words: lignin–carbohydrate complexes, *Populus*, saccharification, suberin, wood cell wall, xylan.

- Wood is the most important repository of assimilated carbon in the biosphere, in the form of large polymers (cellulose, hemicelluloses including glucuronoxylan, and lignin) that interactively form a composite, together with soluble extractives including phenolic and aliphatic compounds. Molecular interactions among these compounds are not fully understood.
- We have targeted the expression of a fungal α -glucuronidase to the wood cell wall of aspen (*Populus tremula* L. \times *tremuloides* Michx.) and *Arabidopsis* (*Arabidopsis thaliana* (L.) Heynh), to decrease contents of the 4-O-methyl glucuronopyranose acid (mGlcA) substituent of xylan, to elucidate mGlcA's functions.
- The enzyme affected the content of aliphatic insoluble cell wall components having composition similar to suberin, which required mGlcA for binding to cell walls. Such suberin-like compounds have been previously identified in decayed wood, but here, we show their presence in healthy wood of both hardwood and softwood species. By contrast, γ -ester bonds between mGlcA and lignin were insensitive to cell wall-localized α -glucuronidase, supporting the intracellular formation of these bonds.
- These findings challenge the current view of the wood cell wall composition and reveal a novel function of mGlcA substituent of xylan in fastening of suberin-like compounds to cell wall. They also suggest an intracellular initiation of lignin–carbohydrate complex assembly.

Introduction

The walls of wood cells of trees are crucial sources of renewable biomass (Bar-On *et al.*, 2018) for producing fuels and chemicals or as a versatile material for solid wood products. Dried wood consists of *c.* 45% cellulose, 25% hemicelluloses, and other polysaccharide matrix components, 20% lignin, 7% extractives, and 3% ash, with wide variation within a tree, among different species of angiosperms, or as a result of environmental stresses. Several wood-chemical analyses have used different approaches to reveal intricate details of the nanostructure of wood (Terashima *et al.*, 2009; Fernandes *et al.*, 2011; Bar-On *et al.*, 2018; Lyczakowski *et al.*, 2019; Terrett *et al.*, 2019; Addison *et al.*, 2020), with the results suggesting that wood properties are largely determined by molecular interactions among different wood components. Hemicelluloses play a unique role in these interactions by mediating the contact between the rigid semicrystalline cellulose

microfibril network and the more flexible lignin network (Berglund *et al.*, 2020). Hemicelluloses coat cellulose hydrophobic and hydrophilic microfibril surfaces according to the presence and distribution of their side chains (Bromley *et al.*, 2013; Busse-Wicher *et al.*, 2014, 2016; Grantham *et al.*, 2017; Martínez-Abad *et al.*, 2017, 2020) and closely interact with lignin at the subnano scale (Kang *et al.*, 2019; Addison *et al.*, 2020) to form 'lignin–carbohydrate complexes' (LCCs; Tarasov *et al.*, 2018; Giummarella *et al.*, 2019; Terrett & Dupree, 2019).

In hardwoods, glucuronoxylan is the main hemicellulose. Its backbone, comprising β -1,4-linked D-Xylp units, favors a threefold screw conformation in solution, but acquires a twofold conformation when interacting with cellulose microfibrils, which requires even spacing of xylan side chains: O-acetyl groups at position O-2, O-3, or both, and 4-O-methyl glucuronopyranose acid (mGlcA) units linked by a 1,2- α -glycosidic bond (Busse-Wicher *et al.*, 2014, 2016; Grantham *et al.*, 2017). The major xylan domain is characterized by even side-group spacing, while the minor domain has tight and uneven glucuronosylation and

[†]Deceased.

acetylation patterns (Busse-Wicher *et al.*, 2014). Both domains can represent different parts of the same or separate molecules and are formed by different xylan glucuronosyl and acetyltransferases (Bromley *et al.*, 2013; Grantham *et al.*, 2017). The minor domain is more difficult to extract because it interacts covalently with lignin (Martínez-Abad *et al.*, 2018).

Glucuronoxylan mediates three main LCCs: phenyl glycosides, linking phenolic C-4 to Xylp C1-O; γ -esters, linking lignin unit γ -carbon to the mGlcA carboxyl group (C6-O); and benzyl ethers, linking lignin unit α -carbon to C2-O or C3-O in Xylp (Tarasov *et al.*, 2018; Giummarella *et al.*, 2019; Terrett & Dupree, 2019). In birch, γ -esters and benzyl ether linkages are found in the highly recalcitrant fraction, whereas phenyl glycosidic LCCs are easily extracted (Martínez-Abad *et al.*, 2018). Molecular dynamic simulations suggested that mGlcA side chains may interact ionically with Ca^{2+} forming intermolecular cross-links analogous to the pectin egg-box structures (Pereira *et al.*, 2017). Thus, the presence and distribution of mGlcA substitutions in xylan are predicted to play crucial roles in determining the cell wall properties of hardwoods.

To assess the molecular implications of mGlcA substitution, we and others examined mutants of xylan glucuronosyl transferases, which form a small clade in the glycosyl transferase family 8 (GT8), and are encoded by *GUX1–GUX5* in *Arabidopsis thaliana* (Mortimer *et al.*, 2010, 2015; Lee *et al.*, 2012; Rennie *et al.*, 2012; Bromley *et al.*, 2013). Recently, similar genes have been described for conifers (Lyczakowski *et al.*, 2021). *GUX1* and *GUX3* generate an even glucuronosylation pattern, typically every eighth or sixth Xylp, respectively, while *GUX2* generates an uneven and consecutive glucuronosylation pattern. Therefore, single, double, and triple mutants of these genes display precise changes in mGlcA patterns in *A. thaliana*. The triple-mutant *gux1gux2gux3* is a dwarf, but the *gux1gux2* mutant grows normally despite the reduced level of xylan glucuronosylation. During saccharification, these plants have moderately and greatly increased glucose and xylose yields, respectively (Lee *et al.*, 2012; Lyczakowski *et al.*, 2017). However, the reduced glucuronosylation increases xylan acetylation because the two substituents compete for the same sites in xylan (Chong *et al.*, 2014; Lee *et al.*, 2014). Moreover, the suppressed GUX activity likely alters substrate pool in the Golgi, resulting in an increase cell wall Xyl content (Lee *et al.*, 2014; Chong *et al.*, 2015). Therefore, the cell wall and lignocellulose properties of the *gux* mutants are likely to be affected by other factors in addition to the change in mGlcA substitution.

To reduce xylan glucuronosylation without introducing additional structural changes, we previously expressed an α -glucuronidase of *Schizophyllum commune* ScAGU115 in *A. thaliana* targeting it to the cell wall (Chong *et al.*, 2015). ScAGU115 belongs to a novel α -glucuronidase family GH115 that acts on polymeric xylan (Tenkanen & Siika-aho, 2000), but *in planta*, it was active only on a small population of mGlcA residues that were accessible to UX1 monoclonal antibody (Chong *et al.*, 2015). The UX1 antibody binds GlcA decorations on deacetylated xylan (Koutaniemi *et al.*, 2012). As the majority of Xylp units decorated by mGlcA are acetylated in native glucuronoxylan (Chong *et al.*, 2014), prior deacetylation of the

xylan would be necessary for hydrolysis of mGlcA by ScAGU115. Here, we used instead an α -glucuronidase of *Aspergillus niger* (*AnAgu67A*) from the family GH67 representing enzymes that remove glucuronosyl residue from terminal nonreducing end of xylo-oligosaccharides (Tenkanen & Siika-aho, 2000), and we targeted it to the cell walls of hybrid aspen (*Populus tremula* L. \times *tremuloides* Michx.) and *A. thaliana*. This uncovered previously unrecognized functions of xylan glucuronosylation in the wood and has led to identification of a novel wood component.

Materials and Methods

Gene cloning and recombinant expression of *AnAgu67A*

The cDNA clone Asn_01446 (GenBank accession: DR701927.1) encoding α -glucuronidase of *Aspergillus niger* Tiegh. (hereinafter *AnAgu67A*) was isolated as part of a fungal species gene discovery program (GenBank BioSample: SAMN00176483; EST: LIBEST_017623), where Q96WX9 and NRRL3_01069 are other identifiers of the same gene. For recombinant expression, *AnAgu67A* cDNA was amplified by PCR and transferred to ANIp7G (Storms *et al.*, 2005) using Gateway LR Clonase™ (Invitrogen). The details of cloning are presented in Supporting Information Methods S1. Enzyme activity assays of recombinant *AnAgu67A* are described in Methods S2.

Plant vector construction

The *A. niger* α -glucuronidase cDNA clone Asn_01446 (GenBank accession: DR701927.1) was used to create a plant expression vector. The native signal peptide sequence was exchanged to the plant signal peptide from the *PxtCel9B3* gene (alias *PttCel9B*) from *P. tremula* L. \times *tremuloides* Michx. (GenBank accession no. AY660968.1; Rudsander *et al.*, 2003) with use of the following primers: OC9Bf1, OC9Br1, FC1f1, FC1r1, and FC1r1s (Table S1) as described previously (Gandla *et al.*, 2015). The entry clone was created using the pENTR/D-TOPO cloning system (Thermo Fisher Scientific, Uppsala, Sweden), and the expression clone was obtained using the Gateway® System (Thermo Fisher Scientific) in either the pK2WG7.0 vector (Karimi *et al.*, 2002) for overexpression using the 35S promoter in hybrid aspen or pK-pGT43B-GW7 (Ratke *et al.*, 2015) for expression specifically in cells developing secondary cell walls in *A. thaliana*. The destination vector pK7FGW2.0 was used to fuse SP_{PttCel9B}:AnAgu67A with GFP (Karimi *et al.*, 2002). All plant vectors were introduced into competent *Agrobacterium tumefaciens* (Smith and Townsend) Conn strain GV3101 using electroporation.

Plant material transformation and growth conditions

Hybrid aspen (*P. tremula* L. \times *tremuloides* Michx., clone T89) was transformed by *A. tumefaciens* and propagated *in vitro* as described previously (Gray-Mitsumune *et al.*, 2008). Five lines with the highest *AnAgu67A* expression were selected out of the 23 analyzed lines. Between nine and 13 trees of each of the five selected lines and 19 wild-type (WT) trees were grown in a

glasshouse for 3 months as described previously (Gandla *et al.*, 2015). The stem height, the average internode length for internodes 19–35, and the stem diameters for internode 40 were determined at the time of harvest.

Arabidopsis thaliana (L.) Heynh (Col-0) was transformed using the floral dip method (Clough & Bent, 1998). Seeds collected from the transformed plants were germinated on ½ Murashige & Skoog medium (½ MS) plates with kanamycin (50 µg ml⁻¹) and homozygotic single insert lines were selected by segregation. Plants of the two highest expressing lines were grown for 8 wk under a 16 h : 8 h, light : dark cycle, 150 µmol m⁻² s⁻¹, at 22°C and 70% humidity.

Immunolocalization of SP^{PttCel9B}:AnAgu67A:GFP

T2 *A. thaliana* seeds carrying the transgene were germinated on ½ MS plates, and 7-d-old seedlings were plasmolyzed in 20% mannitol, fixed in 2% w/v paraformaldehyde, and used for immunolocalization as described previously (Pawar *et al.*, 2016), except that the CyTM5 AffiniPure Donkey Anti-Rabbit IgG (H + L; Jackson ImmunoResearch Europe Ltd, Ely, UK) diluted 1 : 200 was used as secondary antibody. The seedling roots were analyzed by sequential line scanning using a Leica TCS SP2 confocal microscope with 633 nm excitation and 650–798 nm emission (Leica Microsystems, Wetzlar, Germany). The lambda scan was performed every 6 nm between 650 and 800 nm to ensure that the signal matched that of Cy5.

qRT-PCR analysis

RNA was isolated from developing xylem tissues of hybrid aspen as previously described (Gray-Mitsumune *et al.*, 2004) using CTAB buffer (Chang *et al.*, 1993), before being treated with DNaseI (DNA-freeTM DNA Removal Kit; Thermo Fisher Scientific). The cDNA library was made from 1 µg of RNA using an iScriptTM cDNA Synthesis Kit (Bio-Rad Laboratories AB, Hercules, CA, USA), and cDNA diluted 1 : 20 was used for transcript-level analysis. The expression was normalized to tubulin (*Potri.001G464400*) and ubiquitin (*Potri.005G198700*), calculated according to Pfaffl (2001) and presented relative to the lowest-expressing line.

In the case of *A. thaliana*, RNA was isolated from the stems of 6-wk-old plants using TRI Reagent[®] (Applied Biosystems, Bedford, MA, USA). The cDNA libraries were made as described previously from 400 ng of RNA and diluted 10 times for transcript-level analysis. The expression was calculated according to Livak & Schmittgen (2001), was normalized to *ACTIN2* (*AT3G18780*) and *EF1ALPHA* (*AT5G60390*), and presented relative to the lowest-expressing line. The primers details are provided in Table S1.

Alpha-glucuronidase activity assay in transgenic plants

Portions of 100 mg of either developing wood, in the case of hybrid aspen, or stem tissues, in the case of *A. thaliana*, were ground in liquid nitrogen, incubated in 300 µl of buffer A (0.2 M sodium succinate, pH 5.5), 10 mM CaCl₂, and 1% (w/v)

PVPP (aspen) or 1% (w/v) PVP (*A. thaliana*) at 4°C for 1 h with shaking, spun at 20 000 g for 15 min, and the supernatants were collected as soluble protein fractions. The pellets were extracted with 200 µl of buffer B (0.2 M sodium succinate, 10 mM CaCl₂, and 1 M NaCl, pH 5.5) for 1 h at 4°C with shaking, spun as above, and the supernatants were collected as wall-bound protein fractions, which were desalted using Microcon centrifugal filters (30 000 MWCO; Millipore) and equilibrated in buffer A. The protein concentrations were determined by the Bradford method and adjusted to 0.3 and 0.59 mg ml⁻¹ for hybrid aspen and *A. thaliana*, respectively.

The α-glucuronidase activity assay was performed using the K-AGLUA Assay Kit (Megazyme, currently Neogen Europe Ltd, Ayr, UK) using 7.5 µg of proteins from soluble and wall-bound fractions for hybrid aspen, and 14.75 µg of protein from the wall-bound fraction for *A. thaliana* according to manufacturer's instructions. Briefly, the proteins were incubated with a mixture of tri-, tetra-, and penta-aldouronic acid (provided in the kit) for 20 min of a two-step reaction at 40°C, where the α-glucuronidase product (glucuronic acid) was further reacted with nicotinamide adenine dinucleotide (NAD⁺) to form D-glucarate and reduced NADH that was spectrophotometrically measured at 340 nm.

Thin-layer chromatography analysis was used to visualize the α-glucuronidase reaction in hybrid aspen according to Franková & Fry (2011). Details are presented in Methods S3.

Anatomy

Stem segments from internode 42 of hybrid aspen were fixed in FAA (50% ethanol, 4% formaldehyde, 5% acetic acid; v/v/v). Fifty micrometer-thick transverse sections were cut using a vibratome (VT100S; Leica Biosystems) and stained with Mäule reagent (Meshitsuka & Nakano, 1977). Sections were incubated in 1% (w/v) KMnO₄ for 5 min, washed three times with distilled water, and incubated in 37% N HCl for 2 min. The stained sections were mounted in the presence of concentrated NH₄OH and observed under a Dmi8 microscope (Leica Microsystems) in white light with a color DCF7000 T camera. Thicknesses of secondary xylem, secondary phloem, and bark were analyzed in three trees per line.

Suberin localization

Stem sections prepared as above were stained with Fluorol Yellow 088 (FY088; Lux *et al.*, 2005) either directly or after prior removal of soluble extractives as described below. Unstained sections were used as control for lignin autofluorescence. Sections were examined with a Dmi8 microscope using standard GFP settings (excitation, 450–490 nm; dichroic mirror, 495; emission 500–550 nm) and a monochromatic camera DCF9000 GT. Fluorescence was quantified using LasX software (Leica Microsystem CMS GmbH) in the line mode. Three trees were analyzed per genotype, using 3–19 images per tree, and the fluorescence signal was measured at a minimum of 15 positions per image and averaged. The staining and imaging settings were consistent across the lines and treatments that were compared.

Wood grinding for compositional analysis

Hybrid aspen internodes 44–60 were debarked and freeze-dried for 36 h. The pith was removed, and the wood was milled using an A11 Basic Analytical Mill (IKA, Staufen, Germany) followed by grinding in a ZM 200 ultra centrifugal mill (Retsch, Haan, Germany). Rough wood powder (particle size < 0.5 mm) was further milled to a fine wood powder in 10-ml stainless steel jars with one 12-mm grinding ball at 30 Hz for 2 min, using an MM400 bead mill (Retsch).

Pyrolysis coupled to gas chromatography/mass spectrometry (Py-GC/MS)

Portions of $50 \pm 10 \mu\text{g}$ of fine wood powder were applied to a pyrolyzer equipped with an autosampler (PY-2020iD and AS-1020E; Frontier Lab, Koriyama, Japan) connected to a GC/MS (7890A/5975C; Agilent Technologies AB, Santa Clara, CA, USA), and the pyrolysate was separated and analyzed according to Gerber *et al.* (2012).

FT-IR spectroscopy

Samples of fine wood powder (10 mg) were analyzed as described previously (Gandla *et al.*, 2015) using a Bruker IFS 66v/S spectrometer (Bruker Optik GmbH, Ettlingen, Germany) equipped with a diffuse reflectance 16-sample holder accessory (Harrick Scientific Products, Pleasantville, NY, USA). Samples of 9–13 trees of each transgenic line and 19 WT trees were examined.

Wood wet chemistry analyses

The fine wood powders of two trees of the same line were pooled to provide 4–5 biological replicates per line. The alcohol insoluble residue (AIR) was prepared by washing the samples with 4 mM HEPES buffer (pH 7.5) containing 80% ethanol, a methanol : chloroform 1 : 1 (v/v) mixture, and finally with acetone, before drying the residue in a vacuum (Gandla *et al.*, 2015). Type I α -amylase from pig pancreas (Roche, Solna, Sweden: 10102814001; 100 U/100 mg of AIR) was used to remove starch from AIR following two overnight incubations with fresh addition of the enzyme each day.

Methanolysis-TMS analysis was conducted using 500 μg of either starch-free AIR material or dioxane lignin isolated as described below, together with inositol (10 μg ; internal standard) and nine monosaccharide standards, as described previously (Gandla *et al.*, 2015). Silylated monosaccharides were separated by GC/MS (7890A/5975C; Agilent Technologies AB). The resulting raw data MS files were converted to CDF format in Agilent Chemstation Data Analysis (v.E.02.00.493) and exported to R software (v.3.0.2; R Foundation for Statistical Computing). Data pretreatment procedures, such as baseline correction and chromatogram alignment, time-window setting, and multivariate curve resolution (MCR) processing, followed by peak identification were performed in R, and 4-O-methylglucuronic acid was identified according to Chong *et al.* (2013).

The crystalline cellulose content was determined by the Updegraff procedure (Updegraff, 1969), the resulting glucose content was determined using the anthrone method as previously described (Gandla *et al.*, 2015), and the acid-insoluble lignin (Klason lignin) content was determined according to Theander & Westerlund (1986).

Analytical saccharification

Each line was analyzed with four or five biological replicates, each representing a pool of wood powder (particle size: 0.1–0.5 mm) from two trees obtained by fractionation of the rough wood powder using an AS 200 analytical sieve shaker (Retsch). Moisture content in 50 mg wood powder samples was measured using Mettler Toledo HG63 moisture analyzer (Columbus, OH, USA). The acid pretreatment, enzymatic saccharification, and resulting hydrolysate analyses were conducted as previously described previously (Gandla *et al.*, 2015). Briefly, the acid pretreatment was performed in 1% (w/w) sulfuric acid for 10 min at 165°C using an initiator single-mode microwave instrument (Biotage Sweden AB, Uppsala, Sweden). The enzymatic hydrolysis after acid pretreatment was performed at 45°C for 72 h in sodium citrate buffer (50 mM, pH 5.2) using 50 mg of an enzyme mix of Celluclast 1.51 and Novozyme 188 (1 : 1, obtained from Sigma–Aldrich (St Louis, MO, USA)), in a reaction mixture of 1000 mg. Reaction mixtures with wood that had not been pretreated consisted of 50 mg of milled wood, 900 mg of the sodium citrate buffer, and 50 mg of the same enzyme mix. The yield of Glc and Xyl was determined following the method as mentioned by Gandla *et al.* (2015) using a high-performance anion-exchange chromatography system with pulsed amperometric detection (Ion Chromatography System ICS-3000 by Dionex, Sunnyvale, CA, USA).

Dioxane-lignin isolation

Fractionated wood powder (particle size: 0.1–0.5 mm) was pooled from nine trees to obtain a single sample of ≥ 7.5 g. Materials from nine transgenic trees, including three trees each from lines 4, 6, and 23, and nine WT trees were pooled equally by weight to obtain one transgenic and one WT sample. Part of the material (extracted wood) was extracted sequentially in three technical replicates in a Soxhlet apparatus for 6 h with toluene (95% EtOH; 2 : 1; v/v), for 4 h in 95% EtOH, and for 2 h in H₂O, and finally, the extracted wood was dried in an oven at 103°C for 48 h (this step was omitted for nonextracted samples). The material was ground in 0.3–1.2 g portions in a Planetary Micro Mill Pulverisette 7 Premium line (Fritsch, Idar-Oberstein, Germany) with 10 ZrO₂ balls (10-mm diameter) at 500 rpm over five 10-min milling cycles, with a 10-min break between each. The finely ground material was suspended in 1,4-dioxane : water (96 : 4; v/v) with a solid : liquid ratio of 1 : 10 (g ml⁻¹) and shaken at 225 rpm for 24 h at room temperature. The suspension was centrifuged at 4000 g for 10 min, the supernatant was collected, and the pellet was re-extracted with 1,4-dioxane : water a further three times. The four extractions were

combined and filtered through a Whatman glass microfiber filter (pore size 1.2 µm; Merck, Solna, Sweden), following which, two volumes of water were added to precipitate the lignin-carbohydrate mixture. The 1,4-dioxane and water were evaporated in a rotary evaporator (under reduced pressure) at 35°C to almost dryness, before adding 10 ml of water and evaporating again to almost dryness; this process was repeated three times to remove 1,4-dioxane. Finally, 10 ml of water was added to the sample, transferred to a Falcon tube, and lyophilized in a freeze-dryer for 24 h to obtain 'dioxane lignin'.

NMR

Dioxane lignin (10–15 mg) was transferred to 5-mm NMR tubes and dissolved in 600 µl dimethyl sulfoxide- d_6 (Kim *et al.*, 2008). 2D ^1H - ^{13}C heteronuclear single quantum coherence (HSQC) profiles were acquired at 298 K using a Bruker 600 MHz Avance III spectrometer equipped with a 5 mm BBO cryo-probe (Bruker Biospin, Rheinstetten, Germany). A pulse program employing adiabatic ^{13}C refocusing and inversion pulses was used (hsqcetgpp-sisp2.2), with sweep widths of 8.1 ppm in the ^1H dimension and 140 ppm in the ^{13}C dimension. Sixteen scans were recorded for each of the 256 t_1 increments, and the spectra were calibrated using the residual dimethyl sulfoxide peak (d_H : 2.49 ppm and d_C : 39.5 ppm). A Gaussian window function was used in F1 (^{13}C dimension), and a 90-degree shifted square sine bell window function was applied in F2 (^1H dimension). Processing and peak volume integration were performed in Topspin 3.6 (Bruker Biospin), and peak assignments were based on those used in previous studies (Kim *et al.*, 2008; Balakshin *et al.*, 2011; Shakeri Yekta *et al.*, 2019; Correia *et al.*, 2020). Orthogonal partial least square (OPLS) analysis and visualization were performed using an in-house MATLAB application that transforms a batch of 2D spectra to a matrix suitable for multivariate analysis by reshaping each spectrum to a row vector (Hedenström *et al.*, 2009; Öman *et al.*, 2014).

Metabolomic analysis

Metabolites were extracted and analyzed as described by Abreu *et al.* (2020). Briefly, 20 mg of fine wood powder was extracted in 1 ml of extraction buffer (methanol : chloroform : water; 20 : 60 : 20; v/v/v), including internal standards (Gullberg *et al.*, 2004), and 100 µl of each extract was dried in a SpeedVac and dissolved in 20 µl of methanol followed by 20 µl of water. Lipids were extracted in methanol : chloroform (50 : 50, v/v) as described by Melo *et al.* (2021). Metabolomics and lipidomics analyses were performed by liquid chromatography, and the metabolites were detected by an Agilent 6540 Q-TOF mass spectrometer equipped with an electrospray ion source operating in negative and/or positive ion modes (Abreu *et al.*, 2020). The mass files from the metabolomic analysis were processed (Profinder B.08.00; Agilent Technologies AB) by a targeted feature extraction approach using the aspen stem database (Abreu *et al.*, 2020), while those from the lipidomic analysis were processed by an untargeted approach using a recursive feature

extraction as described by Melo *et al.* (2021). The generated data were normalized against the internal standard and weight of each sample. The targeted approach used to process phenolic compounds resulted in the annotation of 135 metabolites (Table S5, see later), which was confirmed by comparison of MS fragments (produced by MS/MS analysis) with the results of previous studies (Kasper *et al.*, 2012; Abreu *et al.*, 2020). Annotation was performed on significant ion mass. The untargeted approach used for the lipid MS files resulted in the detection of 984 (positive) and 980 (negative) features. Lipid compounds were annotated based on mass spectra in the library LIPIDMAPS (<https://www.lipidmaps.org/>). Changes in abundance between transgenic and WT samples were considered as significant if $P \leq 0.05$ (t -test) and, in the case of lipids, $|\text{fold change}| \geq 1.5$. The false discovery rate was < 0.05 .

Transcriptomics

RNA samples were isolated from developing wood, and their concentrations were determined by a NanoDrop 2000 spectrophotometer (Thermo Fisher Scientific). The quality of the RNA was assessed by an Agilent 2100 Bioanalyzer (Agilent Technologies AB) following the manufacturer's instructions, and samples with an integrity number (RIN) ≥ 8 were used for sequencing. Four biological replicates of line 4, three biological replicates of line 6, and eight biological replicates of WT were analyzed. Sequencing was conducted by Novogene (Cambridge, UK) using an Illumina NovaSeq 6000 PE150 platform, as was the quality control and mapping to the *P. tremula* transcriptome v.2.2 (retrieved from PlantGenIE; ftp://plantgenie.org/Data/PopGenIE/Populus_tremula/v2.2/). The raw counts were used for differential expression analysis in R (v3.4.0) using the BIOCONDUCTOR (v.3.4) DESEQ2 package (v.1.16.1) as previously described (Kumar *et al.*, 2019).

Statistical analyses

Univariate analyses were conducted using JMP v.15.0.0. program (SAS Institute). SIMCA-P software (v.16.0.1; Sartorius Stedim Data Analysis AB, Goettingen, Germany), with built-in options, was used for multivariate analysis.

Results

Production of AnAgu67A

The recombinant AnAgu67A protein purified from *A. niger* exhibited α -glucuronidase activity, and a half-life of > 2 h at 40°C and ≈ 1 h at 60°C. Hydrolysis of aldouronic acids by AnAgu67A was optimal at pH 5.0 and between 50°C and 60°C (Fig. S1a,b); the k_{cat} and K_m of AnAgu67A were $4.6 \times 10^{-2} \text{ s}^{-1}$ and 3.5 mg ml^{-1} , respectively. Two pure aldouronic acid fractions were tested as AnAgu67A substrates: UXX, with an mGlcA substituent on the terminal nonreducing end of xylotriase; and XUXX, with an mGlcA substituent at the second Xylp unit from the nonreducing end of xyloetraose. Consistent with the

substrate preferences of the GH67 family, mGlcA was released from the UXX substrate only (Chong *et al.*, 2015). mGlcA was also released from birchwood xylan by the recombinant enzyme (Fig. S2c), indicating that terminal mGlcA decorations at the reducing end are present in native wood xylan.

Ectopically expressed *AnAgu67A*-induced reduction in mGlcA xylan branching has no significant effects on the aspen growth phenotype, wood composition, or saccharification

A chimeric gene was cloned by substituting the *AnAgu67A* signal peptide with the signal peptide of *PtxiCel9B3* (SP_{Cel9B3}) for efficient targeting of the fungal enzyme to the plant cell wall. To verify the proper targeting, the chimeric gene was fused to *eGFP* and *35S::SP_{Cel9B3}::AnAgu67A::eGFP* construct was transferred to *A. thaliana*. As expected, the fusion protein was localized in cell walls in plasmolyzed root cells (Fig. 1a). Transgenic hybrid aspen lines were subsequently produced using the *35S::SP_{Cel9B3}::AnAgu67A* construct (*AnAgu67A* lines or transgenic lines) and grown in a glasshouse. The transgene was found expressed in developing wood in all analyzed lines (Fig. 1b), with the lowest expression in line 9, which was therefore omitted in some analyses.

As plants do not have endogenous α -glucuronidase activity, we examined α -glucuronidase activity in wall-bound protein extracts of developing wood from transgenic plants (Fig. 1c). The extracts of all analyzed transgenic lines hydrolyzed UXX to xylotri-ose and mGlcA, as was observed for *AnAgu67A* protein *in vitro*, whereas no activity was detected in the WT (Fig. 1c). Quantitative analysis of α -glucuronidase activity in the soluble and wall-bound protein fractions extracted from the developing wood of transgenic lines showed predominant activity in the wall-bound fraction (Fig. 1d) in agreement with protein localization to the cell wall and was the highest in lines 4 and 6.

The effects of α -glucuronidase activity on the sugar composition of wood matrix polysaccharides were investigated by methanolysis-trimethylsilyl (TMS) derivatization. A 20–30% reduction in mGlcA units was evident in all transgenic lines except for the low-expressing line 9, while no changes were observed in other sugar-related constituents (Figs 1e, S2a). The wood chemistry was analyzed by pyrolysis-GC/MS (Py-GC/MS), Fourier-transform infrared spectroscopy (FT-IR), Updegraff cellulose analysis, and Klason lignin, with no significant changes observed compared with WT (Fig. S2b–e).

To examine the effects of 20–30% reduction in xylan glucuronosylation on saccharification, wood from transgenic lines with reduced mGlcA was analyzed by analytical enzymatic saccharification with and without acid pretreatment. The results showed no significant change in glucose or xylose release in the transgenic lines compared with WT (Fig. S2f–g), which contrasts with the previously reported improved saccharification in *gux1-gux2* and *gux1gux2gux3* mutants (Lee *et al.*, 2012; Lyczakowski *et al.*, 2017).

The morphology and anatomy of transgenic trees were analyzed to determine whether the reduced xylan glucuronosylation affected plant growth and development, but the only change was

a small but consistent decrease in stem height caused by a decreased internode length (Fig. 1f–h), which might indicate a role of xylan glucuronosylation in stem elongation. Otherwise, no major or consistent changes in stem radial growth or stem anatomy were detected among the analyzed transgenic lines (Fig. S3a–c).

Cell wall-localized *AnAgu67A* α -glucuronidase does not affect γ -linkages

As (m)GlcA substituents of xylan are involved in cross-linking xylan to lignin via γ -ester bonds, we tested whether the α -glucuronidase activity in cell walls impacted γ -ester bonds in LCCs, which can be solubilized from cell walls together with lignin using dioxane (Giummarella *et al.*, 2019). Dioxane-soluble lignin was isolated from transgenic and WT extractive-free wood samples and analyzed by Py-GC/MS. It was found to comprise c. 65% lignin and 35% carbohydrates in both transgenic and WT samples (Fig. S4a). Xylose was the main sugar unit of dioxane lignin, reaching c. 95 mole % in both transgenic and WT samples (Fig. S4b). In agreement with these results, 2D HSQC NMR analysis with peak quantification normalized to lignin aromatic units (Tarasov *et al.*, 2018) showed no significant differences between transgenic and WT samples in either different lignin signals or anomeric signals from xylan (Fig. S4c–e). Therefore, the LCC composition does not differ significantly between transgenic and WT trees. The γ -ester peak, which is in the *O*-alkylated region, was well resolved (Fig. S5), and its integrated signal constituted c. 6% and 7% of total lignin aromatic signals for WT and transgenic samples, respectively (Fig. S4d), which is close to the 5.6% previously reported for birch (Tarasov *et al.*, 2018). Thus, α -glucuronidase activity in cell walls did not impact the LCC composition nor the occurrence of γ -ester bonds.

AnAgu67A α -glucuronidase decreases the content of aliphatic compounds in dioxane lignin

The OPLS modeling of 2D HSQC NMR spectra of dioxane lignin from extractive-free wood of transgenic and WT samples (Fig. S5a,b) revealed the most significant changes between the two samples in the aliphatic region A, followed by the *O*-alkylated region B. The aromatic region C did not contribute to sample separation, which is consistent with the aromatic peak quantitative analysis (Fig. S4c). The high-resolution OPLS loading plots corresponding to regions A and B of the spectra are shown in Fig. 2(a,b). The loadings represent spectra that significantly contributed to the separation of transgenic and WT samples in OPLS. The blue signals, including aliphatic saturated and unsaturated esters, triacylglycerols (TAGs), and diacylglycerols (DAGs), were higher in WT, whereas all black peaks were higher in transgenic lines. Quantitative analysis of the integrated peaks normalized to lignin confirmed the reduced signals from fatty esters, TAGs, and DAGs in the dioxane lignin from transgenic plants from extractive-free wood samples, whereas the corresponding signals obtained from wood with extractives

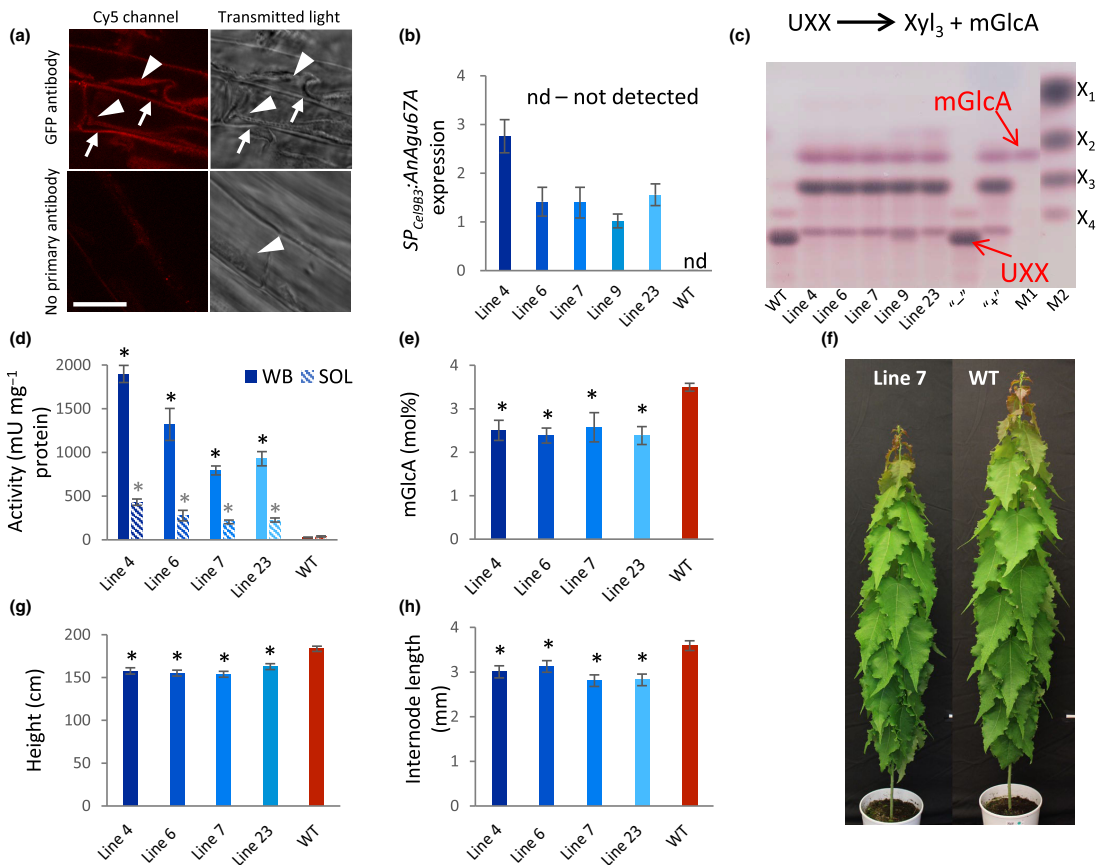


Fig. 1 Characterization of transgenic aspen (*Populus tremula* L. × *tremuloides* Michx.) lines carrying 35S::SP_{Cel9B3}::AnAgu67A construct. (a) Immunolocalization of eGFP in plasmolyzed root cells of *Arabidopsis thaliana* expressing 35S::SP_{Cel9B3}::AnAgu67A:eGFP showing that the protein is targeted to cell walls. Arrowhead, shrunken protoplast; arrow, SP_{Cel9B3}::AnAgu67A:eGFP signal in cell wall. Bar, 15 µm. (b) Relative expression of transgene in transgenic lines normalized to line 9. (c) Visualization of α-glucuronidase activity in wall-bound protein fractions extracted from developing wood of transgenic and wild-type (WT) lines showing products of UXX hydrolysis by thin-layer chromatography. M1 and M2 – size markers, ‘–’ – negative control with buffer instead of protein extract, ‘+’ – positive control with *Geobacillus stearothermophilus* Donk α-glucuronidase. (d) Specific activity of α-glucuronidase in soluble (SOL) and wall-bound (WB) protein fraction extracted from developing wood of transgenic and WT plants. (e) 4-O-MeGlcA reduction in transgenic lines detected in methanolysis-trimethylsilyl analysis. (f) Appearance of 10-wk-old trees. (g) Height. (h) Internode length. Data in (b), (d), (e), (g), and (h) are means ± SE of *n* = 3 (b), *n* = 4 (d, e), *n* = 9–19 (g, h), for 12-wk-old trees. Asterisks mark lines significantly different from WT at *P* < 0.05 (Dunnnett’s test).

(nonextracted wood) were similar for transgenic and WT samples (Fig. 2c). Therefore, *AnAgu67A* affects the extractability of aliphatic compounds, but not their amounts in wood. This conclusion was consistent with the results of transcriptomic analyses of developing wood in transgenic aspen lines 4 and 6 that were most highly expressing *AnAgu67A* and in WT, which did not reveal any changes in expression of lipid-related genes (Table S2).

To identify the most highly extracted aliphatic compounds from wood of transgenic plants compared with WT, we analyzed both samples using untargeted lipidomics approach. Out of *c.* 1000 lipid peaks that were detected in the wood extracts

(Table S3), 115 were significantly changed between transgenic and WT samples (*P* < 0.05 and fold change > 1.5). From the corresponding metabolites, 88 were annotated and classified into nine categories (Fig. 2d; Table S4); the majority (71/88) were increased in transgenic samples (Fig. 2d). Among the fatty acids (FAs) increased in the transgenic extracts, there were 13 suberin monomers, such as 5,9,23-triacontatrienoic acid (77-fold increase), 28-hydroxy-octacosanoic acid, 9-octadecenoic acid, suberic acid, and 9,10-epoxy-octadecanoic acid (Fig. 2d; Table S4). By contrast, three other suberin monomers, comprising tetradecanedioic acid, glutinic acid, and 2-hydroxy-heptanoic

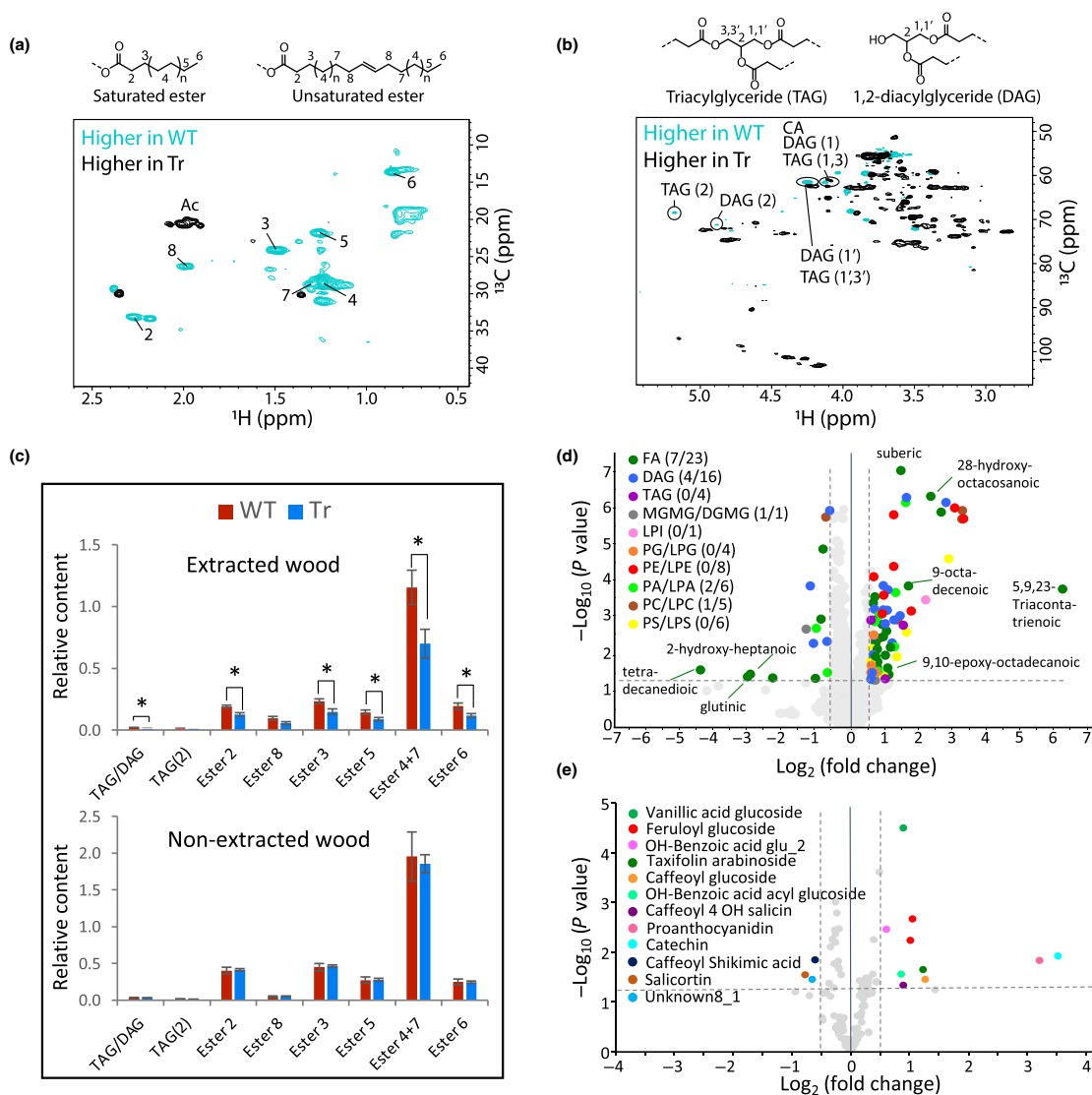


Fig. 2 Aliphatic suberin-like compounds are easier to extract from the wood of transgenic aspen (*Populus tremula* L. \times *tremuloides* Michx.) expressing *AnAgus67A* (Tr) than from wild-type (WT) wood. Two-dimensional (2D) nuclear magnetic resonance spectra of dioxane-soluble lignin isolated after removal of extractives (extracted wood) in the aliphatic (a) and O-alkylated (b) spectral regions that contributed to separation of transgenic and WT samples in orthogonal projections to latent structures (OPLS) analysis. Details of the OPLS models for extracted and nonextracted wood and 2D signals from WT samples are shown in Supporting Information Fig. S5. Ac, acetate; CA, cinnamyl alcohol. (c) Quantitative analysis of integrated peaks from the aliphatic and O-alkylated regions of extracted and nonextracted wood. Means \pm SE, $n = 3$ technical replicates of pooled material from three transgenic lines or from WT, asterisks show peaks significantly different between transgenic and WT samples at $P \leq 0.05$ (t -test). (d, e) Volcano plots showing aliphatic (d) and phenolic (e) metabolites extracted from the wood that differed in abundance between transgenic and WT samples ($P < 0.05$, t -test). The significantly altered metabolites are colored and represent in (d): DAG, diacylglycerols; FA, fatty acids; LPI, monoacylglycerophosphoinositols; MGMTG/DGMTG, (mono/di)glycosylmonoacylglycerols; PA/LPA, (di/mono)acylglycerophosphates; PC/LPC, (di/mono)acylglycerophosphocholines; PE/LPE, (di/mono)acylglycerophosphoethanolamines; PG/LPG, (di/mono)acylglycerophosphoglycerols; TAG, triacylglycerols; PS/LPS, (di/mono)acylglycerophosphoserines; (number of downregulated/upregulated metabolites). Cutin/suberin-related FAs are shown.

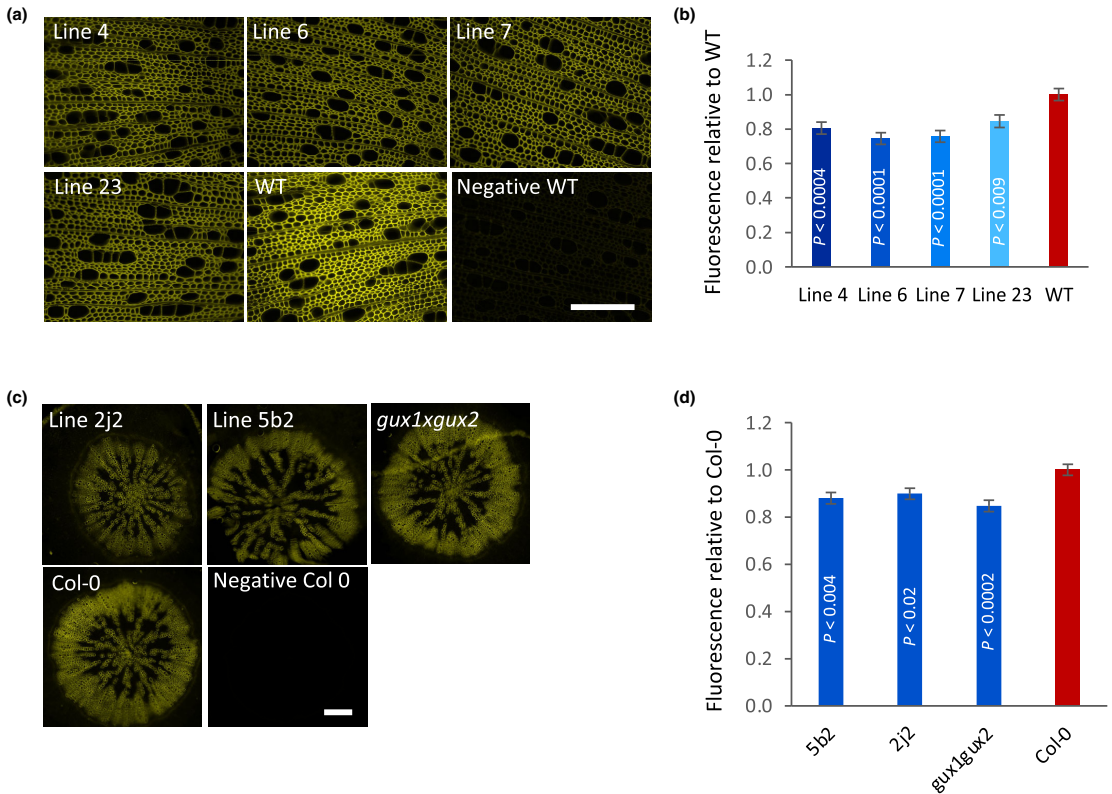


Fig. 3 Histochemical analysis of aliphatic compounds with FY088 in the wood of transgenic plants expressing *AnAgu67A* and wild-type (WT/Col0) after removal of extractives. (a) Representative sections of each line showing differences in suberin-like signals in 12-wk-old aspen (*Populus tremula* L. × *tremuloides* Michx.) stems. (b) Quantification of fluorescence signals in cell walls: means ± SE of $n = 36$. (c) Representative images of signals in 4-wk-old *A. thaliana* hypocotyls in two transgenic lines 5b2 and 2j2, in *gux1gux2* mutant and Col-0. Sections of 12 plants per genotype were analyzed. (d) Quantification of fluorescence signals in cell walls: means ± SE, $n = 12$. *P* values in (b) and (d) correspond to Dunnett's test comparing each genotype to WT/Col-0. Bars, 200 μm. Negative control in (a) and (c) shows autofluorescence signals without FY088.

acid, were reduced in transgenic extracts compared with WT; these FAs were characterized by shorter chains compared with those with increased extractability in the transgenic plants. The generally higher abundance of lipids in transgenic extracts confirms the NMR results, showing that aliphatic compounds are easier to extract when α -glucuronidase *AnAgu67A* is present in cell walls. The high contribution of suberin-related FAs to the extractability suggests that *AnAgu67A* affects the solubility of such compounds in wood. As suberin contains phenolic compounds linked with aliphatic compounds, we also investigated whether extracted phenolic compounds are more abundant in transgenic samples. A targeted metabolomic approach revealed 135 annotated phenolic compounds (Table S5), among which, 10, including tannins and glycosylated derivatives of hydroxycinnamic acids (known suberin components; Bernards, 2002; Graça, 2010), were more abundant in transgenic samples (Fig. 2e; Table S6).

AnAgu67A-sensitive aliphatic compounds are present in sapwood cell walls

To determine the location of α -glucuronidase-sensitive suberin-like compounds in wood, we stained extracted stem sections of transgenic and WT trees with Fluorol Yellow 088 (FY088), which stains suberin (Naseer *et al.*, 2012). The results showed strong yellow fluorescence signals in all lignified cell walls of mature WT wood (Fig. 3a). These extraction-resistant signals were visibly reduced in transgenic lines, which was confirmed by quantitative image analysis (Fig. 3a,b). By contrast, the nonextracted sections of transgenic plants had similar signal intensity to the nonextracted WT sections (Fig. S6a–c), suggesting that *AnAgu67A* was responsible for the enhanced liberation of these cell wall aliphatic compounds by toluene-ethanol solvent.

To investigate whether *AnAgu67A* had a similar effect on cell wall aliphatic compounds in other species, transgenic lines

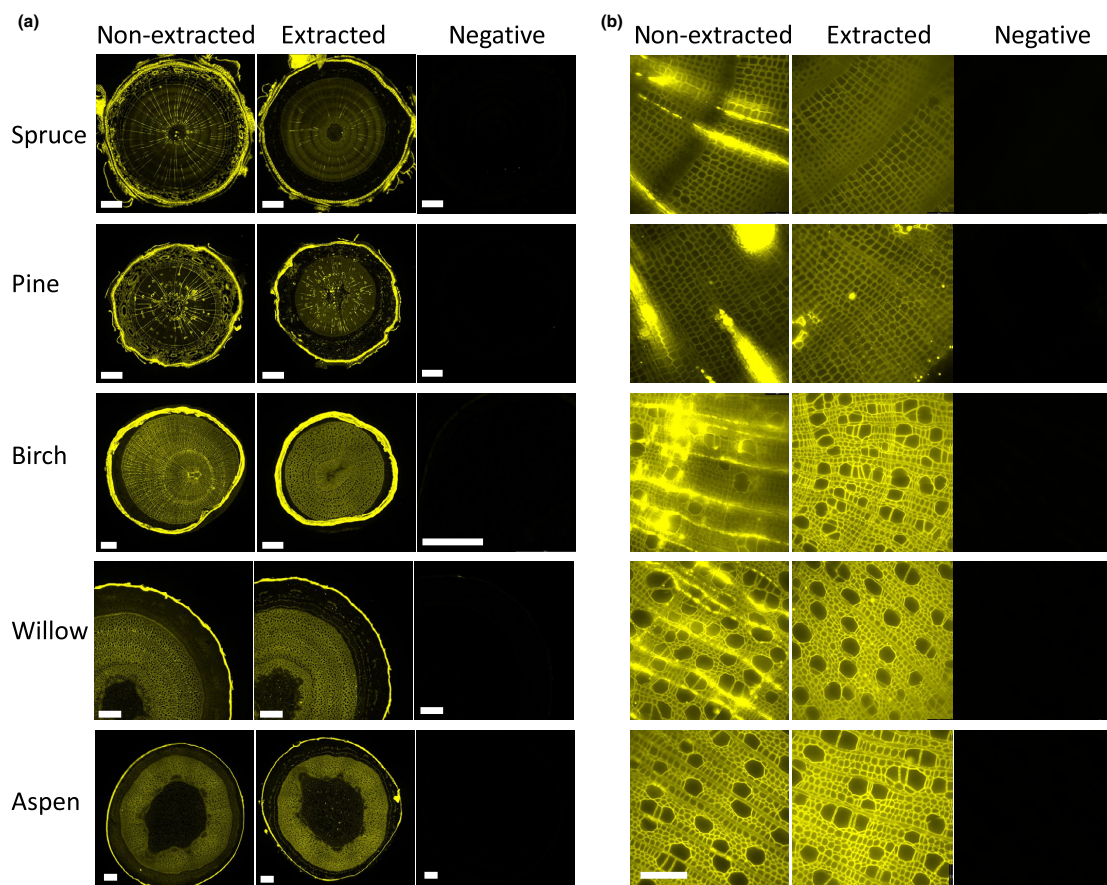


Fig. 4 Histochemical analysis of aliphatic compounds in extracted and nonextracted wood sections of different tree species. Samples collected during dormancy and stained with FY088. (a) Fluorescence channel pictures. Bars, 500 μm . Negative control without FY088 shows signal from lignin autofluorescence. (b) Fluorescence channel pictures at a higher magnification showing wood. Bar, 100 μm , for all micrographs.

expressing *AnAgu67A* under the control of a wood-specific promoter (Ratke *et al.*, 2015) were constructed in *A. thaliana* and their secondarily thickened hypocotyl sections were stained with FY088 before and after removal of extractives. Two independent most highly expressing lines, 2j2 and 5b2, each exhibiting α -glucuronidase activity (Fig. S7a–c), showed the mobilization of FY088-stained toluene-ethanol-resistant lipids from the cell walls of secondary xylem (Figs 3c,d, S7d), similar to transgenic aspen.

To determine whether the mobilization of suberin-like lipids is mediated by the reduction in mGlcA decorations on the xylan backbone or the presence of α -glucuronidase activity in the cell walls, we analyzed the extraction-resistant lipids by FY088 staining in the *gux1gux2* mutant (deficient in the main xylan glucuronosyl transferases responsible for secondary wall xylan glucuronosylation; Mortimer *et al.*, 2010), which under our conditions exhibited *c.* fourfold reduction in xylan glucuronosylation level (Chong *et al.*, 2014). The mutant displayed reduced levels

of solvent-resistant aliphatic compounds in the cell walls, whereas its total aliphatic compound levels were unaffected (Figs 3c,d, S7d), indicating increased mobility of cell wall lipids compared with WT (Col-0). Thus, the solvent-resistant suberin-like fraction is dependent on the presence of mGlcA decorations on xylan.

Presence of aliphatic compounds in different woody species

The presence of aliphatic, solvent-resistant compounds in the cell walls of healthy xylem tissue has not been previously recognized in woody species. Therefore, we investigated whether such compounds could be detected in softwoods (Norway spruce (*Picea abies* L.) and Scots pine (*Pinus sylvestris* L.)) and in other hardwoods (downy birch (*Betula pubescens* Ehrh.), goat willow (*Salix caprea* L.), and European aspen (*P. tremula* L.)). Wood samples collected during winter dormancy were sectioned and stained

with FY088 before and after the removal of extractives. In both extracted and nonextracted wood sections, strong, specific staining was observed in the cell walls of mature wood and cork (Fig. 4a,b). Nonextracted samples showed additional signals from live ray cells and resin canals, corresponding to lipids stored for winter dormancy and resin, respectively. The disappearance of these signals in extracted sections confirmed the effective removal of wood extractives (Fig. 4b). Quantification of the FY088 signal in the cell walls (Fig. S8) demonstrated weaker staining in spruce and pine cell walls compared with that observed in the hardwoods. Moreover, the wood of pine, birch, and willow exhibited stronger signals after removal of extractives, suggesting the presence interfering or masking compounds in the extractives. The signal remaining in cell walls after extractives removal corresponding to wall-bound lipids could be clearly seen in all analyzed species.

To analyze the distribution of these lipids in different wood cell wall layers, we examined normal and reaction woods (tension and compression woods) in all studied species at a higher resolution (Fig. 5). In spruce and pine, the solvent-resistant FY088 signals were distributed evenly throughout the primary and secondary wall layers of normal and compression woods, but were weaker in the compression wood. In birch, willow, and aspen, the signals were associated with lignified cell wall layers of normal and tension woods and were excluded from nonlignified gelatinous cell wall layers.

Discussion

Aspergillus niger α -glucuronidase *AnAgu67A* was shown to hydrolyze only mGlcA xylan decorations exposed at the nonreducing xylan end, typical to GH67 family of α -glucuronidases. When expressed in hybrid aspen and targeted to cell walls, it could remove c. 30% of mGlcA decorations. *PtxXyn10A* xylan endotransglycosylase is the only known GH10 family gene expressed in developing wood that could expose mGlcA for *AnAgu67A* hydrolysis (Derba-Maceluch *et al.*, 2015). GH10 enzymes were not analyzed for their ability to hydrolyze the xylan backbone at Xylp residues carrying mGlcA covalently linked to lignin, but it is rather unlikely that such bulky molecules could fit in the binding pocket at their +1 subsite. Therefore, we assume that *PtxXyn10A* cleaves the xylan backbone beside unbound mGlcA. Moreover, as the catalytic site of the GH67 α -glucuronidase of *Cellvibrio japonicus* has been shown to interact with the mGlcA carboxyl residue (Nagy *et al.*, 2003), *AnAgu67A* is also predicted to remove only unbound mGlcA xylan decorations; this would affect γ -ester linkages to lignin if these linkages are formed in the cell wall. However, if the γ -ester linkages are formed intracellularly, then their frequency is not expected to be affected by cell wall-localized *AnAgu67A*. As we found no reduction in the presence of γ -ester linkages in transgenic aspen lines with a 30% reduction in mGlcA, and no decrease in amount of xylan associated to lignin by either methanolysis-TMS or by NMR analyses, we propose that these linkages are formed intracellularly. The process could be envisioned as an intracellular addition of benzyl substitutions to UDP-linked GlcA, analogous to the addition of ferulate or *p*-coumarate substitutions on UDP-

linked arabinose by BAHD family acyl transferases, followed by the incorporation of acylated sugar units to the xylan backbone, as is suggested for grasses (Piston *et al.*, 2010; Bartley *et al.*, 2013; Rennie & Scheller, 2014; Buanafina *et al.*, 2016; Feijao *et al.*, 2022). The intracellular γ -ester linkages formation suggested by the results of this study is in agreement of the recent computational analysis of LCC formation showing that glucuronic acid is less likely to be involved in the nucleophilic attack on quinone methide intermediate compared with neutral sugars or water; thus, it is unlikely to participate in LCC formation in cell walls (Beck *et al.*, 2022). As *AnAgu67A* did not affect γ -ester linkages, we did not detect any positive effect of removal of mGlcA on saccharification in transgenic lines.

Our results showed that introducing α -glucuronidase to secondary cell walls or mutating *GUX1* and *GUX2* (encoding the main GlcA transferases involved in secondary wall xylan biosynthesis; Mortimer *et al.*, 2010, 2015; Lee *et al.*, 2012; Rennie *et al.*, 2012; Bromley *et al.*, 2013), both increased the solubility of the suberin-like aliphatic compounds, indicating that glucuronoxylan with mGlcA decorations is involved in anchoring them to wood cell walls. In agreement, no FY088 staining was detected in the gelatinous layers that contain little or no glucuronoxylan (Gorshkova *et al.*, 2015; Guedes *et al.*, 2017). Monomers of cutin and suberin are commonly present in wood extractives, which constitute 1–5% of the dry wood weight (Björklund Jansson & Nilvebrant, 2009) and we extracted more such monomers from transgenic plants expressing *AnAgu67A* compared with WT. Suberin monomers have also been identified in the xylem sap of several angiosperm species (Schenk *et al.*, 2021). Wood extractives are known to permeate cell walls in heartwood, which makes them resistant to solvents, suggesting their polymerization and/or covalent linking with other cell wall polymers (Björklund Jansson & Nilvebrant, 2009; Donaldson *et al.*, 2019). Present data suggest their linking to cell walls *via* mGlcA xylan decorations.

The suberin has been shown to remain in the wood cell wall after refluxing wood with lipid solvents (Pearce & Holloway, 1984), although this was previously only thought to occur in infected or damaged wood tissue (Biggs, 1987; Pearce, 1990; Kashyap *et al.*, 2022). Suberin was also demonstrated in cells adjacent to epithelial cells of resin canals in pine (Donaldson *et al.*, 2015). Low suberin levels (0.2–1% of the dry wood weight) were also reported in healthy oak wood, but it was thought to be associated with tyloses or with the inner cell wall layer of tracheary elements, based on Sudan IV and FM1-43 staining patterns (Pearce & Holloway, 1984; Biggs, 1987; Schenk *et al.*, 2021), whereas we identified lipids in all lignified cell wall layers, including the compound middle lamella and the secondary wall layers, using FY088. Sudan IV and FM1-43 are larger than FY088, and may not be able to penetrate more compact and heavily lignified outermost cell wall layers (Ruel *et al.*, 2006; Donaldson *et al.*, 2019) explaining their contrasting labeling pattern compared with FY088. The FY088 labeling pattern is supported by previous time-of-flight secondary ion mass spectrometry imaging, detecting FAs, and DMGs/TMGs in the entire cell wall of tracheids in larch (Fu *et al.*, 2018).

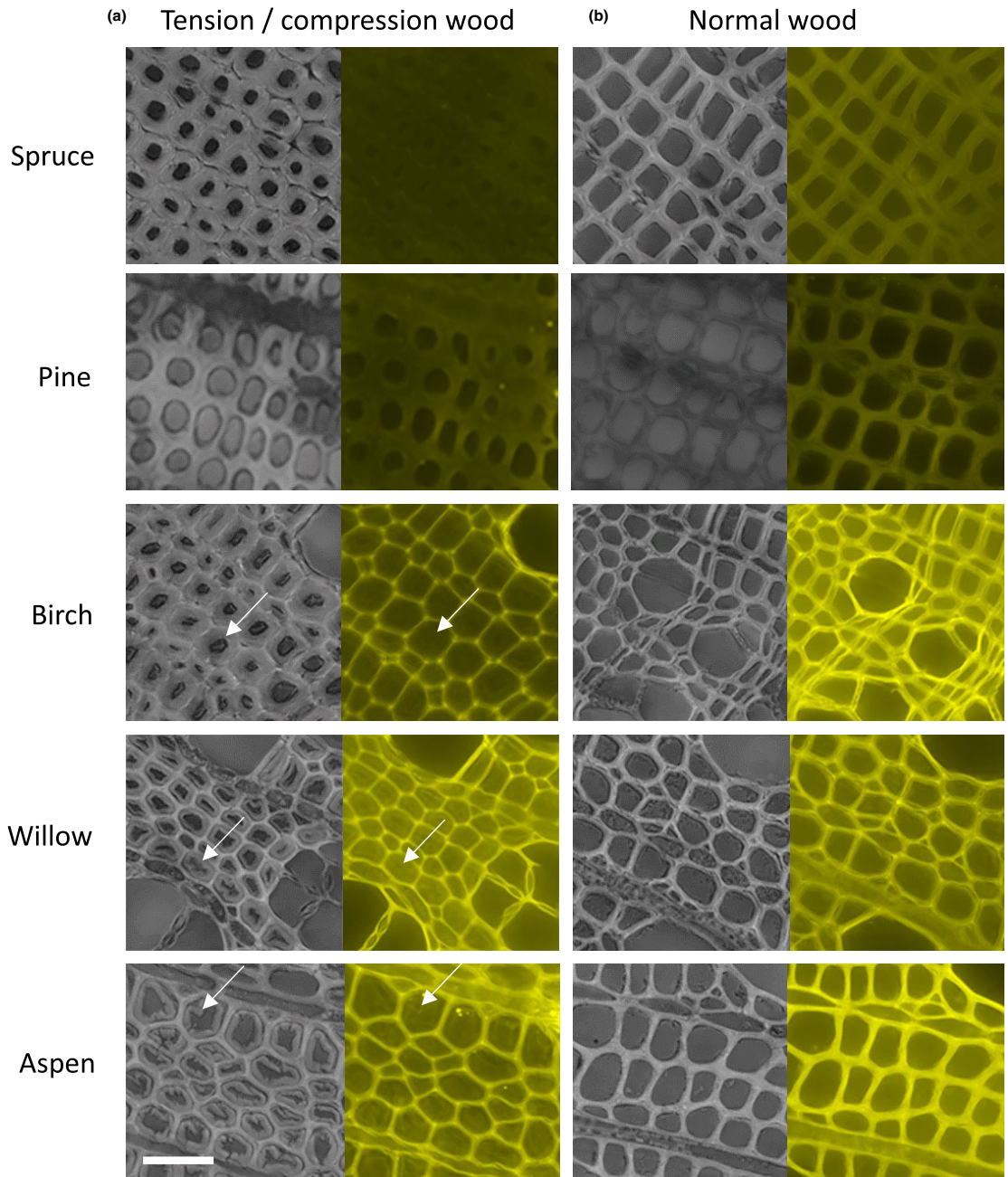


Fig. 5 Histochemical analysis of aliphatic compounds in extracted normal and reaction wood sections of different tree species. Samples collected during dormancy and stained with FY088. (a) Tension or compression wood. (b) Normal wood. Bright field (left) and fluorescence (right) channel pictures. Note the lack of signal in gelatinous cell wall layers (arrows). Bar, 25 μm .

Future studies should focus on elucidating the structure of these suberin-like components of wood cell walls and their connection to xylan mGlcA. The awareness of the presence of such compounds in wood cell walls is crucial for our understanding of wood physiology, particularly water conduction and wood decay processes. It has also bearing on the utilization of lignocellulose as a renewable resource, for developing novel technological processes of cell wall disintegration, and for solving problems of pitch on machinery observed during wood processing (Back & Allen, 2000).

Acknowledgements

We wish to thank Dr J. Takahashi-Schmidt of the Biopolymer Analytical Platform of KBC at Umeå University for her help with the cell wall analyses; Dr A. Gorzsás of the Vibrational Spectroscopy Core Facility of KBC at Umeå University for his help with the FT-IR analyses; and the Umeå Plant Science Centre (UPSC) Microscopy Facility. We are grateful to Prof. M. Tenkanen, University of Helsinki for the donation of the enzyme substrates and mGlcA. This work was supported by grants from the Knut and Alice Wallenberg Foundation (KAW), the Swedish Governmental Agency for Innovation Systems (VINNOVA), the Swedish Foundation for Strategic Research (SSF; project Value-Tree RBP14-0011), Kempestiftelsen, the Swedish Research Council VR, FORMAS, Bio4Energy, the Swedish University of Agricultural Sciences (SLU), Genome Canada, and Genome Quebec.

Competing interests

None declared.

Author contributions

MD-M, ERM and EJM designed the experiments. MD-M conducted most of the experiments with help from the other co-authors. MH performed NMR analyses. AT, JP and ERM identified, cloned, and characterized the *AnAgu67A* of *A. niger*. XL conducted the initial glasshouse phenotyping of transgenic aspen lines; MLG and LJJ analyzed the saccharification of transgenic wood. FRB characterized the transgenic *Arabidopsis* lines expressing *AnAgu67A*. MM, INA and TM analyzed the phenolics and lipids extracted from the wood. END and JU conducted the transcriptomic analysis of transgenic aspen. MD-M and EJM wrote the manuscript with help from the co-authors. All the authors read and commented on the manuscript.

ORCID

Ilka N. Abreu  <https://orcid.org/0000-0003-4728-0161>
 Félix R. Barbut  <https://orcid.org/0000-0001-5395-6776>
 Marta Derba-Maceluch  <https://orcid.org/0000-0002-8034-3630>
 Evgeniy N. Donev  <https://orcid.org/0000-0002-7279-0481>
 Madhavi L. Gandla  <https://orcid.org/0000-0003-2798-6298>

Mattias Hedenström  <https://orcid.org/0000-0002-0903-6662>
 Leif J. Jönsson  <https://orcid.org/0000-0003-3866-0111>
 Xiaokun Liu  <https://orcid.org/0000-0002-4889-8361>
 Emma R. Master  <https://orcid.org/0000-0002-6837-9817>
 Ewa J. Mellerowicz  <https://orcid.org/0000-0001-6817-1031>
 Madhusree Mitra  <https://orcid.org/0000-0002-8653-8770>
 Thomas Moritz  <https://orcid.org/0000-0002-4258-3190>
 Adrian Tsang  <https://orcid.org/0000-0002-5892-4797>
 János Urbancsik  <https://orcid.org/0000-0003-3237-6806>

Data availability

The data supporting the findings of this study are available within the paper and/or its [Supporting Information](#). RNA sequencing data are available at ENA (<https://www.ebi.ac.uk/ena/browser/home>) under accession number: PRJEB53456.

References

- Abreu IN, Johansson AI, Sokolowska K, Niittylä T, Sundberg B, Hvidsten TR, Street NR, Moritz T. 2020. A metabolite roadmap of the wood-forming tissue in *Populus tremula*. *New Phytologist* **228**: 1559–1572.
- Addison B, Stengel D, Bharadwaj VS, Happs RM, Doepcke C, Wang T, Bomble YJ, Holland GP, Harman-Ware AE. 2020. Selective one-dimensional ^{13}C spin-diffusion solid-state nuclear magnetic resonance methods to probe spatial arrangements in biopolymers including plant cell walls, peptides, and spider silk. *The Journal of Physical Chemistry. B* **124**: 9870–9883.
- Back EL, Allen LH. 2000. *Pitch control, wood resin and deresination*. Atlanta, GA, USA: TAPPI Press.
- Balakshin M, Capanema E, Gracz H, Chang HM, Jameel H. 2011. Quantification of lignin-carbohydrate linkages with high-resolution NMR spectroscopy. *Planta* **233**: 1097–1110.
- Bar-On YM, Phillips R, Milo R. 2018. The biomass distribution on earth. *Proceedings of the National Academy of Sciences, USA* **115**: 6506–6511.
- Bartley LE, Peck ML, Kim SR, Ebert B, Manisseri C, Chiniquy DM, Sykes R, Gao L, Rautengarten C, Vega-Sánchez ME *et al.* 2013. Overexpression of a BAHD acyltransferase, *OsAt10*, alters rice cell wall hydroxycinnamic acid content and saccharification. *Plant Physiology* **161**: 1615–1633.
- Beck S, Choi P, Mushrif SH. 2022. Origins of covalent linkages within the lignin-carbohydrate network of biomass. *Physical Chemistry Chemical Physics* **24**: 20480–20490.
- Berglund J, Mikkelsen D, Flanagan BM, Dhital S, Gaunitz S, Henriksson G, Lindström ME, Yakubov GE, Gidley MJ, Vilaplana F. 2020. Wood hemicelluloses exert distinct biomechanical contributions to cellulose fibrillar networks. *Nature Communications* **11**: 4692.
- Bernards MA. 2002. Demystifying suberin. *Canadian Journal of Botany* **80**: 227–240.
- Biggs AR. 1987. Occurrence and location of suberin in wound reaction zones in xylem of 17 tree species. *Phytopathology* **77**: 718–725.
- Björklund Jansson M, Nilvebrant N-O. 2009. Wood extractives. In: Ek M, Gellerstedt G, Henriksson G, eds. *Wood chemistry and wood biotechnology*. Berlin, Germany: de Gruyter, 147–171.
- Bromley JR, Busse-Wicher M, Tryfona T, Mortimer JC, Zhang Z, Brown DM, Dupree P. 2013. GUX1 and GUX2 glucuronyltransferases decorate distinct domains of glucuronoxylan with different substitution patterns. *The Plant Journal* **74**: 423–434.
- Buanafina MM, Fescemyer HW, Sharma M, Shearer EA. 2016. Functional testing of a PF02458 homologue of putative rice arabinoxylan feruloyl transferase genes in *Brachypodium distachyon*. *Planta* **243**: 659–674.
- Busse-Wicher M, Gomes TC, Tryfona T, Nikolovski N, Stott K, Grantham NJ, Bolam DN, Skaf MS, Dupree P. 2014. The pattern of xylan acetylation suggests xylan may interact with cellulose microfibrils as a twofold helical screw

- in the secondary plant cell wall of *Arabidopsis thaliana*. *The Plant Journal* 79: 492–506.
- Busse-Wicher M, Li A, Silveira RL, Pereira CS, Tryfona T, Gomes TC, Skaf MS, Dupree P. 2016. Evolution of xylan substitution patterns in gymnosperms and angiosperms: implications for xylan interaction with cellulose. *Plant Physiology* 171: 2418–2431.
- Chang SJ, Puryear J, Cairney J. 1993. A simple and efficient method for isolating RNA from pine trees. *Plant Molecular Biology Reporter* 11: 113–116.
- Chong SL, Derba-Maceluch M, Koutaniemi S, Gómez LD, McQueen-Mason SJ, Tenkanen M, Mellerowicz EJ. 2015. Active fungal GH115 α -glucuronidase produced in *Arabidopsis thaliana* affects only the UX1-reactive glucuronate decorations on native glucuronoxylans. *BMC Biotechnology* 15: 56.
- Chong SL, Koutaniemi S, Virkki L, Pynnönen H, Tuomainen P, Tenkanen M. 2013. Quantitation of 4-O-methylglucuronic acid from plant cell walls. *Carbohydrate Polymers* 91: 626–630.
- Chong SL, Virkki L, Maaheimo H, Juvonen M, Derba-Maceluch M, Koutaniemi S, Roach M, Sundberg B, Tuomainen P, Mellerowicz EJ *et al.* 2014. O-acetylation of glucuronoxylan in *Arabidopsis thaliana* wild type and its change in xylan biosynthesis mutants. *Glycobiology* 24: 494–506.
- Clough SJ, Bent AF. 1998. Floral dip: a simplified method for *Agrobacterium* mediated transformation of *Arabidopsis thaliana*. *The Plant Journal* 16: 735–743.
- Correia VG, Bento A, Pais J, Rodrigues R, Haliński LP, Frydrych M, Greenhalgh A, Stepnowski P, Vollrath F, King AWT *et al.* 2020. The molecular structure and multifunctionality of the cryptic plant polymer suberin. *Materials Today Bio* 5: 100309.
- Derba-Maceluch M, Awano T, Takahashi J, Lucenius J, Ratke C, Kontro I, Busse-Wicher M, Kosik O, Tanaka R, Winzell A *et al.* 2015. Suppression of xylan endotransglycosylase *PtxXyn10A* affects cellulose microfibril angle in secondary wall in aspen wood. *New Phytologist* 205: 666–681.
- Donaldson LA, Nanayakkara B, Radotić K, Djikanović-Golubović D, Mitrović A, Bogdanović Pristov J, Simonović Radosavljević J, Kalauzi A. 2015. Xylem parenchyma cell walls lack a gravitropic response in conifer compression wood. *Planta* 242: 1413–1424.
- Donaldson LA, Singh A, Raymond L, Hill S, Schmitt U. 2019. Extractive distribution in *Pseudotsuga menziesii*: effects on cell wall porosity in sapwood and heartwood. *IAWA Journal* 40: 721–740.
- Feijao C, Morreel K, Anders N, Tryfona T, Busse-Wicher M, Kotake T, Boerjan W, Dupree P. 2022. Hydroxycinnamic acid-modified xylan side chains and their cross-linking products in rice cell walls are reduced in the xylosyl arabinosyl substitution of xylan 1 mutant. *The Plant Journal* 109: 1152–1167.
- Fernandes AN, Thomas LH, Altaner CM, Callow P, Forsyth VT, Apperley DC, Kennedy CJ, Jarvis MC. 2011. Nanostructure of cellulose microfibrils in spruce wood. *Proceedings of the National Academy of Sciences, USA* 108: E1195–E1203.
- Franková L, Fry SC. 2011. Phylogenetic variation in glycosidases and glycanases acting on plant cell wall polysaccharides, and the detection of transglycosidase and trans- β -xylanase activities. *The Plant Journal* 67: 662–681.
- Fu T, Elie N, Brunelle A. 2018. Radial distribution of wood extractives in European larch *Larix decidua* by TOF-SIMS imaging. *Phytochemistry* 150: 31–39.
- Gandla LM, Derba-Maceluch M, Liu X, Gerber L, Master ER, Mellerowicz EJ, Jönsson LJ. 2015. Expression of a fungal glucuronoyl esterase in *Populus*: effects on wood properties and saccharification efficiency. *Phytochemistry* 112: 210–220.
- Gerber L, Eliasson M, Trygg J, Moritz T, Sundberg B. 2012. Multivariate curve resolution provides a high-throughput data processing pipeline for pyrolysis gas chromatography/mass spectrometry. *Journal of Analytical and Applied Pyrolysis* 95: 95–100.
- Giummarella N, Pu Y, Ragauskas AJ, Lawoko M. 2019. A critical review on the analysis of lignin carbohydrate bonds. *Green Chemistry* 21: 1573–1595.
- Gorshkova T, Mokshina N, Chernova T, Ibragimova N, Salnikov V, Mikshina P, Tryfona T, Banasiak A, Immerzeel P, Dupree P *et al.* 2015. Aspen tension wood fibers contain β -(1 \rightarrow 4)-galactans and acidic arabinogalactans retained by cellulose microfibrils in gelatinous walls. *Plant Physiology* 169: 2048–2063.
- Graça J. 2010. Hydroxycinnamates in suberin formation. *Phytochemistry Reviews* 9: 85–91.
- Grantham NJ, Wurman-Rodrich J, Terrett OM, Lyczakowski JJ, Stott K, Iuga D, Simmons TJ, Durand-Tardif M, Brown SP, Dupree R *et al.* 2017. An even pattern of xylan substitution is critical for interaction with cellulose in plant cell walls. *Nature Plants* 3: 859–865.
- Gray-Mitsumune M, Mellerowicz EJ, Abe H, Schrader J, Winzell A, Sterky F, Blomqvist K, McQueen-Mason S, Teeri TT, Sundberg B. 2004. Expansins abundant in secondary xylem belong to subgroup A of the α -expansin gene family. *Plant Physiology* 135: 1552–1564.
- Gray-Mitsumune M, Mellerowicz EJ, Abe H, Schrader J, Winzell A, Sterky F, Blomqvist K, McQueen-Mason S, Teeri TT, Sundberg B. 2008. Ectopic expression of a wood-abundant expansin PrtEXP1A promotes cell expansion in primary and secondary tissues in aspen. *Plant Biotechnology Journal* 6: 62–72.
- Guedes FTP, Laurans F, Quemener B, Assor C, Lainé-Prade V, Boizot N, Vigouroux J, Lesage-Descauses MC, Lepélé JC, Déjardin A *et al.* 2017. Non-cellulosic polysaccharide distribution during G-layer formation in poplar tension wood fibers: abundance of rhamnogalacturonan I and arabinogalactan proteins but no evidence of xyloglucan. *Planta* 246: 857–878.
- Gullberg J, Jonsson P, Nordström A, Sjöström M, Moritz T. 2004. Design of experiments: an efficient strategy to identify factors influencing extraction and derivatization of *Arabidopsis thaliana* samples in metabolomic studies with gas chromatography-mass spectrometry. *Analytical Biochemistry* 331: 283–295.
- Hedenström M, Wiklund-Lindström S, Oman T, Lu F, Gerber L, Schatz P, Sundberg B, Ralph J. 2009. Identification of lignin and polysaccharide modifications in *Populus* wood by chemometric analysis of 2D NMR spectra from dissolved cell walls. *Molecular Plant* 2: 933–942.
- Kang X, Kirui A, Dickwella Widanage MC, Mentink-Vigier F, Cosgrove DJ, Wang T. 2019. Lignin-polysaccharide interactions in plant secondary cell walls revealed by solid-state NMR. *Nature Communications* 10: 1–9.
- Karimi M, Inzé D, Depicker A. 2002. Gateway vectors for *Agrobacterium*-mediated plant transformation. *Trends in Plant Science* 7: 193–195.
- Kashyap A, Jiménez-Jiménez AL, Zhang W, Capellades M, Srinivasan S, Laromaine A, Serra O, Figueras M, Rencoret J, Gutiérrez A *et al.* 2022. Induced ligno-suberin vascular coating and tyramine-derived hydroxycinnamic acid amides restrict *Ralstonia solanacearum* colonization in resistant tomato. *New Phytologist* 234: 1411–1429.
- Kasper PT, Rojas-Chertó M, Mistrik R, Reijmers T, Hankemeier T, Vreeken RJ. 2012. Fragmentation trees for the structural characterisation of metabolites. *Rapid Communications in Mass Spectrometry* 26: 2275–2286.
- Kim H, Ralph J, Akiyama T. 2008. Solution-state 2D NMR of ball-milled plant cell wall gels in DMSO-d₆. *Bioenergy Research* 1: 56–66.
- Koutaniemi S, Guillon F, Tranquet O, Bouchet B, Tuomainen P, Virkki L, Petersen HL, Willats WG, Saulnier L, Tenkanen M. 2012. Substituent-specific antibody against glucuronoxylan reveals close association of glucuronic acid and acetyl substituents and distinct labeling patterns in tree species. *Planta* 236: 739–751.
- Kumar V, Hainaut M, Delhomme N, Mannapperuma C, Immerzeel P, Street NR, Henrissat B, Mellerowicz EJ. 2019. Poplar carbohydrate-active enzymes: whole-genome annotation and functional analyses based on RNA expression data. *The Plant Journal* 99: 598–609.
- Lee C, Teng Q, Zhong R, Ye ZH. 2012. Arabidopsis GUX proteins are glucuronyltransferases responsible for the addition of glucuronic acid side chains onto xylan. *Plant & Cell Physiology* 53: 1204–1216.
- Lee C, Teng Q, Zhong R, Ye ZH. 2014. Alterations of the degree of xylan acetylation in *Arabidopsis* xylan mutants. *Plant Signaling & Behavior* 9: 1186–1199.
- Livak KJ, Schmittgen TD. 2001. Analysis of relative gene expression data using real-time quantitative PCR and the 2^{- $\Delta\Delta$ CT} method. *Methods* 25: 402–408.
- Lux A, Morita S, Abe J, Ito K. 2005. An improved method for clearing and staining free-hand sections and whole-mount samples. *Annals of Botany* 96: 989–996.
- Lyczakowski JJ, Bourdon M, Terrett OM, Helariutta V, Wightman R, Dupree P. 2019. Structural imaging of native cryo-preserved secondary cell walls reveals the presence of microfibrils and their formation requires normal cellulose, lignin and xylan biosynthesis. *Frontiers in Plant Science* 10: 1398.
- Lyczakowski JJ, Wicher KB, Terrett OM, Faria-Blanc N, Yu X, Brown D, Krogh KBRM, Dupree P, Busse-Wicher M. 2017. Removal of glucuronic acid

- from xylan is a strategy to improve the conversion of plant biomass to sugars for bioenergy. *Biotechnology for Biofuels* 10: 224.
- Lyczakowski JJ, Yu L, Terrett OM, Fleischmann C, Temple H, Thorlby G, Sorieul M, Dupree P. 2021. Two conifer GUX clades are responsible for distinct glucuronic acid patterns on xylan. *New Phytologist* 231: 1720–1733.
- Martínez-Abad A, Berglund J, Toriz G, Gatenholm P, Henriksson G, Lindström M, Wohler J, Vilaplana F. 2017. Regular motifs in xylan modular molecular flexibility and interactions with cellulose surfaces. *Plant Physiology* 175: 1579–1592.
- Martínez-Abad A, Giummarella N, Lawoko M, Vilaplana F. 2018. Differences in extractability under subcritical water reveal interconnected hemicellulose and lignin recalcitrance in birch hardwoods. *Green Chemistry* 20: 2534–2546.
- Martínez-Abad A, Jiménez-Quero A, Wohlert J. 2020. Influence of the molecular motifs of mannan and xylan populations on their recalcitrance and organization in spruce softwoods. *Green Chemistry* 22: 3956–3970.
- Melo T, Figueiredo ARP, da Costa E, Couto D, Silva J, Domingues MR, Domingues P. 2021. Ethanol extraction of polar lipids from *Nannochloropsis oceanica* for food, feed, and biotechnology applications evaluated using lipidomic approaches. *Marine Drugs* 19: 593.
- Meshitsuka G, Nakano J. 1977. Studies on the mechanism of lignin color reaction XI. Mäule color reaction. *Mokuzai Gakkaishi* 23: 232–236.
- Mortimer JC, Faria-Blanc N, Yu X, Tryfona T, Sorieul M, Ng YZ, Zhang Z, Stott K, Anders N, Dupree P. 2015. An unusual xylan in *Arabidopsis* primary cell walls is synthesised by GUX3, IRX9L, IRX10L and IRX14. *The Plant Journal* 83: 413–426.
- Mortimer JC, Miles GP, Brown DM, Zhang Z, Segura MP, Weimar T, Yu X, Seffen KA, Stephens E, Turner SR *et al.* 2010. Absence of branches from xylan in *Arabidopsis gux* mutants reveals potential for simplification of lignocellulosic biomass. *Proceedings of the National Academy of Sciences, USA* 107: 17409–17414.
- Nagy T, Nurizzo D, Davies GJ, Biely P, Lakey JH, Bolam DN, Gilbert HJ. 2003. The alpha-glucuronidase, GlcA67A, of *Cellvibrio japonicus* utilizes the carboxylate and methyl groups of aldobioinonic acid as important substrate recognition determinants. *The Journal of Biological Chemistry* 278: 20286–20292.
- Naser S, Lee Y, Lapierre C, Franke R, Nawrath C, Geldner N. 2012. Casparian strip diffusion barrier in *Arabidopsis* is made of a lignin polymer without suberin. *Proceedings of the National Academy of Sciences, USA* 109: 10101–10106.
- Öman T, Tessem MB, Bathen TF, Bertilsson H, Angelsen A, Hedenström M, Andreassen T. 2014. Identification of metabolites from 2D ¹H-¹³C HSQC NMR using peak correlation plots. *BMC Bioinformatics* 15: 413.
- Pawar PM, Derba-Maceluch M, Chong SL, Gómez LD, Miedes E, Banasiak A, Ratke C, Gaertner C, Mouille G, McQueen-Mason SJ *et al.* 2016. Expression of fungal acetyl xylan esterase in *Arabidopsis thaliana* improves saccharification of stem lignocellulose. *Plant Biotechnology Journal* 14: 387–397.
- Pearce RB. 1990. Occurrence of decay-associated xylem suberization in a range of woody species. *European Journal of Forest Pathology* 20: 275–289.
- Pearce RB, Holloway PJ. 1984. Suberin in the sapwood of oak (*Quercus robur* L.): its composition from a compartmentalization barrier and its occurrence in tyloses in undecayed wood. *Physiological Plant Pathology* 24: 71–81.
- Pereira CS, Silveira RL, Dupree P, Skaf MS. 2017. Effects of xylan side-chain substitutions on xylan–cellulose interactions and implications for thermal pretreatment of cellulosic biomass. *Biomacromolecules* 18: 1311–1321.
- Pfaff MW. 2001. A new mathematical model for relative quantification in real-time RT-PCR. *Nucleic Acids Research* 29: e45.
- Piston F, Uauy C, Fu L, Langston J, Labavitch J, Dubcovsky J. 2010. Down-regulation of four putative arabinoxylan feruloyl transferase genes from family PF02458 reduces ester-linked ferulate content in rice cell walls. *Planta* 231: 677–691.
- Ratke C, Pawar PM, Balasubramanian VK, Naumann M, Duncranz ML, Derba-Maceluch M, Gorzús A, Endo S, Ezcurra I, Mellerowicz EJ. 2015. Populus GT 43 family members group into distinct sets required for primary and secondary wall xylan biosynthesis and include useful promoters for wood modification. *Plant Biotechnology Journal* 13: 26–37.
- Rennie EA, Hansen SF, Baidoo EE, Hadi MZ, Keasling JD, Scheller HV. 2012. Three members of the *Arabidopsis* glycosyltransferase family 8 are xylan glucuronosyltransferases. *Plant Physiology* 159: 1408–1417.
- Rennie EA, Scheller HV. 2014. Xylan biosynthesis. *Current Opinion in Biotechnology* 26: 100–107.
- Rudsander UJ, Denman S, Raza S, Teeri TT. 2003. Molecular features of family GH9 cellulases in hybrid aspen and the filamentous fungus *Phanerochaete chrysosporium*. *Journal of Applied Glycoscience* 50: 253–256.
- Ruel K, Chevalier-Billosta V, Guillemin F, Sierra JB, Joseleau J-P. 2006. The wood cell wall at the ultrastructural scale- formation and topochemical organization. *Maderas Ciencia y Tecnología* 8: 107–116.
- Schenk HJ, Michaud JM, Mocko K, Espino S, Melendres T, Roth MR, Welti R, Kaack L, Jansen S. 2021. Lipids in xylem sap of woody plants across the angiosperm phylogeny. *The Plant Journal* 105: 1477–1494.
- Shakeri Yekta S, Hedenström M, Svensson BH, Sundgren I, Dario M, Enrich-Prast A, Hertkorn N, Björn A. 2019. Molecular characterization of particulate organic matter in full scale anaerobic digesters: an NMR spectroscopy study. *Science of the Total Environment* 685: 1107–1115.
- Storms R, Zheng Y, Li H, Sillaois S, Martínez-Pérez A, Tsang A. 2005. Plasmid vectors for protein production, gene expression and molecular manipulations in *Aspergillus niger*. *Plasmid* 53: 191–204.
- Tarasov D, Leitch M, Fatehi P. 2018. Lignin–carbohydrate complexes: properties, applications, analyses, and methods of extraction: a review. *Biotechnology for Biofuels* 11: 269.
- Tenkanen M, Siika-aho M. 2000. An alpha-glucuronidase of *Schizophyllum commune* acting on polymeric xylan. *Journal of Biotechnology* 78: 149–161.
- Terashima N, Kitano K, Kojima M, Yoshida M, Yamamoto H, Westermark U. 2009. Nanostructural assembly of cellulose, hemicellulose, and lignin in the middle layer of secondary wall of ginkgo tracheid. *Journal of Wood Science* 55: 409–416.
- Terrett OM, Dupree P. 2019. Covalent interactions between lignin and hemicelluloses in plant secondary cell walls. *Current Opinion in Biotechnology* 56: 97–104.
- Terrett OM, Lyczakowski JJ, Yu L, Iuga D, Franks WT, Brown SP, Dupree R, Dupree P. 2019. Molecular architecture of softwood revealed by solid-state NMR. *Nature Communications* 10: 4978.
- Theander O, Westerlund EA. 1986. Studies on dietary fiber. 3. Improved procedures for analysis of dietary fiber. *Journal of Agricultural and Food Chemistry* 34: 330–336.
- Updegraff D. 1969. Semimicro determination of cellulose in biological materials. *Analytical Biochemistry* 32: 420–424.

Supporting Information

Additional Supporting Information may be found online in the Supporting Information section at the end of the article.

Fig. S1 Enzymatic activity of recombinant *AnAgu67A* purified from *Aspergillus niger* Tiegh.

Fig. S2 Chemical analyses and saccharification sugar yields of wood of transgenic aspen (*Populus tremula* L. × *tremuloides* Michx.) lines ectopically expressing *SP_{Cel9B3}::AnAgu67A*.

Fig. S3 Characterization of transgenic aspen (*Populus tremula* L. × *tremuloides* Michx.) lines carrying *35S::SP_{Cel9B3}::AnAgu67A* construct.

Fig. S4 Chemical analysis of dioxane lignin of transgenic and wild-type wood samples extracted with toluene-ethanol.

Fig. S5 NMR spectral characterization of dioxane-extracted lignin without removal of extractives (nonextracted wood) and after extractives removal (extracted wood).

Fig. S6 Histochemical analysis of lipophilic substances in wood with FY088 staining.

Fig. S7 General characterization of transgenic *Arabidopsis* lines carrying *WP::SP_{Cel9B3}:AnAgu67A* construct.

Fig. S8 Histochemical analysis of aliphatic compounds in cell walls in the wood of different species with FY088 staining.

Methods S1 Gene cloning and recombinant expression of *AnAgu67A*.

Methods S2 Enzyme activity of recombinant *AnAgu67A*.

Methods S3 Thin-layer chromatography for detecting of *AnAgu67A* alpha-glucuronidase activity.

Table S1 Primers used for RT-PCR analyses and cloning of hybrid genes for expression vectors.

Table S2 Differentially expressed genes in developing wood of transgenic aspen (*Populus tremula* L. × *tremuloides* Michx.) lines 4 and 6 expressing *SP_{Cel9B3}:AnAgu67A* compared with wild-type.

Table S3 List of lipidomics peaks (Mass@retention time) detected in wood extracts by liquid chromatography–mass spectrometry in positive and negative modes and analysis of differences in their integrated signal intensities between transgenic and wild-type samples by *t*-test.

Table S4 List of identified lipidic compounds in wood extracts that differed in abundance between transgenic and wild-type samples.

Table S5 List of all signals from metabolomics analysis.

Table S6 List of identified phenolic compounds in wood extracts that differed in abundance between transgenic and wild-type samples.

Please note: Wiley is not responsible for the content or functionality of any Supporting Information supplied by the authors. Any queries (other than missing material) should be directed to the *New Phytologist* Central Office.

See also the Commentary on this article by Oliveira, 238: 8–10.

IV

Modification of xylan in secondary walls alters cell wall biosynthesis and wood formation programs

Pramod Sivan^{1,6,#}, János Urbancsok^{1,#}, Evgeniy N. Donev¹, Marta Derba-Maceluch¹, Félix R. Barbut¹, Zakiya Yassin², Madhavi L. Gandla³, Madhusree Mitra¹, Saara E. Heinonen^{6,7}, Jan Šimura¹, Kateřina Cermanová⁴, Michal Karady⁴, Gerhard Scheepers², Leif J. Jönsson³, Emma R. Master⁵, Francisco Vilaplana^{6,7}, Ewa J. Mellerowicz^{1*}

¹ Umeå Plant Science Centre, Swedish University of Agricultural Sciences, Department of Forest Genetics and Plant Physiology, 901 83 Umeå, Sweden

² RISE Research Institutes of Sweden, Drottning Kristinas väg 61, 11428 Stockholm, Sweden

³ Department of Chemistry, Umeå University, 901 87 Umeå, Sweden

⁴ Laboratory of Growth Regulators, Palacký University, Institute of Experimental Botany, The Czech Academy of Sciences & Faculty of Science, Olomouc, CZ-783 71 Czechia

⁵ Department of Chemical Engineering and Applied Chemistry, University of Toronto, M5S 3E5 Canada

⁶ Division of Glycoscience, Department of Chemistry, KTH Royal Institute of Technology, AlbaNova University Centre, 106 91 Stockholm, Sweden

⁷ Wallenberg Wood Science Centre (WWSC), KTH Royal Institute of Technology, 100 44 Stockholm, Sweden

These authors contributed equally to this work.

*Author for correspondence:

Ewa J. Mellerowicz : ewa.mellerowicz@slu.se

Find this paper online for Supp tables: <https://www.biorxiv.org/content/10.1101/2024.05.02.592170v2>

Authors e-mail, ORCID

1. Pramod Sivan, psivan@kth.se 0000-0001-5297-2221
2. János Urbancsok, urbancsok.janos@gmail.com 0000-0003-3237-6806
3. Evgeniy N. Donev, evgeniy.donev@slu.se 0000-0002-7279-0481
4. Marta Derba-Maceluch, Marta.Derba-Maceluch@slu.se 0000-0002-8034-3630
5. Félix R. Barbut, felix.barbut@slu.se 0000-0001-5395-6776
6. Zakiya Yassin, zakiya.yassin@ri.se 0000-0001-6878-3361
7. Madhavi L. Gandla, madhavi.latha.gandla@umu.se 0000-0003-2798-6298
8. Madhusree Mitra, madhusree.mitra@slu.se 0000-0002-8653-8770

9. Saara E. Heinonen sehei@kth.se 0000-0002-5069-2370
10. Jan Šimura, jan.simura@slu.se 0000-0002-1567-2278
11. Kateřina Cermanová, katerina.cermanova01@upol.cz 0009-0006-5809-0733
12. Michal Karady, michal.karady@upol.cz 0000-0002-5603-706X
13. Gerhard Scheepers gerhard.scheepers@ri.se 0000-0002-5630-1377
14. Leif J. Jönsson, leif.jonsson@umu.se 0000-0003-3866-0111
15. Emma R. Master, emma.master@utoronto.ca 0000-0002-6837-9817
16. Francisco Vilaplana, franvila@kth.se 0000-0003-3572-7798
17. Ewa J. Mellerowicz, Ewa.Mellerowicz@slu.se 0000-0001-6817-1031

Key words: Glucuronoxylan, fungal xylanases, transgenic aspen, wood development, lignocellulose, secondary cell wall, hardwood genetic engineering

Word count: Intro 935, Results 2312, Discussion 2069, MM 2400, Total 7716 (max 7000).

Abstract

Wood of broad-leaf tree species is a valued source of renewable biomass for biorefinery and a target for genetic improvement efforts to reduce its recalcitrance. Glucuronoxylan (GX) plays a key role in recalcitrance through its interactions with cellulose and lignin. To reduce recalcitrance, we modified wood GX by expressing GH10 and GH11 endoxylanases from *Aspergillus nidulans* in hybrid aspen (*Populus tremula* L. x *tremuloides* Michx.) and targeting the enzymes to cell wall. The xylanases reduced tree height, modified cambial activity by increasing phloem and reducing xylem production, and reduced secondary wall deposition. Xylan molecular weight was decreased, and the spacing between acetyl and MeGlcA side chains was reduced in transgenic lines. The transgenic trees produced hypolignified xylem having thin secondary walls and deformed vessels. Glucose yields of enzymatic saccharification without pretreatment almost doubled indicating decreased recalcitrance. The transcriptomics, hormonomics and metabolomics data provided evidence for activation of cytokinin and ethylene signaling pathways, decrease in ABA levels, transcriptional suppression of lignification and a subset of secondary wall biosynthetic program, including xylan glucuronidation and acetylation machinery. Several candidate genes for perception of impairment in xylan integrity were detected. These candidates could provide a new target for uncoupling negative growth effects from reduced recalcitrance. In conclusion, our study supports the hypothesis that xylan modification generates intrinsic signals and evokes novel pathways regulating tree growth and secondary wall biosynthesis.

Introduction

Plant cell wall is a highly dynamic and heterogenous structure made by complex chemical organization of cellulose, diverse matrix polysaccharides, structural proteins and polyphenols (Albersheim et al., 2010). The structure, composition and molecular interaction of matrix polysaccharides determine cell shape and tensile properties necessary for the mechanical strength of cell wall. Xyloglucans and pectins form the matrix of primary cell wall and their interactions with cellulose microfibrils within highly hydrated architecture facilitate cell expansion. The secondary

walls (SWs) are deposited in xylem cells after cell expansion and have a denser and thicker network of cellulose microfibrils with a SW-specific combination of matrix polysaccharides including glucuronoxylan (GX) and glucomannan. Deposition of this SW polysaccharide network and its subsequent lignification starting from the primary wall makes further cell expansion impossible but provides xylem cells with mechanical strength and rigidity. The primary and secondary walls constitute wood biomass which is the most abundant renewable resource on Earth for sustainable production of eco-friendly materials, chemicals and energy carriers (Keegan et al. 2013; Bar-On et al. 2018; Martínez-Abad et al. 2018).

Biosynthesis of cell wall components has been largely investigated by studying cell wall mutants like *murus* (*mur*) (Mertz et al., 2012), *irregular xylem* (*irx*) (Turner and Somerville, 1997), *fragile stem* (*fra*) (Zhong et al., 2005), *trichome birefringence-like* (*tbl*) (Potikha and Delmer, 1995) and by systematic gene sequence analyses (Cantarel et al., 2009; Kumar et al., 2019). The enzymatic activities of several proteins have been characterized (e.g. Cavalier and Keegstra 2006; Maris et al. 2011). However, it is still not well understood how the different activities are coordinated during cell wall biosynthesis to produce cell walls of required properties. Knowledge on the dynamic macromolecular changes during cell wall formation and modification in response to developmental and environmental changes is fundamental for our efforts to create plants with desired cell wall chemical composition suitable for industrial applications such as biorefinery and production of biomaterials (Somerville and Bonetta 2001; Pauly and Keegstra, 2008, 2010).

The secondary cell wall of hardwood xylem contains approx. 25% (dry weight) of GX. GX has been reported to have distinct structural variants in terms of relative abundance of acetylation and glucuronidation and the pattern of these decorations resulting in the major xylan domain that forms a two-fold helical screw conformation, forming a compatible region for hydrogen bonding to the hydrophilic surface of cellulose, and a minor domain forming a three-fold screw making regions interacting with lignin (Bromley et al., 2013; Busse-Wicher et al., 2014; Simmons et al., 2016; Yuan et al., 2016a; 2016b; 2016c; Grantham et al., 2017). The unsubstituted xylan surface can form stacking interactions on the hydrophobic surface of cellulose (Gupta et al., 2021). Thus, xylan molecules can differently affect cell wall architecture, and how their biosynthetic process is controlled to ensure formation of functional cell wall is not understood. This is complicated by the fact that in addition to enzymatically driven xylan biosynthesis and modification there are spontaneous processes that may occur in the cell wall changing its properties. For example, there is a long-standing hypothesis that xylan provides nucleation sites for lignin polymerization. In grasses, the ferulic acid linked to arabinose side chains of xylan is believed to initiate lignification (Markwalder & Neukom, 1976; Hartley et al., 1990; Ralph et al., 1995). In poplar, Ruel et al (2006) proposed that hemicellulose-lignin covalent linkage serves as an anchor for lignin polymerization. The extracellular lignin analysis in spruce cell cultures suggests that exogenously supplied xylan can act as a nucleation center for lignin polymerization, depending on the amount and solubility of the xylan provided (Sapouna et al., 2023).

Postsynthetic modification of the cell wall by overexpression of xylan-modifying microbial enzymes represents a promising strategy to examine the contributions of different xylan structures to cell wall functions and to investigate mechanisms regulating cell wall biosynthesis in response to xylan integrity defects (Pogorelko et al., 2011). The cell wall modification by overexpression of xylan-acting microbial enzymes has also been demonstrated to decrease biomass recalcitrance (Pogorelko et al., 2011; Gandla et al., 2015; Pawar et al., 2016; 2017; Pramod et al., 2021). Similarly, xylan structure defects caused by suppression of native xylan biosynthetic genes altered plant cell wall architecture and improved saccharification (Donev et al., 2018). These experiments demonstrated the potential use of plants compromised in xylan integrity for biorefinery applications, and in some cases revealed activation of biotic stress and growth responses triggered by xylan modification. However, their effects on cell wall developmental pathway received little or no attention.

In the present study, we report changes in xylem cell wall chemistry and resulting modifications in cell wall biosynthesis and xylem cell developmental programs in transgenic aspen overexpressing endo-1,4- β -D-xylanases of GH10 and GH11 families from *Aspergillus nidulans* in apoplast of developing xylem cells. Endo-1,4- β -D-xylanases (EC 3.2.1.8) cleave internal 1,4- β -xylosidic bonds in xylan backbones, producing low molecular weight (MW) heteroxylans and unsubstituted or branched xylo-oligosaccharides (XOS) (Reilly, 1981; Pollet et al., 2010). The products of GH10 and GH11 xylanases slightly differ because only GH10 can accommodate a substituted xylosyl residue at the -1 subsite of the active site whereas both families require unsubstituted xylosyl residue at the +1 subsite (Biely et al., 1997; Pell et al., 2004; Kolenová et al., 2006; Vardakou et al., 2008; Kojima et al., 2022). The expression of xylanases altered xylem cell wall biosynthetic program and modified cambial activity suggesting the loss of xylan integrity in SWs is sensed by differentiating xylem cells. The resulting lignocellulosic biomass had substantially increased saccharification potential. However the plants' growth was affected and uncoupling of the two effects is needed before such a strategy could be used for practical deployment.

Results

Microbial xylanases affected growth and vascular tissue differentiation pattern in aspen

Transgenic aspen expressing fungal xylanases showed clear morphological changes (**Fig. 1A**). All growth parameters (stem height and diameter, aboveground and root biomass) were significantly affected compared to the wild-type (WT) (**Fig. 1B**). Transgene transcript levels were higher in 35S promoter lines than in WP lines (**Fig. S1**), which did not correlate with growth penalty. However, in three WP:GH10 lines with different transgene levels, there was a clear negative impact of transgene transcript level on height and biomass production. Although radial growth was not affected in the majority of transgenic lines, the measurement of secondary vascular tissues from transverse sections revealed increased secondary phloem and decreased secondary xylem production (**Fig. 1C**). The pith area of transgenic lines was also significantly increased. These observations indicate that xylanases stimulated growth of pith and had a major impact on cambial activity shifting it from xylem to phloem production.

Intriguingly, the appearance of freshly cut stems of transgenic lines was altered. All lines, but the low-expressing line WP:GH10_11, showed a markedly increased zone of wet xylem, which normally indicates developing not fully lignified xylem (**Fig. 2A**). The stems were also much easier to cut, suggesting changes in cell wall properties. Indeed, SilviScan analysis (**Fig. 2B**) showed that several transgenic lines had higher wood density or increased cellulose microfibril angle (MFA). The number of xylem cells per radial file was reduced in transgenic lines confirming microscopy analyses. Furthermore, an increase in vessel fraction with concomitant decrease in vessel perimeter and an increase in fiber diameter were observed in several transgenic lines, suggesting that xylem cell fate and xylem cell expansion were also affected by the xylanases.

Analysis of semi-thin transverse sections stained with toluidine blue O (TBO) revealed a substantial decrease in cell wall thickness and frequent occurrence of *irregular xylem (irx)* phenotype (**Fig. 2CD, Fig. S2**). Moreover, a shift in TBO color from cyan in WT to violet-blue in transgenic lines suggested decrease in lignification. This was confirmed by analysis of lignin autofluorescence in the wood sections of transgenic and WT plants (**Fig. S3**). Lignin autofluorescence images also revealed large wood areas in transgenic plants with very low signal, which possibly represent patches of tension wood (TW). All these changes were attenuated in the line WP:GH10_11 that had lower transgene expression compared to other lines.

Xylanase expression had a major impact on the content and composition of wood matrix sugars and lignin

Sulfuric acid hydrolysis showed no consistent changes in cellulose (glucan) content (**Fig. 3A**). On the other hand, acid methanolysis-TMS analysis showed significant changes in matrix sugars (**Fig. 3B**): xylose, MeGlcA and GlcA contents decreased in most or all transgenic lines, mannose contents decreased in most lines but WP:GH10 and most lines had lower glucose unit content than WT. WP:GH10 lines showed increase in pectin-related sugars including rhamnose, galacturonic acid, galactose and arabinose, whereas the opposite trend or no change was observed for other lines. Wood analysis by Py-GC/MS revealed a significant decrease in total lignin and guaiacyl (G) unit contents in transgenic lines (**Fig. 3C**). Whereas the G-lignin units were substantially reduced in all transgenic lines, the syringil (S) lignin units were decreased only in GH11-expressing lines. The content of other phenolics was on the other hand increased in the majority of the transgenic lines. Spatial distribution pattern of lignin and xylan in cell walls analyzed by transmission electron microscopy revealed a severe depletion of lignin in the compound middle lamellae and SW layers of xylem fibers in transgenic trees (**Fig. 4A**) and a significant decrease in gold particle density labeling LM10 xylan epitopes in transgenic lines (**Fig. 4BC**). Thus, cell wall analyses revealed major impact of xylanases on the lignin and xylan in wood cell walls.

Detailed xylan analysis revealed that xylanases affected its molecular structure

The yield of xylan in 20 and 30 min subcritical water extracts (SWE) determined as sum of xylose and MeGlcA contents was increased in WP:GH11 lines indicating increased xylan solubility compared to WT (**Fig. 5A**). The xylan from 30 min extracts of transgenic lines was characterized by a higher degree of acetylation (**Fig. 5B**). The molar mass distribution of 30 min SWE determined by size exclusion chromatography revealed a decrease in molecular weight in transgenic trees indicating the reduction in the degree of polymerization of xylan according to the expected cleavage activity of expressed xylanases (**Fig. 5C**).

The oligomeric mass profiling (OLIMP) of acetylated xylan from SWE and digested with GH30 glucuronoxylanase showed an increased population of oligomers representing closer glucuronidation spacing and higher acetyl substitution (X_2UA , X_3UA) and a decreased abundance of oligomers representing more spaced substitutions (X_4UA , X_5U , X_6U) in transgenic lines (**Fig. 5D, S4**). OLIMP of alkali-extracted xylan showed in opposite a significant decrease in oligomers representing closer glucuronidation (X_3U to X_5U) and increase in those representing more spaced glucuronidation (X_6U to $X_{10}U$) (**Fig. 5E, S5**). Altogether these data indicate that the xylan domains with close MeGlcA and acetyl substitution are protected from GH10 and GH11 xylanases expressed in transgenic lines, and that regions with highly spaced glucuronidation are most likely hindered from GH10 and GH11 xylanases by high acetyl substitution.

Xylanases-induced cell wall chemical changes improved saccharification potential of wood

Wood of xylanase-expressing lines showed substantial reduction of recalcitrance which was particularly evident in saccharification without pretreatment. Glucose production rate, and glucose and xylose yields increased up to 210%, 190% and 300% of WT levels, respectively (**Fig. 6A**). The improvements for GH11 were more substantial compared to GH10 (even when disregarding line WP:GH10_11), as supported by $P_{\text{contrast GH10 vs GH11}} \leq 0.0001$ for all three parameters. After pretreatment, glucose production rates were also increased in transgenic lines, but to a lesser extent (up to 130%), whereas only GH11 lines showed higher glucose yields (up to 130%) than WT (**Fig. 6B**). Total xylose yields were increased for some lines (35s:GH11) but reduced for others (35s:GH10 and WP:GH11) reflecting the net decrease in xylose unit content of these lines. Furthermore, the yields of mannan and galactan in pretreatment liquid were altered in many transgenic samples reflecting changes in their content and solubility (**Fig. S6**).

Changes in hormonomics and metabolomics provide evidence for intrinsic regulation of vascular differentiation and cell wall lignification in transgenic trees

To understand mechanism of developmental changes triggered by xylan integrity impairments in SWs, we analyzed hormones in developing wood of WP:GH10 and WP:GH11 lines and WT. There was an overall similarity in hormonal changes induced by GH10 and GH11, with many cytokinin forms, some auxin forms, abscisic acid (ABA) and the ethylene precursor 1-aminocyclopropane-1-carboxylic acid (ACC) being significantly affected, whereas no changes were seen in jasmonates (JA) or salicylic acid (**Fig. 7A**). Significant increases in active forms of cytokinins, trans-zeatin and N⁶-isopentenyladenine, and their riboside precursors were evident indicating elevated cytokinin signaling (**Fig. 7B**). In contrast, the levels of indole-3-acetic acid (IAA) were decreased with concomitant increases in inactivated IAA forms. The ABA showed a two-fold decrease while ACC concentration increased almost four times in transgenic trees, indicating altered stress signaling *via* ABA and ethylene. This provides evidence that hormones regulating the cambial activity, xylem differentiation and stress responses were affected by expression of xylanases in xylem cells forming SWs.

Xylanases induced striking changes in the metabolomes of transgenic lines, which were highly similar between WP:GH10 and WP:GH11 lines as shown by the volcano plots and Venn diagrams (**Fig. 8AB**). Significantly affected compounds detected by GC-MS analysis were mostly upregulated. They comprised amino acids and sugars, including xylose (Xyl) and xylobiose (Xyl-B) (**Fig. 8C**). LC-MS analysis revealed metabolites mostly reduced in transgenic lines of which the most affected were lignols (some with over 30-fold decrease), phenolic glycosides and phenyl propanoid-related metabolites (**Fig. 8A-C**), demonstrating the specific impact on lignin biosynthetic pathway.

Transcriptomic changes

Overview of transcriptomic changes in WP:GH10 and WP:GH11 transgenic lines

RNA-seq analysis of developing xylem identified 1600 - 2700 differentially expressed genes (DEG) in WP:GH10 and WP:GH11 lines, with an overrepresentation of upregulated genes (**Fig. 9A, Supplementary Table S4**). The core genes affected in common for all xylanase-expressing lines included 391 upregulated and 239 downregulated genes (**Supplementary Table S5**). Gene ontology (GO) enrichment analysis of these genes revealed upregulation in GO terms related to the photosynthesis, chlorophyll binding, generation of energy and stress and downregulation in categories related to lipid, protein and amino acid metabolism, oxidoreductase activities, and cell wall biosynthesis (**Fig. 9B, Supplementary Table S6**).

The exclusive functional classification of the core genes (**Fig. 9C, Supplementary Table S7**) showed that signaling, stress and transcription factors functions were most highly represented among both up- and downregulated genes. Interestingly, many of the stress-related genes were annotated as responsive to anoxia. "Amino acid metabolism" and "cell wall" categories were highly represented among the downregulated genes whereas a . This indicates that changes seen in about 10% of upregulated genes were associated with photosynthesis.

Transcriptomic changes in signaling and stress response genes

Since the signaling was the most represented function among DEGs, we analyzed these genes in more detail. Transcripts for different kinases and calcium signaling genes were the two most highly represented groups in the signaling category (**Fig. 9C, Table 1**). Of the hormone-related genes, those related to ABA, ethylene, and cytokinins were most highly represented, which is in good agreement with the hormone analyses.

Transcriptomic changes in secondary wall-related genes

To find out if SW formation was affected by the xylanases at the transcript levels, we identified differentially regulated genes in transgenic lines with 35S:GH10, WP:GH10 and WP:GH11 constructs among known SW-related genes expressed in the wood forming tissues (**Supplementary Table S8**). Among cellulose-related genes, several genes from family GH9 encoding cellulases were found downregulated (**Table 2**). Among xylan-related genes, those involved in mGlcA substitution (*PtGUX1-A*, *PtGUX4-A* and *PtGXMI*), and acetylation (*PtXOAT1*, *PtRWA-A* and *PtRWA-B*) were found downregulated. Lignin biosynthesis pathway was also affected due to downregulation of genes involved in monolignol biosynthesis (*PtPAL4*, *PtCald5H2*, homolog of *AtCAD6*, *Pt4CL3* and 5, *PtCCoAOMT1* and 2) and polymerization (*PtLAC12/AtLAC17*). This indicates that specific programs modifying cellulose, responsible for xylan substitution and lignin biosynthesis were downregulated. Among the master switches regulating these programs in *Populus* (Zhong et al., 2010; Ohtani et al., 2011), we identified two *VND6* genes *PtVND6-A2* and *PtVND6-C2* genes (named after Li et al., 2012 as listed in Takata et al., 2019) and their downstream TFs, *PtMYB199* homologous to *AtMYB85* - an activator of lignin biosynthesis, *PtSND2* and *PtNAC124* (homologous to *AtSND2*) and *PtMYB90*, *PtMYB161* homologous to *AtMYB52* activating cellulose and hemicellulose biosynthetic pathways (Zhong et al., 2008; Schuetz et al., 2013) downregulated in xylanase-expressing lines (**Table 2**). This suggests that specific sub-programs of SW biosynthesis have been downregulated via SW transcriptional cascade in transgenic lines. On the other hand, we also observed a strong downregulation of four *AtMYB4* homologs, including *PtLTF1* that regulates lignification in response to stress (Gui et al., 2019), upregulation of *PtMYB55* homologous to *AtMYB61* reported to positively regulate SW development in *Arabidopsis* coordinating a small network of downstream genes (Romano et al., 2012), and three homologs of *AtMYB73* involved in salinity stress response and lateral root development (Kim et al., 2013; Wang et al., 2021).

Co-expression networks formed by genes commonly affected in WP:GH10 and WP:GH11 lines

To identify co-expression networks of DEGs that might operate in developing wood we used AspWood database (Sundell et al., 2017). Eight networks were identified, the main network and seven side networks, and expression of the genes of each network in wood forming tissues, in different tree organs and in different xylanase-expressing lines was illustrated as heatmaps (**Fig. 10, Supplementary Figs S7-S10, Supplementary Table S7**). The main network included mostly genes expressed late during xylogenesis, but it contained smaller subnetworks of genes expressed during SW formation and during primary wall stage of xylem differentiation (**Supplementary Fig. S7**). It was dominated by signaling- and stress-related genes (**Fig. 10, Supplementary Table S7**), including many kinases, calcium signaling components, genes related to hormones (peptide - *PAF1s*, ethylene, ABA - *AtAFP2*, and *AtNCED1*, cytokinin - *AtARR6*), sugar responses, and stress (dehydration, salt, freezing and anoxia). The highly interconnected transcriptional factors included upregulated *AtWRKY75*, *AtERF110/PtERF57* and *AtLBD21/PtLBD047* and downregulated *AtLBD19/PtLBD043* and several *AtNAC074* homologs. The cell wall-related genes included downregulated *PtGH9B11*, *PtGH9_18*, *PtGUX4A*, and upregulated *AtXTH28/PtXTH40*.

Among the side networks, network 3 included genes differentially expressed in the cambium (**Fig. 10, Supplementary Fig. S9**), with three transcription factors, *AtMYB61*, *AtSCREAM-like* and *AtbZIP44*, the calcium-signaling related gene *AtMLO4* and transporters *AtZIF1* and *AtAVP1*. Side networks 4 and 6 were grouping genes expressed in the phloem that were almost all upregulated in transgenic lines (**Fig. 10, Supplementary Fig. S10**). Network 4 included *AtCLE45* encoding a peptide hormone and transcription factors *AtCES* and *AtBBX15*, whereas network 6 included a kinase (*AtMPK2*), peroxidase *AtPRX72* and stress-related genes (*AtGSTF11* and *AtKTI5*).

The side networks 1 and 2 (**Supplementary Fig. S9**) grouped genes highly upregulated by xylanases, expressed in the leaves, phloem and mature xylem zone, and involved in photosynthesis (*AtLHCA3*, *AtLHCB5*, *AtPSAD*, *AtPSAE*, *AtPSBR*, *AtPSBO2*) and photorespiration (*AtGOX1*).

Side networks 5 and 7 (**Supplementary Fig. S10 and 11**) grouped genes expressed at primary-SW transition in developing xylem and low expressed in extraxylary tissues, which were downregulated except one, *AtZPR1* encoding LITTLE ZIPPER1. Network 7 included *AtSTP10* encoding hexose-H⁺ proton symporter and *AtGNL2* encoding GNOM-like 2 an ARF guanidine exchange factor regulating vesicle trafficking.

Unique transcriptomic changes induced by the two families of xylanases

Venn diagrams (**Fig. 9A**) showed that 120 genes were jointly upregulated in two lines of WP:GH10 construct but were not affected in any of the lines of WP:GH11 construct whereas 230 genes were upregulated only in the GH11 expressing lines. Similar analysis of downregulated genes revealed 62 specifically downregulated in WP:GH10 and 117 in GH11 lines. Thus, GH11 altered expression of approx. two times more genes than GH10 and these genes were more frequently upregulated (**Supplementary Table S9**). GO analysis of these xylanase family-specific genes (**Supplementary Table 10**) revealed that GH11 induced more intense activation of stress and in particular raffinose stress-related genes than GH10.

Discussion

Fungal xylanases reduced xylan content and altered its structure in aspen secondary walls

The majority of transgenic lines expressing fungal GH10 and GH11 xylanases in cell walls had reduced TMS xylose content, and reduced molecular weight of SWE xylan. This was accompanied by reduced signals from LM10 antibodies in SWs and increased content of soluble xylose and xylobiose. Jointly these data demonstrate that the xylanases were active on cell wall xylan in aspen, cleaving the backbone. However, not all domains of xylan were equally susceptible to cell wall-targeted GH10 and GH11 xylanases. Analysis of degree of acetylation and OLIMP profiles after GH30 glucuronoxylanase digestion of SWE xylan indicated that highly acetylated and tightly glucuronidated regions of xylan were less prone to hydrolysis by these xylanases as these substitutions are known to restrict xylan backbone digestion by GH10 and GH11 xylanases (Biely et al., 2016; Kojima et al., 2022).

Fungal xylanases affected wood cell wall structure and composition

Irregular xylem phenotype (irx) with thin-walled fibers and collapsed vessels is typical for mutants impaired in biosynthesis of SWs or one of its main components like cellulose, xylan and lignin (Jones et al., 2001; Turner et al., 2001; Brown et al., 2005; Persson et al., 2007; Hao et al., 2014). Here we show that *irx* phenotype was also induced by SW-targeted fungal xylanases. This SW thinning was without any change in cellulose content but with prominent decrease in lignin content and composition. While all lines had reduced content of G-lignin, only GH11-expressing lines had lower S-lignin content. Similarly, *Arabidopsis thaliana* expressing GH10 and GH11 xylanases had decreased lignin, especially G-lignin content in secondary xylem (Barbut et al., unpublished). Moreover, mutations in xylan biosynthetic genes were also observed to lead to the same lignin defects (Hao et al., 2014; Barbut et al., unpublished) suggesting an interdependence of lignification on xylan in SWs.

Whereas one mechanism of this interdependence has been proposed *via* xylan acting as a nucleation point for the polymerization of monolignols (Sapouna et al., 2023) our data point to a different possibility. First, we observed a severe decrease in mono- and oligolignols as well as phenolic glycosides suggesting severely decreased lignin monomer biosynthesis in xylanase-expressing lines. If the polymerization was affected *via* reduced lignin nucleation sites, one would expect increased content of unpolymerized lignols instead. Second, we observed downregulation of transcripts of lignification-specific *MYBs* and several genes involved in monolignol biosynthesis and

polymerization. Similarly, key lignin biosynthetic genes were downregulated in *ixr8/gaut12* mutant (Hao et al., 2014). Moreover, two negative regulators of phenylpropanoid biosynthesis encoding F-box proteins *AtKFB* and *AtKMD2* targeting phenylalanine ammonia-lyase for ubiquitination (Zhang et al., 2013) were upregulated in xylanase-expressing lines (**Supplementary Table S7**). It is noteworthy that *AtKMD2* was upregulated in xylobiose-treated *Arabidopsis* (Dewangan et al., 2023) and in *ixr9* mutant (Faria-Blanc et al., 2018) that was also hypolignified (Petersen et al., 2012), making it a strong candidate for downregulation of phenylpropanoid pathway in xylan-compromised plants.

Xylanase-expressing aspen lines showed also downregulation of some key genes required for biosynthesis of MeGlcA and acetyl substitutions of GX. This could be a reaction counteracting the changes in GX substitution induced by xylanases in developing SW. This specific downregulation of GX biosynthesis subprogram likely involves specific branches of the SW regulatory program (Ohtani et al., 2011; Zhong et al., 2011; Taylor-Teeples et al., 2015; Chen et al., 2019), possibly including *VND6* homologs, the first layer master switches, and several members of the third layer master switchers. Some of these master switchers, like *PtMYB161* (Wang et al., 2020a) or *PtLTF1* (Gui et al., 2019), could also participate in a feedback regulation of the SW biosynthesis in response to stress. An additional layer of suppression of SW program in transgenic plants could be mediated by decreased ABA levels since ABA signaling is needed to activate NST1 by phosphorylation (Liu et al., 2021). These observations are in line with our previous hypothesis based on observations in aspen with suppressed *PtGT43BC* expression that SW impairment is sensed by plants resulting in general shutdown of SW biosynthetic program (Ratke et al., 2018).

Expression of fungal xylanases altered growth and vascular differentiation pattern in aspen

Modification of xylan backbone by SW-targeted GH10 and GH11 xylanases led to substantial decrease in height and biomass of trees. The previous experiments suppressing xylan backbone biosynthesis by knocking down *PtGT43A* and *B* (Lee et al., 2011), *PtGT43B* and *C* (Ratke et al., 2018), *PtGT47C* (Lee et al., 2009) or *PtGAUT12* (Li et al., 2011; Biswal et al., 2015) reported in contrast either no or positive effects on growth in *Populus*, especially when WP promoter was used. Intriguingly, the xylanases affected cambial growth by specifically inhibiting xylem formation and increasing phloem formation, which was correlated with increased cytokinin content. Phloem differentiation and cambial cell division are known to be regulated by local maxima in cytokinins which in turn exclude auxin maxima by regulating distribution of PIN transporters inhibiting auxin-dependent activation of HD-ZIPIII transcription factors and xylem differentiation (Bishopp et al., 2011; Immanen et al., 2016; Haas et al., 2022). Moreover, we found three homologs of *ZPR1* that is known to inactivate HD-ZIPIII transcription factors (Wenkel et al., 2007) upregulated in xylanase-expressing lines, which would provide additional mechanism suppressing xylem formation. Therefore, modification of xylan in SW appears to positively affect mitotic divisions in the cambium, enhance phloem differentiation, and in case of xylanase-expressing lines, inhibit xylem fate *via* transcriptional and hormonal regulation.

Hormonal signaling pathways are affected in xylanase-expressing lines

Impairment of xylan integrity in SW by fungal xylanases induced severe systemic changes such as reduced plant height, reprogramming of cambial activity from xylem to phloem production, and suppression of SW formation program in differentiating xylem. Such changes require long- and short-distance signaling, which likely starts in differentiating xylem cells and involves plant hormones.

Decrease in ABA content and signaling was supported by a downregulation of a key ABA biosynthetic gene, homolog of *AtNCED1*, and the upregulation of homologs of negative regulators of ABA signaling pathway: *AtATAF1* (Garapati et al., 2015) and *AtKING1* (Papdi et al., 2008) in

xylanase-expressing aspen. ABA forms a regulatory feedback loop with FERONIA (FER), a key RLK sensing cell wall integrity (Bacete and Hamann, 2020). ABA biosynthesis has been found to be downregulated after cell wall integrity signaling mediated by *AtTHESEUS1* (*AtTHE1*) (Bacete et al., 2022), after stem mechanical disturbance (Urbancsok et al., 2023) and following *Botrytis cinerea* infection (Windram et al., 2012). On the other hand, ABA signaling was needed for increased biotic resistance in *Arabidopsis irx* mutants with defects in SW *CesA* genes (Hernández-Blanco et al., 2007).

Strigolactones (SLs) and/or related carotenoids have been previously shown to mediate *irx* phenotype and freezing tolerance of *esk1/tbl29* and other SW mutants impaired in cellulose and xylan biosynthesis in *Arabidopsis* (Ramírez and Pauly, 2019). In xylanase-expressing aspen lines the upregulation of a functional homolog of *AtDWARF14* (*AtD14*), *PtD14a*, encoding an SL receptor (Zheng et al., 2016) and *AtSMXL8* - involved in feedback regulation of SL signaling (Wang et al., 2020b)- supports activation of signaling by SLs. Moreover, a downregulation of a chalcone synthase transcript *AtTT4* which controls flavonoid biosynthesis downstream SLs (Richmond et al., 2022) was observed in common in xylanase-expressing aspen and xylobiose-treated *Arabidopsis* (Dewangan et al., 2023). Xylanases also induced *BYPASS1* (*BPS1*) encoding a plant-specific inhibitor of a carotene-related xylem-transported hormone inhibiting shoot development (Van Norman and Sieburth, 2007).

Xylanases also affected ethylene signaling as evidenced by increased ACC levels, and upregulation of several ethylene related genes including *ETHYLENE RESPONSE FACTORS* (*ERFs*) which were also induced in xylobiose-treated *Arabidopsis* (Dewangan et al., 2023), and a homolog of *ERF1* regulating growth under stress (Hoang et al., 2020). Upregulated JA signaling was also evident based on transcriptome analysis. This signaling pathway has been implicated in cell wall integrity response downstream of THE1 (Bacete et al., 2022). Both ethylene and JA signaling pathways were stimulated in the developing xylem by mechanical stress (Urbancsok et al., 2023).

Upregulation of cytokinins in xylanase-expressing aspen expectantly would increase plastid multiplication resulting in strong upregulation of photosynthesis-related genes, and lipid and amino acid metabolism. Transcriptomics data supported these hypotheses with upregulation of a homolog of *AtPLASTID DIVISION2* (*AtPDV2*) that regulates plastid division (Chang et al., 2017) and many genes involved in plastid organization and photosynthesis. Among several cytokinin-related DEGs, a homolog of *AtARR6* encoding a negative regulator of cytokinin response was downregulated. *ARR6* has been implicated in cell wall modification and immunity (Bacete et al., 2020).

Thus, xylan integrity impairment caused by xylanases affected signaling *via* ABA, strigolactones/carotenes, ethylene and cytokinins, which overlaps with primary cell wall integrity signaling, and responses to mechanical and other abiotic and biotic stresses (Bacete and Hamann, 2020; Rivero et al., 2021).

Local candidates for stress perception in secondary wall-forming cells

The perception of xylan impairment in SW expectedly would involve local sensors including xylobiose (DAMP) sensors (Dewangan et al., 2023) and other cell wall integrity sensing components (Bacete and Hamann, 2020). One of them could be *HPCAI* encoding a novel RLK responsible for H₂O₂ perception at the plasma membrane and activation of calcium influx (Wu et al., 2020). Several other calcium signaling-related genes were upregulated, including mechanosensitive calcium channel *AtOSCA1.8* (Yuan et al., 2014; Murthy et al., 2018), defense-activated calcium channel *AtZARI* (Bi et al., 2021), *AtMDL3* known to be dependent on activity of mechanically activated MCA channels (Mori et al., 2018), *AtLBD38* regulated by calcium influx via cyclic nucleotide-gated channel CNG15 (Tipper et al., 2023). Furthermore, *AtMLO4* and *AtMLO1* homologs were downregulated. *AtMLO4* is a calcium channel involved in mechanical stress and gravitropism signaling (Zhu et al., 2021). Among candidates expressed at primary-SW transition other transporters

were also identified, including *PtVPI.1* (*AtAVPI*) encoding a pyrophosphate-fueled proton pump regulating apoplastic pH and involved in stress responses (Yang et al., 2015), *AtSTP10* encoding a proton-coupled sugar symporter responsible for uptake of monosaccharides from apoplast into plant cells (Bavnhøj et al., 2021), and *AtGNL2* involved in ER-Golgi trafficking of proteins (Teh and Moore, 2007). Some of these genes were regulated in common with xylobiose-treated *Arabidopsis* (Dewangan et al., 2023) (**Supplementary Table S7**).

Xylanase-induced changes in cell wall chemistry improved wood saccharification potential

Xylan binds to cellulose surfaces and interconnects lignin and was shown to impede the enzymatic saccharification (De Martini et al., 2013). Moreover, as it is the main source of yeast-inhibiting acetic acid, it is predicted to inhibit the fermentation (Donev et al., 2018). Therefore, decreasing xylan content and its modification are considered as effective strategies for improving biomass biorefinery properties. Here, we show that expressing either GH10 or GH11 xylanases in aspen SWs greatly improved glucose yield and production rate per wood weight in saccharification without pretreatment which were doubled or even tripled compared to WT. Previous experiments with *HvXyl1* expressed in poplar reported a 50% increase in glucose yield in saccharification after steam pretreatment (Kaida et al., 2009). Even milder xylan reduction by suppressing *GT43* genes of clades B and C resulted in increased in glucose yield in saccharification without pretreatment by 30% to 40%, but a negligible effect was observed after acid pre-treatment (Lee et al., 2011; Ratke et al., 2018). The high glucose yields observed in the present study were however associated with growth penalties. On the other hand, no such penalties were observed in *GT43*-suppressed aspen either in the greenhouse or in the field (Ratke et al., 2015; Derba-Maceluch et al., 2023). It is therefore evident that saccharification benefits and growth are not necessarily negatively linked. Our current analysis of transcriptomic and metabolomic changes revealed many candidates for uncoupling regulation of growth and development from xylan reduction in xylanase-expressing lines. Elucidation of their function could lead to designing better strategies to obtain saccharification-improved plants that grow just as well as WT or even better.

Conclusions

This study evaluated the effects of postsynthetic modification of xylan backbone by overexpression of fungal xylanases on growth, secondary cell wall characteristics and wood properties in aspen. Our results demonstrated that xylanases decreased the content of xylan and its molecular weight, and modified its substitution pattern. This inhibited tree growth, wood production, SW development and lignin biosynthesis. The hormonomics, metabolomics and transcriptomics analyses revealed that xylan impairment activated hormonal signaling and affected genetic regulatory pathways that modified cambial growth and adjusted SW biosynthesis program, suggesting the activation of SW integrity sensing. Although the benefits of highly enhanced glucose yield in saccharification from transgenic wood biomass were offset by growth penalty, the identified candidates for the SW integrity sensing mechanism could be used to uncouple beneficial and undesirable effects for developing improved lignocellulose in aspen for biorefinery.

Experimental Procedures

Generation of transgenic lines

The *Aspergillus nidulans* cDNA clones encoding GH10 (AN1818.2; GenBank: ABF50851.1) and GH11 (ANIA_03613; NCBI_GeneID:2873037, XP_661217.1) xylanases (Bauer et al., 2006) were used to generate expression vectors. The signal peptide of GH10 was replaced by the hybrid aspen (*Populus tremula* L. x *tremuloides* Michx.) signal peptide from gene *PtxtCel9B3* (alias *PttCel9B*) (GenBank AY660968.1; Rudsander et al., 2003) as described previously (Gandla et al., 2015),

whereas native fungal signal peptide was used for GH11 vector. The cloning primers are listed in **Supplementary Table S11**. The entry clones generated using the pENTR/D-TOPO cloning system (Thermo Fisher Scientific, Uppsala, Sweden) were used to make the expression clones in either pK2WG7.0 (Karimi et al., 2002) for ectopic expression using 35S promoter or in pK-pGT43B-GW7 (Ratke et al., 2015) for expression specifically in cells developing secondary cell walls driven by the wood-specific promoter (WP). The resulting vectors (35S:GH10, 35S:GH11, WP:GH10 and WP:GH11) were introduced into competent *Agrobacterium tumefaciens* (Smith and Townsend, 1907) Conn 1942, strain GV3101 using electroporation. Binary vectors were transformed into hybrid aspen (*Populus tremula* L. × *tremuloides* Michx., clone T89) as described previously (Derba-Maceluch et al., 2015). Lines with the highest transgene expression were selected from 20 independent lines for further analyses.

Plant growth in the greenhouse

In vitro propagated saplings were planted in soil (K-jord, Hasselfors Garden AB, Örebro, Sweden) in 7 L plastic pots, watered to 25% - 30% (v:v) soil moisture content, covered with transparent 8 L plastic bags, and grown for nine weeks in the phenotyping platform (WIWAM Conveyor, custom designed by SMO, Eeklo, Belgium) as described by Wang et al. (2022) under 18 h /6 h (day/night) light regime with 160-230 $\mu\text{mol m}^{-2} \text{s}^{-1}$ light intensity during the day, 22 °C /18 °C temperature, and the average air relative humidity of 60%. White light (FL300 LED Sunlight v1.1) and far-red light (FL100 LED custom-made, 725-735 nm) lamps from Senmatic A/S (Søndersø, Denmark) were used for illumination. After two weeks the bags were removed, and plants were watered automatically based on weight, their height was automatically measured.

At the end of experiment, trees were photographed, and stems diameters at base and aboveground fresh weights were recorded. A 30 cm-long stem segment above internode 37 was debarked, frozen in liquid nitrogen and stored at -70 °C for RNA, metabolomics and hormonomics analyses. The stem below was used for determining internode length. The 38th and 39th internodes were used for microscopy analyses. The four-cm long bottom segment was used for SilviScan analysis, and the remaining stem was debarked and freeze-dried for 48 h for wood chemistry analyses. Belowground biomass was determined by weighing cleaned and air-dried roots.

Wood microscopy analysis

For light microscopy, samples of three trees per line were fixed in FAA (4% formaldehyde, 5% acetic acid, 50% ethanol). Transverse sections (40-50 μm -thick) were prepared with a vibratome (Leica VT1000S, Leica Biosystems, Nussloch, Germany) and stained with safranin-alcian blue (Urbancsok et al., 2023). Lignin autofluorescence was analyzed at 470 nm (Kitin et al., 2020). Images were acquired by Leica DMI8 inverted microscope (Leica Biosystems, Germany) equipped with digital camera and analyzed with ImageJ software.

Another set of samples from the same trees were fixed in 0.1% glutaraldehyde, 4% paraformaldehyde, 50 mM sodium cacodylate buffer for 4 h at room temperature and embedded in LR white resin as described elsewhere (Pramod et al., 2014). Two μm -thick sections were cut using an ultramicrotome (RMC Powertome XL, USA) and stained with toluidine blue O for light microscopy analysis. Transverse ultrathin sections (70-90 nm-thick) were prepared using an ultramicrotome Ultracut E (Leica Biosystems) with a diamond knife and mounted on copper grids. For lignin localization, sections were stained with KMnO_4 (Donaldson, 1992). The xylan immunogold labelling with LM10 monoclonal antibody was carried out as described by Pramod et al. (2014). All sections were examined with a transmission electron microscope (FEI TALOS L120C) at an accelerating voltage of 100 kV. Cell wall thickness and gold particle density was determined using ImageJ based on ten and twenty measurements per tree, respectively, for two lines per construct.

SilviScan analyses

A SilviScan instrument (RISE, Stockholm, Sweden) was used for determining wood and fiber properties of six trees per line, 24 per WT as described by Urbancsok et al. (2023).

Cell wall chemical analyses

For initial pyrolysis and TMS analyses, wood powder from three trees per line was obtained by filing the freeze-dried wood and sieving the sawdust with Retsch AS 200 analytical sieve shaker (Retsch GmbH, Haan, Germany) to 50-100 μm .

Py-GC/MS assay used 50 μg (\pm 10 μg) of powder in a pyrolyser equipped with autosampler (PY-2020iD and AS-1020E, Frontier Lab, Japan) connected to a GC/MS (7890A/5975C, Agilent Technologies Inc., Santa Clara, CA, USA). The pyrolysate was processed and analyzed according to Gerber et al. (2012).

Alcohol-insoluble residue (AIR) was prepared as described by Gandla et al. (2015). AIR was destarched by α -amylase (from pig pancreas, cat. nr. 10102814001, Roche, USA) and amyloglucosidase (from *A. niger* cat. nr.10102857001, Roche) enzymes and the matrix sugar composition was analyzed by methanolysis-trimethylsilyl (TMS) procedure as described by Pramod et al. (2021). The silylated monosaccharides were separated by GC/MS (7890A/5975C; Agilent Technologies Inc., Santa Clara, CA, USA) according to Gandla et al. (2015). Raw data MS files from GC/MS analysis were converted to CDF format in Agilent Chemstation Data Analysis (v.E.02.00.493) and exported to R software (v.3.0.2). 4-*O*-Methylglucuronic acid was identified according to Chong et al. (2013). The amount of monosaccharide units per destarched AIR weight was calculated assuming their polymeric form.

For the remaining cell wall analyses, the pith was removed from debarked and freeze-dried stem segments the segments of seven trees per line were ground together using Retsch Ultra Centrifugal Mill ZM 200 (Retsch GmbH, Haan, Germany) equipped with a 0.5 mm ring sieve. The resulting wood powder was then sieved by Retsch AS 200 vibratory sieve shaker to isolate powder with particle size of 50-100 and 100-500 μm .

The 50-100 μm fraction was used in triplicates for monosaccharide analysis by a two-step sulfuric acid hydrolysis (Saeman et al., 1954). In brief, 1 mg of sample was incubated with 125 μL of 72% H_2SO_4 at room temperature for 3 h, then diluted with 1375 μL of deionized water and incubated at 100°C for 3 h. Hydrolyzates were diluted 10 times with MilliQ water, filtered through 0.2 mm syringe filter (Chromacol 17-SF-02-N) into HPAEC-PAD vials and analyzed by high performance anion exchange chromatography with pulsed amperometric detection (HPAEC-PAD) (ICS-6000 DC, Dionex) equipped with a CarboPac PA1 column (4 \times 250 mm, Dionex) at 30°C using the eluent gradients previously reported (McKee et al., 2016). Quantification of monosaccharides was performed by standard calibration of ten monosaccharides (Ara, Rha, Fuc, Xyl, Man, Gal, Glc, GalA, MeGlcA and GlcA) with concentrations between 0.005 and 0.1 g L⁻¹.

For subcritical water extraction, 2 g of 100-500 μm wood powder was extracted with 0.2 M formate buffer, pH 5.0, at 170 °C and 100 bar in an accelerated solvent extractor (ASE-300, Dionex, USA). Extraction proceeded in 4 steps with residence times of 10, 20, 30 and 60 min according to Sivan et al., (2023). Low-molecular weight compounds were removed by dialysis using Spectra/Por 3 membranes (Spectrum, USA), and the extracted polymers were freeze-dried.

For alkaline extraction, 1 g of wood powder with particle size 100-500 μm was incubated with 24% KOH for 24 h at room temperature (Escalante et al., 2012; Timell, 1961), filtered through 60 μm wire mesh and neutralized with 0.4 vol of acetic acid. Hemicellulose was precipitated with 96% ethanol (4 °C for overnight), centrifuged, washed in 80% ethanol, dissolved in distilled water and freeze-dried. Molar mass of extracts was determined by size exclusion chromatography coupled to

refractive index and UV-detectors (SECurity 1260, Polymer Standard Services, Mainz, Germany). The samples (2 mg) were dissolved in 1 mL of dimethyl sulfoxide (DMSO Anhydrous, Sigma-Aldrich) with 0.5% w/w LiBr (Anhydrous free-flowing Redi-Dri, Sigma-Aldrich) at 60 °C, and filtered through 0.45 µm PTFE syringe filters (VWR). The separation was carried through GRAM Analytical columns of 100 and 10000 Å (Polymer Standard Services, Mainz, Germany) at a flow rate of 0.5 mL min⁻¹ and 60 °C. The columns were calibrated using pullulan standards between 345 and 708 000 Da (Polymer Standard Services, Mainz, Germany).

The acetyl content of water extracts was determined in duplicates by overnight saponification of approx. 5 mg of sample in 1.2 mL of 0.8 M NaOH at 60 °C with constant mixing, neutralization with 90 µL of 37% HCl and filtration through 0.45 mm Chromacol syringe filters (17-SF-02(N), Thermo Fisher Scientific). The released acetic acid was detected by UV at 210 nm using high pressure liquid chromatography with UV detector (Dionex-ThermoFisher Ultimate 3100, USA) and separation by a Rezex ROA-organic acid column (300 x 7.8 mm, Phenomenex, USA) at 50 °C in 2.5 mM H₂SO₄ at 0.5 mL/min. Propionic acid was used as an internal standard.

For oligosaccharide mass profiling (OLIMP), the alkaline and 30 min water extracts were digested using GH10 endo-β-(1-4)-xylanase from *Cellvibrio mixtus* (Megazyme), a GH11 endo-1,4-β-xylanase from *Neocallimastix patriciarum* (Megazyme) and GH30 endo-1,4-β glucuronoxylanase (kindly provided by Prof. James F. Preston, University of Florida), incubating 1 mg of extract in 1 mL of 20 mM sodium acetate buffer (pH 5.5) and 10 U enzyme for 16 h at 37 °C. After enzyme inactivation at 95°C for 10 min, the hydrolysates were ten times diluted in acetonitrile 50 % (v/v) with 0.1 % (v/v) formic acid and filtered through Chromacol 0.2 µm filters (Scantec Nordic, Sweden). Samples were then briefly passed through a ZORBAX Eclipse Plus C18 column 1.8 µm (2.1 × 50 mm) (Agilent Technologies, Santa Clara, CA) and the oligosaccharide profiles were analyzed by HPAEC-PAD as reported previously (McKee et al., 2016) using xylooligosaccharides (X₂-X₆; Megazyme) as external standards and electrospray ionization mass spectrometry (ESI-MS) with a Synapt HDMS mass spectrometer (Waters, USA) in positive-ion mode and capillary and cone voltage set to 3 kV and 70 kV, respectively. The oligosaccharides were detected as [M + Na]⁺ adducts.

Oligosaccharide sequencing was achieved after the separation of labeled oligosaccharides by tandem LC-ESI-MS/MS. Derivatization was performed by reductive amination with anthranilic acid as previously described (Mischnick, 2012). The labelled oligosaccharides were separated through an ACQUITY UPLC HSS T3 column (150 × 2.1 mm, Waters, USA) at a flow rate of 0.3 mL min⁻¹ and a gradient of increasing acetonitrile content (10–30%) over 40 min. Mass spectrometric analysis was performed in positive mode with the capillary voltage and cone set to 3 kV and 70 kV, respectively. MS² was performed by selecting the ion of interest [M + Na]⁺ through single ion monitoring and subjecting it to collision-induced dissociation using argon as the collision gas, at a ramped voltage of 35–85 V. Assignment of proposed structures was performed by reference to labeled standards and analysis of the fragmentation spectra using ChemDraw (PerkinElmer, Waltham, Massachusetts, USA).

Saccharification assay

Three technical replicates from each line and six from WT were used for analytical-scale saccharification. Wood powder moisture content was measured using Mettler Toledo HG63 moisture analyzer (Columbus, OH, USA) and 50 mg of dry material was used per sample. Acid pretreatment was carried out using an Initiator single-mode microwave instrument (Biotage Sweden AB, Uppsala, Sweden) with 1% (w/w) sulfuric acid at 165 °C for 10 min. Enzymatic hydrolysis without or after acid pretreatment was performed at 45 °C using 4 mg of the liquid enzyme mixture Cellic CTec2 (cat. nr. SAE0020, Sigma-Aldrich, Saint Louis, MO, USA) as previously described (Gandla et al., 2021). Samples were analyzed for glucose production rate at 2 h by using an Accu-Chek[®] Aviva

glucometer (Roche Diagnostics Scandinavia AB, Solna, Sweden) following the calibration with a set of glucose standard solutions. After 72 h, the yields of monosaccharides were quantified using HPAEC-PAD (Ion Chromatography System ICS-5000 by Dionex, Sunnyvale, CA, USA) (Wang et al., 2018).

RNA analyses

Developing xylem tissues were scrapped from the debarked frozen stem and ground in a mortar with a pestle in liquid nitrogen. Approximately 100 mg of fine tissue powder was extracted with CTAB/chloroform:isoamylalcohol (24:1) followed by LiCl and sodium acetate/ethanol precipitation to isolate total RNA (Chang et al., 1993).

RNA samples from three trees per line were DNase treated with DNA-free™ kit (cat. nr. AM1906, Thermo Fisher Scientific, Waltham, MA, USA) then reverse-transcribed using iScript™ cDNA synthesis kit (cat. nr. 1708891) (Bio-Rad Laboratories, Hercules, CA, USA) following the manufacturers' instructions. Quantitative polymerase chain reactions (qPCRs) were performed using LIGHTCYCLER 480 SYBR GREEN I Master Mix (Roche, Indianapolis, IN, USA) in a Bio-Rad CFX384 Touch Real-Time PCR Detection System with 10 µL reaction volume. PCR program was 95°C for 3 min, then 50 cycles of 95°C for 10 s, 55°C for 10 s and 72°C for 15 s. UBQ-L (Potri.005G198700) and ACT11 (Potri.006G192700) were selected as reference genes from four tested genes based on GeNorm (Vandesompele et al., 2002). The primer sequences are listed in **Supplementary Table S11**. The relative expression level was calculated according to Pfaffl (2001)

For transcriptomics, RNA was purified as described previously (Urbancsok et al., 2023) and four or five biological replicates per transgenic line and eight biological replicates of the WT with RNA integrity number (RIN) ≥ 8 were used for cDNA preparation and sequencing using NovaSeq 6000 PE150 at Novogene Co., Ltd. (Cambridge, United Kingdom). Quality control and mapping to the *P. tremula* transcriptome (v.2.2), retrieved from the PlantGenIE resource (<https://plantgenie.org>; Sundell et al., 2015) were carried out by Novogene. Raw counts were used for differential expression analysis in R (v3.4.0) with the Bioconductor (v.3.4) DESeq2 package (v.1.16.1), as previously detailed (Kumar et al., 2019). The best BLAST hits were identified in *Populus trichocarpa* (v3.1) and *Arabidopsis thaliana* (v11.0).

Hormonomics and metabolomics

Frozen developing xylem samples were ground as described above. Hormone profiling was done according to Šimura et al. (2018), with slight modifications (Urbancsok et al., 2023). ACC (1-aminocyclopropane-1-carboxylic acid) was quantified according to Karady et al. (2024).

Metabolites were extracted and analyzed as described by Abreu et al. (2020) and Urbancsok et al. (2023) and processed by an untargeted approach. The generated data were normalized against the internal standard and weight of each sample. Changes in abundance between transgenic and WT samples were considered as significant if $P \leq 0.05$ (t-test) and $|\text{fold change}| \geq 1.5$. The false discovery rate was < 0.05 .

Statistical analyses

Unless otherwise stated, statistical analyses were performed in JMP Pro (v.16.0) software (SAS Institute Inc., Cary, NC, USA).

Acknowledgements

This work was supported by the Knut and Alice Wallenberg (KAW) Foundation, the Swedish Governmental Agency for Innovation Systems (VINNOVA), Swedish Research Council, Kempestiftelserna, T4F, Bio4Energy and the SSF program ValueTree RBP14-0011 to EJM. MK was supported by The Czech Science Foundation (GAČR) via 20-25948Y junior grant.

We are grateful to the undergraduate student Rakesh Vaasan, KTH, for help with cell wall analyses. We acknowledge the Umeå Plant Science Centre (UPSC) Tree Phenotyping Platform, Bioinformatics Facility, Microscopy Facility, Biopolymer Analytical Platform, and the Swedish Metabolomics Centre in Umeå.

Author Contributions

PS performed majority of wood chemistry and microscopy analyses, interpreted the data and wrote the manuscript. JU processed wood material, extracted RNA, analyzed transgene expression and prepared samples for omics analyses. JU, END and FRB carried the greenhouse experiment and tree phenotyping. END performed bioinformatic analyses. MDM created transgenic aspen and collected samples for Silviscan analysis. ZY and GS carried out wood SilviScan analyses. JŠ, KC and MK analysed hormones. MLG and LJJ analysed saccharification potential. MM analyzed metabolomics data. EH and FV carried out hemicellulose analyses. ERM designed cloning strategy. EJM designed and coordinated the research, secured the funding, and finalized the paper with contributions from all authors.

Data availability

The raw RNA-Seq data that support the findings of this study are available in the European Nucleotide Archive (ENA) at EMBL-EBI (<https://www.ebi.ac.uk/ena/browser/home>), under accession no. PRJEB61635 and

References

- Abreu, I.N., Johansson, A.I., Sokołowska, K., Niittylä, T., Sundberg, B., Hvidsten, T.R., Street, N.R. and Moritz, T. (2020) A metabolite roadmap of the wood-forming tissue in *Populus tremula*. *New Phytol.* **228**,1559–1572.
- Albersheim, P., Darvill, A., Roberts, K., Sederoff, R. and Staehelin, A. (2010) *Plant cell walls*. Garland Science, Taylor & Francis Group, LLC, New York.
- Bacete, L. and Hamann, T. (2020) The role of mechanoperception in plant cell wall integrity maintenance. *Plants* **9**, 574.
- Bacete, L., Mérida, H., López, G., Dabos, P., Tremousaygue, D., Denancé, N., Miedes, E., Bulone, V., Goffiner, D. and Molina, A. (2020) ARABIDOPSIS RESPONSE REGULATOR 6 (ARR6) modulates plant cell-wall composition and disease resistance. *Mol. Plant Microbe Interact.* **33**, 767-780.
- Bar-On, Y.M., Phillips, R. and Milo, R. (2018) The biomass distribution on Earth. *Proc. Natl. Acad. Sci. U. S. A.* **115**, 6506-6511.
- Bauer, S., Vasu, P., Persson, S., Mort, A. J., and Somerville, C. R. (2006). Development and application of a suite of polysaccharide-degrading enzymes for analyzing plant cell walls. *Proc. Natl. Acad. Sci. U. S. A.* **103**, 11417–11422.
- Bavnhøj, L., Paulsen, P.A., Flores-Canales, J.C., Schiøtt, B. and Pedersen, B.P. (2021) Molecular mechanism of sugar transport in plants unveiled by structures of glucose/H⁺ symporter STP10. *Nat. Plants* **7**, 1409-1419.
- Bi, G., Su, M., Li, N., Liang, Y., Dang, S., Xu, J., Hu, M., Wang, J., Zou, M., Deng, Y., Li, Q., Huang, S., Li, J., Chai, J., He, K., Chen, Y. H., & Zhou, J. M. (2021). The ZAR1 resistosome is a calcium-permeable channel triggering plant immune signaling. *Cell* **184**, 3528–3541.e12.
- Biely, P., Vrsanská, M., Tenkanen, M. and Kluepfel, D. (1997) Endo-beta-1,4-xylanase families: differences in catalytic properties. *J. Biotechnol.* **57**, 151-166.
- Biely, P., Singh, S., & Puchart, V. (2016). Towards enzymatic breakdown of complex plant xylan structures: State of the art. *Biotechnol. Adv.* **34**, 1260–1274.

- Bishopp, A., Benková, E. and Helariutta, Y. (2011) Sending mixed messages: auxin-cytokinin crosstalk in roots. *Curr. Opin. Plant Biol.* **14**, 10-16.
- Biswal, A.K., Hao, Z., Pattathil, S., Yang, X., Winkeler, K., Collins, C., Mohanty, S.S., Richardson, E.A., Gelineo-Albersheim, I., Hunt, K., Ryno, D., Sykes, R.W., Turner, G.B., Ziebell, A., Gjersing, E., Lukowitz, W., Davis, M.F., Decker, S.R., Hahn, M.G. and Mohnen, D. (2015) Downregulation of *GAUT12* in *Populus deltoides* by RNA silencing results in reduced recalcitrance, increased growth and reduced xylan and pectin in a woody biofuel feedstock. *Biotechnol. Biofuels* **8**, 41.
- Bromley, J.R., Busse-Wicher, M., Tryfona, T., Mortimer, J.C., Zhang, Z., Brown, D.M. and Dupree, P. (2013) GUX1 and GUX2 glucuronyltransferases decorate distinct domains of glucuronoxytan with different substitution patterns. *Plant J.* **74**, 423-434.
- Brown, D.M., Zeef, L.A., Ellis, J., Goodacre, R. and Turner, S.R. (2005) Identification of novel genes in *Arabidopsis* involved in secondary cell wall formation using expression profiling and reverse genetics. *Plant Cell* **17**, 2281-2295.
- Busse-Wicher, M., Gomes, T.C.F., Tryfona, T., Nikolovski, N., Stott, K., Grantham, N.J., Bolam, D.N., Skaf, M.S. and Dupree, P. (2014) The pattern of xylan acetylation suggests xylan may interact with cellulose microfibrils as a twofold helical screw in the secondary plant cell wall of *Arabidopsis thaliana*. *Plant J.* **79**, 492-506.
- Cantarel, B.L., Coutinho, P.M., Rancurel, C., Bernard, T., Lombard, V. and Henrissat, B. (2009) The Carbohydrate-Active EnZymes database (CAZy): an expert resource for Glycogenomics. *Nucleic Acids Res.* **37**, D233-238.
- Chang, S., Puryear, J. and Cairney, J. (1993) A simple and efficient method for isolating RNA from pine trees. *Plant Mol. Biol. Rep.* **11**, 113-116.
- Chang, N., Sun, Q., Li, Y., Mu, Y., Hu, J., Feng, Y., Liu, X., & Gao, H. (2017). PDV2 has a dosage effect on chloroplast division in *Arabidopsis*. *Plant Cell Rep.* **36**, 471-480.
- Chen, H., Wang, J. P., Liu, H., Li, H., Lin, Y. J., Shi, R., Yang, C., Gao, J., Zhou, C., Li, Q., Sederoff, R. R., Li, W., & Chiang, V. L. (2019). Hierarchical transcription factor and chromatin binding network for wood formation in black cottonwood (*Populus trichocarpa*). *Plant Cell* **31**, 602-626.
- Chong, S.L., Koutaniemi, S., Virkki, L., Pynnönen, H., Tuomainen, P. and Tenkanen, M. (2013) Quantitation of 4-O-methylglucuronic acid from plant cell walls. *Carbohydr. Polym.* **91**, 626-630.
- DeMartini, J.D., Pattathil, S., Miller, J.S., Li, H., Hahn, M.G. and Wyman, C.E. (2013) Investigating plant cell wall components that affect biomass recalcitrance in poplar and switchgrass. *Energy Environ. Sci.* **6**, 898-909.
- Derba-Maceluch, M., Awano, T., Takahashi, J., Lucenius, J., Ratke, C., Kontro, I., Busse-Wicher, M., Kosik, O., Tanaka, R., Winzell, A., Kallas, Å., Leśniewska, J., Berthold, F., Immerzeel, P., Teeri, T.T., Ezcurrea, I., Dupree, P., Serimaa, R. and Mellerowicz, E.J. (2015) Suppression of xylan endotransglycosylase *PtxtXyn10A* affects cellulose microfibril angle in secondary wall in aspen wood. *New Phytol.* **205**, 666-81.
- Derba-Maceluch, M., Sivan, P., Donev, E.N., Gandla, M.L., Yassin, Z., Vaasan, R., Heinonen, E., Andersson, S., Amini, F., Scheepers, G., Johansson, U., Vilaplana, F.J., Albrechtsen, B.R., Hertzberg, M., Jönsson, L.J. and Mellerowicz, E.J. (2023) Impact of xylan on field productivity and wood saccharification properties in aspen. *Front. Plant Sci.* **14**, 1218302.
- Dewangan, B.P., Gupta, A., Sah, R.K., Das, S., Kumar, S., Bhattacharjee, S. and Pawar, P.A. (2023) Xylobiose treatment triggers a defense-related response and alters cell wall composition. *Plant Mol. Biol.* **113**, 383-400.
- Donaldson, L.A. (1992) Lignin distribution during late wood formation in *Pinus radiata* D. Don. *IAWA Bulletin* **13**, 381-387.

- Donev, E., Gandla, M.L., Jönsson, L.J. and Mellerowicz, E.J. (2018) Engineering non-cellulosic polysaccharides of wood for the biorefinery. *Front. Plant Sci* **9**, 1537.
- Escalante, A., Gonçalves, A., Bodin, A., Stepan, A., Sandström, C., Toriz, G. and Gatenholm, P. (2012) Flexible oxygen barrier films from spruce xylan. *Carbohydr. Polym.* **87**, 2381-2387.
- Faria-Blanc, N., Mortimer, J. C., and Dupree, P. (2018). A transcriptomic analysis of xylan mutants does not support the existence of a secondary cell wall integrity system in *Arabidopsis*. *Frontiers Plant Sci.* **9**, 384. <https://doi.org/10.3389/fpls.2018.00384>
- Gandla, L.M., Derba-Maceluch, M., Liu, X., Gerber, L., Master, E.R., Mellerowicz, E.J. and Jönsson, L.J. (2015) Expression of a fungal glucuronoyl esterase in *Populus*: effects on wood properties and saccharification efficiency. *Phytochemistry* **112**, 210-220.
- Gandla, M.L., Mähler, N., Escamez, S., Skotare, T., Obudulu, O., Möller, L., Abreu, I.N., Bygdell, J., Hertzberg, M., Hvidsten, T.R., Moritz, T., Wingsle, G., Trygg, J., Tuominen, H. and Jönsson, L.J. (2021) Overexpression of vesicle-associated membrane protein *PttVAP27-17* as a tool to improve biomass production and the overall saccharification yields in *Populus* trees. *Biotechnol Biofuels.* **14**,43.
- Garapati, P., Xue, G.P., Munné-Bosch, S. and Balazadeh, S. (2015) Transcription Factor ATAF1 in *Arabidopsis* Promotes Senescence by Direct Regulation of Key Chloroplast Maintenance and Senescence Transcriptional Cascades. *Plant Physiol.* **168**, 1122-1139.
- Gerber, L., Eliasson, M., Trygg, J., Moritz, T. and Sundberg, B. (2012) Multivariate curve resolution provides a high-throughput data processing pipeline for pyrolysis-gas chromatography/mass spectrometry. *J. Anal. Appl. Pyrolysis* **95**, 95-100.
- Grantham, N.J., Wurman-Rodrich, J., Terrett, O.M., Lyczakowski, J.J., Stott, K., Iuga, D., Simmons, T.J., Durand-Tardif, M., Brown, S.P., Dupree, R., Busse-Wicher, M. and Dupree, P. (2017) An even pattern of xylan substitution is critical for interaction with cellulose in plant cell walls. *Nat. Plants* **3**, 859-865.
- Gui, J., Luo, L., Zhong, Y., Sun, J., Umezawa, T., and Li, L. (2019). Phosphorylation of LTF1, an MYB transcription factor in *Populus*, acts as a sensory switch regulating lignin biosynthesis in wood cells. *Mol. Plant* **12**, 1325-1337.
- Gupta, M., Rawal, T.B., Dupree, P., Smith, J.C. and Petridis, L. (2021) Spontaneous rearrangement of acetylated xylan on hydrophilic cellulose surfaces. *Cellulose* **28**, 3327-3345.
- Haas, A.S., Shi, D. and Greb, T. (2022) Cell fate decisions within the vascular cambium—initiating wood and bast formation. *Front. Plant Sci.* **13**, 864422.
- Han, H., Zhang, G., Wu, M., & Wang, G. (2016). Identification and characterization of the *Populus trichocarpa* CLE family. *BMC Genomics* **17**, 174.
- Hao, Z., Avci, U., Tan, L., Zhu, X., Glushka, J., Pattathil, S., Eberhard, S., Sholes, T., Rothstein, G.E., Lukowitz, W., Orlando, R., Hahn, M.G. and Mohnen, D. (2014) Loss of *Arabidopsis GAUT12/IRX8* causes anther indehiscence and leads to reduced G lignin associated with altered matrix polysaccharide deposition. *Front. Plant Sci.* **5**,357.
- Hartley, R.D., Morrison, W.H., Himmelsbach, D.S. and Borneman, W.S. (1990) Cross-linking of cell wall phenolic arabinoxylans in graminaceous plants. *Phytochemistry* **29**, 3705-3709.
- Hernández-Blanco, C., Feng, D. X., Hu, J., Sánchez-Vallet, A., Deslandes, L., Llorente, F., Berrocal-Lobo, M., Keller, H., Barlet, X., Sánchez-Rodríguez, C., Anderson, L. K., Somerville, S., Marco, Y., & Molina, A. (2007). Impairment of cellulose synthases required for *Arabidopsis* secondary cell wall formation enhances disease resistance. *Plant Cell* **19**, 890–903.
- Hoang, N. V., Choe, G., Zheng, Y., Aliaga Fandino, A. C., Sung, I., Hur, J., Kamran, M., Park, C., Kim, H., Ahn, H., Kim, S., Fei, Z., & Lee, J. Y. (2020). Identification of conserved gene-regulatory networks that integrate environmental sensing and growth in the root cambium. *Current Biol.* **30**, 2887–2900.e7.
- Immanen, J., Nieminen, K., Smolander, O.-P., Kojima, M., Alonso Serra, J., Koskinen, P., Zhang, J., Elo, A., Mähönen, Ari P., Street, N., Bhalerao, Rishikesh P., Paulin, L., Auvinen, P.,

- Sakakibara, H. and Helariutta, Y. (2016) Cytokinin and auxin display distinct but interconnected distribution and signaling profiles to stimulate cambial activity. *Curr. Biol.* **26**, 1990-1997.
- Jones, L., Ennos, A.R. and Turner, S.R. (2001) Cloning and characterization of irregular xylem4 (irx4): a severely lignin-deficient mutant of *Arabidopsis*. *Plant J* **26**, 205-216.
- Kaida, R., Kaku, T., Baba, K., Oyadomari, M., Watanabe, T., Nishida, K., Kanaya, T., Shani, Z., Shoseyov, O. and Hayashi, T. (2009) Loosening xyloglucan accelerates the enzymatic degradation of cellulose in wood. *Mol. Plant.* **2**, 904-909.
- Karady, M., Hladík, P., Cermanová, K., Jiroutová, P., Antoniadis, I., Casanova-Sáez, R., Ljung, K. and Novák, O. (2024). Profiling of 1-aminocyclopropane-1-carboxylic acid and selected phytohormones in *Arabidopsis* using liquid chromatography-tandem mass spectrometry. *Plant Methods* **20**, 41.
- Karimi, M., Inzé, D. and Depicker, A. (2002) GATEWAY vectors for Agrobacterium-mediated plant transformation. *Trends Plant Sci.* **7**, 193–195.
- Keegan, D., Kretschmer, B., Elbersen, B. and Panoutsou, C. (2013) Cascading use: a systematic approach to biomass beyond the energy sector. *Biofuels, Bioprod. Bioref.* **7**, 193-206.
- Kim, J.H., Nguyen, N.H., Jeong, C.Y., Nguyen, N.T., Hong, S.W. and Lee, H (2013) Loss of the R2R3 MYB, *AtMYB73*, causes hyper-induction of the SOS1 and SOS3 genes in response to high salinity in *Arabidopsis*. *J. Plant Physiol.* **170**, 1461-1465.
- Kitin, P., Nakaba, S., Hunt, C.G., Lim, S. and Funada, R. (2020) Direct fluorescence imaging of lignocellulosic and suberized cell walls in roots and stems. *AoB Plants* **12**, plaa032.
- Kojima, K., Sunagawa, N., Yoshimi, Y., Tryfona, T., Samejima, M., Dupree, P., & Igarashi, K. (2022). Acetylated xylan degradation by glycoside hydrolase family 10 and 11 xylanases from the white-rot fungus *Phanerochaete chrysosporium*. *J. Appl. Glycosci.* **69**, 35–43.
- Kolenová, K., Vrsanská, M. and Biely, P. (2006) Mode of action of endo-beta-1,4-xylanases of families 10 and 11 on acidic xylooligosaccharides. *J. Biotechnol.* **121**, 338-345.
- Kumar, V., Hainaut, M., Delhomme, N., Mannapperuma, C., Immerzeel, P., Street, N.R., Henrissat, B. and Mellerowicz, E.J. (2019) Poplar carbohydrate-active enzymes: whole-genome annotation and functional analyses based on RNA expression data. *Plant J.* **99**, 589-609.
- Lee, C., Teng, Q., Huang, W., Zhong, R. and Ye, Z.-H. (2009) Down-regulation of *PoGT47C* expression in poplar results in a reduced glucuronoxylan content and an increased wood digestibility by cellulase. *Plant Cell Physiol.* **50**, 1075-1089.
- Lee, C., Teng, Q., Zhong, R. and Ye, Z.-H. (2011) Molecular dissection of xylan biosynthesis during wood formation in poplar. *Mol. Plant* **4**, 730-747.
- Li, Q., Lin, Y.C., Sun, Y.H., Song, J., Chen, H., Zhang, X.H., Sederoff, R.R. and Chiang, V.L. (2012) Splice variant of the SND1 transcription factor is a dominant negative of SND1 members and their regulation in *Populus trichocarpa*. *Proc. Natl. Acad. Sci. U.S.A* **109**, 14699-14704.
- Liu, C., Yu, H., Rao, X., Li, L., & Dixon, R. A. (2021). Abscisic acid regulates secondary cell-wall formation and lignin deposition in *Arabidopsis thaliana* through phosphorylation of NST1. *Proc. Nat. Acad. Sci. USA* **118**, e2010911118.
- Maris, A., Kaewthai, N., Eklöf, J.M., Miller, J.G., Brumer, H., Fry, S.C., Verbelen, J.P. and Vissenberg, K. (2011) Differences in enzymic properties of five recombinant xyloglucan endotransglucosylase/hydrolase (XTH) proteins of *Arabidopsis thaliana*. *J. Exp. Bot.* **62**, 261-271.
- Markwalder, H.U. and Neukom, H. (1976) Diferulic acid as a possible crosslink in hemicelluloses from wheat germ. *Phytochemistry* **15**, 836-837.
- Martínez-Abad, A., Giummarella, N., Lawoko, M. and Vilaplana, F. (2018) Differences in extractability under subcritical water reveal interconnected hemicellulose and lignin recalcitrance in birch hardwoods. *Green Chem.* **20**, 2534-2546.

- McKee, L.S., Sunner, H., Anasontzis, G.E., Toriz, G., Gatenholm, P., Bulone, V., Vilaplana, F. and Olsson, L. (2016b) A GH115 α -glucuronidase from *Schizophyllum commune* contributes to the synergistic enzymatic deconstruction of softwood glucuronoarabinoxylan. *Biotechnol. Biofuels* **9**, 2.
- Mertz, R.A., Olek, A.T. and Carpita, N.C. (2012) Alterations in cell-wall glycosyl linkage structure of *Arabidopsis murus* mutants. *Carbohydr. Polym.* **89**, 331-339.
- Mischnick, P. (2012) Mass spectrometric characterization of oligo- and polysaccharides and their derivatives. *Advances in Polymer Science*, pp.105-174. Vol. **248**, Springer, Berlin, Heidelberg.
- Mori, K., Renhu, N., Naito, M., Nakamura, A., Shiba, H., Yamamoto, T., Suzaki, T., Iida, H. and Miura, K. (2018) Ca(2+)-permeable mechanosensitive channels MCA1 and MCA2 mediate cold-induced cytosolic Ca(2+) increase and cold tolerance in *Arabidopsis*. *Sci. Rep.* **8**, 550.
- Murthy, S.E., Dubin, A.E., Whitwam, T., Jojoa-Cruz, S., Cahalan, S.M., Mousavi, S.A.R., Ward, A.B. and Patapoutian, A. (2018) OSCA/TMEM63 are an evolutionarily conserved family of mechanically activated ion channels. *Elife* **7**.
- Ohtani, M., Nishikubo, N., Xu, B., Yamaguchi, M., Mitsuda, N., Goué, N., Shi, F., Ohme-Takagi, M. and Demura, T. (2011) A NAC domain protein family contributing to the regulation of wood formation in poplar. *Plant J.* **67**, 499-512.
- Papdi, C., Ábrahám, E., Joseph, M.P., Popescu, C., Koncz, C. and Szabados, L.S. (2008) Functional identification of *Arabidopsis* stress regulatory genes using the controlled cDNA overexpression system. *Plant Physiol.* **147**, 528-542.
- Pauly, M. and Keegstra, K. (2008) Cell-wall carbohydrates and their modification as a resource for biofuels. *Plant J.* **54**, 559-568.
- Pauly, M. and Keegstra, K. (2010) Plant cell wall polymers as precursors for biofuels. *Curr. Opin. Plant Biol.* **13**, 305-312.
- Pawar, P.M.-A., Derba-Maceluch, M., Chong, S.-L., Gandla, M.L., Bashar, S.S., Sparrman, T., Ahvenainen, P., Hedenström, M., Özparpucu, M., Rüggeberg, M., Serimaa, R., Lawoko, M., Tenkanen, M., Jönsson, L.J. and Mellerowicz, E.J. (2017) *In muro* deacetylation of xylan affects lignin properties and improves saccharification of aspen wood. *Biotechnol. Biofuels* **10**, 98.
- Pawar, P.M., Derba-Maceluch, M., Chong, S.L., Gómez, L.D., Miedes, E., Banasiak, A., Ratke, C., Gaertner, C., Mouille, G., McQueen-Mason, S.J., Molina, A., Sellstedt, A., Tenkanen, M. and Mellerowicz, E.J. (2016) Expression of fungal acetyl xylan esterase in *Arabidopsis thaliana* improves saccharification of stem lignocellulose. *Plant Biotechnol. J.* **14**, 387-397.
- Pell, G., Taylor, E.J., Gloster, T.M., Turkenburg, J.P., Fontes, C.M., Ferreira, L.M., Nagy, T., Clark, S.J., Davies, G.J. and Gilbert, H.J. (2004) The mechanisms by which family 10 glycoside hydrolases bind decorated substrates. *J. Biol. Chem.* **279**, 9597-9605.
- Persson, S., Caffall, K.H., Freshour, G., Hilley, M.T., Bauer, S., Poindexter, P., Hahn, M.G., Mohnen, D. and Somerville, C. (2007) The *Arabidopsis irregular xylem8* mutant is deficient in glucuronoxyylan and homogalacturonan, which are essential for secondary cell wall integrity. *Plant Cell* **19**, 237-255.
- Petersen, P. D., Lau, J., Ebert, B., Yang, F., Verhertbruggen, Y., Kim, J. S., Varanasi, P., Suttangkakul, A., Auer, M., Loqué, D., and Scheller, H. V. (2012). Engineering of plants with improved properties as biofuels feedstocks by vessel-specific complementation of xylan biosynthesis mutants. *Biotechnol. Biofuels* **5**, 84. <https://doi.org/10.1186/1754-6834-5-84>
- Pfaffl, M.W. (2001) A new mathematical model for relative quantification in real-time RT-PCR. *Nucleic Acids Res.* **29**, e45.
- Pogorelko, G., Fursova, O., Lin, M., Pyle, E., Jass, J. and Zabortina, O.A. (2011) Post-synthetic modification of plant cell walls by expression of microbial hydrolases in the apoplast. *Plant Mol. Biol.* **77**, 433-445.

- Pollet, A., Delcour, J.A. and Courtin, C.M. (2010) Structural determinants of the substrate specificities of xylanases from different glycoside hydrolase families. *Crit. Rev. Biotechnol.* **30**, 176-191.
- Potikha, T. and Delmer, D.P. (1995) A mutant of *Arabidopsis thaliana* displaying altered patterns of cellulose deposition. *Plant J.* **7**, 453-460.
- Pramod, S., Gandla, M.L., Derba-Maceluch, M., Jönsson, L.J., Mellerowicz, E.J. and Winestrand, S. (2021) Saccharification potential of transgenic greenhouse- and field-grown aspen engineered for reduced xylan acetylation. *Front. Plant Sci.* **12**, 704960.
- Pramod, S., Patel, V.R., Rajput, K.S. and Rao, K.S. (2014) Distribution of tension wood like gelatinous fibres in the roots of *Acacia nilotica* (Lam.) Willd. *Planta* **240**, 1191-1202.
- Ralph, J., Grabber, J.H. and Hatfield, R.D. (1995) Lignin-ferulate cross-links in grasses: active incorporation of ferulate polysaccharide esters into ryegrass lignins. *Carbohydrate Research* **275**, 167-178.
- Ramírez, V. and Pauly, M. (2019) Genetic dissection of cell wall defects and the strigolactone pathway in *Arabidopsis*. *Plant Direct* **3**, e00149.
- Ratke, C., Pawar, P.M., Balasubramanian, V.K., Naumann, M., Duncranz, M.L., Derba-Maceluch, M., Gorzsás, A., Endo, S., Ezcurra, I. and Mellerowicz, E.J. (2015) *Populus GT43* family members group into distinct sets required for primary and secondary wall xylan biosynthesis and include useful promoters for wood modification. *Plant Biotechnol. J.* **13**, 26-37.
- Ratke, C., Terebieniec, B.K., Winestrand, S., Derba-Maceluch, M., Grahn, T., Schiffthaler, B., Ulvcróna, T., Özparpucu, M., Rüggeberg, M., Lundqvist, S.-O., Street, N.R., Jönsson, L.J. and Mellerowicz, E.J. (2018) Downregulating aspen xylan biosynthetic *GT43* genes in developing wood stimulates growth via reprogramming of the transcriptome. *New Phytol.* **219**, 230-245.
- Reilly, P.J. (1981) Xylanases: structure and function. *Basic Life Sci.* **18**, 111-129.
- Richmond, B.L., Coelho, C.L., Wilkinson, H., McKenna, J., Ratchinski, P., Schwarze, M., Frost, M., Lagunas, B. and Gifford, M.L. (2022) Elucidating connections between the strigolactone biosynthesis pathway, flavonoid production and root system architecture in *Arabidopsis thaliana*. *Physiol. Plant.* **174**, e13681.
- Rivero, R.M., Mittler, R., Blumwald, E. and Zandalinas, S.I. (2022) Developing climate-resilient crops: improving plant tolerance to stress combination. *Plant J.* **109**, 373-389.
- Romano, J.M., Dubos, C., Prouse, M.B., Wilkins, O., Hong, H., Poole, M., Kang, K.-Y., Li, E., Douglas, C.J., Western, T.L., Mansfield, S.D. and Campbell, M.M. (2012) *AtMYB61*, an R2R3-MYB transcription factor, functions as a pleiotropic regulator via a small gene network. *New Phytol.* **195**, 774-786.
- Rudsander, U.J., Denman, S., Raza, S., Teeri, T.T. (2003) Molecular features of family GH9 cellulases in hybrid aspen and the filamentous fungus *Phanerochaete chrysosporium*. *Journal of Applied Glycoscience* **50**, 253-256.
- Ruel, K., Chevalier-billosta, V., Guillemin, F., Sierra, J.B. and Joseleau, J-P. (2006) The wood cell wall at the ultrastructural scale - formation and topochemical organization. *Maderas Cienc.Tecnol.* **8**, 107-116.
- Saeman J.F., Moore W.E., Mitchell R.L. and Millett M.A. (1954). Technique for the determination of pulp constituents by quantitative paper chromatography. *Tappi J.* **37**, 336-343.
- Sapouna, I., Kärkönen, A. and McKee, L.S. (2023) The impact of xylan on the biosynthesis and structure of extracellular lignin produced by a Norway spruce tissue culture. *Plant Direct* **7**, e500.
- Schuetz, M., Smith, R. and Ellis, B. (2012) Xylem tissue specification, patterning, and differentiation mechanisms. *J. Exp. Bot.* **64**, 11-31.

- Simmons, T.J., Mortimer, J.C., Bernardinelli, O.D., Pöppler, A.-C., Brown, S.P., deAzevedo, E.R., Dupree, R. and Dupree, P. (2016) Folding of xylan onto cellulose fibrils in plant cell walls revealed by solid-state NMR. *Nat. Commun.* **7**, 13902.
- Simura, J., Antoniadi, I., Siroka, J., Tarkowska, D., Strnad, M., Ljung, K. and Novak, O. (2018) Plant hormonomics: multiple phytohormone profiling by targeted metabolomics. *Plant Physiol.* **177**, 476–489.
- Sivan, P., Heinonen, E., Latha Gandla, M., Jiménez-Quero, A., Özeren, H.D., Jönsson, L.J., Mellerowicz, E.J. and Vilaplana, F. (2023) Sequential extraction of hemicelluloses by subcritical water improves saccharification of hybrid aspen wood grown in greenhouse and field conditions. *Green Chem.* **25**, 5634–5646.
- Somerville, C.R. and Bonetta, D. (2001) Plants as factories for technical materials. *Plant Physiol.* **125**, 168–171.
- Sundell, D., Mannapperuma, C., Netotea, S., Delhomme, N., Lin, Y.C., Sjödin, A., Van de Peer, Y., Jansson, S., Hvidsten, T.R. and Street, N.R. (2015) The plant genome integrative explorer resource: PlantGenIE.org. *New Phytol.* **208**, 1149–1156.
- Sundell, D., Street, N.R., Kumar, M., Mellerowicz, E.J., Kucukoglu, M., Johnsson, C., Kumar, V., Mannapperuma, C., Delhomme, N., Nilsson, O., Tuominen, H., Pesquet, E., Fischer, U., Niittylä, T., Sundberg, B. and Hvidsten, T.R. (2017) AspWood: high-spatial-resolution transcriptome profiles reveal uncharacterized modularity of wood formation in *Populus tremula*. *Plant Cell* **29**, 1585–1604.
- Takata, N., Awano, T., Nakata, M.T., Sano, Y., Sakamoto, S., Mitsuda, N. and Taniguchi, T. (2019) *Populus NST/SND* orthologs are key regulators of secondary cell wall formation in wood fibers, phloem fibers and xylem ray parenchyma cells. *Tree Physiol.* **39**, 514–525.
- Taylor-Teeples, M., Lin, L., de Lucas, M., Turco, G., Toal, T. W., Gaudinier, A., Young, N. F., Trabucco, G. M., Veling, M. T., Lamothe, R., Handakumbura, P. P., Xiong, G., Wang, C., Corwin, J., Tsoukalas, A., Zhang, L., Ware, D., Pauly, M., Kliebenstein, D. J., Dehesh, K., ... Brady, S. M. (2015). An *Arabidopsis* gene regulatory network for secondary cell wall synthesis. *Nature* **517**, 571–575.
- Teh, O. K., & Moore, I. (2007). An ARF-GEF acting at the Golgi and in selective endocytosis in polarized plant cells. *Nature* **448**, 493–496.
- Timell, T.E. (1961) Isolation of galactoglucomannans from the wood of gymnosperms. *Tappi* **44**, 88–96.
- Tipper, E., Leitão, N., Dangeville, P., Lawson, D. M., & Charpentier, M. (2023). A novel mutant allele of *AtCNGC15* reveals a dual function of nuclear calcium release in the root meristem. *J. Exp. Bot.* **74**, 2572–2584.
- Turner, S.R. and Somerville, C.R. (1997) Collapsed xylem phenotype of *Arabidopsis* identifies mutants deficient in cellulose deposition in the secondary cell wall. *Plant Cell* **9**, 689–701.
- Turner, S.R., Taylor, N. and Jones, L. (2001) Mutations of the secondary cell wall. *Plant Mol. Biol.* **47**, 209–219.
- Urbancsok, J., Donev, E.N., Sivan, P., van Zalen, E., Barbut, F.R., Derba-Maceluch, M., Šimura, J., Yassin, Z., Gandla, M.L., Karady, M., Ljung, K., Winstrand, S., Jönsson, L.J., Scheepers, G., Delhomme, N., Street, N.R. and Mellerowicz, E.J. (2023) Flexure wood formation via growth reprogramming in hybrid aspen involves jasmonates and polyamines and transcriptional changes resembling tension wood development. *New Phytol.* **240**, 2312–2334.
- Van Norman, J.M. and Sieburth, L.E. (2007) Dissecting the biosynthetic pathway for the bypass1 root-derived signal. *Plant J.* **49**, 619–628.
- Vandesompele, J., De Preter, K., Pattyn, F., Poppe, B., Van Roy, N., De Paepe, A. et al. (2002) Accurate normalization of real-time quantitative RT-PCR data by geometric averaging of multiple internal control genes. *Genome Biol.* **3**, 0034.

- Vardakou, M., Dumon, C., Murray, J.W., Christakopoulos, P., Weiner, D.P., Juge, N., Lewis, R.J., Gilbert, H.J. and Flint, J.E. (2008) Understanding the structural basis for substrate and inhibitor recognition in eukaryotic GH11 xylanases. *J. Mol. Biol.* **375**, 1293-1305.
- Wang, Z., Mao, Y., Guo, Y., Gao, J., Liu, X., Li, S., Lin, Y. J., Chen, H., Wang, J. P., Chiang, V. L., & Li, W. (2020a). MYB transcription factor161 mediates feedback regulation of secondary wall-associated NAC-domain family genes for wood formation. *Plant Physiol.* **184**, 1389–1406.
- Wang, L., Wang, B., Yu, H., Guo, H., Lin, T., Kou, L., Wang, A., Shao, N., Ma, H., Xiong, G., Li, X., Yang, J., Chu, J. and Li, J. (2020b) Transcriptional regulation of strigolactone signalling in *Arabidopsis*. *Nature* **583**, 277-281.
- Wang, W., Talide, L., Viljamaa, S., & Niittylä, T. (2022). Aspen growth is not limited by starch reserves. *Current Biol.* **32**, 3619–3627.
- Wang, X., Niu, Y. and Zheng, Y (2021) Multiple functions of MYB transcription factors in abiotic stress responses. *Int. J. Mol. Sci.* **22**, 6125.
- Wang, Z., Winstrand, S., Gillgren, T. and Jönsson, L.J. (2018) Chemical and structural factors influencing enzymatic saccharification of wood from aspen, birch and spruce. *Biomass Bioenergy* **109**, 125–134.
- Wenkel, S., Emery, J., Hou, B. H., Evans, M. M., & Barton, M. K. (2007). A feedback regulatory module formed by LITTLE ZIPPER and HD-ZIPIII genes. *Plant Cell* **19**, 3379–3390.
- Windram, O., Madhou, P., McHattie, S., Hill, C., Hickman, R., Cooke, E., Jenkins, D.J., Penfold, C.A., Baxter, L., Breeze, E., Kiddle, S.J., Rhodes, J., Atwell, S., Kliebenstein, D.J., Kim, Y.S., Stegle, O., Borgwardt, K., Zhang, C., Tabrett, A., Legaie, R., Moore, J., Finkenstadt, B., Wild, D.L., Mead, A., Rand, D., Beynon, J., Ott, S., Buchanan-Wollaston, V. and Denby, K.J. (2012) *Arabidopsis* defense against *Botrytis cinerea*: chronology and regulation deciphered by high-resolution temporal transcriptomic analysis. *Plant Cell* **24**, 3530-3557.
- Wu, F., Chi, Y., Jiang, Z., Xu, Y., Xie, L., Huang, F., Wan, D., Ni, J., Yuan, F., Wu, X., Zhang, Y., Wang, L., Ye, R., Byeon, B., Wang, W., Zhang, S., Sima, M., Chen, S., Zhu, M., Pei, J., Johnson, D.M., Zhu, S., Cao, X., Pei, C., Zai, Z., Liu, Y., Liu, T., Swift, G.B., Zhang, W., Yu, M., Hu, Z., Siedow, J.N., Chen, X. and Pei, Z.M. (2020) Hydrogen peroxide sensor HPCA1 is an LRR receptor kinase in *Arabidopsis*. *Nature* **578**, 577-581.
- Yang, Y., Tang, R. J., Li, B., Wang, H. H., Jin, Y. L., Jiang, C. M., Bao, Y., Su, H. Y., Zhao, N., Ma, X. J., Yang, L., Chen, S. L., Cheng, X. H., & Zhang, H. X. (2015). Overexpression of a *Populus trichocarpa* H⁺-pyrophosphatase gene *PtVPL1* confers salt tolerance on transgenic poplar. *Tree Physiol.* **35**, 663–677.
- Yuan, F., Yang, H., Xue, Y., Kong, D., Ye, R., Li, C., Zhang, J., Theprungsirikul, L., Shrift, T., Krichilsky, B., Johnson, D.M., Swift, G.B., He, Y., Siedow, J.N. and Pei, Z.-M. (2014) OSCA1 mediates osmotic-stress-evoked Ca²⁺ increases vital for osmosensing in *Arabidopsis*. *Nature* **514**, 367-371.
- Yuan, Y., Teng, Q., Zhong, R. and Ye, Z.H. (2016b) TBL3 and TBL31, Two *Arabidopsis* DUF231 domain proteins, are required for 3-o-monoacetylation of xylan. *Plant Cell Physiol.* **57**, 35-45.
- Yuan, Y., Teng, Q., Zhong, R., Haghghat, M., Richardson, E.A. and Ye, Z.H. (2016a) Mutations of *Arabidopsis* TBL32 and TBL33 affect xylan acetylation and secondary wall deposition. *PLoS One* **11**, e0146460.
- Zhang, X., Gou, M. and Liu, C.J. (2013) *Arabidopsis* Kelch repeat F-box proteins regulate phenylpropanoid biosynthesis via controlling the turnover of phenylalanine ammonia-lyase. *Plant Cell* **25**, 4994-5010.
- Zheng, K., Wang, X., Weighill, D.A., Guo, H.B., Xie, M., Yang, Y., Yang, J., Wang, S., Jacobson, D.A., Guo, H., Muchero, W., Tuskan, G.A. and Chen, J.G. (2016) Characterization of *DWARF14* genes in *Populus*. *Sci. Rep.* **6**, 21593.

- Zhong, R., Peña, M. J., Zhou, G. K., Nairn, C. J., Wood-Jones, A., Richardson, E. A., Morrison, W. H., 3rd, Darvill, A. G., York, W. S., & Ye, Z. H. (2005). *Arabidopsis* *FRAGILE FIBER8*, which encodes a putative glucuronyltransferase, is essential for normal secondary wall synthesis. *Plant Cell* **17**, 3390–3408.
- Zhong, R., Lee, C. and Ye, Z.H. (2010) Functional characterization of poplar wood-associated NAC domain transcription factors. *Plant Physiol.* **152**, 1044-1055.
- Zhong, R., Lee, C., Zhou, J., McCarthy, R.L. and Ye, Z.-H. (2008) A battery of transcription factors involved in the regulation of secondary cell wall biosynthesis in *Arabidopsis*. *Plant Cell* **20**, 2763-2782.
- Zhong, R., McCarthy, R.L., Lee, C. and Ye, Z.H. (2011) Dissection of the transcriptional program regulating secondary wall biosynthesis during wood formation in poplar. *Plant Physiol.* **157**, 1452-1468.
- Zhu, L., Zhang, X. Q., Ye, D., & Chen, L. Q. (2021). The MILDEW RESISTANCE LOCUS O 4 interacts with CaM/CML and is involved in root gravity response. *Int. J Mol. Sci.* **22**, 5962.

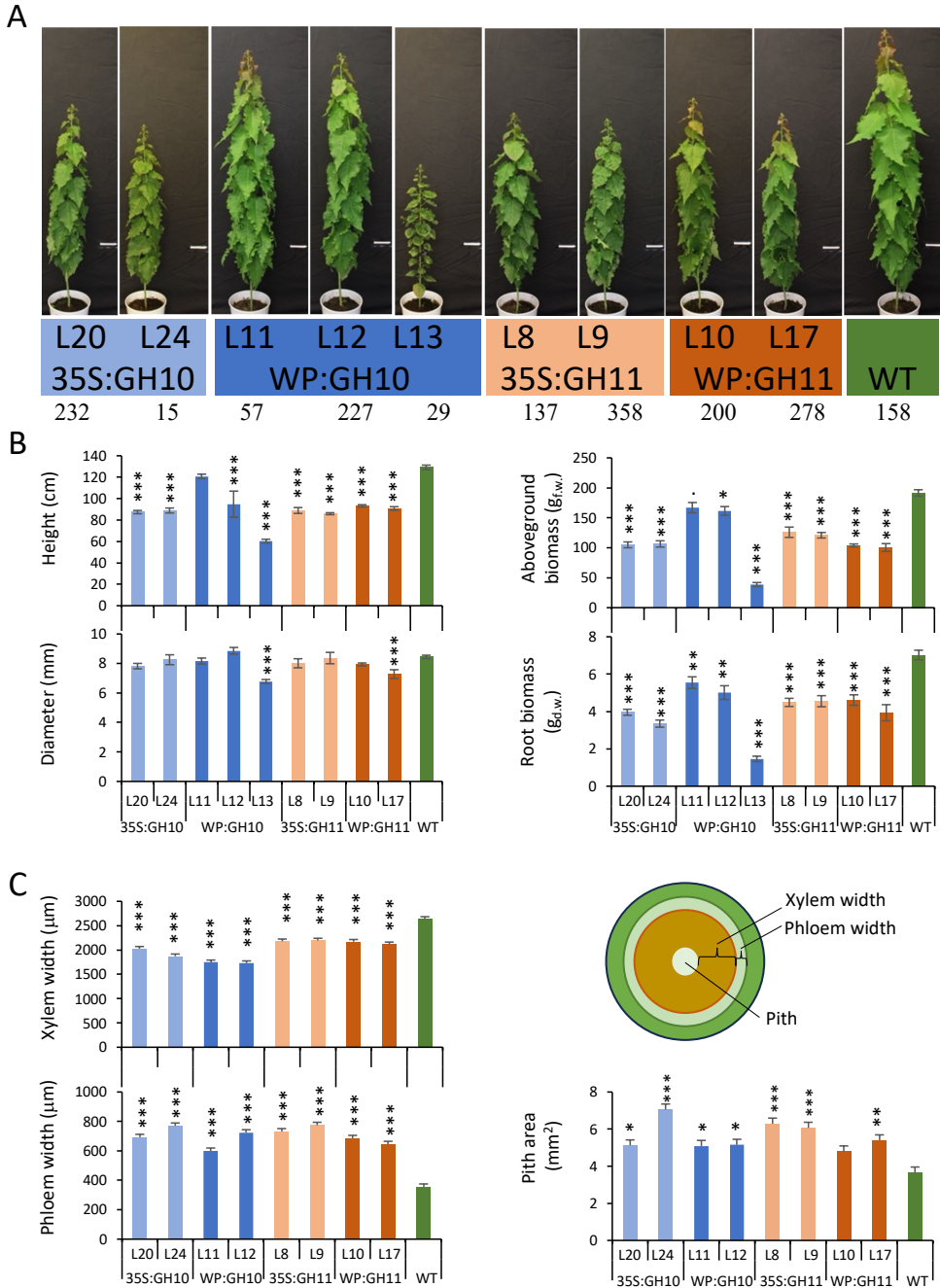


Figure 1. Growth of transgenic lines expressing GH10 and GH11 xylanases. (A) Morphology of 9-week-old plants. Size bar = 10 cm. **(B)** Plant size. **(C)** The width of secondary xylem and secondary phloem and the area of pith measured in stem cross sections of internode 40, as shown on the diagram. Data are means \pm SE; N=6 trees for transgenic lines and 14 for WT for (B), 2 trees \times 10 radii or 2 trees \times 2 sections in (C). * - $P \leq 0.05$; ** - $P \leq 0.01$; *** - $P \leq 0.001$ for comparisons with WT by Dunnett's test.

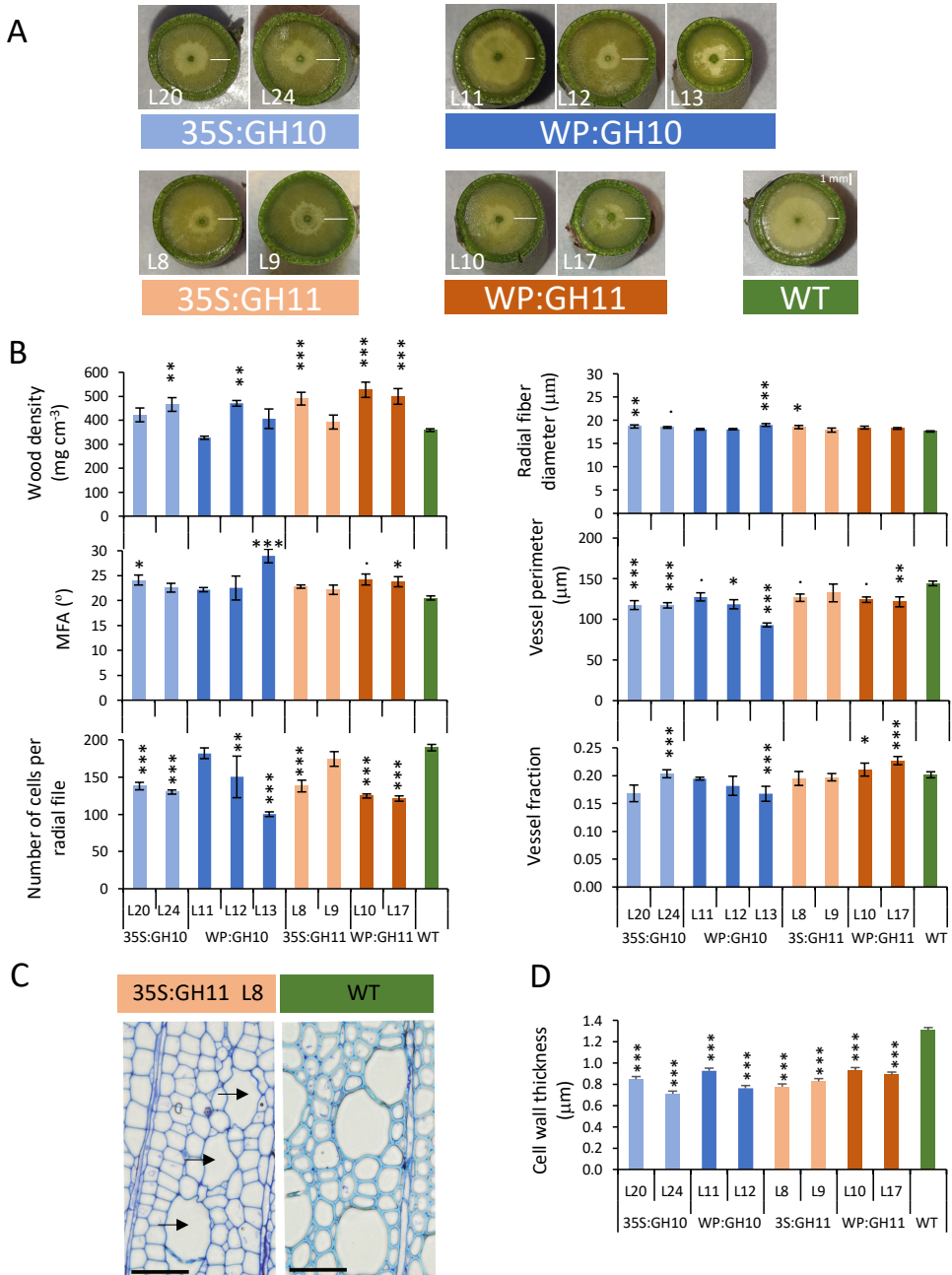


Figure 2. Wood quality traits of transgenic lines expressing GH10 and GH11 xylanases determined by SilviScan and anatomical analyses. (A) Appearance of SilviScan wood samples freshly dissected from the stems. Note the wider wet-looking zone (white bars) in transgenic lines. **(B)** Different wood quality traits measured by SilviScan. **(C)** Typical appearance of wood in xylanase-expressing plants. Note a reduction in cell wall thickness, *irregular xylem* phenotype (collapsed vessels, black arrows) and altered cell wall staining properties. Toluidine blue stained wood cross sections. Sections of other lines are shown in Supplementary Figure S2. **(D)** Secondary wall thickness measured by transmission electron microscopy analysis. WT-wild type, MFA – cellulose microfibril angle. Data in B and D are means \pm SE, N = 6 for transgenic lines and 24 for WT in B, or 2 trees \times 3 images \times 4 measurement in D. * - $P \leq 0.05$; ** - $P \leq 0.01$; *** - $P \leq 0.001$ for comparisons with WT by Dunnett's test.

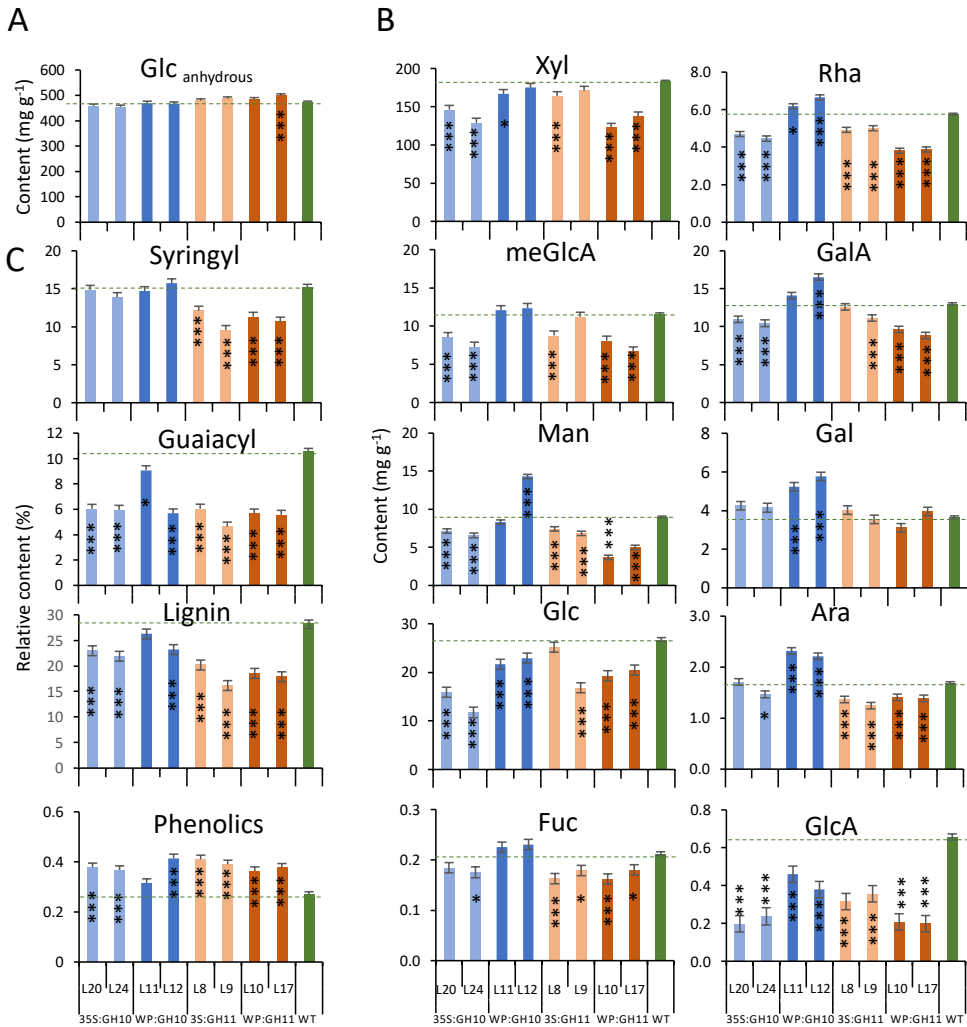


Figure 3. Chemical composition of wood in transgenic lines expressing GH10 and GH11 xylanases. Glucan (anhydrous glucose) content in dry wood determined by sulfuric acid hydrolysis (A). Matrix sugar content (hydrous) determined by methanolysis-TMS per dry weight of dry destarched alcohol-insoluble wood (B). Relative content of syringyl (S) and guaiacyl (G) monolignols, total lignin (S+G+H) and phenolics in wood powder determined by the pyrolysis GC-MS (C). H - *p*-hydroxyphenyl units. Data are means \pm SE, N = 3 technical replicates of pooled material from 6 trees in A; N = 9 (3 technical and 3 biological replicates in B; N = 3 biological replicates for C, * - $P \leq 0.05$; ** - $P \leq 0.01$; *** - $P \leq 0.001$ for comparisons with WT by Dunnett's test.

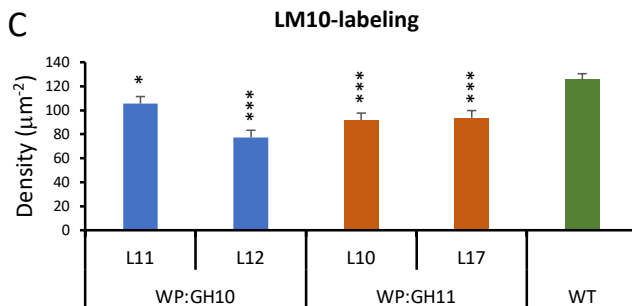
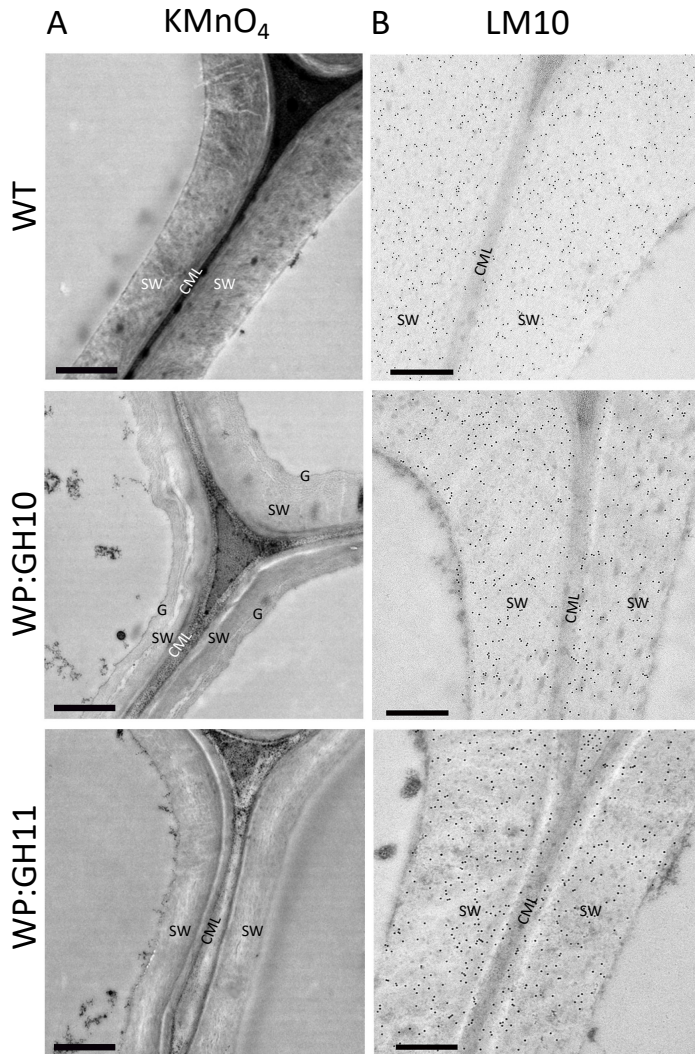


Figure 4. Transmission electron microscopy of cell walls in the xylem of transgenic lines expressing GH10 and GH11 xylanases showing differences in lignin and xylan content compared to wild type (WT). (A) Lignin in the fiber walls detected with KMnO_4 which is seen as a dark deposit in the compound middle lamella (CML) and secondary walls (SW) is highly reduced in transgenic lines. Note also the presence of G-layer (G) in one of the transgenic samples. **(B, C)** Immunogold localization of xylan in fiber cell walls using LM10 antibody **(B)** and quantification of gold particle density over secondary walls **(C)**. Scale bar = 1 μm in A and 500 nm in B; data in C are means \pm SE, N = 2 trees \times 3 images \times 4 measurements. * - $P \leq 0.05$; ** - $P \leq 0.01$; *** - $P \leq 0.001$ for comparisons with WT by Dunnett's test.

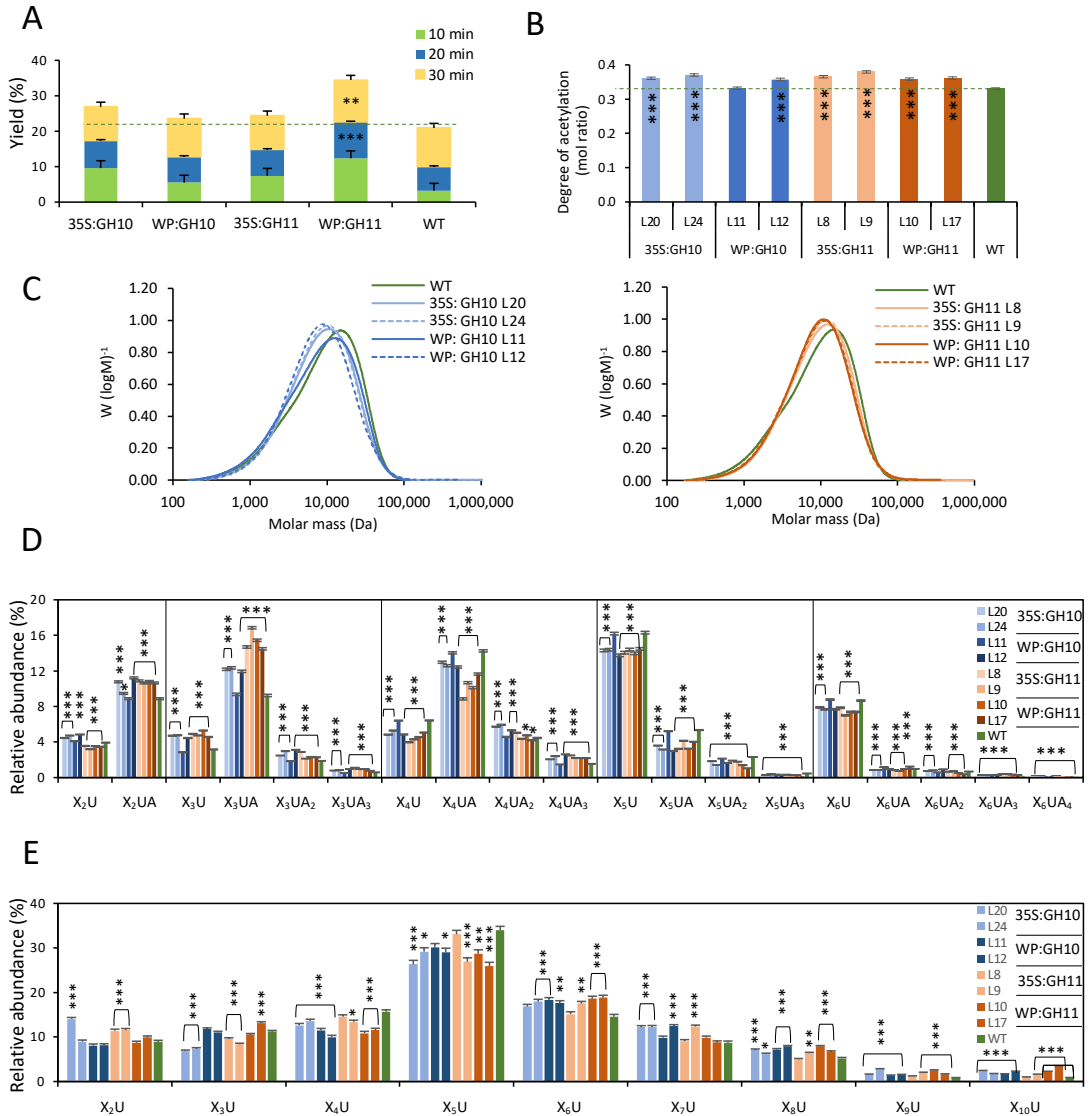


Figure 5. Characterization of xylan structure in transgenic lines expressing GH10 and GH11 xylanases. (A) Xylan yields during successive steps of subcritical water extraction relative to starting xylan weight. **(B)** The degree of acetylation of xylan extracted by SWE for 30 min. **(C)** Size exclusion chromatography of 30 min SWE extract. **(D, E)** Oligomeric mass profiling (OLIMP) by ESI-MS of SWE-extracted glucuronoxylan **(D)** or alkali-extracted glucuronoxylan **(E)** hydrolyzed with GH30 glucuronoxylanase. Relative abundance of oligosaccharides in D and E are calculated from the total ESI-MS intensities. Data in A, B, D, E are means \pm SE, N= 2 lines in A, 2 technical replicates in B, and 3 technical replicates in D and E, * - P \leq 0.05; ** - P \leq 0.01; *** - P \leq 0.001 for comparisons with WT by Dunnett's test.

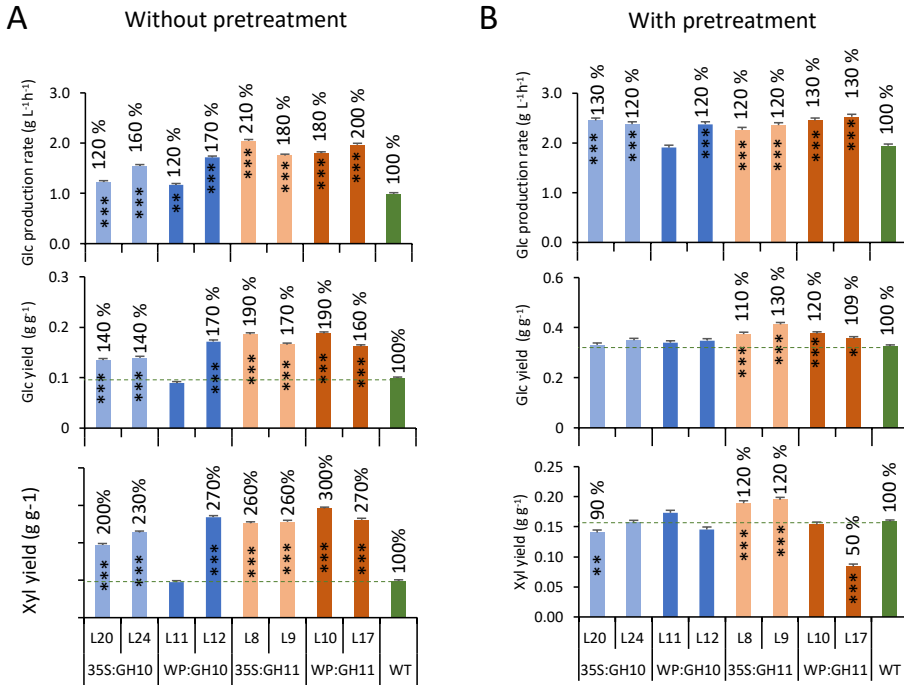


Figure 6. Effects of *in planta* expression of GH10 and GH11 xylanases on saccharification of wood. Glucose production rates, and glucose and xylose yields in saccharification without (A) and with (B) acid pretreatment. Data are means \pm SE, N = 3 or 6 technical replicates from the pooled material of 6 trees for transgenic lines and WT, respectively. * - $P \leq 0.05$; ** - $P \leq 0.01$; *** - $P \leq 0.001$ for comparisons with WT by Dunnett's test.

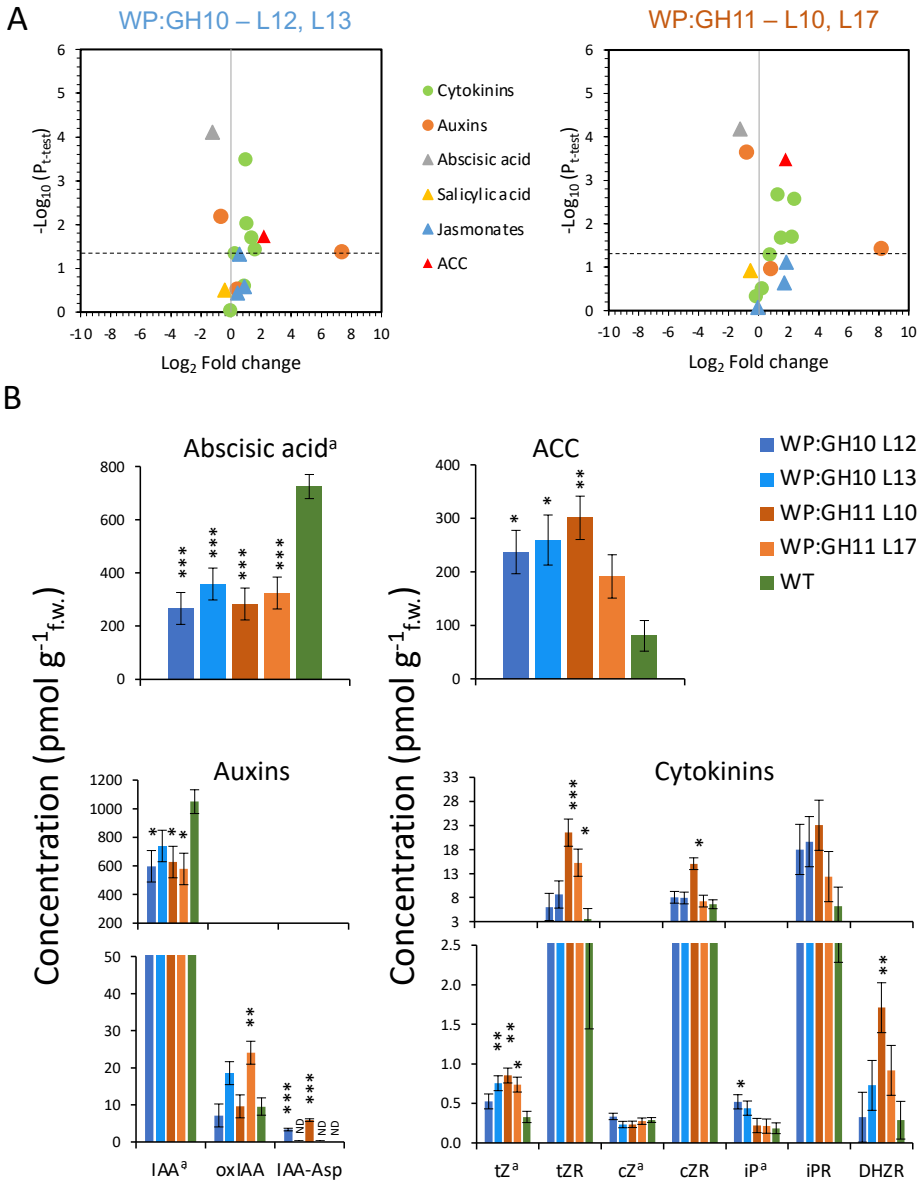


Figure 7. Changes in hormonal status in wood forming tissues of transgenic lines expressing GH10 or GH11 xylanases. (A) Volcano plots showing all detected hormones. Colored signs above the dashed lines show the hormones that were either significantly increased or reduced in the transgenic lines at $P \leq 0.05$ compared with wild type (WT). **(B)** Bar plots showing mean contents of abscisic acid, ACC, auxins and cytokinins in transgenic lines as compared to WT. Data are means \pm SE, $N = 4$ trees for transgenic lines and 7 for WT; * - $P \leq 0.05$; ** - $P \leq 0.01$; *** - $P \leq 0.001$ for comparisons with WT by Dunnett's test. ND – not detected; active hormones are marked with "a". ACC – 1-aminocyclopropane-1-carboxylic acid; IAA – indole-3-acetic acid; oxIAA – 2-oxoindole-3-acetic acid; IAA-Asp – IAA-aspartate; tZ – *trans*-zeatin; tZR – *trans*-zeatin riboside; cZ – *cis*-zeatin; cZR – *cis*-zeatin riboside; iP – N⁶-isopentenyladenine; iPR – N⁶-isopentenyladenosine; DHZR – dihydrozeatin riboside.

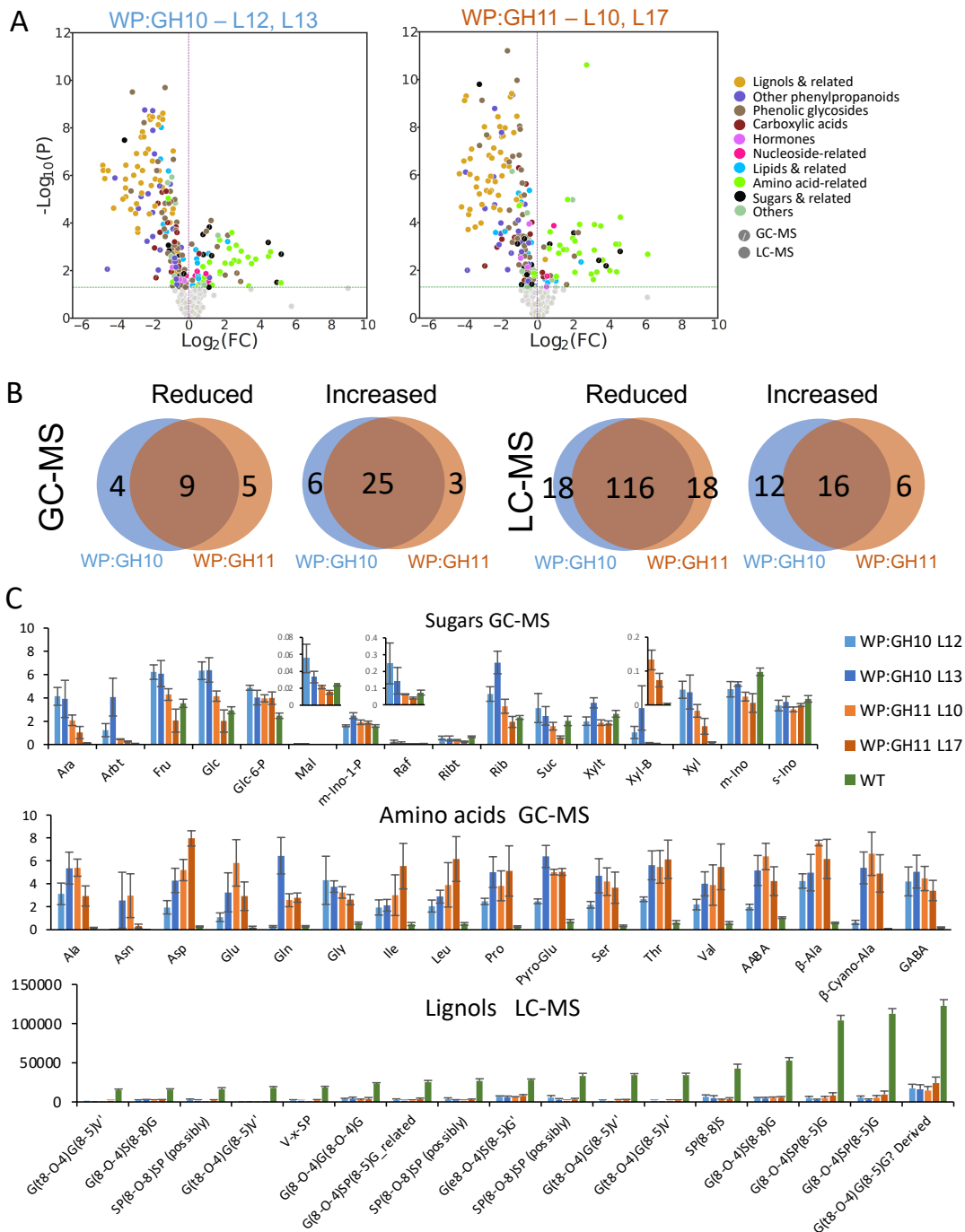
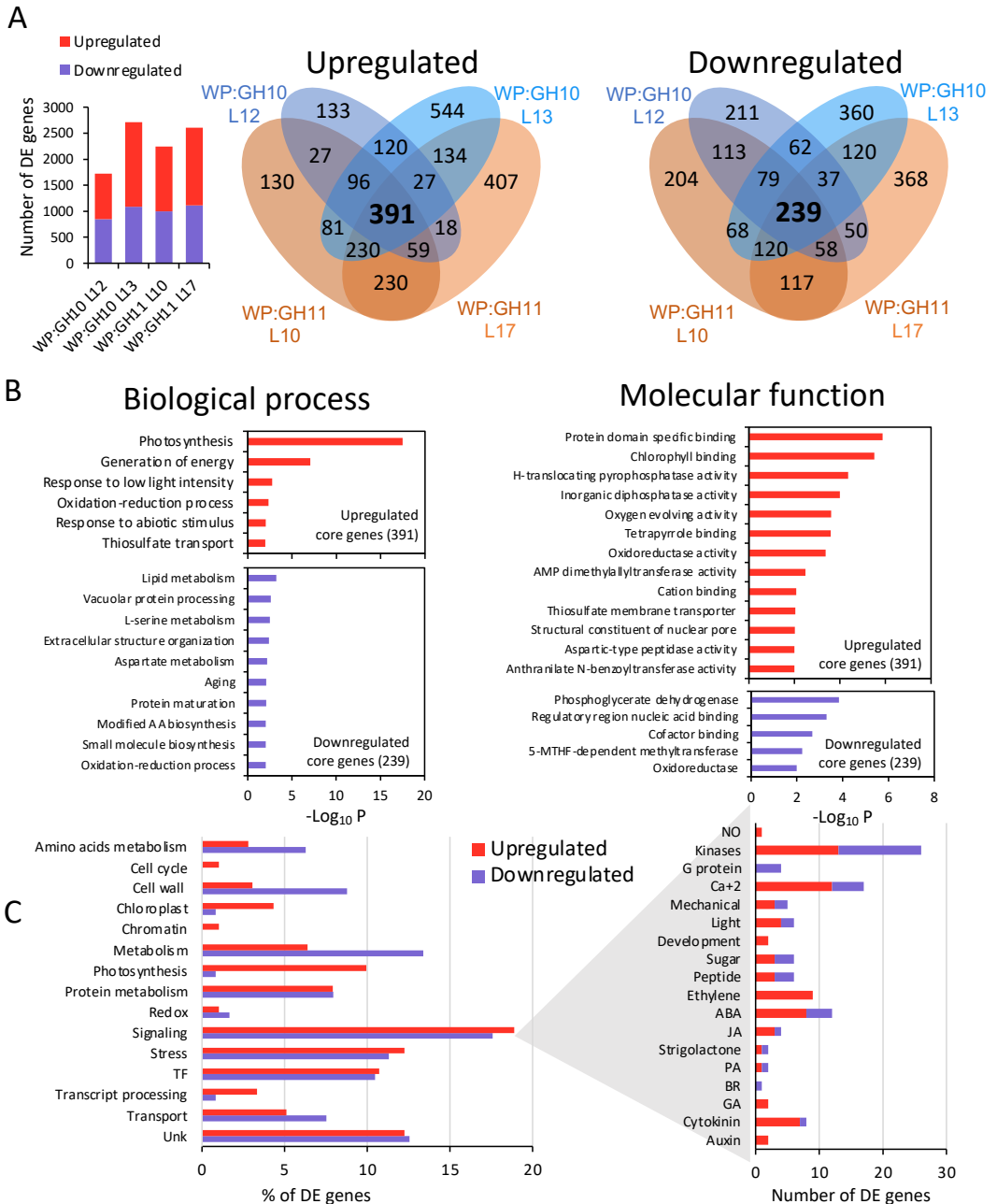


Figure 8. Metabolomes of developing wood in transgenic lines expressing xylanases show massive changes in several groups of compounds. (A) Volcano plots of metabolites analyzed by LC-MS and GC-MS showing groups of compounds significantly affected ($P \leq 0.05$, t-test) in transgenic lines compared to wild type (WT). (B) Venn diagrams showing number of metabolites significantly affected transgenic lines compared to WT. (C) Quantitative variation in integrated peaks (in relative units) corresponding to the most affected groups of compounds (amino acids, sugars and most abundant lignols). Data are means \pm SE, $N = 8$ trees for WT and 4 for transgenic lines. Complete lists of metabolites are shown in Tables S1 – S3.



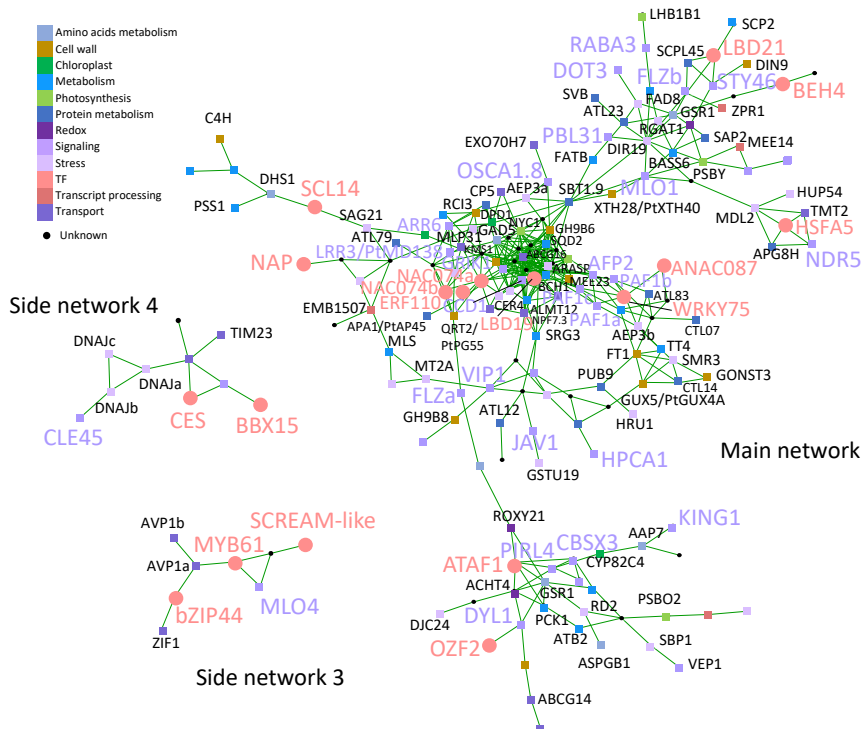


Figure 10. Co-expression networks of the core genes differentially expressed in GH10- and GH11-expressing aspen lines. Gene exclusive functional classification is indicated by the colors of the nodes, as listed in Table S7. Signaling- and stress-related genes and transcription factors are shown on large colored fonts. All gene names use *Arabidopsis* gene symbols, unless indicated by prefix Pt. For the gene expression data and all identified networks, please see Figures S7-S10.

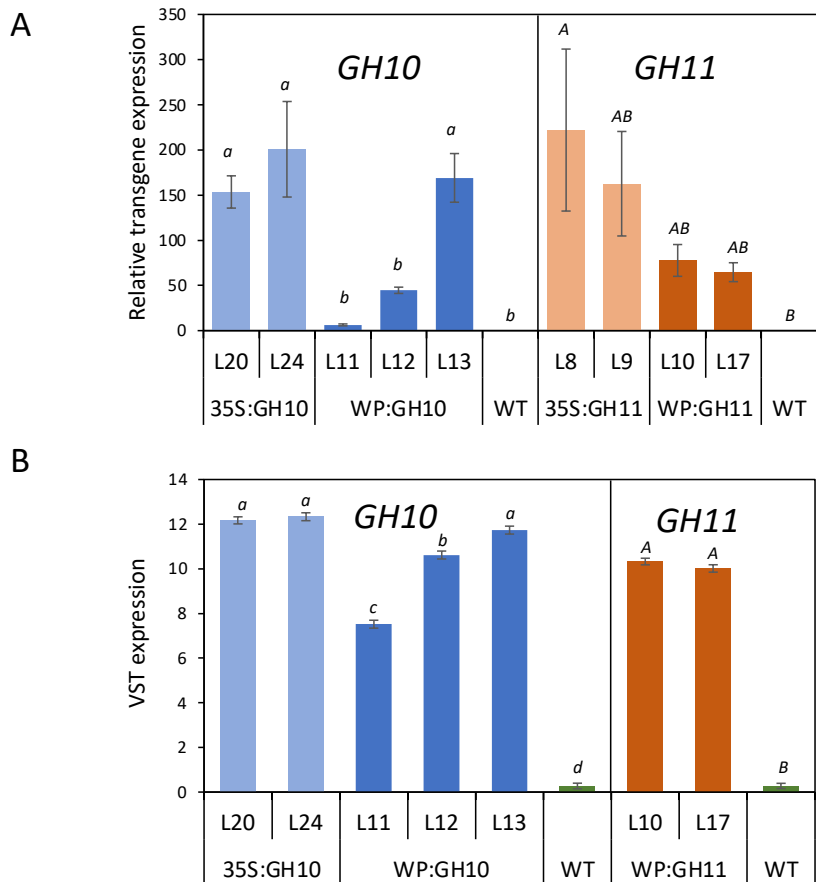
Table 1. Signaling-related genes significantly up- (U) or downregulated (D) in common by GH10 and GH11 xylanases.

Category	<i>P. tremula</i> v. 2.2 <i>Potra2n</i>	<i>P. trichocarpa</i> v. 3.1 <i>Potri</i>	Ath Diamond BLAST	Ath name	U/D	Category	<i>P. tremula</i> v. 2.2 <i>Potra2n</i>	<i>P. trichocarpa</i> v. 3.1 <i>Potri</i>	Ath Diamond BLAST	Ath name	U/D
ABA	7c15809	007G101700	AT5G63910	<i>AtFLCY</i>	U	JA	16c29395	016G017900	AT3G22160	<i>AtJAV1</i>	U
ABA	13c26213	013G009800	AT3G58450	<i>AtGRUSP/USP</i>	U	JA	432s35660	001G015500	AT3G45140	<i>AtLOX2</i>	U
ABA	8c17204	008G065000	AT2G39980		U	JA	10c21496	010G108200	AT3G17860	<i>AtIAZ3</i>	U
ABA	5c12343	005G058200	AT2G38820		U	JA	13c25422	013G102700	AT1G76690	<i>AtOPR2</i>	D
ABA	6c15263	006G014500	AT5G47550	<i>AtCY55</i>	U	Kinases	1069s36958	005G014700	AT2G19130		U
ABA	9c18899	009G139400	AT4G38470	<i>AtSTY46</i>	U	Kinases	743s36657	005G014700	AT2G19130		U
ABA	9c19650	009G054000	AT1G50920	<i>AtNOG1-1</i>	U	Kinases	3c7707	003G090100	AT4G35470	<i>AtPIRL4</i>	U
ABA	1c767	001G092500	AT5G53160	<i>AtRCAR3</i>	U	Kinases	11c22893	011G110200	AT1G78850	<i>AtGAL2, MBL1</i>	U
ABA	18c32305	018G107800	AT5G46220	<i>AtTOD1</i>	D	Kinases	12c24522	012G097000	AT3G48530	<i>AtKING1</i>	U
ABA	4c9033	004G067400	AT1G73390		D	Kinases	18c32838	018G048100	AT5G21940		U
ABA	17c31097	017G094500	AT1G13740	<i>AtAFP2</i>	D	Kinases	6c13385	006G219800	AT5G21940		U
ABA	6c13197	018G043500	AT3G63520	<i>AtNCED1/CCD1</i>	D	Kinases	8c18059	008G156000	AT3G22750		U
Auxin	3c7907	003G063400	AT1G54200	<i>AtBG3</i>	U	Kinases	12c24080	012G043200	AT1G73500	<i>AtMAPKK9</i>	U
Auxin	1c3599	001G410400	AT5G54510	<i>AtDFL1/GH3.6</i>	U	Kinases	4c9196	004G086000	AT5G37660	<i>AtPDL7</i>	U
BR	5c11696	005G124000	AT3G50660	<i>AtDWF4</i>	D	Kinases	158s34765	019G050500	AT5G16810		U
Ca ²⁺	2c6269	002G019800	AT1G20080	<i>AtSYTB</i>	U	Kinases	15c28339	015G094700	AT3G48530	<i>AtKING1</i>	U
Ca ²⁺	6c14829	006G062800	AT1G30270	<i>AtCIPK23</i>	U	Kinases	2c6154	002G032100	AT1G59580	<i>AtMPK2</i>	U
Ca ²⁺	14c27171	014G104200	AT1G01140	<i>AtCIPK9</i>	U	Kinases	8c17227	008G067900	AT2G40090	<i>AtATH9</i>	D
Ca ²⁺	19c33304	019G128100	AT2G30360	<i>AtCIPK11</i>	U	Kinases	8c17956	008G144900	AT1G10850		D
Ca ²⁺	7c16155	007G055100	AT5G67480	<i>AtBT4</i>	U	Kinases	2c6116	002G036200	AT1G03920	<i>AtNDR5</i>	D
Ca ²⁺	1c1997	001G231100	AT2G44310		U	Kinases	10c20345	010G231000	AT3G52790		D
Ca ²⁺	18c30319	018G027300	AT4G32300	<i>AtSD2-5</i>	U	Kinases	11c23439	011G034900	AT1G61400		D
Ca ²⁺	3c6844	003G181900	AT5G25110	<i>AtCIPK25</i>	U	Kinases	3c7017	003G164200	AT1G03080	<i>AtNET1D</i>	D
Ca ²⁺	114s34562	015G126800	AT5G62390	<i>AtBAG7</i>	U	Kinases	6c13382	006G220100	AT2G26330	<i>AtER</i>	D
Ca ²⁺	1c19	001G002000	AT1G55500	<i>AtECT4</i>	U	Kinases	10c20401	010G225300	AT2G39110	<i>AtPBL38</i>	D
Ca ²⁺	6c15264	006G014400	AT3G50950	<i>AtZAR1</i>	U	Kinases	8c18004	008G150200	AT3G05990	<i>AtLLR3</i>	D
Ca ²⁺	3c6476	003G222700	AT3G13460	<i>AtECT2</i>	U	Kinases	203s34959	007G039800	AT5G66850	<i>AtMAPKKK5</i>	D
Ca ²⁺	17c31919	017G000900	AT4G02600	<i>AtMLO1</i>	D	Kinases	2c5709	002G077900	AT1G77280		D
Ca ²⁺	4c10336	004G218500	AT1G11000	<i>AtMLO4</i>	D	Kinases	2c6370	002G009400	AT1G76360	<i>AtPBL31</i>	D
Ca ²⁺	8c17563	008G103900	AT5G49480	<i>AtCP1</i>	D	Kinases	4c10446	004G231600	AT5G49760	<i>AtHPCA1</i>	U
Ca ²⁺	6c13702	006G187500	AT4G30993		D	Light	5c11650	005G130700	AT5G66560		D
Ca ²⁺	4c10186	004G202200	AT2G27480		D	Light	7c15989	005G090000	AT5G04190	<i>AtPK54</i>	U
Cytokinins	6c13614	006G196900	AT1G15670	<i>AtKMD2</i>	U	Light	13c24949	013G159000	AT2G30520	<i>AtRPT2</i>	U
Cytokinins	10c21288	008G117100	AT1G13260	<i>AtRAV1</i>	U	Light	5c11293	005G175800	AT1G21920	<i>AtMORN3</i>	U
Cytokinins	10c22148	010G030500	AT5G19040	<i>AtIPT5</i>	U	Light	11c22895	011G109900	AT2G42610	<i>AtLSH7, LSH10</i>	D
Cytokinins	5c11275	005G177600	AT1G21830		U	Light	13c26086	013G024400	AT5G64330	<i>AtDOT3/NPH3</i>	D
Cytokinins	9c19633	009G055800	AT1G01550	<i>AtBPS1</i>	U	Mech.	243s35083	T092400	AT3G51660	<i>AtMDL3</i>	U
Cytokinins	8c18492	008G202200	AT5G19040	<i>AtPTS5</i>	U	Mech.	3c7622	003G099800	AT1G32090	<i>AtOSCA1.8</i>	U
Cytokinins	15c29002	015G023200	AT4G27950	<i>AtCRF4</i>	U	Mech.	19c33668	019G079300	AT1G72160	<i>AtPATL3</i>	U
Cytokinins	15c28518	015G078200	AT5G62960	<i>AtARR6</i>	D	Mech.	5c11148	002G069500	AT1G43700	<i>AtVIP1/SUE3</i>	D
Development	15c28320	015G096500	AT3G48550		U	Mech.	8c17949	008G144300	AT2G02170		D
Development	14c26462	014G019500	AT4G24220	<i>AAV131/VEP1</i>	U	NO	7c15899	007G092300	AT3G05030		U
Ethylene	19c34043	T069600	AT5G39890	<i>AtHU43/PCO2</i>	U	PA	1c3393	001G388900			U
Ethylene	4c2902	004G086600	AT2G38540	<i>AtLTP1/LP1</i>	U	PA	3c7590	003G103600	AT1G31830	<i>AtPUT2/PQR2</i>	D
Ethylene	11c22474	011G156200	AT1G06650		U	Peptides	18c32791	018G057100	AT5G25930	<i>AtHSL3/NUT</i>	U
Ethylene	17c30762	017G135800	AT1G06620		U	Peptides	10c20934	010G169300		<i>AtCLE45</i>	U
Ethylene	8c18146	008G164400	AT3G23150	<i>AtETR2</i>	U	Peptides	3c7873	003G074000	AT1G72300	<i>AtPSY1R</i>	U
Ethylene	18c32128	018G130800	AT5G25350	<i>AtEBF2, EBF1</i>	U	Peptides	3c6613	003G206000	AT5G12950	<i>AtPAF1</i>	D
Ethylene	1c65	001G007100	AT3G13610	<i>AtDLO2</i>	U	Peptides	154s34742	003G206000	AT5G12950	<i>AtPAF1</i>	D
Ethylene	16c29776	016G059700	AT3G58040	<i>AtSINAT2</i>	U	Peptides	3c6614	003G206000	AT5G12950	<i>AtPAF1</i>	D
Ethylene	1c3337	001G381700	AT1G17020	<i>AtSRG1</i>	U	SL	2c5333	002G118900	AT3G03990	<i>AtD14</i>	U
G proteins	2c4810	002G175700	AT1G01200	<i>RABA3</i>	D	SL	8c17236	008G069100	AT2G40130	<i>AtSMXL8</i>	D
G proteins	18c32613	018G075300	AT5G19610	<i>AtGNL2</i>	D	Sugar	4c8814	004G047100	AT1G28330	<i>AtDYL1/DRM1</i>	U
G proteins	14c27157	014G102200	AT1G01200	<i>AtRABA3</i>	D	Sugar	1c105	001G010700	AT3G45240	<i>AtGRIK1</i>	U
G proteins	2c4342	002G231900	AT2G43120	<i>AtPRN2</i>	D	Sugar	1c1918	001G220800	AT5G21170	<i>AtKINBETA1</i>	U
GA	1c3303	001G378400	AT1G78440	<i>AtGA2OX1</i>	U	Sugar	14c27762	014G167400	AT5G21170	<i>AtKINBETA1</i>	D
GA	5c10699	005G239100	AT1G75750	<i>AtGASA1</i>	U	Sugar	7c15922	007G089200	AT1G78020	<i>AtFLZ6</i>	D
						Sugar	2c5564	002G092000	AT1G78020	<i>AtFLZ6</i>	D

Table 2. Cell wall-related genes significantly ($P_{adj} \leq 0.05$) up- or downregulated in transgenic lines expressing GH10 and GH11 xylanases. Shown are values of Log_2 fold change from WT levels. Values in grey are not significantly different from WT.

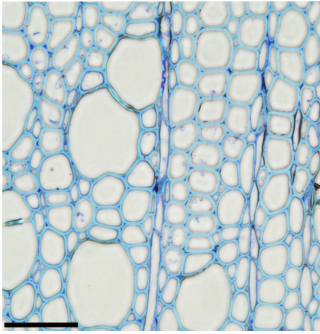
<i>P. tremula</i> v. 2.2 Potra2n	<i>P. trichocarpa</i> v. 3.1	Populus name	Ath best BLAST	Ath name	Log_2FC				Functi on	
					WP:GH10		WP:GH11			
					L12	L13	L10	L17		
19c33790	Potri.019G069300	<i>PtGH9B3</i>	AT1G71380	<i>AtCEL3</i>	-0.65	-0.59	-0.81	-1.47	CEL	
2c6226	Potri.002G023900	<i>PtGH_28</i>	AT1G19940	<i>AtGH9B5</i>	-0.42	-1.29	-1.01	-0.99		
14c27669	Potri.014G157600	<i>PtGH9B11</i>	AT2G32990	<i>AtGH9B8</i>	-1.01	-1.33	-1.02	-1.21		
6c13189	Potri.006G240200	<i>PtGT43G</i>	AT1G27600	<i>AtIRX9-L</i>	-0.55	-0.92	-0.72	-1.03	GX biosynthesis	
7c15752	Potri.007G107200	<i>PtGUX1-A</i>	AT3G18660	<i>AtGUX1</i>	-0.43	-0.84	-0.63	-0.67		
5c12551	Potri.005G033500	<i>PtGUX4-A</i>	AT1G08990	<i>AtGUX5</i>	-0.88	-2.90	-2.33	-2.28		
3c8387	Potri.004G226800	<i>PtGXM1</i>	AT1G09610	<i>AtGXM1</i>	-0.22	-0.63	-0.34	-0.56		
14c26628	Potri.014G040300	<i>PtGATL1-A</i>	AT1G19300	<i>AtPARVUS</i>	-0.38	-0.84	-0.72	-1.06		
1c2626	Potri.001G300800	<i>CE6</i>	AT4G34215	<i>At4G34215</i>	-0.74	-0.87	-0.87	-0.89	GX acetylation	
8c17245	Potri.008G069900	<i>PtXOAT1</i>	AT3G55990	<i>AtESK1</i>	-0.32	-0.60	-0.33	-0.60		
10c20767	Potri.010G187600	<i>PtXOAT2</i>	AT3G55990	<i>AtESK1</i>	-0.41	-0.67	-0.25	-0.52		
8c17246	Potri.008G070000	<i>PtXOAT6</i>	AT3G55990	<i>AtESK1</i>	-0.48	-1.45	-1.68	-1.37		
562s35967	Potri.001G376700	<i>PtXOAT8</i>	AT1G73140	<i>AtTBL31</i>	-0.38	-0.96	-0.48	-1.05		
1c3105	Potri.001G352300	<i>PtRWA_A</i>	AT2G34410	<i>AtRWA3</i>	-0.29	-0.83	-0.48	-0.70		
11c23099	Potri.011G079400	<i>PtRWA_B</i>	AT2G34410	<i>AtRWA3</i>	-0.42	-0.95	-0.58	-0.91		
10c20411	Potri.010G224100	<i>PtPAL4</i>	AT2G37040	<i>AtPAL1</i>	-0.50	-1.08	-0.57	-0.85	Lignin biosynthesis	
16c29966	Potri.016G078300		AT4G37970	<i>AtCAD6</i>	-0.47	-0.51	-0.59	-0.62		
1c2649	Potri.001G304800	<i>PtCCoAOMT2</i>	AT4G34050	<i>AtCCoAOMT1</i>	-0.55	-1.15	-0.56	-0.60		
9c19246	Potri.009G099800	<i>PtCCoAOMT1</i>	AT4G34050	<i>AtCCoAOMT1</i>	-0.39	-0.77	-0.38	-0.56		
3c6783	Potri.003G188500	<i>Pt4CL5</i>	AT1G51680	<i>At4CL1</i>	-1.00	-1.80	-1.06	-0.67		
1c307	Potri.001G036900	<i>Pt4CL3</i>	AT1G51680	<i>At4CL1</i>	-0.50	-0.96	-0.52	-0.58		
6c14571	Potri.006G087500	<i>PtLAC12</i>	AT5G60020	<i>AtLAC17</i>	-0.10	-0.47	-0.45	-0.95		
1c3502	Potri.001G401300	<i>PtLAC7</i>	AT5G60020	<i>AtLAC17</i>	-0.54	-0.48	-0.35	-0.37		
7c15861	Potri.007G096200		AT2G22420	<i>AtPRX17</i>	1.59	2.42	1.04	1.55		PRX
6c14751	Potri.006G069600		AT2G41480	<i>AtPRX25</i>	1.83	2.37	1.69	1.50		
19c34464	Potri.T045500		AT4G33420	<i>AtPRX47</i>	-1.26	-2.19	-1.35	-0.88		
5c11750	Potri.005G118700		AT5G66390	<i>AtPRX72</i>	1.50	2.49	1.44	1.27		
16c30396	Potri.016G125000		AT5G64120	<i>AtPRX71</i>	4.63	3.76	1.68	5.00		
14c27236	Potri.014G111200	<i>PtMYB055</i>	AT1G09540	<i>AtMYB61</i>	0.16	0.72	0.82	0.72	Master switchers	
2c5298	Potri.002G122600	<i>PtMYB177</i>	AT4G37260	<i>AtMYB73</i>	1.64	1.31	1.02	0.56		
5c11563	Potri.005G142600	<i>PtMYB029</i>	AT4G37260	<i>AtMYB73</i>	0.97	1.17	0.87	1.28		
611s36153	Potri.009G096000	<i>PtMYB019</i>	AT4G37260	<i>AtMYB73</i>	1.26	1.49	1.50	1.55		
19c34420	Potri.T011400		AT4G38620	<i>AtMYB4</i>	-1.28	-1.34	-1.38	-1.38		
4c9673	Potri.004G138000	<i>PtMYB093</i>	AT4G38620	<i>AtMYB4</i>	-0.96	-0.69	-0.74	-1.03		
4c9980	Potri.004G174400	<i>PtLTF1</i>	AT4G38620	<i>AtMYB4</i>	-1.59	-1.80	-1.38	-1.51		
9c18946	Potri.009G134000		AT4G38620	<i>AtMYB4</i>	-1.02	-1.04	-0.86	-0.94		
12c24760	Potri.012G127700	<i>PtMYB199</i>	AT4G22680	<i>AtMYB85</i>	-0.66	-0.88	-0.51	-0.52		
11c23287	Potri.011G058400	<i>PtNAC124</i>	AT4G28500	<i>AtSND2</i>	-0.57	-0.75	-0.89	-0.96		
4c8837	Potri.004G049300	<i>PtSND2</i>	AT4G28500	<i>AtSND2</i>	-0.70	-0.96	-0.73	-0.80		
12c24750	Potri.012G126500	<i>PtVND6-A2</i>	AT1G12260	<i>AtVND4</i>	-0.52	-0.51	-0.33	-0.33		
5c11773	Potri.005G116800	<i>PtVND6-C2</i>	AT2G18060	<i>AtVND1</i>	-0.96	-0.47	-0.34	-0.87		
15c28915	Potri.015G033600	<i>PtMYB090</i>	AT1G17950	<i>AtMYB52</i>	-0.30	-0.68	-0.47	-0.72		
7c15498	Potri.007G134500	<i>PtMYB161</i>	AT1G17950	<i>AtMYB52</i>	-0.45	-0.87	-0.73	-0.82		

CEL – cellulase; GX – glucuronoxylan, PRX - peroxidase

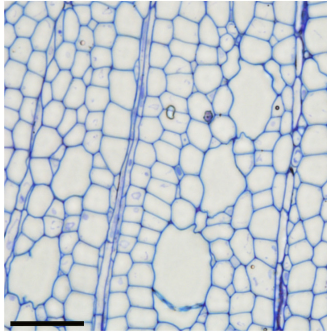


Supplementary Figure S1. Transgene expression levels in developing wood of transgenic lines expressing GH10 and GH11 xylanases. (A) Expression by RT-PCR using actin and ubiquitin genes for calibration and normalized to the lowest-expressing transgenic line. WT expression represents the noise. **(B)** Transcript quantitation based on RNA sequencing. Data are means \pm SE, N = 3 for transgenic lines and 6 for WT in (A) or N=5 for transgenic lines and 8 for WT in (B). Different letters above the bars in (A) or (B) indicate significant difference among averages ($P \leq 0.05$, Tukey test).

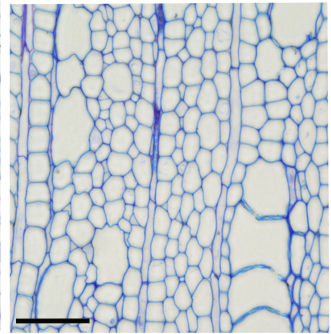
WT



35S:GH11 L8

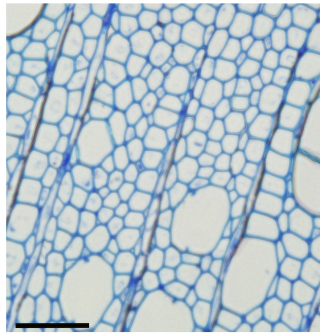


35S:GH11 L9

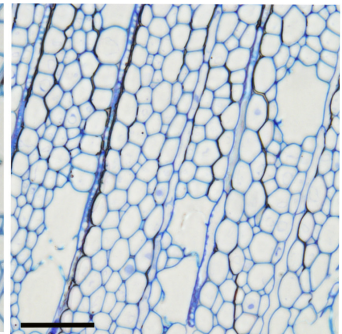


Supplementary Figure S2.
Toluidine blue stained wood sections showing reduction in cell wall thickness and change in staining indicative of reduced lignin content in transgenic lines expressing xylanases. Some vessel elements in most affected lines show *irregular xylem phenotype (irx)*. The phenotype is visible in all analyzed lines except WP:GH10_line 11, which had lower transgene expression than other lines. Scale bar = 50 μ m

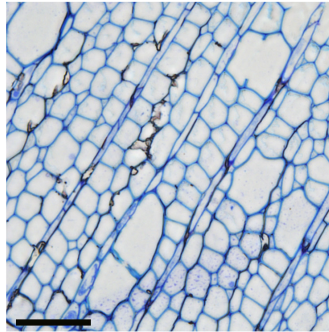
WP:GH11 L10



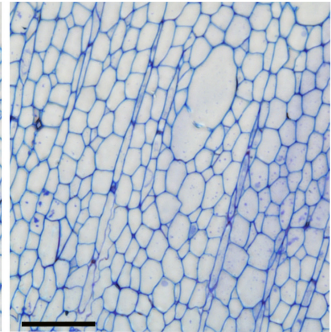
WP:GH11 L17



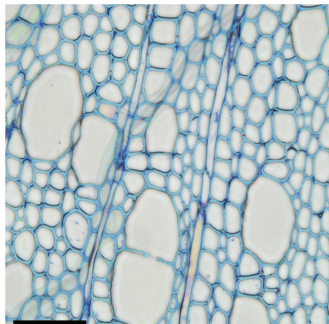
35S:GH10 L20



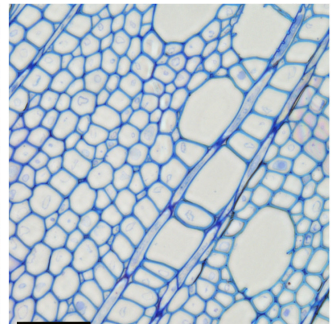
35S:GH10 L24

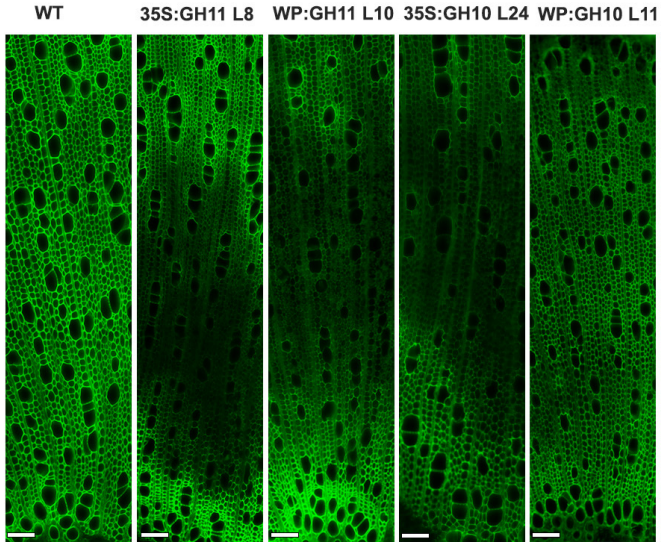


WP:GH10 L11

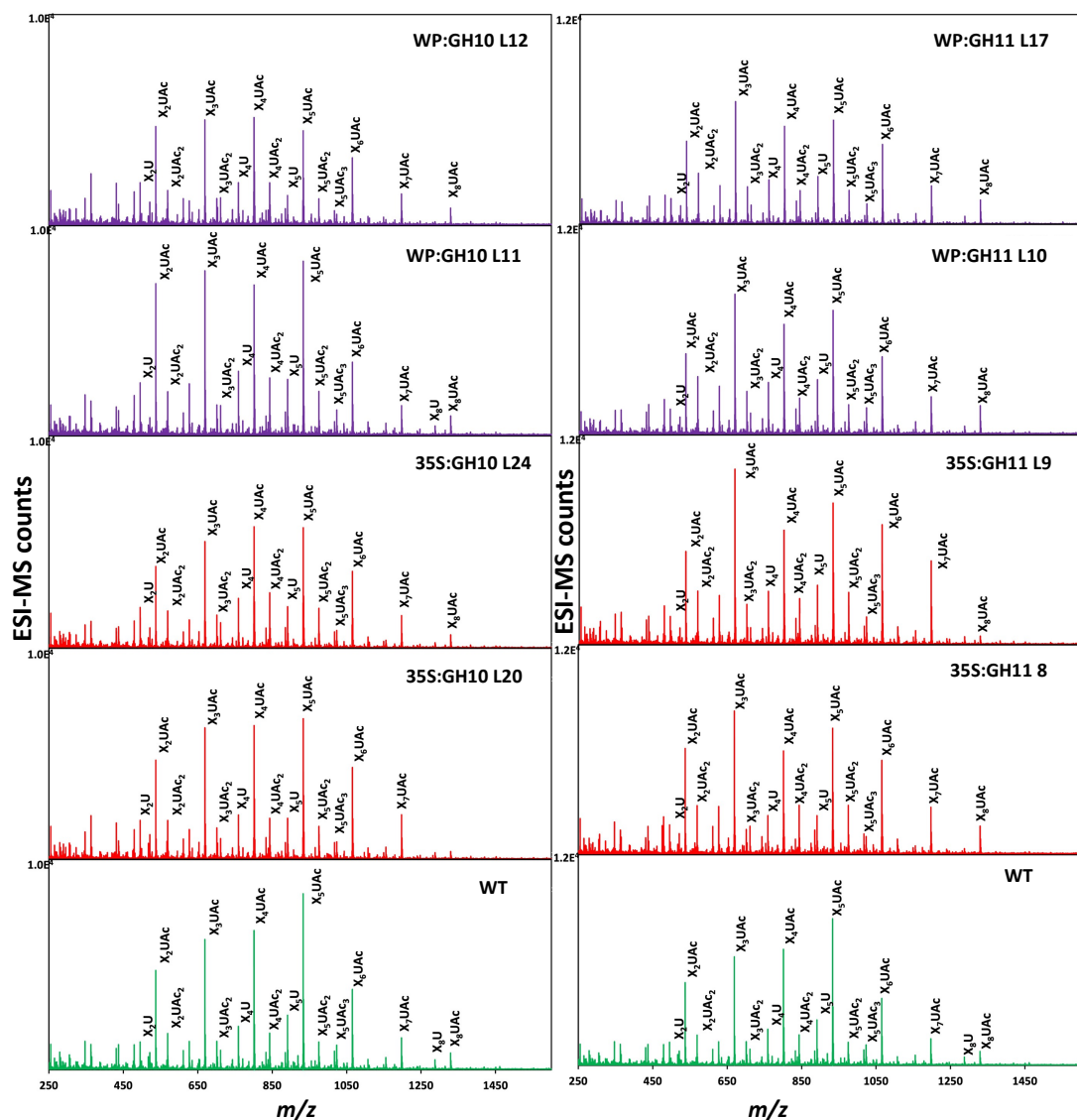


WP:GH10 L12

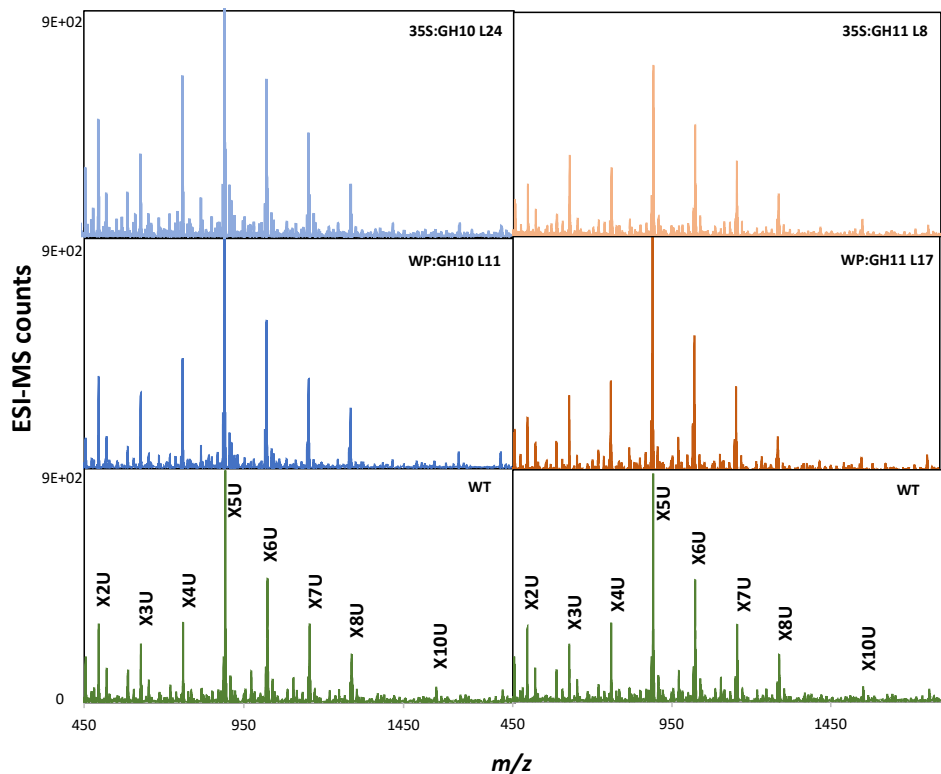




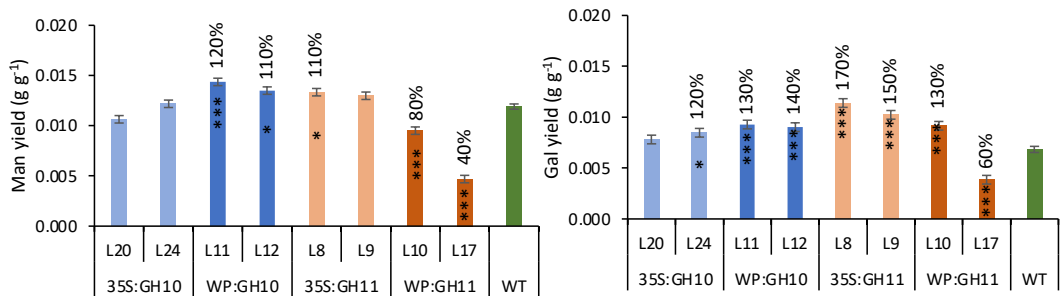
Supplementary Figure S3. Fluorescence microscopy for detection of lignin in the wood tissue of transgenic lines expressing GH10 and GH11 xylanases. Note the weak autofluorescence from the irregular xylem phenotypes of transgenic line. Scale bar= 50 μ m.



Supplementary Figure S4. Oligomeric mass profiling (ESI-MS) of acetylated glucuronoxylan extracted with 30 min subcritical water extraction from transgenic lines expressing GH10 and GH11 xylanases. The oligomers are released by incubating the extracted hemicellulose with GH30 glucuronoxylanase.

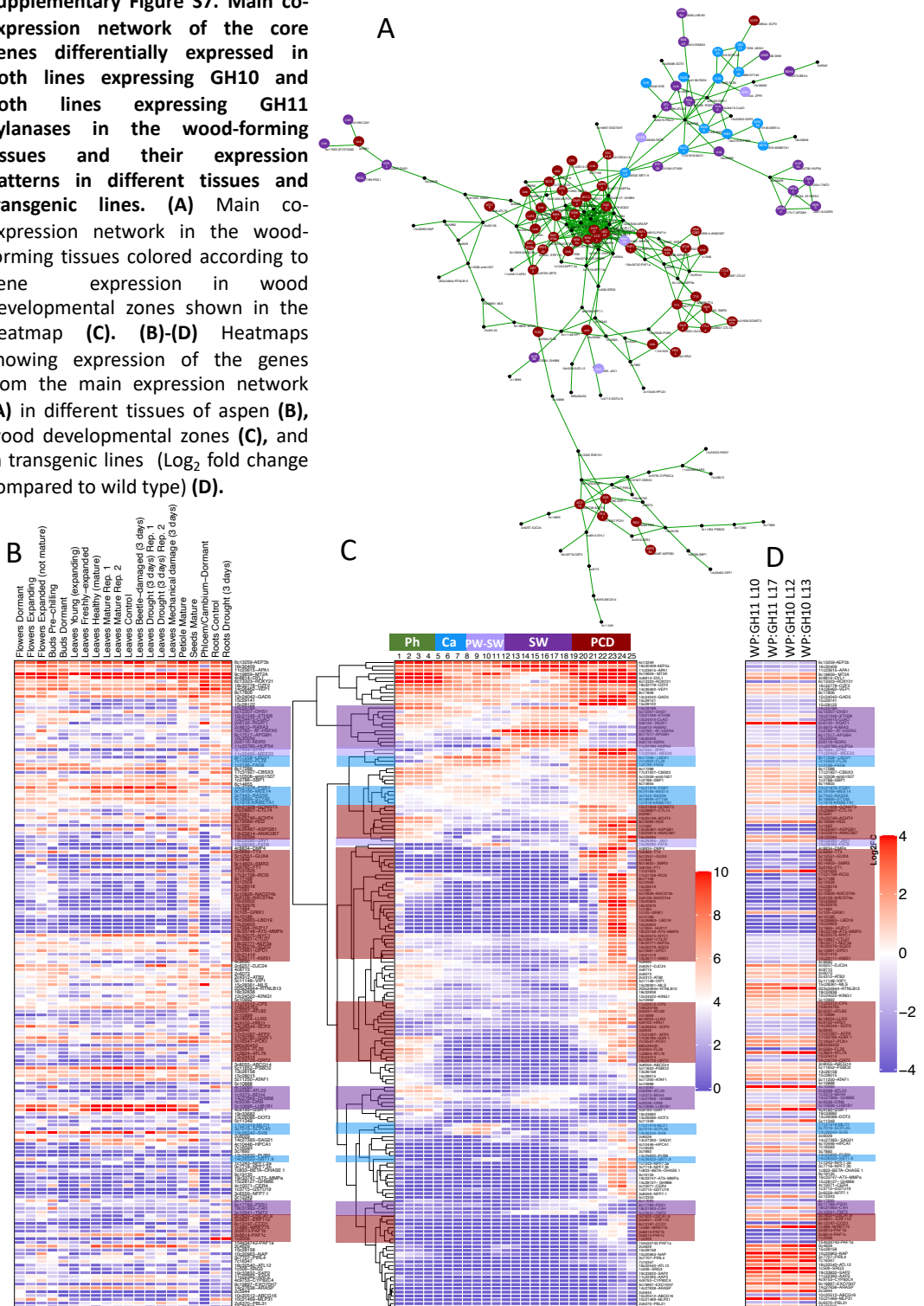


Supplementary Figure S5. Oligomeric mass profiling (ESI-MS) of glucuronoxylan extracted with alkali from transgenic lines expressing GH10 and GH11 xylanases. The oligomers are released by incubating the extracted hemicellulose with GH30 glucuronoxylanase.

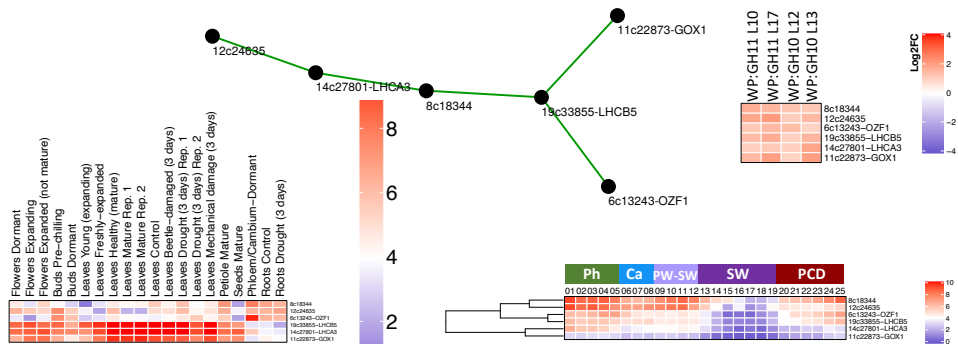


Supplementary Figure S6. Saccharification yields of mannose and galactose obtained from wood of transgenic lines expressing GH10 and GH11 xylanases. The sugars were released during acid pretreatment. Data are means \pm SE, N = 3 or 6 technical replicates from the pooled material of 6 trees for transgenic lines and WT, respectively. * - $P \leq 0.05$; ** - $P \leq 0.01$; *** - $P \leq 0.001$ for comparisons with WT by Dunnett's test.

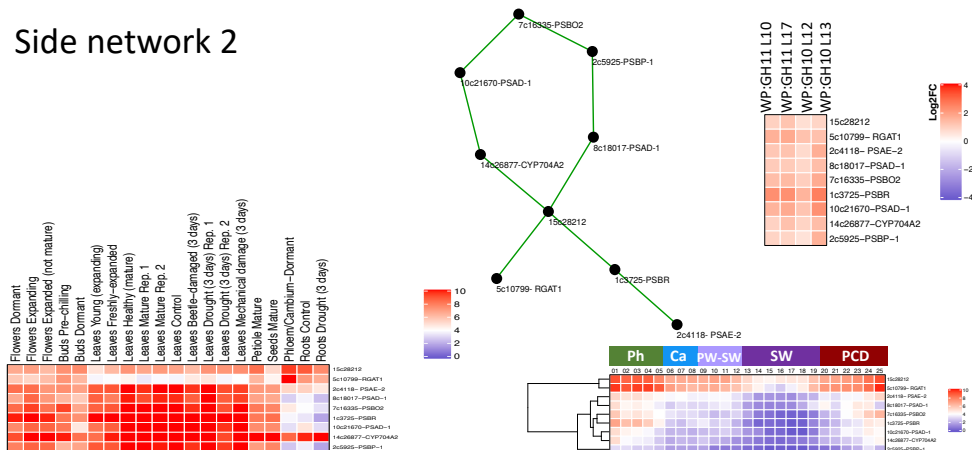
Supplementary Figure S7. Main co-expression network of the core genes differentially expressed in both lines expressing GH10 and both lines expressing GH11 xylanases in the wood-forming tissues and their expression patterns in different tissues and transgenic lines. (A) Main co-expression network in the wood-forming tissues colored according to gene expression in wood developmental zones shown in the heatmap **(C)**. **(B)-(D)** Heatmaps showing expression of the genes from the main expression network **(A)** in different tissues of aspen **(B)**, wood developmental zones **(C)**, and in transgenic lines (Log_2 fold change compared to wild type) **(D)**.



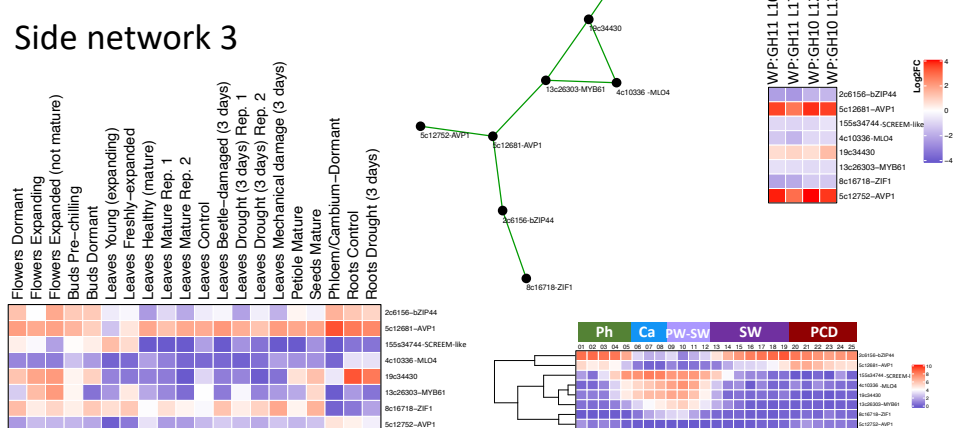
Side network 1



Side network 2

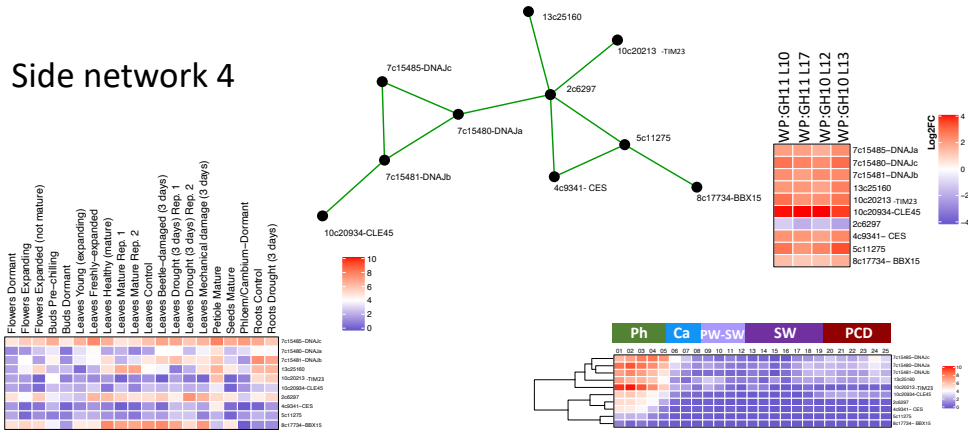


Side network 3

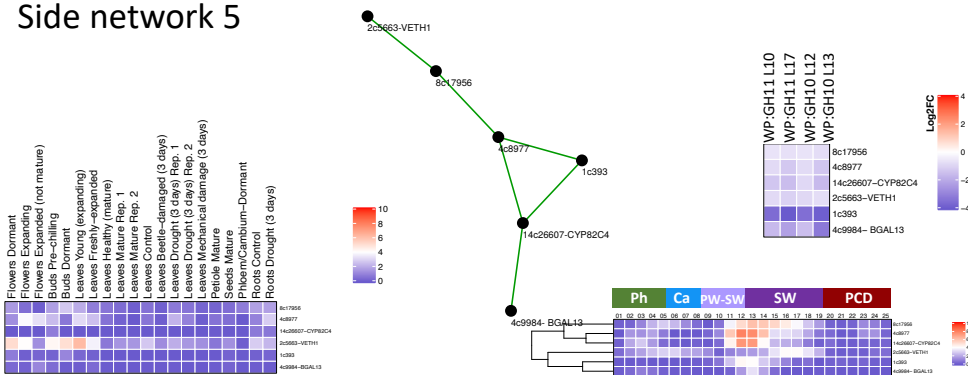


Supplementary Figure S8. Side co-expression networks 1-3 of the core genes differentially expressed in both lines expressing GH10 and both lines expressing GH11 xylanases in the wood-forming tissues and their expression patterns in different tissues and in transgenic lines. Note that network 3 includes genes downregulated or upregulated in the cambium.

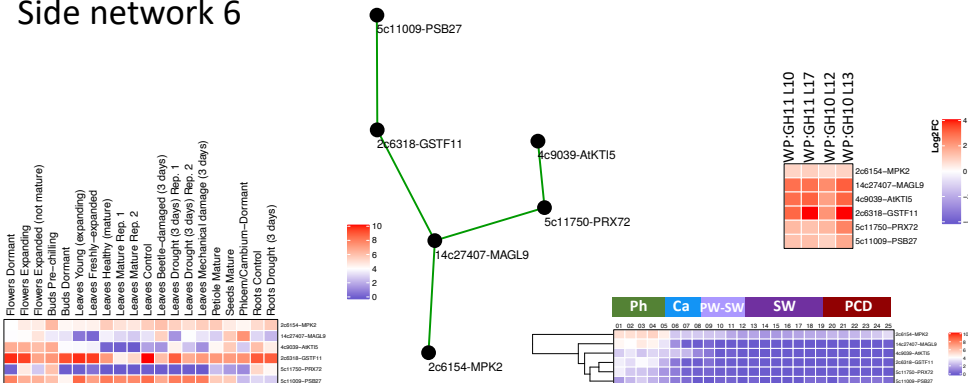
Side network 4



Side network 5

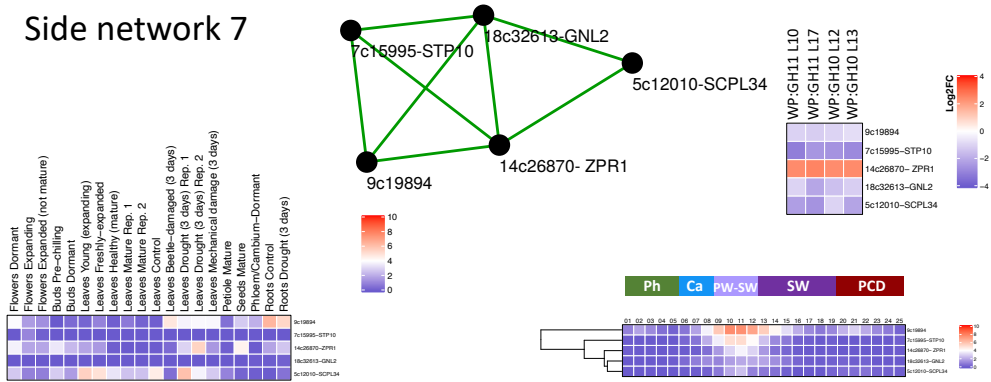


Side network 6



Supplementary Figure S9. Side co-expression networks 4-6 of the core genes differentially expressed in both lines expressing GH10 and both lines expressing GH11 xylanases in the wood-forming tissues and their expression patterns in different tissues and in transgenic lines. Note that networks 4 and 6 include genes specifically expressed in the phloem, which are mostly upregulated in transgenic lines, whereas network 5 includes genes upregulated during primary to secondary wall transition, which are downregulated in transgenic lines.

Side network 7



Supplementary Figure S10. Side co-expression network 7 of the core genes differentially expressed in both lines expressing GH10 and both lines expressing GH11 xylanases in the wood-forming tissues and their expression patterns in different tissues and in transgenic lines. Note that network 7 includes genes specifically upregulated during primary to secondary wall transition, which are downregulated in transgenic lines except for one, ZPR1.